THE UNIVERSITY
of EDINBURGH

The role of mononuclear phagocytes in prion pathogenesis

Barry Matthew Bradford

A thesis submitted in partial fulfilment of the requirements of the University of Edinburgh for the degree of Doctor of Philosophy

This programme of research was carried out at the Roslin Institute and R(D)SVS, the University of Edinburgh

2016

Table of Contents

Declaration

I declare that the work presented in this thesis is my own, except where otherwise stated. All experiments were designed by myself, in collaboration with my supervisors Professor Neil Mabbott, and Dr. Andreas Lengeling, unless otherwise stated. No part of this work has been, or will be submitted for any other degree, or professional qualification.

Barry M. Bradford
September 2016

Abstract

Prion diseases are fatal infectious neurodegenerative disorders hypothesised to be caused by misfolding of the prion protein. Following prion infection, the infectious agent is sequestered to and replicates upon follicular dendritic cells (FDC) within lymphoid follicles prior to neuroinvasion. The mechanism of transport of the prion infectious agent from the site of infection to FDC is unknown. One of the postulated routes of transport is the specific migration of antigen presenting cells (APC) to FDC. APC specifically capture antigenic material and transport and present that material to effector cells and FDC in order to generate an appropriate acquired immune response. FDC reside within the B-cell follicle of secondary lymphoid organs. FDC organise and maintain the B-cell follicular structure by secretion of the chemokine CXCL13 which stimulates chemotactic movement of cells which express the CXCR5 receptor, e.g. B cells.

Dendritic cells are specialised APC that are commonly characterised by their expression of CD11c. Transport of the prion infectious agent from the site of infection to FDC was observed to be blocked or severely delayed following depletion of $CD11c^+$ cells. To determine whether $CD11c^+$ cells acquire prions and subsequently deliver them to the FDC, the chemokine receptor CXCR5 was depleted from $CD11c^+$ cells using a conditional transgenic mouse model. These mice were characterised for normal lymphoid organogenesis and monitored for their responses to oral infection with either prions or intestinal helminths.

Data in this thesis show that the CD11c-mediated depletion of CXCR5 resulted in a delay in peripheral prion pathogenesis after oral exposure and significantly reduced disease susceptibility. These data suggest that efficient prion transport to FDC requires delivery by APC and is potentially mediated by CXCR5 chemotaxis. Following oral exposure to the intestinal helminth (*Trichuris muris*) CD11c-mediated depletion of CXCR5 prevented the establishment of a protective T_H2 response. As a consequence the mice mounted a T_H1-dominated response and were unable to clear the infection. These data also confirm that the effective generation of T_H2 responses to oral helminth infection also requires APC localisation to B-cell follicles via CXCR5.

Acknowledgements

I would like to express my thanks and sincere gratitude to my supervisors and advisors Professor Neil Mabbott, Dr. Andreas Lengeling, Dr. Dave Sester and Professor David Hume for all their help, support and guidance during my studies.

I would like to thank the following for provision of mouse line and reagents:
Professor Boris Reizis, Bart Vanhasebroeck and Wayne Pearce (Dept. Microbiology & Immunity, Columbia University, New York) for providing CD11c-cre mice. Professor David Hume, Dr. Dave Sester and Dr. Kristin Sauter (The Roslin Institute, Edinburgh) for provision of and assistance with MacGreen mice. Dr Steffan Jung (Weizmann Institute of Science, Rehovot, Israel) for providing CD11c-DTR mice. Professor Paul Crocker (University of Dundee) for provision of sialoadhesin-deficient mice and assistance with analysis of studies undertook with this model. Dr. Liqun Luo (Stanford University, Howard Hughes Medical Institute, Stanford, CA) for providing mTmG cre-reporter mice. Professor Kathryn Else (University of Manchester) for provision of the *T. Muris* infection model

Parts of chapter 1 have been previously published as (Bradford and Mabbott, 2012, Mabbott and Bradford, 2015). Parts of Chapter 3 have been previously published as (Bradford et al., 2011). Parts of chapter 7 have been previously published as (Bradford et al., 2014). Parts of Chapter 8 have been published as (Bradford et al., 2016)

I would like to thank the staff and students of the Roslin Institute and R(D)SVS the university of Edinburgh, in particular Kris Hogan, Sally Carpenter, Fraser Laing & Dave Davies for assistance and management of transgenic mouse colonies and all other related animal work within the Roslin Institute Biological Research Facility. Gillian McGregor, Sandra Mack, Aileen Boyle & Dawn Drummond for assistance with all aspects of histopathological processing and analysis. Members of the Mabbott Group including, Gwen Wathne and Laura McCulloch and especially Dr David Donaldson for his assistance with the *T. Muris* studies and Dr Karen Brown for assistance with SIGN-R1-depletion study, plus all members of the Roslin Institute Neurobiology division for helpful discussion, assistance with laboratory techniques, and all their helpful feedback and suggestions during my studies.

I would like to thank my students; Matthew Helsby, ‘Angeline’ Kah Heng Yap, Mark Laloo and Caroline Wood for their part in mini-projects. I would like to thank my colleagues and friends Dr. Herbert Baybutt, Dr. Robert Somerville, Boon Chin Tan, Andrew Castle, Karen Fernie, Dr. Wilfred Goldman, Professor Nora Hunter and Angie Chong with whom I spent many delightful hours broadening my knowledge. I would especially like to thank my great friend and mentor Professor Pedro Piccardo. Finally I would like to thank Paula Stewart, Liz Stewart and Bobby Stewart for all their love and support during my studies and my son Robin Bradford for making it all worthwhile.

Abbreviations

ANOVA	analysis of variance
APC	antigen presenting cell
B220	heavily glycosylated CD45R, mw 220 kDa
bp	base-pair
BSE	bovine spongiform encephalopathy
C	Complement component
CCL	CC chemokine ligand
CCR	CC chemokine receptor
cDNA	copy deoxyribose nucleic acid
cDC	conventional dendritic cell
CDS	coding sequence (of a gene)
CD4	Glycoprotein co-receptor assists TCR with APC
CD8α	Transmembrane glycoprotein co-receptor assists TCR, binds MHC-I
CD11b	Integrin alpha m subunit, Itgam
CD11c	Integrin alpha x subunit, Itgax
CD19	B lymphocyte antigen
CD68	Macrosialin
CD103	Integrin alpha E subunit, Itgae
CD169	Sialoadhesin, Sn, Siglec-1
CJD	Creutzfeldt-Jakob's disease
c-KIT	tyrosine protein kinase, CD117, SCFR
CNS	central nervous system
CP	Cryptopatch
CR	complement receptor
Cre	cyclization recombinase enzyme
CSF1	colony stimulating factor 1, M-CSF
CSF1-R	colony stimulating factor 1 receptor
CX3CR1	CX3C chemokine receptor 1, fractalkine receptor, GPR13
CX3CL1	fractalkine
CXCL13	CXC chemokine ligand 13, B lymphocyte chemokine (BLC)
CXCR5	CXC chemokine receptor 5, BLC receptor (BCR), CD185
$CXCR5^{fl}$	CXCR5 floxed transgenic mouse model
DC	dendritic cell
DNA	deoxyribose nucleic acid
DTR	diphtheria toxin receptor
DTX	diphtheria toxin
eGFP	enhanced green fluorescent protein
ELISA	enzyme-linked immunosorbent assay
ES	embryonic stem (cell)
FACS	fluorescent activated cell sorting
FAE	follicle associated epithelium
Fc	fragment crystallisable (invariant) portion of immunoglobulin
FDC	follicular dendritic cell
FITC	Fluorescein isothiocyanate
FLPe	flipase (enhanced) recombinase enzyme
FM	follicular mantle
g	gravity

GALT	gut-associated lymphoid tissue
GC	germinal centre
IEL	intra-epithelial lymphocyte
IFN	interferon
IFR	interfollicular region of the Peyer's patch
Ig	immunoglobulin
IgA	immunoglobulin class A
IgG	immunoglobulin class G
IgM	immunoglobulin class M
IHC	immunohistochemistry
Il	interleukin
ILF	isolated lymphoid follicle
Itgam	integrin alpha M subunit, CD11b
Itgax	integrin alpha X subunit, p150, CR4, CD11c
kDA	KiloDalton
KO	knockout i.e. transgenic gene deletion/ablation
loxP	locus of cross-over of bacteriophage P1, Cre recognition sequence
LC	Langerhans cell
LTα	lymphotoxin alpha
LTβ	lymphotoxin beta
LTβR	lymphotoxin beta receptor
LTi	lymphoid tissue inducer (cell)
MACS	magnetic-activated cell sorting
MadCAM	mucosal vascular addressin cell adhesion molecule
MALT	mucosa-associated lymphoid tissue
M-cell	microfold cell
MHC	major histocompatibility complex
MNP	mononuclear phagocyte(s)
mPDCA1	murine Plasmacytoid dendritic cell antigen 1, BST2, CD317
mTmG	double transgenic Cre reporter mouse model
MZ	marginal zone
PC	paracortex region of the lymph node
PBS	Phosphate buffered saline
PCR	polymerase chain reaction
pDC	plasmacytoid dendritic cell
PET	paraffin-embedded tissue (blot)
PK	proteinase K
PLP	Periodate-lysine-paraformaldehyde fixative
PNS	peripheral nervous system
PrP	Prion protein
PrP^{C}	Prion protein cellular isoform
PrP^{d}	Prion protein disease specific
PrP^{Sc}	Prion protein scrapie-associated isoform
R	receptor
RNA	ribose nucleic acid
RP	red pulp region of the spleen
SCID	severe combined immunodeficiency
SED	sub-epithelial dome region of the Peyer's patch
SIGLEC	sialic acid binding Ig-like lectin
SIGN-R1	specific intercellular adhesion molecule-3-grabbing non-integrin related 1
Sn	Sialoadhesin, SIGLEC-1, CD169

TFH	T follicular-helper cell
TH	T helper cell
TNF	tumour necrosis factor
TSE	transmissible spongiform encephalopathy
VCAM	vascular cell adhesion molecule
WP	white pulp region of the spleen

Chapter 1. Introduction

1.1 Prion Disease

1.1.1 Prion diseases

Prion diseases are classically defined as neurodegenerative disorders of the central nervous system (CNS) which affect both humans and animals (Table 1.1). Prion diseases can arise spontaneously, result from genetic predisposition or be transmitted via infection. As a group these diseases share certain characteristics which include lengthy incubation periods and distinctive pathology, most notably the spongiform appearance of the brain tissue due to vacuolation. Concurrent with this spongiform change, neuronal loss, activated glial response and deposition of both amyloid and protease resistant prion protein (PrP) may be associated to varying degrees. Due to the infectious nature of some of these disease and the stereotypical neuropathological changes they are often referred to as transmissible spongiform encephalopathies (TSE). Currently prion diseases have no known curative or prophylactic treatment and are therefore invariably fatal. Prion diseases do not elicit a classical immune response (Bradford and Mabbott, 2012).

Table 1.1 Prion diseases

Prion Disease	Affected species	Identified
Atypical BSE (BASE)	Cattle	2004
Atypical Scrapie (e.g. Nor98)	Sheep	1998
Bovine Spongiform Encephalopathy (BSE)	Cattle	1986
Chronic Wasting Disease (CWD)	Mule Deer, Elk	1967
Exotic Ungulate Encephalopathy (EUE)	Nyala, Gemsbok, Kudu, Eland, Oryx	Mid 1980's
Familial Creutzfeldt-Jakob's Disease (fCJD)	Human	1924
Fatal Familial Insomnia (FFI)	Human	1974
Feline Spongiform Encephalopathy (FSE)	Domestic cat, Puma, Ocelot, Lynx, Lion, Leopard Cat, Tiger	1990
Gerstmann-Straussler-Scheinker Syndrome (GSS)	Human	1928/1936
Kuru	Human	1941
Variant Creutzfeldt-Jakob's Disease (vCJD)	Human	1996
Scrapie	Sheep, Goat	1732
Sporadic Creutzfeldt-Jakob's Disease (sCJD)	Human	1920/1921
Transmissible Mink Encephalopathy (TME)	Mink	1947

1.1.2 The prion infectious agent

The causative infectious agent in prion disease has been subject to much heated debate. The prion infectious agent was initially classified as a virus, as scrapie was shown to be transmissible between sheep in cell-free filtrates (Gordon, 1957). The extraordinary resistance of the scrapie agent to heat inactivation (Stamp, 1962) and formalin (Pattison, 1965) were well documented. The long incubation periods observed with scrapie were compared with other diseases such as Rida, and maedi visna virus infections resulting in the description of scrapie as a slow virus infection (Sigurdsson, 1954, Sigurdsson and Palsson, 1958). Further characterisation of the scrapie agent with electron beam and ultraviolet irradiation suggested it was of extremely small size and potentially devoid of nucleic acid components, or that nucleic acid was not required for its replication (Alper et al., 1966, Alper et al., 1967). It had been suggested that the scrapie infectious agent may be comprised solely of protein (Alper et al., 1967, Griffith, 1967). A theory later developed into the prion hypothesis (Prusiner, 1982). Following the transmission of the scrapie agent to mice (Chandler, 1961), investigation of the encephalopathy caused (Morris and Gajdusek, 1963, Eklund et al., 1967) highlighted the similarities between scrapie in sheep, encephalopathy of mink (Hartsoug and Burger, 1965) and kuru in humans (Gajdusek and Gibbs, 1964), thus forming an early basis for the grouping of prion diseases from different species into a group of diseases with possibly the same type of causative infectious agent. PrP was first associated with prion disease by co-purification of the protein with infection (Bolton et al., 1982), surprisingly PrP was discovered to be a host-encoded protein (Oesch et al., 1985).

Deposited protease-resistant or disease associated PrP is known under several monikers. In this text the term PrP^{Sc}, the acronym for PrP scrapie, will be used. Conversely, the term PrP^{C} will be used in reference to the normal cellular isoform, or protease-sensitive PrP. Upon refolding into PrP^{Sc}, the alpha-helical content is reduced and beta-sheet content increased (Riesner, 2003). PrP^{Sc} appears to have a greater propensity to form polymeric structures or aggregates, hence the amyloid deposits. Refolding of the protein also bestows a variable protease resistance, usually manifest experimentally by digestion of infected material with proteinase K (PK). Following PK treatment PrP^{Sc} is reduced to a protease resistant core of 27-30 kDa following variable truncation of the amino-terminal residues up to residues in the region 90-110 (McKinley et al., 1983). Lysozymal proteolysis of PrP^{Sc} has been observed *in vitro* (Caughey et al., 1991) and *in vivo* in infected individuals, and may play an important role in the spread of infection particularly in the CNS (Lawson et al., 2001, Ayers et al., 2009). The

prion hypothesis suggests a PrP^{Sc} template-mediated conversion process of PrP^{C} as the integral component of the infectious process. Cell-free conversion of PrP^{C} to PrP^{Sc} has been demonstrated (Kocisko et al., 1994), however, attempts to generate de-novo infection from PrP^{C} only appear to remain elusive.

1.1.3 Routes of infection

The most common likely form of exposure is via dietary consumption of infected material as evidenced by the propagation of bovine spongiform encephalopathy (BSE) within the UK cattle population via BSE contaminated meat and bone meal supplements (Taylor, 1993). BSE has also transmitted to other animals such as both domestic cats and large cats, bovid ruminants and non-human primates within zoo collections (Sigurdson and Miller, 2003) as well as humans via the food chain (Will and Ironside, 1999). Prions are highly resistant to denaturation and are capable of contaminating the environment for appreciable time periods (Brown and Gajdusek, 1991). This resistant nature of prions to decontamination (Dickinson and Taylor, 1978, Taylor et al., 1994, Manuelidis, 1997, Taylor, 2000) is hypothesised to underlie the basis of their infectious nature and also their ability to survive transit through the digestive tract (Krüger et al., 2009). The spread of Kuru within humans has also been attributed to oral transmission due to the practice of ritual cannibalistic feasts and the decrease in disease incidence once these practices were halted (Collinge et al., 2006).

In other cases of natural horizontal transmission, such as scrapie in sheep and goats and CWD in mule deer and elk a variety of potential routes exist. As well as oral transmission, prions are known to readily transmit through lesions in skin (Taylor et al., 1996) and oral mucosa (Carp, 1982). The potential for vertical e.g. maternal transmission exist and some evidence exists for its occurrence in scrapie (Hoinville et al., 2010) but not BSE-infected sheep (Foster et al., 2004). Furthermore iatrogenic transmission of prion diseases have occurred via surgical intervention (Thadani et al., 1988) and blood transfusion (Llewelyn et al., 2004) in humans. Experimental transmission of prion disease such as scrapie between sheep (Cuille and Chelle, 1936), to goats (Pattison, 1957, Pattison et al., 1959) and to mice (Chandler, 1961) have all been performed by intracerebral inoculation. Intraperitoneal, intravenous and subcutaneous (Kimberlin and Walker, 1978) and intragastric (Kimberlin and Walker, 1989) routes have been shown to be effective in mice, though less efficient than the intracerebral route of inoculation. Intraocular (Fraser and Dickinson, 1985), intraspinal (Kimberlin et al., 1987) and intraneural

(Kimberlin et al., 1983) prion inoculations in mice often produce shorter disease incubation periods than intracerebral inoculation but with varying efficiency of transmission.

1.1.4 Strains of prion agent

The occurrence of prion diseases in several animal species and their species range, zoonotic potential and clinical presentation suggest that several distinct prion diseases exist. Serial transmission of sheep-derived scrapie in goats (Pattison et al., 1959) revealed differing clinical symptoms classified as scratching or nervous/drowsy syndromes that occurred either 16 or 22 months post inoculation (Pattison and Millson, 1961), indicative of variations in the disease characteristics of both incubation period and clinical outcome elicited by scrapie prions and the first evidence for different strains of prion agent. On attempted transmission of scratching or drowsy goat scrapie to a panel of mice including C57Bl, CBA and Swiss White mice, only Swiss White mice succumbed to the drowsy goat inoculum revealing variable susceptibility to scrapie prions in inbred mouse lines (Chandler, 1961). Serial passage of the 'Chandler' drowsy goat scrapie in mice yielded the 139A mouse-adapted strain of scrapie prions (Bruce and Dickinson, 1987). Transmission of sheep scrapie directly to mice generated the ME7 mouse-adapted strain of scrapie prions (Zlotnik and Rennie, 1963) used in this thesis. This led to the further discovery of a specific gene, termed *Sinc* for scrapie incubation period, in mice with alleles for short $Sinc^{S7}$ or prolonged $Sinc^{P7}$ effect on ME7 scrapie incubation period and their heterozygote cross with alterations also observed in the type and patterns of brain lesion produced in these mice (Dickinson et al., 1986). The *Sinc* gene was initially thought to be linked to the PrP gene (Hunter et al., 1987) and was later shown to be congruent with *Prnp* using targeted gene-replacement transgenic mice (Moore et al., 1998).

1.1.4 Prion neuroinvasion

To cause disease, the infectious agent must gain access to the CNS, a process that has been termed neuroinvasion. The long incubation periods, or lag phase following experimental transmission via peripheral routes, occur due to the stages of infection prior to neuroinvasion. This is exemplified by experimental transmission routes such as intracerebral delivery to the CNS (Kimberlin and Walker, 1986), and intraneural delivery to the peripheral nervous system (PNS), having the shortest disease incubation period (Kimberlin and Walker, 1986, Kimberlin et al., 1987). Transport of the infectious agent to the CNS can occur through the PNS by defined anatomical routes (McBride and Beekes, 1999, Beekes and McBride, 2000, McBride

et al., 2001). Once into the PNS the spread of the infectious agent occurs at a relatively uniform rate regardless of the strain of agent (Bartz et al., 2002, Kunzi et al., 2002).

1.1.6 Prion neuropathology

The common pathological presentation in the CNS is spongiosis, due to vacuolation of the grey matter (Figure 1.1A) when compared to uninfected brain tissue (Figure 1.1B). Following experimental transmission of sheep scrapie isolates to mice, several distinct strains of agent have been distinguished, each with highly reproducible characteristics (Bruce, 1993). The degree of vacuolation and PrP^{Sc} deposition and their targeting to specific brain areas is dependent upon many variables (Bruce et al., 1994). Concurrent with the appearance of vacuolation, disease-associated PrP (PrP^{d}) deposition (Figure 1.1C) and neuronal loss (Figure 1.1B), the CNS responds to infection via astrocytic (Diedrich et al., 1991)(Figure 1.1E) and microglial responses (Williams et al., 1994)(Figure 1.1G) not normally observed in uninfected brain tissue (Figure 1.1 C, F & H). The strain of agent, route of infection and host PrP sequence have a large influence in determining disease duration, clinical and pathological outcome (Bruce, 2003).

The range of clinical presentation is vast even amongst the human subtypes of CJD, however the majority of clinical symptoms result from underlying neurological abnormality usually within the CNS, though some prion diseases present with neuropathy of the PNS also. These diseases were considered for a long time as a purely neurological disease eliciting a minimal immune response. However, investigation into the spread of infection from sites of exposure suggests an implicit link between these diseases and the immune system, and study of the neurodegenerative nature of these diseases has revealed a significant role for microglial cells within the CNS. The exact cause of death from these diseases is still elusive, however experimental evidence suggests that progression of neuronal loss and dysfunction in critical target areas of the brain results in the loss of vital functions (Mirabile et al., 2014). Sporadic CJD in humans typically presents with a variety of symptoms but usually includes dementia, myoclonia, cerebellar ataxia, visual disturbances and periodic electroencephalography, whereas vCJD typically is clinically characterized by psychiatric abnormalities, sensory symptoms and ataxia preceding dementia alongside other clinical symptoms similar to sporadic CJD (Brandel, 1999).

Figure 1.1 Typical prion disease neuropathology

Coronal hippocampal sections of mouse brain stained with haematoxylin & eosin reveal vacuolation and neuronal loss following prion infection (A) giving the brain a characteristic spongiform appearance, not normally observed in uninfected brain tissue (B). Immunohistochemical staining with anti-PrP antibody reveals deposition of disease-associated PrP (PrP^d) (C) not present in uninfected brain (D). Immunohistochemical staining with anti-GFAP antibody reveals morphologically activated astrocytes in infected brain tissue (E) when compared to uninfected brain (F). Immunohistochemical staining with anti-iba1 antibody reveals morphologically activated microglia and accumulation of microglia in infected brain tissue (G) when compared to uninfected brain (H). Scale bar = 100 µm.

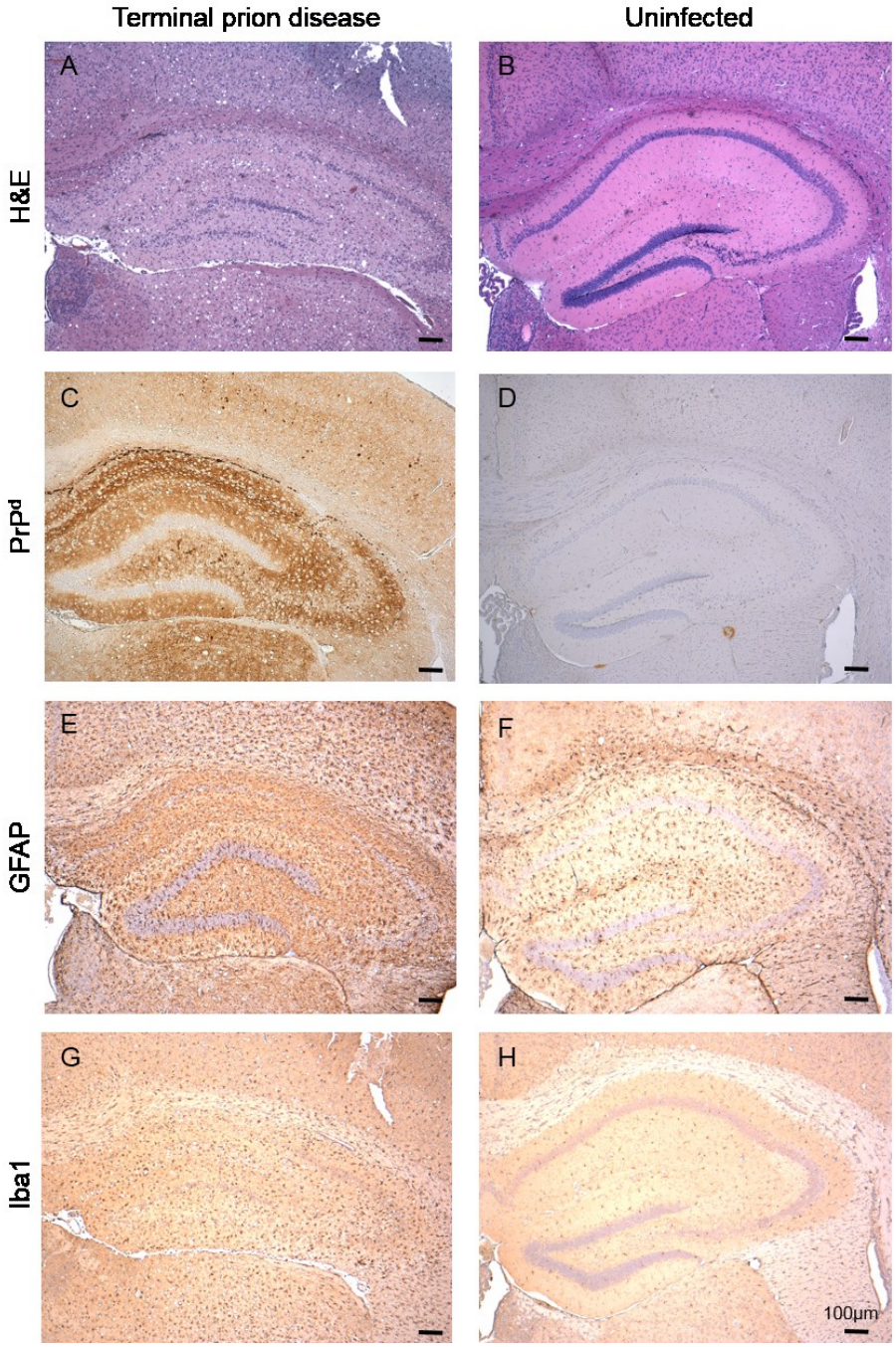

1.2 Prion protein

1.2.1 Cellular prion protein

PrP^C is a 209 amino acid, 35 kilodalton (kDa) protein (in humans) folded into a predominantly alpha-helical structure. The immature protein has a 23 amino acid residue signal sequence at the amino-terminus directing protein translocation through the endoplasmic reticulum to insertion at the cell membrane during which the sequence is cleaved (Hegde et al., 1998). Mature PrP^C has a glycosylphosphatidylinositol (GPI) anchor attached at the carboxy-terminus fixing the mature protein to the cell membrane (Stahl et al., 1987). The protein sequence includes a disulphide bridge and two N-linked glycosylation sites that may be variably occupied leading to three major classes of glycoform variants namely unglycosylated, monoglycosylated and diglycosylated (Oesch et al., 1985). Variation within the sugar moieties attached results in a large number of sub-variant glycoforms (Stimson et al., 1999, Rudd et al., 2001). The protein is encoded by the *Prnp* gene which consists of 2 exons with the complete coding sequence for PrP contained within exon 2. The *Prnp* gene sequence varies between species as well as by identified mutations that encode polymorphic changes, repeats or deletions but remains reasonably highly conserved throughout mammalian species (Mastrianni, 2010, Minikel et al., 2016). Ablation of the *Prnp* gene in transgenic mice initially revealed little phenotypic alteration, other than their complete resistance to prion disease (Bueler et al., 1993, Manson et al., 1994).

1.2.2 Prion protein expression

PrP^C is widely expressed in many tissues (Figure 1.2A), though the expression level is higher within the nervous system (Oesch et al., 1985, Kretzschmar et al., 1986) than in most other tissues, including lymphoid tissues (Caughey et al., 1988, Mabbott et al., 1997, Dodelet and Cashman, 1998). There has been much debate regarding which cells of the immune system do or do not express appreciable levels of PrP. It has long been known that PrP is expressed on hematopoietic stem cells within the bone-marrow compartment, specific lineages appear to lose or down-regulate this expression during differentiation (Kubosaki et al., 2001, Liu et al., 2001). Maturation of cells in response to all-trans retinoic acid is one mechanism known to down-regulate PrP expression (Rybner et al., 2002). In light of the current debate regarding hematopoietic differentiation and retention or loss of PrP^C expression data on the expression of the prion protein gene (*Prnp*) transcripts in various innate immunity relevant cellular compartments is presented (Figure 1.2B). The ability to detect *Prnp* gene expression and PrP^C differ, indeed it appears that the mature protein is often more labile or difficult to detect than its corresponding mRNA message, possibly accounting for some of the reported discrepancies (Ford et al., 2002a, Ford et al., 2002b). The data presented here clearly depicts altered *Prnp* expression levels between subcomponents of the hematopoietic system with macrophage, conventional dendritic cell (cDC), microglia, Langerhans cells and interferon-producing killer dendritic cells displaying high levels of *Prnp* transcript. In contrast mast cells appear to specifically upregulate *Prnp* expression during their differentiation from HSC (Haddon et al., 2009).

Figure 1.2 *Prnp* expression levels in various murine tissues and isolated immune cell subtypes

(A) *Prnp* gene expression data in mouse tissues from BioGPS.org (Wu et al., 2009). (B) *Prnp* gene expression data in immune cell subsets; BM, bone marrow; HSC, hematopoietic stem cells; CMP, common myeloid progenitor; GMP, granulocyte-macrophage progenitor; CLP, common lymphoid progenitor; BMDM, bone marrow-derived macrophage; LC, Langerhans cell; BMDC, bone marrow-derived dendritic cell; DC, dendritic cell; pDC, plasmacytoid dendritic cell; IKDC, interferon-producing killer dendritic cell; NK, natural killer. Using Affymetrix GeneChip Mouse Genome 430 2.0 Array probe set 1448233_at, data from (Mabbott et al., 2010).

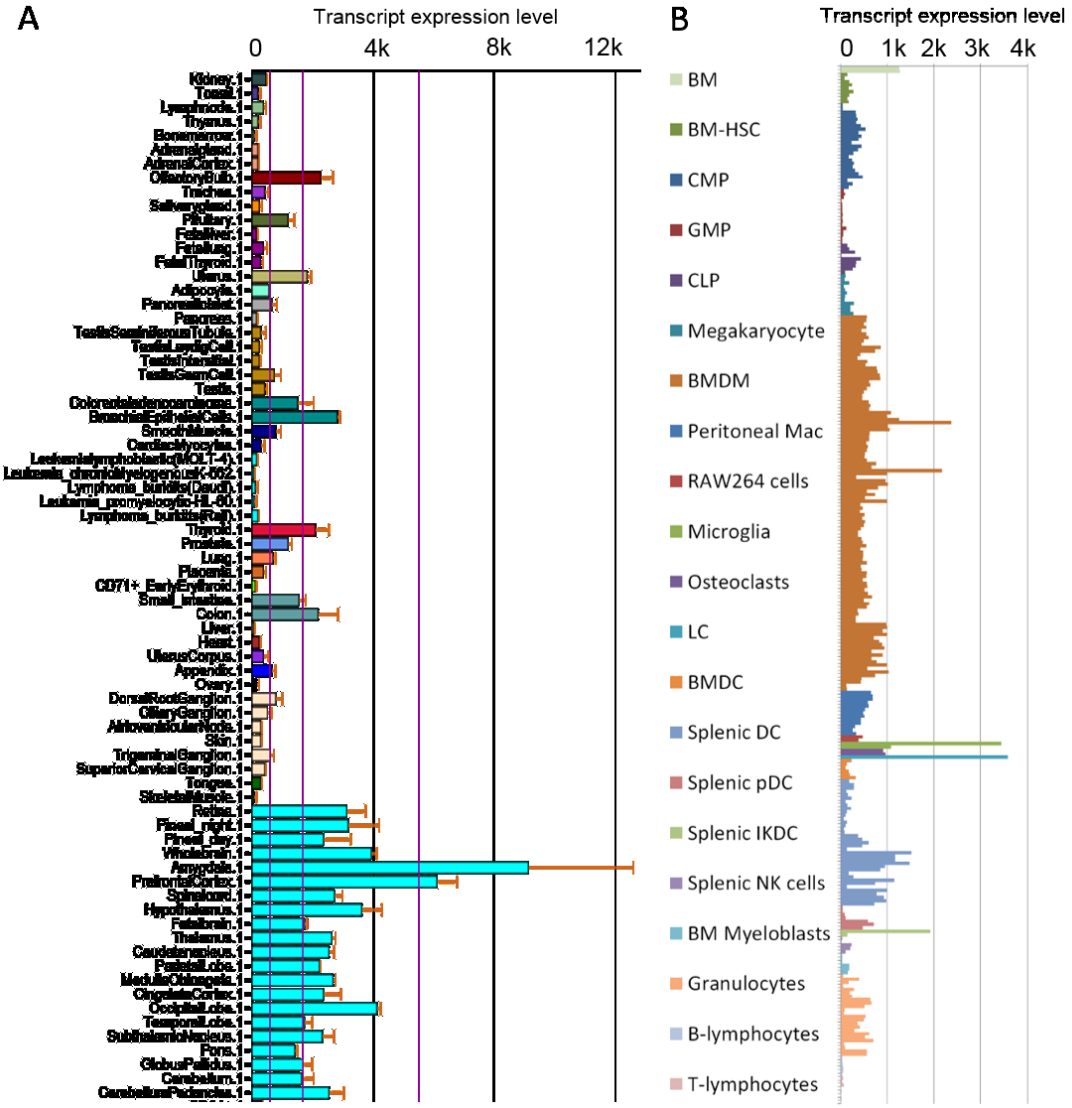

1.2.3 Prion protein functions

The exact physiological function or functions of PrP^C are still under debate. PrP^C is expressed widely in many tissues but most highly within the CNS. Understandably most of the initial investigations into PrP^C function have focussed on neuronal cells and the nervous systems, despite that fact that PrP^C is not restricted to neurones. One of the major functional deficits discovered in PrP-knockout mice was the failure of myelin maintenance (Bremer et al., 2010). Due to the availability of conditional PrP-knockout mice (Tuzi et al., 2004), this cell-cell signalling function of PrP^C was shown to be directly attributable to the expression of PrP upon neuronal cells as the loss of PrP from myelinating cells had no effect on myelin maintenance (Bradford et al., 2009, Bremer et al., 2010). Indeed PrP^C may serve as a receptor for heparan sulfate (Pan et al., 2002), laminin (Graner et al., 2000), vitronectin (Hajj et al., 2007), nerve cell adhesion molecule (Schmitt-Ulms et al., 2001), various synaptic proteins (Spielhaupter and Schätzl, 2001) and stress-inducible protein-1 (Zanata et al., 2002). Other studies of complete PrP-knockout mice have revealed deficits in learning, memory and sleep (Tobler et al., 1996), increased sensitivity to seizures (Walz et al., 1999), exacerbated reactions to stroke (Weise et al., 2006) and exacerbated reaction to experimental autoimmune encephalomyelitis (Tsutsui et al., 2008). Much of these neurological and neuroinflammatory response disorders may well be attributable to the potential cell-cell signalling function of PrP^C. Recent investigation of a novel PrP-knockout mouse constructed on C57Bl/6 background recapitulated the chronic demyelinating phenotype which has been robustly observed in all PrP-knockout mice lines produced so far, further indicating the true function PrP^C performs within the nervous system (Nuvolone et al., 2016)

Other than the potential possible role or function of PrP^C in neurones, roles for PrP^C have also been suggested within the immune system (Isaacs et al., 2006) including immunological senescence (Bakkebø et al., 2015). PrP^C is upregulated during T-cell activation (Cashman et al., 1990) and present within T cell-cDC interactions at the immunological synapse (Paar et al., 2007). Indeed PrP-knockout mice display reduced antigen-presenting cell function (Ballerini et al., 2006) and was reported to modulate phagocytic uptake by macrophages (de Almeida et al., 2005, Krebs et al., 2006), however these observation have since been attributed to the 129/Ola variant of the SIRPα gene nearby to *Prnp* as a substantial genetic background and linkage effect has occurred following the PrP-knockout transgene construction and breeding into other mouse strains (Nuvolone et al., 2013). This caveat is similarly applicable to most of the above-mentioned findings in PrP-knockout mice and so the precise function and

physiological role of PrP^C within either the nervous or immune systems or elsewhere still remains elusive.

PrP^C is most highly and notably expressed upon cell types that possess (a) complex cell shapes with extensive membrane morphology (neurones, astrocytes, myelinating cells, FDC, LC, cDC, macrophages), (b) activity which involves a lot of recycling of membrane components such as vesicular uptake and release e.g. neurotransmitter release and recycling (neurones & astrocytes), myelin maintenance (myelinating cells) degranulation (mast cells), or antigen presentation (FDC, LC, cDC, macrophages, T-cells) and (c) undergo extensive cell-cell interaction in order to perform their normal functions. It is likely therefore that if PrP^C has a specific role to play it will be in the regulation or assistance of these functions. However functional investigations into PrP-deficient cells have revealed no impact upon FDC (McCulloch et al., 2013) or mast cell (Haddon et al., 2009) functions to date.

1.3 The role of the immune system in prion pathogenesis

1.3.1 Gut associated lymphoid tissue

The gut associated lymphoid tissue (GALT), a subclass of the mucosa-associated lymphoid tissue (MALT), can be categorised by its relative structures and includes Peyer's patches, isolated lymphoid follicles (ILF) and cryptopatches (CP). Peyer's patches are identified as thickened layers of the gut wall, and consist of multiple highly organised B cell rich follicles resident in the lamina propia layer, separated by T cell rich interfollicular regions. Each follicle consists of a germinal centre (GC) which includes B cell centrocytes and centroblasts surrounding follicular dendritic cells (FDC) (Figure 1.3). The germinal centre is surrounded by the follicular mantle (FM), consisting of B cells which have not passed through the GC. This in turn is surrounded by the marginal zone (MZ) memory B cells, resembling either centrocytes or monocytes, capable of migrating to the GC (Macpherson et al., 2008, Suzuki et al., 2010). The cDC rich sub-epithelial dome covers each follicle, extending into the submucosal layer of epithelium and covered by follicle associated epithelium (FAE). Lymph nodes associated with MALT process the draining extracellular fluid through the afferent lymphatic vessels. In the case of GALT, the lymph drains to the mesenteric lymph nodes resident in a chain between the layers of mesentery with each node corresponding to a specific area of the intestine (Houston et al., 2015). Once processed in the lymph nodes the remaining fluid exits via the efferent lymphatic vessel and re-joins the blood via the venous system. In a similar fashion to the processing of lymph via the lymph nodes, the blood is processed via transition through the spleen.

The earliest indication of oral prion disease in hamsters experimentally infected with 263K strain of scrapie prions is the presence of PrP^{Sc} in the ileal Peyer's patches and mesenteric lymph nodes (Beekes and McBride, 2000). Prion accumulation occurs within the lymphoreticular systems following oral infection before prions are detectable within the nervous system of naturally scrapie-infected sheep (Andreoletti et al., 2000, Heggebo et al., 2000), CWD-infected mule deer (Sigurdson et al., 1999) and scrapie-infected mice (Prinz et al., 2003c, Glaysher and Mabbott, 2007). In fact the presence of specific gut-associated lymphoid tissues (GALT) have been shown critical for efficient oral scrapie infection of mice (Mabbott et al., 2003, Prinz et al., 2003c, Glaysher and Mabbott, 2007, Donaldson et al., 2015). Whilst similar GALT structures exist in both the small and large intestine, only the small intestinal lymphoid tissues appear critical to oral prion infection (Donaldson et al., 2015).

Figure 1.3 Initial events in oral prion pathogenesis

Prions present in the gut lumen following consumption of contaminated food are taken up into Peyer's patches by microfold (M) cells on the follicle-associated epithelium (FAE). Following uptake prions may by recognised by complement components or taken up directly by MNP. Macrophage uptake is likely to result in prion degradation. Transport of prions from the sub-epithelial dome (SED) to follicular dendritic cells (FDC) in the germinal centres (GC) separated by interfollicular (IFR) regions may occur via cell-free complement-mediated or conventional dendritic cell (cDC) chemotaxis–mediated mechanisms. Amplification of prions by FDC may be a requirement prior to prion neuroinvasion.

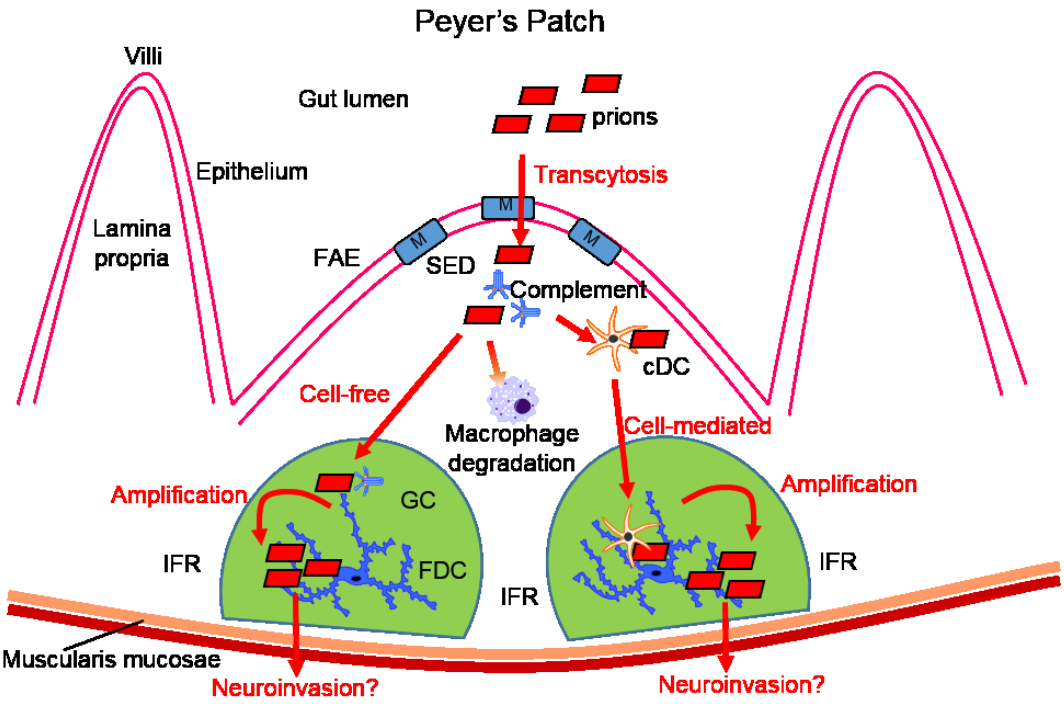

1.3.2 Microfold cells

Microfold cells (M-cells) are specialised for the transport of antigen across the epithelial barrier (Neutra et al., 1996). For this purpose, M-cells are localised to the follicle-associated epithelium (FAE) structures covering Peyer's patches. M-cells are critical for gut immune surveillance and function to sample antigens in the gut lumen and allow rapid presentation to the resident lymphoid cells situated immediately against their basal aspect (Mabbott et al., 2013).

Following oral challenge the prion infectious agent must pass from the gut lumen across the epithelial gut wall to cause infection. Depletion of M-cells prior to oral prion infection blocked the uptake and accumulation of prions upon FDC in Peyer's patches. Furthermore M-cell depletion prior to infection also blocked neuroinvasion and development of disease (Donaldson et al., 2012). Evidence of prion uptake directly into FAE enterocytes has been reported, with localisation to large multivesicular endosomes (Kujala et al., 2011), however in light of the findings following M-cell depletion it appears trans-enterocyte access of prions alone is insufficient to cause infection.

1.3.3 Complement

The complement system is composed of numerous blood borne proteins that are generally synthesized in the liver and circulate as inactive precursors or pro-proteins. Significant amounts of complement components are also synthesized locally by tissue-resident MNP (Colten et al., 1979, Colten et al., 1986), epithelial and stromal cells such as FDC (Schwaeble et al., 1995). The complement system is activated by numerous triggers that establish a proteolytic cleavage cascade, amplifying the response and typically resulting in the formation of the membrane attack complex (MAC). The classical complement activation pathway is triggered mainly by antigen-antibody complexes. Alternative activation pathways exist wherein complement component C3b may bind directly to foreign material (alternative pathway) or where mannose-binding lectin recognizes and binds to sugar moieties (lectin pathway) both associated with pathogenic microorganisms. The MAC functions to form transmembrane pores, thereby punching holes in pathogenic cells with the aim of promoting cell lysis and death (Sarma and Ward, 2010).

Complement has been shown to be activated early during prion pathogenesis by as yet undetermined mechanisms and may constitute the first active response to infection. PrP has been shown to be directly bound by C1q and Factor H (Mitchell et al., 2007) and this binding occurs specifically when PrP is conformationally modified to represent the conversion to the disease-associated isoform (Blanquet-Grossard et al., 2005). Prions are opsonized by complement components including C1q and C3, most likely via the classical complement activation pathway, which may aid in their targeting of the agent to lymphoid follicles (Mabbott, 2004). Mice lacking in complement components C1qa, C2 or C3 revealed deficient peripheral prion pathogenesis following intraperitoneal exposure to limiting amounts of prions (Klein et al., 2001, Mabbott et al., 2001). Whereas mice lacking complement components C3, C4 (Haybaeck et al., 2011) and C5 (Mabbott and Bruce, 2004) reveal unaltered prion pathogenesis. The local production of complement components by MNP has been shown to alter their function (Hartung and Hadding, 1983). C1q enhances the receptor-mediated uptake of disease-associated PrP by cDC (Flores-Langarica et al., 2009). The role of complement during prion pathogenesis is further complicated by the observation that the individual complement components mediating interaction with PrP^{Sc} appear to differ dependent upon the strain of infectious agent (Hasebe et al., 2012). Cell-autonomous and complement-assisted cell-mediated waves of prion trafficking occurs to lymphoid follicles, the relevance of each transport mechanism to disease pathogenesis remains undetermined (Michel et al., 2012). The role of the complement system within the CNS has also been extensively reviewed (Yanamadala and Friedlander, 2010, Veerhuis et al., 2011). There is currently little evidence supporting a role for complement in prion pathogenesis within the CNS as mice lacking C1qa, C2 or C3 revealed unaltered responses to intracerebral prion infection (Klein et al., 2001).

1.3.4 Mononuclear phagocytes

MNP constitute a system of highly phagocytic cells that have a common origin in the bone marrow and circulate or reside in the body tissues in order to sample their environment via uptake of foreign, and self, material (Hume, 2006, Geissmann et al., 2010). The role of MNP in prion pathogenesis have been subject to recent review and are considered diverse, reflecting the diversity of MNP and their functions (Wathne and Mabbott, 2012, Mabbott and Bradford, 2015). Evidence suggests that macrophages, generally identifiable by the markers CD11b, CD68 or the F4/80 antigen, degrade the prion agent (Sassa et al., 2010). The degradative and prion clearance abilities of macrophages appears to be down-regulated when macrophage activation is stimulated by other danger signal molecules (Gilch et al., 2007). Cellular degradation of PrP^{Sc} has been shown to be inhibited by cysteine protease inhibitors (Luhr et al., 2004). Cleavage of PrP^{C} has been shown to protect against infection (Lewis et al., 2009), whilst cleavage of PrP^{Sc} has been shown to modulate prion propagation in a similar fashion (Yadavalli et al., 2004).The uptake of prions likely involves complement, lectin or scavenger receptors while there is evidence that Fc (Klein et al., 2001) (FcγR, RII and RIII deficient mice reveal no deficit following intracerebral or intraperitoneal inoculation), or toll-like receptors (Prinz et al., 2003b) (at least via the Myd88-dependent pathway) have little role in peripheral pathogenesis under steady state conditions. The cellular ability to uptake and degrade prions appears to be independent of PrP^{C} expression (Rybner-Barnier et al., 2006, Paquet et al., 2007).

Figure 1.4 The role of resident MNP during prion uptake in the splenic marginal zone.

Prions arriving at the spleen may gain access to FDC via either cell-free or cell-mediated mechanisms. Following entry through the central arteriole, cell-free complement-bound prions may gain entry to the B-cell follicle and be recognised by FDC. Complement-bound or unbound prions may be phagocytosed by specialised resident macrophages in the marginal zone (MZ) using receptors such as sialoadhesin on marginal zone metallophilic (MZM) macrophages or SIGN-R1 for subsequent processing and transference into the B-cell follicle. Prions arriving on $CXCR5^{+}$ cDC may gain direct access to the B-cell follicle or cDC may collect prions in the marginal zone and subsequently migrate to FDC.

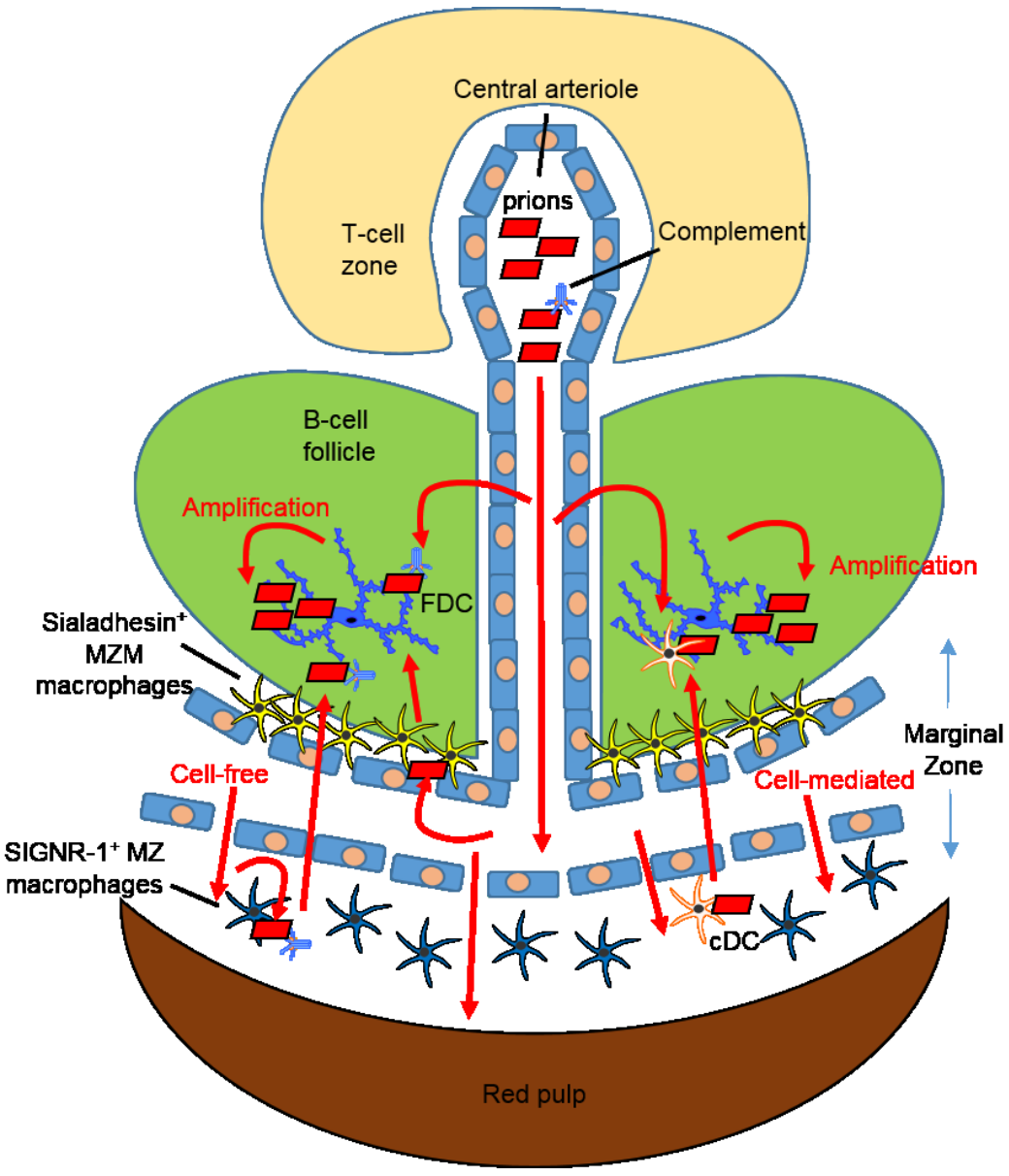

Temporary depletion of $CD11c^+$ cells during experimental prion infection revealed a significant block to agent accumulation in the GALT and a reduction in susceptibility to disease (Raymond et al., 2007). The depletion of $CD11c^+$ cells affects the lymphoid microarchitecture as specific resident MNP cell types are also $CD11c^+$. The specific loss of sialoadhesin (CD169) expressing marginal zone macrophages was observed in the CD11c-depletion model (Raymond et al., 2007, Bradford et al., 2011). In aged mice a similar loss of the specific intercellular adhesion molecule-3-grabbing non-integrin related 1 (SIGN-R1, CD209b) from the splenic marginal zone was also observed concurrent with a reduction in prion susceptibility (Brown and Mabbott, 2014). Both of these receptors are expressed on specific subsets of macrophage populations, resident cells of the splenic marginal zone (see Figure 1.4) which function to regulate the clearance of blood-borne immune-complexes and proteoglycans into the FDC-containing B cell follicles (Aichele et al., 2003, Cinamon et al., 2008).

1.3.5 Conventional Dendritic cells

cDC usually possess stellate morphology and act as the antigen presenting cells (APC) of the innate immune system and possess a potent ability to stimulate naïve T cells, thereby providing the bridge between innate and adaptive immunity. cDC arise from a common DC precursor (Naik et al., 2007, Onai et al., 2007) and are categorised into three major groups; type 1 for CD8α+ and CD103+ DC dependent upon the transcription factor BATF3 for development, type 2 for CD11b+ and CD172a+ DC dependent upon the transcription factor IRF4 for development, and the E2-2 transcription factor-dependent pDC (Guilliams et al., 2014). cDC may degrade some antigen to peptide lengths for presentation on major histocompatibility complex (MHC) class I and II molecules (Trombetta et al., 2003, Delamarre et al., 2005). MHC class I and II bound antigen complexes are recognized by, and stimulate, cytotoxic T lymphocytes (CTL) or T helper cells (T_H) respectively. MHC class I induction and generation of cytotoxic T lymphocytes results in recognition of, and usually destruction of, the activating antigen. MHC class II mediated response however activates T helper cells which have expansive immune-regulatory function, thus tolerising the immune system to the antigen. cDC are also capable of internalizing and retaining complete, or cognate, antigen for later presentation (Bergtold et al., 2005). The migration of cDC is acutely regulated by chemokinesis and the differential expression of their chemokine receptors (Foti et al., 1999, Caux et al., 2000, Cyster, 2000, Randolph, 2001).

Following oral prion infection altered homeostasis in cDC levels has been reported in intestinal Peyer's patches (Dorban et al., 2007). Depletion of $CD11c^+$ cells revealed the ability to completely block or severely impair prion pathogenesis via oral and intraperitoneal routes (Raymond et al., 2007, Cordier-Dirikoc and Chabry, 2008). This depletion strategy was observed to eliminate all MNP types from the intestine, including cDC and macrophages, suggesting that neither transport nor degradation are actively occurring during depletion (Bradford et al., 2011). Depletion models of $CD11c^+$ $CD8^+$ (in this case CD8αα) cDC subsets restricts intraperitoneal but not oral pathogenesis suggesting that alternative cDC subsets may be employed following different infection routes. CD8 knockout mice revealed no alteration of prion pathogenesis, suggesting no direct role for CD8 (Klein et al., 1997). Prion infection of 'plt' mice (deficient in CC chemokine ligand 19 & 21 CCL-19/CCL-21) revealed delayed pathogenesis following transcutaneous infection attributable to impaired CCR7-mediated chemotaxis of cDC (Levavasseur et al., 2007). This paradigm seems more clearly established in the parenteral 'skin scarification' model route of infection. In this model numerous cDC and Langerhans cell (LC, expressing the marker Langerin) MNP types are known to interact with the prion agent but the depletion of non-epidermal $CD11c^+$ cells had the biggest impact upon pathogenesis (Wathne et al., 2012). Extracted cell populations representing cDC and plasmacytoid DC (pDC) have been shown to be capable of transfer of infection *in vivo* (Aucouturier et al., 2001) and *in vitro* (Castro-Seoane et al., 2012) respectively. These findings strongly link these cell types to the retention of intact prion agent and, in the case of cDC, traffic of the agent in the pre-neuroinvasion stage of prion infection.

1.3.6 Chemokines and their receptors

Chemokines are small secreted proteins that induce strong chemotaxis in responsive cells possessing the relevant receptors. Chemokine receptors are G-protein coupled seven-transmembrane structured receptors that mediate two modes of cellular movement, namely chemotaxis and chemokinesis (Rossi and Zlotnik, 2000). Chemotaxis is defined as an organised directional movement response by cells towards chemokines, chemokinesis on the other hand is a random, i.e. non-vectorial, movement caused by a change in migratory or motile behaviour of the cell. Chemokines can be broadly separated into homeostatic or pro-inflammatory types.

Homeostatic chemokines and chemokine receptors play an important part in both the development of lymphoid structures and in regulating the entry and localisation of lymphocytes within mature lymphoid organs (Cyster, 1999, Ansel et al., 2000, Ansel and Cyster, 2001, Andrian, 2003, Campbell et al., 2003, Cupedo and Mebius, 2003, Ohl et al., 2003). The expression of the homeostatic chemokine receptor CCR6 by immature cDC facilitates their migration to environmental contact sites expressing its ligand CCL20, such as the FAE (Cook et al., 2000). Pro-inflammatory chemokines function to activate and mobilise previously localised cells in order to create an immune response to infection or other insult. During maturation and following antigen capture, cDC down regulate CCR6 and upregulate CCR7 expression (Sallusto et al., 1998). Mature cDC migrate towards immune priming sites in secondary lymphoid organs, mediated by CCR7 recognising chemokines CCL19 and CCL21 (Dieu et al., 1998) expressed by stromal cells particularly in the high endothelial venule (HEV). cDC have also been reported presenting antigen directly to B cells (Wykes et al., 1998) and do so by trafficking to the B cell follicle using the chemokine receptor CXCR5 (Saeki et al., 2000, Yu et al., 2002). Indeed a specific subset of cDC, identifiable by their ability to bind a specific fusion protein, have been shown to preferentially traffic to B cell regions (Berney et al., 1999). Furthermore, modification of bone-marrow derived DC to express CXCR5 has been shown to allow traffic to B cell regions and may also alter subsequent antigen-specific immune responses generated (Wu et al., 2001).

1.3.7 Follicular Dendritic cells

FDC are specialised stromal cells which reside within lymphoid organ germinal centres and function to sequester antigen in the form of immune-complexes (Chen et al., 1978). FDC are generated from ubiquitous perivascular precursor identified by their expression of platelet-derived growth factor receptor β (Krautler et al., 2012). FDC status is maintained by lymphotoxin signalling from both hematopoietic and stromal components. Removal of lymphotoxin alpha (LTα) signalling from B cells results in a failure of FDCs to develop (Fu et al., 1997, Gonzalez et al., 1998). FDCs also rely on stromal lymphotoxin beta receptor (LTβR) expression and B cell derived lymphotoxin beta (LTβ) and tumour necrosis factor (TNF) for maturation and maintenance (Endres et al., 1999). FDC capture antigens in the form of immune-complexes via the complement receptors expressed upon their surface including complement receptor 1 (CR1/CD35), indeed originally the FDC-specific marker FDC-M2 was used to identify these cells has been shown to be captured complement component 4 (C4)

(Taylor et al., 2002). FDC contribute to the regulation of humoral immune responses, including organising the B cell follicle via expression of the chemokine CXCL13 (Vermi et al., 2008, Wang et al., 2011) and inducing the germinal centre reaction by expression of B-cell activating factor (BAFF), Interleukin-6 (IL-6) and Complement 4b binding protein (C4bBP) (El Shikh and Pitzalis, 2012). FDC function as dynamic antigen libraries and are essential for the production of IgM, Ig class-switching and high-affinity IgG antibodies (Aydar et al., 2005), late signals promoting somatic hypermutation in B cells (Wu et al., 2008) and the development of B cell memory (Heesters et al., 2013, Heesters et al., 2014). Secreted protein (FDC-SP) from FDC has also been shown critical to the regulation of IgA production (Hou et al., 2014). FDC allow lymph-node resident cDC to continually sample antigen from them for presentation to $CD8^+$ T cells (McCloskey et al., 2011) as well as allowing acquisition of antigen–antibody immune complexes to cognate B cells for further processing and presentation to follicular helper T cells (T_{FH}) (Suzuki et al., 2009). FDC also secrete immune-complex laden iccosomes for either B cell uptake or degradation by tingible body macrophages (Szakal et al., 1988).

Following prion infection, PrP^{Sc} is observed accumulating upon FDCs within Peyer's Patches and draining lymph nodes nearest the infection site and later in the spleen (Brown et al., 1999, Beekes and McBride, 2000). This lymphotropic phase of prion pathogenesis is usually dependent upon FDC in secondary lymphoid organs (Kitamoto et al., 1991, Klein et al., 1998, Brown et al., 1999, Zabel et al., 2007). This process is dependent upon the expression of PrP^C by FDC (McCulloch et al., 2011) which is expressed at high levels (Mabbott et al., 2011). The neuroinvasion of prions into the PNS from FDC is postulated to occur due to replication of prions upon FDC above a certain threshold level (McBride et al., 1992, Mabbott et al., 2003, Prinz et al., 2003c, Glaysher and Mabbott, 2007). One of the physical limitations to FDC-PNS transition of prions may be due to the distance between FDC and peripheral nerve endings, as shortening this distance accelerates prion pathogenesis (Prinz et al., 2003a, von Poser-Klein et al., 2008). A profound effect on the susceptibility to prion disease is revealed either through loss of B cells alone (Klein et al., 1997) or B and T cells, for example in severe combined immunodeficiency (SCID) mice (Lasmezas et al., 1996, Taylor et al., 1996). This effect can be rectified by replenishing the lymphocyte population, by bone marrow transplantation for example (Fraser et al., 1996). Notably the lack of PrP expression by B cells has no effect on prion disease, suggesting that B cell impact upon prion pathogenesis occurs indirectly via it effect upon FDC maturation state (Klein et al., 1998). Similarly impairment of the maturation of FDC by blockade of the lymphotoxin signalling system (Mabbott et al., 2000, Montrasio et

al., 2000, Prinz et al., 2002, Mabbott et al., 2003) also impacts significantly on prion disease. The maturation state and regression cycle of FDCs and their ability to trap immune-complexes appears also to be adversely effected during prion infection (McGovern et al., 2009). The potential acquisition of prions by FDC may occur through either cell-free complement-mediated mechanisms and/or by cell mediated antigen presentation from prion-loaded $CXCR5^{+}$ cDC.

1.3.8 Microglia

Microglia are specialised MNP that reside within the CNS and mediate innate immune responses. Microglial development is dependent upon signalling via the CSF1-R (Erblich et al., 2011), however microglial population of the CNS appears to require both CSF-1R ligands; interleukin-34 (IL-34) (Wang et al., 2012) and CSF-1 (Kondo and Duncan, 2009). Microglia activated by amyloidogenic peptides including $PrP^{106-126}$ also reveal enhanced survival and proliferative responses to CSF-1 (Hamilton et al., 2002). Following peripheral prion infection the microglia show signs of activation after neurons and astrocytes have responded. These findings suggest that microglia do not respond directly to presence of PrP^{Sc} *per se* but may require priming by other CNS cell types. Following priming the microglial cells undergo chemotaxis to the site of insult (Marella and Chabry, 2004), impairment of this chemotaxis by knockout of CXCR3 revealed altered central prion pathogenesis (Riemer et al., 2008). Once activated the microglial population expands and has been shown to upregulate various markers including Trem2, SiglecF, CD200R, and Fcγ receptors in a non-classical immune-response (Lunnon et al., 2011). In fact many of the CNS gene expression profiling studies focused on prion infected CNS have repeatedly identified genes strongly associated with MNP activation (Bradford and Mabbott, 2012). Together these data suggest that MNP constitute the most clinically relevant target innate immune cell population both within and without the CNS during prion pathogenesis.

1.4 Aims

The main aims of this thesis are to examine the role of mononuclear phagocytes on peripheral prion pathogenesis. Previous studies have shown that $CD11c^+$ cells can either carry (Aucouturier et al., 2001) or degrade (Luhr et al., 2002, Luhr et al., 2004) infectious prions, and deletion of $CD11c^+$ cells *in vivo* critically affects prion uptake and transport from the infection site to FDC. How this uptake, processing and transport occur and through which receptors and signal transduction mechanisms prions are recognised by MNP is unknown. Understanding how prions are recognised and processed by MNP is critical to our understanding of prion pathogenesis and potentially the basis to natural susceptibility or resistance to prion infection. The hypothesis that CD11c is a valid marker for cDC is investigated Chapter 3 using cell fate-mapping in CD11c and CSF1-R transgenic mouse models, validating the use of CD11c-specific transgenic mouse models later in this thesis. A novel $CXCR5^{fl}$ conditional transgenic mouse model is generated and characterised in which expression of the chemokine receptor CXCR5 can be conditionally ablated. Furthermore the use of a CD11c-mediated Cre model allows the investigation of the effects of removal of CXCR5 from $CD11c^+$ cells in Chapter 4. The hypothesis that $CXCR5^+$ $CD11c^+$ cells transport prions to FDC is tested in Chapter 5 by investigating oral prion infection in CD11cCre:$CXCR5^{fl}$ mice. The hypothesis that $CXCR5^+$ $CD11c^+$ cells are critical to the formation of protective helper T cell type-2 (T_H2) responses is tested by infection of CD11cCre:$CXCR5^{fl}$ mice with a high dose of the gastrointestinal endoparasite *Trichuris muris* in Chapter 6. The hypotheses that the uptake of cell-free prions is mediated by sialoadhesin is tested in Chapters 7 via investigation of intraperitoneal prion infection in sialoadhesin-deficient mice. The hypothesis that the uptake of cell-free prions is mediated by SIGN-R1 is tested in Chapter 8 via antibody-mediated depletion of SIGN-R1 prior to intravenous prion infection. For all prion infections the aim was to determine if the alteration to MNP had effects on the trafficking of prions to FDC, thereby altering either susceptibility or disease incubation period.

Chapter 2. Materials and methods

2.1 Transgenic mouse Lines

2.1.1 B6N.Cg-Tg(CXCR5)^{tm1Edin} (CXCR5^{fl})

Transgenic mouse line B6N.Cg-Tg(CXCR5)^{tm1Edin} hereafter referred to as CXCR5^{fl} were generated during this thesis. These mice possess unidirectional LoxP sequences surrounding the CXCR5 gene CDS in Exon 2 such that they express CXCR5 normally. Following expression of Cre, recombination of the CXCR5^{fl} gene removes the CDS for the major functional portion of the CXCR5 gene.

2.1.2 B6.Cg-Tg(Itgax-cre)1-1Reiz/J (CD11cCre)

Transgenic mouse line B6.Cg-Tg(Itgax-cre)1-1Reiz/J hereafter referred to as CD11cCre were used in this study. These mice express Cre recombinase under control of the mouse integrin alpha X (CD11c) promoter (Caton et al., 2007).

2.1.3 B6;129S4-Gt(ROSA)26Sor^{tm1Sho} (ROSA26LacZ)

Transgenic mouse line B6;129S4-Gt(ROSA)26Sor^{tm1Sho} hereafter referred to as ROSA26LacZ were used in this study. These mice contain the β-galactosidase neomycin phosphotransferase fusion gene (β geo). Expression of Cre recombinase removes a *loxP* flanked STOP sequence within this construct and the resulting cells express β-galactosidase enzyme which is utilised as a reporter for Cre recombinase activity (Mao et al., 1999).

2.1.4 B6.129(Cg)-Gt(ROSA)26Sor$^{tm4(ACTB-tdTomato,-EGFP)Luo}$/J (mTmG)

Transgenic mouse line B6.129(Cg)-Gt(ROSA)26Sor$^{tm4(ACTB-tdTomato,-EGFP)Luo}$/J hereafter referred to as mTmG were used in this study. These mice possess loxP sites on either side of a membrane-targeted tdTomato (mT) cassette and express strong red fluorescence in all tissues and cell types examined. Tail or whole body epifluorescence is sufficient to identify mTmG homozygotes. When bred to Cre recombinase expressing mice, the resulting offspring have the mT cassette deleted in the Cre expressing tissue(s), allowing expression of the membrane-targeted EGFP (mG) cassette located just downstream.

2.1.5 B6.FVB-Tg(Itgax-DTR/EGFP)57Lan/J (CD11cDTR)

Transgenic mouse line B6.FVB-Tg(Itgax-DTR/EGFP)57Lan/J hereafter referred to as CD11cDTR were used in this study. These mice express the simian diphtheria toxin receptor (DTR) under control of the mouse integrin alpha X (CD11c) promoter. Application of diptheria toxin results in temporary deletion of CD11c-expressing cells.

2.1.6 B6N.Cg-Tg(Csf1r-EGFP)1Hume/J (*Csf1r*-eGFP)

Transgenic mouse line containing the *Csf1r*-eGFP transgene were used in this study. These *Csf1r*-eGFP transgenic mice express the eGFP, enhanced green fluorescent protein, under the control of the mouse *Csf1r*, colony stimulating factor 1 receptor, promoter. Transgene expression (eGFP positive cells) mimics endogenous gene expression patterns.

2.1.7 B6.129SV-Tg (Siglec1)^{tm1Croc} (sialoadhesin-deficient)

Transgenic mouse line B6.129SV-Tg (Siglec1)^{tm1Croc} hereafter referred to as sialoadhesin-deficient mice were used in this study. In sialoadhesin-deficient mice, the Siglec1 (Sialoadhesin) gene was subjected to a targeted null/knockout by insertion of a neomycin resistance gene expression cassette into Exon 3.

2.1.8 Tg(Prnp)a20Cwe (Tga20)

Transgenic mouse line Tg(Prnp)a20Cwe hereafter referred to as Tga20 were used in this study. In Tga20 an insertion of a transgene encodes a wild-type mouse prion protein. Expression studies demonstrated that this line expresses Prnp transcripts in the brain 6- to 7-fold compared to wild-type.

2.2 Compound transgenic mouse lines

All compound transgenic mice were retained on a C57BL/6 genetic background.

2.2.1 *Csf1r*-eGFP:CD11cDTR

Heterozygous *Csf1r*-eGFP mice (Sasmono et al., 2003) were crossbred with homozygous CD11cDTR mice (Jung et al., 2002) to produce F1 generation offspring termed *Csf1r*-

eGFP:CD11cDTR compound transgenic mice. These mice were used in this study to determine the effect of deleting CD11c-expressing cells from the pattern of *Csf1r*-eGFP expression.

2.2.2 CD11cCre:mTmG

Homozygous CD11cCre and mTmG mice were crossbred to produce F1 heterozygous offspring termed CD11cCre:mTmG used in this study to investigate the localisation and activity of CD11cCre expression.

2.2.3 CD11cCre:CXCR5^{fl}

Homozygous CXCR5^{fl} mice were sequentially crossbred with heterozygous CD11Cre mice to generate CD11Cre$^{+/-}$:CXCR5$^{fl/fl}$ final genotype offspring for the investigation of CD11Cre-mediated removal of CXCR5 (i.e. 'dendritic cell' specific CXCR5 knockout).

2.3 In vivo techniques

2.3.1 Diptheria toxin mediated cell depletion

To deplete CD11c-expressing cells CD115-eGFP/CD11c-DTR compound transgenic mice were injected intraperitoneally with 100 ng diphtheria toxin (DTX) or vehicle (5% lactose in phosphate buffer [pH7.4]) as a control. Mice were sacrificed 48 hr post-treatment and tissues harvested for analysis as detailed below.

2.3.2 SIGN-R1 depletion

Transient depletion of SIGN-R1 was induced by intravenous injection of 100 µg of 22D1 antibody or Hamster Ig isotype as a control, as reported previously (Kang et al., 2004).

2.3.3 Passive immunizations

To assess antigen trapping in vivo, mice were passively immunized by intravenous injection with 100 µl pre-formed peroxidase–anti peroxidase (PAP) immune complexes (Sigma, St Louis, MO) as described (McCulloch et al., 2011) or 70 000 molecular weight dextran-FITC

(Sigma) as described previously (Kang et al., 2003). PrP^{Sc} was enriched from the brains of mice terminally affected with ME7 scrapie prions and fluorescently labelled (Alexa-PrP^{Sc}) as described previously (Gousset et al., 2009, Wathne et al., 2012).

2.3.4 Prion infection

For intracerebral prion challenge experiments each animal was inoculated with 20 µl of 1 % homogenate, either terminal ME7 scrapie-infected brain or spleen for bioassay, directly into the right cerebral hemisphere (mid temporal cortex) via a 26 gauge hypodermic needle sheathed to restrict the needle point penetration to a maximum of 2 mm and a 1 ml syringe. Inoculation was performed whilst animals were under light halothane-induced anaesthesia, recovery from inoculation and anaesthesia was closely monitored.

For oral prion challenge experiments each animal was removed from their standard housing on the morning of the inoculation date and housed singly without food. Individually housed animals were given one standard food pellet dosed with 50 µl 1 % terminal ME7 scrapie-infected brain homogenate and left until pellet was completely consumed mice were returned to their original (grouped) housing. Water was provided ad libitum throughout.

For intravenous prion challenge experiments animal was inoculated with 20 µl of 0.1 % terminal ME7 scrapie-infected brain homogenate into the tail vein via a 26 gauge hypodermic needle.

2.3.5 *Trichuris muris* infection

For high dose *Trichuris muris* infection 250 embryonated eggs in PBS were introduced by oral gavage. Adult and juvenile worms were counted by hand using a dissecting microscope (Leica).

2.3.6 Chicago Sky Blue 6B

For the investigation of lymphoid tissues, mice were injected intraperitoneally with 0.3ml of 1% Chicago Sky Blue 6B in sterile PBS. Mice were sacrificed 1 week post treatment for gross anatomical identification of lymphoid tissues.

2.3.7 Ethical Statement

All animal studies and breeding were performed via standard methods and conducted under the provisions of the UK Animals Scientific Procedures Act 1986 and approved by the Institute's Ethical Review Committee.

2.4 DNA extraction

2.4.1 Murine genomic DNA extraction

Genomic DNA was extracted from ear biopsy samples using the Qiagen DNeasy blood and tissue kit (Qiagen #69056). Biopsy samples were stored at -20°C prior to DNA extraction. Tissues were lysed in 180 µl ATL buffer (Qiagen) with 20µl proteinase K (Qiagen) for 8 hours minimum at 55°C on an orbital shaker. Lysed samples were spun at 16,100 x *g* in a 5145R centrifuge (eppendorf) to pellet debris and then individually decanted into sterile 1.5 ml flip-top microtubes containing 400 µl of a 1:1 mix of buffer AL (Qiagen) and 99.9% Ethanol. Samples were mixed via vortex at full speed for 15 seconds and decanted onto Qiagen columns. Columns were centrifuged at 5,900 x *g* for 1 minute and flow through discarded. Columns were washed via centrifugation at 5,900 x *g* for 1 minute following addition of 500 µl of AW1 buffer (Qiagen), then at 16,100 x *g* for 3 minutes after addition of 500 µl of AW2 buffer (Qiagen), discarding flow through after each centrifugation. Buffers AW1 and AW2 were supplemented with the relevant volume of 99% ethanol as per manufacturer's instructions prior to use. DNA was recovered from the column by addition of 200 µl (tail) or 100 µl (ear) of AE buffer (Qiagen) incubated for 1 minute at ambient temperature and centrifugation into a sterile 1.5 ml flip-top eppendorf at 5,900 x *g* for 1 minute.

2.4.2 Phenol/chloroform DNA extraction

Following prion infection, mouse genotypes were re-confirmed before grouping and statistical analyses were performed. To purify genomic DNA away from potential infectious prion contamination, DNA was extracted from mouse tail-tip via overnight digestion at 37 °C in: 0.02 mg/ml PK, 0.5 M sodium acetate, 1 % v/v sodium dodecyl sulphate (SDS), 0.05 mM tris-HCl (pH 8.0) and 0.01 mM ethylenediaminetetraacetic acid (EDTA), following digestion samples are mixed with 1:1 phenol / chloroform (pH 8.0) and phase separated via centrifugation at 16,000 g for 1 minute. Following aqueous phase extraction, DNA is

precipitated via addition of 3 mM sodium acetate and 100 % isopropanol and collected via centrifugation at 16,000 g for 1 minute. DNA pellets were washed in 70 % ethanol and air dried before suspension in 100 µl AE Buffer (Qiagen) / mm tail for subsequent genotype analysis. Samples from TSE challenge experiments were treated as Hazard Category 2 material. All steps prior to phenol treatment including aqueous phase extraction were performed in a Category 2 biological safety cabinet except for the overnight 37 °C incubation.

2.5 Polymerase chain reaction

2.5.1 Genotyping via PCR

Genotyping of mouse genomic DNA samples to identify the presence or absence of various transgenes, or detection of gene expression from copy DNA (cDNA), was performed to identify the presence or absence of various transgenes via the polymerase chain reaction (PCR) method. Individual reactions consisted of 40.3 µl ultra-pure water (Millipore, MilliQ), 5 µl 10x PCR buffer (Invitrogen), 1.5 µl 50 mM magnesium chloride ($MgCl_2$) (Invitrogen), 1 µl 10 mM deoxynucleotide triphosphate (dNTP) mixture (Promega #U1240), 0.5 µl of each oligonucleotide primer as detailed below, 0.2 µL Recombinant Taq Polymerase (Invitrogen #10342-020) and 1 µl DNA sample. Oligonucleotides were obtained lyophilized from eurofins MWG operon, reconstituted for use at 100 pmol / µl as per synthesis details provided using ultra-pure water and stored frozen at -20°C prior to use. For multiple samples master mixes were calculated and produced lacking addition of DNA, prior to aliquoting at 49 µl into a 0.5 ml flip-top PCR tube for each sample. Reactions were mixed via vortex following addition of each genomic DNA sample, DNA control or water control. PCR reactions were run on either a T3 or T3000 thermocycler (Biometra) under the following conditions; 94°C for 3 minutes, then 30 cycles of 94°C for 30 seconds, 60°C for 30 seconds and 72°C for 45 seconds unless stated otherwise. At the end of the cycle samples were kept at 72°C for 10 minutes before cooling to 4°C for storage. Heated lids were kept at constant 99°C during the whole program.

Oligonucleotide primers for CXCR5 and CXCL13 were designed in Primer3 v0.4.0 (http://frodo.wi.mit.edu/primer3/) using the NCBI reference sequences NM_007551 and NM_018866.2 respectively and setting the product length range from 190 to 210 base pairs.

Table 2.1 Oligonucleotide primer sequences used in DNA polymerase chain reactions.

PCR	Product size (bp)	Primer name	Oligonucleotide sequence
CD11cCre	wt no product CD11cCre 313	CD11c-Cre.1	ACTTGGCAGCTGTCTCCAAG
		CD11c-Cre.2	GCGAACATCTTCAGGTTCTG
CD11cDTR	wt no product CD11cDTR 600	DTR1	GCCACCATGAAGCTGCTGCCG
		DTR2	TCAGTGGGAATTAGTCATGCC
Cre Recombinase	wt no product Cre 786	CreScreen1	CGAGTGATGAGGTTCGCAAGAACC
		CreScreen3	GCTAAGTGCCTTCTCTACACCTGC
Cre (RT)	wt no product Cre 196	Cre-529	CTGATTTCGACCAGGTTCGT
		Cre-725	GCTAACCAGCGTTTTCGTTC
CXCR5	203	CXCR5-307	GTCTTCATCCTGCCTTTTGC
		CXCR5-509	ATGTGGATGGAGAGGAGTCG
***Csf1r*-eGFP**	753	cFMS-GFP1	GAGGAGGATGGATGGTCTCA
		cFMS-GFP2	GAACTTCAGGGTCAGCTTGC
CXCR5^{fl} 5' loxP	wt 214 fl 375 recombined 292	CXCR5Fl 5' For	AGGAGGCCATTTCCTCAGTT
		CXCR5Fl 5' Rev	GGCTTAGGGATTGCAGTCAG
		CXCR5Fl 3' Rev	TTCCTTAGAGCCTGGAAAAGG
CXCR5 ^{fl} 3' loxP	wt 170 fl 250	CXCR5Fl 3' For	TCAGCCCCATGTTACTGGAT
		CXCR5Fl 3' Rev	TTCCTTAGAGCCTGGAAAAGG
FLPe*	~750	FLP-For2	CACTGATATTGTAAGTAGTTTGC
		FLP-Rev2	CTAGTGCGAAGTAGTGATCAGG
ROSA26-LacZ	~300	LACZ1ROSA26	TACCACAGCGGATGGTTCGG
		LACZ2ROSA26	GTGGTGGTTATGCCGATCGC
Sialoadhesin-deficient	wt 471 KO 234	Neo	CGTTGGCTACCCGTGATATTGC
		SND1F3	CACCACGGTCACTGTGACAA
		SND2R2	GGCCATATGTAGGGTCGTCT
T cell receptor Delta (TCRD)	210	oIMR0015(WTF)	CAAATGTTGCTTGTCTGGTG
		oIMR0016(WTR)	GTCAGTCGAGTGCACAGTTT

2.5.2 CD11cCre PCR

To detect the CD11cCre transgene a primer pair spanning the *Itgax* promoter and Cre coding sequence were used to amplify a 313bp product, not detectable in wild type mice

2.5.3 CD11cDTR PCR

The CD11cDTR transgene was detected using the method as described previously (Jung et al., 2002). Briefly, a ~600bp product corresponding to the DTR was amplified in mice carrying the transgene.

2.5.4 Cre recombinase PCR

For the generic detection of Cre recombinase a primer pair specific to the Cre coding sequence were used to amplify a 786bp product, not detectable in wild type mice.

2.5.5 Cre recombinase RT-PCR

To confirm the expression of Cre recombinase a 196bp product corresponding to a portion of the Cre coding sequences was amplified from cDNA using specific primers. No product was observed in wild type mice.

2.5.6 CXCR5 PCR

To confirm the presence of CXCR5, a 203bp product corresponding to a portion of the coding sequence contained within exon 2 was amplified using specific primers. No product was observed in wild type mice.

2.5.7 *Csf1r*-eGFP PCR

A 753 bp sequence spanning the *c-fms* promoter and eGFP sequences was amplified to genotype the MacGreen transgenic element from mouse genomic DNA as described (Bradford et al., 2011). A 210bp T cell receptor delta (TCRD) sequence was amplified in all samples as an internal control for each PCR reaction.

2.5.8 CXCR5$^{fl/R}$ PCR

For the routine genotyping of conditional CXCR5 expressing mice a 375bp fragment was amplified spanning the *loxP* sequence inserted 5' to CXCR5 exon 2. In wild type mice a shorter 214bp fragment was amplified lacking the *loxP* sequence. Recombination of the conditional CXCR5 allele was confirmed by inclusion of the 3' *loxP* reverse primer yielding a 292bp fragment spanning the genomic region only in the absence of CXCR5 exon2.

2.5.9 CXCR5^{fl} 3'*loxP* PCR

The presence of the CXCR5 3' *loxP* sequence was confirmed by amplification of a 250bp fragment or a 170bp fragment from wild type mice.

2.5.10 FLPe PCR

During the establishment of the CXCR5^{fl} transgenic mouse line the presence of FLPe transgene was confirmed by amplification of a ~750bp fragment, not detectable in wild type mice.

2.5.11 ROSA26LacZ PCR

To detect the Rosa26LacZ transgene, a primer pair specific to a portion of the βgeo element were used to amplify ~300bp product, not detectable in wild type mice

2.5.12 Sialoadhesin-deficient PCR

A 234 bp sequence spanning the Sialoadhesin gene and targeted Neo insert was amplified to genotype the sialoadhesin-deficient transgenic element from mouse genomic DNA as described (Oetke et al., 2006). In the absence of the insert a 471 bp sialoadhesin sequence was amplified spanning the insertion point in wild type mice.

2.5.13 T cell receptor delta control PCR

To confirm the presence of viable genomic DNA and successful PCR, in particular in any of the above PCR reactions that return no product in wild type mice, a 210bp fragment of the T cell receptor delta gene was amplified to act as an internal control.

2.6 Agarose gel electrophoresis

PCR reaction products were mixed 10:1 via vortex with a loading buffer consisting of Xylene cyanol FF and Bromophenol blue at 25 nM each in 10% glucose solution. Reactions were pipette loaded onto and separated by agarose gel in 1% Agarose MP (Roche #11388991001) using a Tris-Borate-EDTA (TBE) buffer. Agarose gels were run in Horizon gel tanks (Biometra) at 125 mV for 1 to 3 hours dependent upon the expected product size. 1Kb DNA ladder (Invitrogen) was run alongside samples for the purpose of sizing fragment bands. Gels were transferred to a UV transilluminator and imaged via an Oncor Appligene Baby Imager.

2.7 Gene expression analysis

2.7.1 RNA extraction

Tissues were homogenised in RNA-BEE RNA Isolation reagent (AMS Biotechnology), small tissues such as lymph nodes were disrupted using Lysing Matrix D tubes and FastPrep (MP Biomedicals). After lysis samples were centrifuged at 12000g for 10 minutes at 4°C and supernatants removed, discarding pellet. Supernatants were mixed vigorously with Chloroform and incubated for 10 minutes on ice. Samples were centrifuged at 12000g for 15 minutes at 4°C for phase separation. Upper, aqueous phase were removed and mixed 1:1 with 70% ethanol. Samples were transferred to RNeasy (Qiagen) spin columns and the remaining washing and elution steps were performed as per the manufacturer's instructions using the kit reagents.

2.7.2 cDNA synthesis

Total cDNA synthesis or mRNA cDNA synthesis were performed using Superscript III first strand cDNA synthesis kit (Invitrogen), with either random hexamer or polyA oligomers respectively, as per the manufacturer's instructions. PCR with cDNA referred to as reverse transcriptase PCR (RTPCR) were performed as 2.3.1. see table 2.1 for oligonucleotide sequences used.

2.7.3 Real-time quantitative PCR (RT-qPCR)

Real-time quantitative PCR were performed using Faststart Universal Sybr Green Rox Master mix (Roche) on an MX3000P (Stratagene). Briefly 20 µl reactions were setup in 96 well plates using 10 µl Faststart, 7 µl upH_2O, 1 µl premixed 1:1 and pre-diluted to 30 µM oligonucleotide primers and 2 µl cDNA, reactions were mixed by vortex and centrifugation. All samples/plates included control primer set for the ribosomal protein L19 (*Rpl19*) gene, which is normally expressed ubiquitously and equally in almost all cell types throughout the life of all individuals (Dawoud Al-Bader and Ali Al-Sarraf, 2005, Chari et al., 2010, Zhou et al., 2010, Facci et al., 2011), used in subsequent analysis for relative gene expression changes using the ΔΔCT calculation method. RT-qPCR primer sets for genes of interest were retrieved from qPrimerDepot https://mouseprimerdepot.nci.nih.gov/ as follows.

Gene Name: ***Acvr1*** RefSeq ID: NM_007394 Chromosome: chr2 Strand: -
Transcription: 58469527-58399808 Number of introns: 9
Right primer sequence: **GAGGCCCTCACACACACAC**
Position: 202 Length: 19 GC%: 63.158 Tm: 60.157
Left primer sequence: **TGCTAATGATGATGGCTTTCC**
Position: 111 Length: 21 GC%: 42.857 Tm: 60.052
cDNA amplicon size:92 Estimated genomic amplicon size:20647

Gene Name: ***Blr1*** RefSeq ID: NM_007551 Chromosome: chr9 Strand: -
Transcription: 44630396-44615762 Number of introns: 1
Right primer sequence: **TCCTGTAGGGGAATCTCCGT**
Position: 149 Length: 20 GC%: 55 Tm: 60.842
Left primer sequence: **ACTAACCCTGGACATGGGC**
Position: 54 Length: 19 GC%: 57.895 Tm: 59.794
cDNA amplicon size:96 Estimated genomic amplicon size:12116

Gene Name: ***Ccl5*** RefSeq ID: NM_013653 Chromosome: chr11 Strand: -
Transcription: 83132151-83127440 Number of introns: 3
Right primer sequence: **CCACTTCTTCTCTGGGTTGG**
Position: 212 Length: 20 GC%: 55 Tm: 59.691
Left primer sequence: **GTGCCCACGTCAAGGAGTAT**
Position: 103 Length: 20 GC%: 55 Tm: 59.997
cDNA amplicon size:110 Estimated genomic amplicon size:3201

Gene Name: ***Ccl11*** RefSeq ID: NM_011330 Chromosome: chr11 Strand: +
Transcription: 81671253-81676283 Number of introns: 2
Right primer sequence: **TAAAGCAGCAGGAAGTTGGG**
Position: 149 Length: 20 GC%: 50 Tm: 60.378
Left primer sequence: **TCCACAGCGCTTCTATTCCT**
Position: 56 Length: 20 GC%: 50 Tm: 59.978
cDNA amplicon size:94 Estimated genomic amplicon size:3730

Gene Name: ***Ccr1*** RefSeq ID: NM_009912 Chromosome: chr9 Strand: -
Transcription: 123983607-123977523 Number of introns: 1
Right primer sequence: **TGCTGAGGAACTGGTCAGG**
Position: 213 Length: 19 GC%: 57.895 Tm: 59.963
Left primer sequence: **AGGCCCAGAAACAAAGTCTG**
Position: 105 Length: 20 GC%: 50 Tm: 59.328
cDNA amplicon size:109 Estimated genomic amplicon size:3488

Gene Name: ***Ccr2*** RefSeq ID: NM_009915 Chromosome: chr9 Strand: +
Transcription: 124117691-124124059 Number of introns: 3
Right primer sequence: **AGCACATGTGGTGAATCCAA**
Position: 90 Length: 20 GC%: 45 Tm: 59.967
Left primer sequence: **TGCCATCATAAAGGAGCCA**
Position: 0 Length: 19 GC%: 47.368 Tm: 60.166
cDNA amplicon size:91 Estimated genomic amplicon size:1838

Gene Name: ***Ccr3*** RefSeq ID: NM_009914 Chromosome: chr9 Strand: +
Transcription: 124037502-124046343 Number of introns: 1
Right primer sequence: **CATAGGGTGTGGTCTCAAAGC**
Position: 145 Length: 21 GC%: 52.381 Tm: 59.607
Left primer sequence: **AAAGGACTTAGCAAAATTCACCA**
Position: 50 Length: 23 GC%: 34.783 Tm: 59.215
cDNA amplicon size:96 Estimated genomic amplicon size:6542

Gene Name: ***Ccr4*** RefSeq ID: NM_009916 Chromosome: chr9 Strand: -

Transcription: 114423978-114419056 Number of introns: 1
Right primer sequence: **GGGTACCAGCAGGAGAAGC**
Position: 114 Length: 19 GC%: 63.158 Tm: 59.818
Left primer sequence: C**GACGGCATTGCTTCATAG**
Position: 24 Length: 19 GC%: 52.632 Tm: 60.373
cDNA amplicon size:91 Estimated genomic amplicon size:3535

Gene Name: ***Ccr5*** RefSeq ID: NM_009917 Chromosome: chr9 Strand: +
Transcription: 124137439-124143048 Number of introns: 1
Right primer sequence: **GCAGGGTGCTGACATACCAT**
Position: 139 Length: 20 GC%: 55 Tm: 60.956
Left primer sequence: **ATCCGTTCCCCCTACAAGAG**
Position: 37 Length: 20 GC%: 55 Tm: 60.319
cDNA amplicon size:103 Estimated genomic amplicon size:2818

Gene Name: ***Cd4*** RefSeq ID: NM_013488 Chromosome: chr6 Strand: -
Transcription: 125506852-125483335 Number of introns: 9
Right primer sequence: **CAAGCGCCTAAGAGAGATGG**
Position: 198 Length: 20 GC%: 55 Tm: 60.11
Left primer sequence: **CACCTGTGCAAGAAGCAGAG**
Position: 89 Length: 20 GC%: 55 Tm: 59.77
cDNA amplicon size:110 Estimated genomic amplicon size:8496

Gene Name: ***Cd80*** RefSeq ID: NM_009855 Chromosome: chr16 Strand: +
Transcription: 38316215-38353405 Number of introns: 5
Right primer sequence: **GGCAAGGCAGCAATACCTTA**
Position: 162 Length: 20 GC%: 50 Tm: 60.23
Left primer sequence: **CTCTTTGTGCTGCTGATTCG**
Position: 69 Length: 20 GC%: 50 Tm: 59.74
cDNA amplicon size:94 Estimated genomic amplicon size:14702

Gene Name: ***Cxcr4*** RefSeq ID: NM_009911 Chromosome: chr1 Strand: -
Transcription: 128429292-128425228 Number of introns: 1
Right primer sequence: **ACTCACACTGATCGGTTCCA**
Position: 139 Length: 20 GC%: 50 Tm: 59.101
Left primer sequence: **AGGTGCAGGTAGCAGTGACC**
Position: 45 Length: 20 GC%: 60 Tm: 60.329
cDNA amplicon size:95 Estimated genomic amplicon size:2366

Gene Name: ***Ifng*** RefSeq ID: NM_008337 Chromosome: chr10 Strand: +
Transcription: 118128981-118133827 Number of introns: 3
Right primer sequence: **TGAGCTCATTGAATGCTTGG**
Position: 193 Length: 20 GC%: 45 Tm: 59.948
Left primer sequence: **ACAGCAAGGCGAAAAAGGAT**
Position: 104 Length: 20 GC%: 45 Tm: 61.117
cDNA amplicon size:90 Estimated genomic amplicon size:2448

Gene Name: ***Il1b***
Right primer sequence: **CTGAACTCAACTGTGAAATGCCA**
Left primer sequence: **AAAGGTTTGGAAGCAGCCCT**

Gene Name: ***Il2*** RefSeq ID: NM_008366 Chromosome: chr3 Strand: -
Transcription: 36927692-36922460 Number of introns: 3
Right primer sequence: **CGCAGAGGTCCAAGTTCATC**
Position: 202 Length: 20 GC%: 55 Tm: 60.801
Left primer sequence: **AACTCCCCAGGATGCTCAC**
Position: 106 Length: 19 GC%: 57.895 Tm: 60.064

cDNA amplicon size:97 Estimated genomic amplicon size:2519

Gene Name: ***Il4*** RefSeq ID: NM_021283 Chromosome: chr11 Strand: -
Transcription: 53258404-53252206 Number of introns: 3
Right primer sequence: **CGAGCTCACTCTCTGTGGTG**
Position: 199 Length: 20 GC%: 60 Tm: 59.757
Left primer sequence: **TGAACGAGGTCACAGGAGAA**
Position: 107 Length: 20 GC%: 50 Tm: 59.388
cDNA amplicon size:93 Estimated genomic amplicon size:4206

Gene Name: ***Il5*** RefSeq ID: NM_010558 Chromosome: chr11 Strand: +
Transcription: 53360532-53364842 Number of introns: 3
Right primer sequence: **CCCACGGACAGTTTGATTCT**
Position: 215 Length: 20 GC%: 50 Tm: 59.966
Left primer sequence: **GCAATGAGACGATGAGGCTT**
Position: 109 Length: 20 GC%: 50 Tm: 60.37
cDNA amplicon size:107 Estimated genomic amplicon size:1976

Gene Name: ***Il6*** RefSeq ID: NM_031168 Chromosome: chr5 Strand: +
Transcription: 28413047-28419859 Number of introns: 4
Right primer sequence: **ACCAGAGGAAATTTTCAATAGGC**
Position: 179 Length: 23 GC%: 39.13 Tm: 59.867
Left primer sequence: **TGATGCACTTGCAGAAAACA**
Position: 71 Length: 20 GC%: 40 Tm: 58.994
cDNA amplicon size:109 Estimated genomic amplicon size:3171

Gene Name: ***Il9*** RefSeq ID: NM_008373 Chromosome: chr13 Strand: -
Transcription: 55585280-55582310 Number of introns: 4
Right primer sequence: **AACAGTCCCTCCCTGTAGCA**
Position: 187 Length: 20 GC%: 55 Tm: 59.721
Left primer sequence: **AAGGATGATCCACCGTCAAA**
Position: 78 Length: 20 GC%: 45 Tm: 60.317
cDNA amplicon size:110 Estimated genomic amplicon size:1296

Gene Name: ***Il10*** RefSeq ID: NM_010548 Chromosome: chr1 Strand: +
Transcription: 130890034-130895158 Number of introns: 4
Right primer sequence: **TGTCAAATTCATTCATGGCCT**
Position: 202 Length: 21 GC%: 38.095 Tm: 60.324
Left primer sequence: **ATCGATTTCTCCCCTGTGAA**
Position: 95 Length: 20 GC%: 45 Tm: 59.483
cDNA amplicon size:108 Estimated genomic amplicon size:1729

Gene Name: ***Il12a*** RefSeq ID: NM_008351 Chromosome: chr3 Strand: +
Transcription: 69032929-69040747 Number of introns: 8
Right primer sequence: **GCTTCTCCCACAGGAGGTTT**
Position: 202 Length: 20 GC%: 55 Tm: 60.628
Left primer sequence: **CTAGACAAGGGCATGCTGGT**
Position: 108 Length: 20 GC%: 55 Tm: 60.277
cDNA amplicon size:95 Estimated genomic amplicon size:2409

Gene Name: ***Il12b*** RefSeq ID: NM_008352 Chromosome: chr11 Strand: +
Transcription: 44039797-44053752 Number of introns: 7
Right primer sequence: **GGAGACACCAGCAAAACGAT**
Position: 205 Length: 20 GC%: 50 Tm: 60.119
Left primer sequence: **GATTCAGACTCCAGGGGACA**
Position: 97 Length: 20 GC%: 55 Tm: 60.048
cDNA amplicon size:109 Estimated genomic amplicon size:3921

Gene Name: ***Il12rb1*** RefSeq ID: NM_008353 Chromosome: chr8 Strand: +
Transcription: 69847655-69860584 Number of introns: 15
Right primer sequence: **TGGATAAACGGGAAATCTGC**
Position: 173 Length: 20 GC%: 45 Tm: 59.901
Left primer sequence: **CAGCCGAGTGATGTACAAGG**
Position: 64 Length: 20 GC%: 55 Tm: 59.314
cDNA amplicon size:110 Estimated genomic amplicon size:2088

Gene Name: ***Il12rb2*** RefSeq ID: NM_008354 Chromosome: chr6 Strand: -
Transcription: 67488911-67404791 Number of introns: 15
Right primer sequence: **CCCTTGCCTCTGATGGATTC**
Position: 175 Length: 20 GC%: 55 Tm: 61.9
Left primer sequence: **GGAAGAGCCTGTTGGGATATT**
Position: 66 Length: 21 GC%: 47.619 Tm: 59.433
cDNA amplicon size:110 Estimated genomic amplicon size:20389

Gene Name: ***Il13*** RefSeq ID: NM_008355 Chromosome: chr11 Strand: -
Transcription: 53274441-53271062 Number of introns: 3
Right primer sequence: **CACACTCCATACCATGCTGC**
Position: 186 Length: 20 GC%: 55 Tm: 60.144
Left primer sequence: **TGTGTCTCTCCCTCTGACCC**
Position: 87 Length: 20 GC%: 60 Tm: 60.243
cDNA amplicon size:100 Estimated genomic amplicon size:1380

Gene Name: ***Il17*** RefSeq ID: NM_010552 Chromosome: chr1 Strand: +
Transcription: 20939781-20943372 Number of introns: 2
Right primer sequence: **TGAGCTTCCCAGATCACAGA**
Position: 198 Length: 20 GC%: 50 Tm: 59.499
Left primer sequence: **TCCAGAAGGCCCTCAGACTA**
Position: 98 Length: 20 GC%: 55 Tm: 59.943
cDNA amplicon size:101 Estimated genomic amplicon size:1414

Gene Name: ***Il17e*** RefSeq ID: NM_080729 Chromosome: chr14 Strand: +
Transcription: 46905385-46908449 Number of introns: 2
Right primer sequence: **GTCTGTAGGCTGACGCAGTG**
Position: 230 Length: 20 GC%: 60 Tm: 59.648
Left primer sequence: **AGCAGGGCCATCTCTCCT**
Position: 121 Length: 18 GC%: 61.111 Tm: 59.903
cDNA amplicon size:110 Estimated genomic amplicon size:1988

Gene Name: ***Il18*** RefSeq ID: NM_008360 Chromosome: chr9 Strand: +
Transcription: 50725961-50742431 Number of introns: 5
Right primer sequence: **TCCTTGAAGTTGACGCAAGA**
Position: 195 Length: 20 GC%: 45 Tm: 59.566
Left primer sequence: **TCCAGCATCAGGACAAAGAA**
Position: 90 Length: 20 GC%: 45 Tm: 59.369
cDNA amplicon size:106 Estimated genomic amplicon size:9847

Gene Name: ***Il27ra*** RefSeq ID: NM_016671 Chromosome: chr8 Strand: -
Transcription: 83309596-83297344 Number of introns: 13
Right primer sequence: **AATATCTCCAGCCCCAAACC**
Position: 206 Length: 20 GC%: 50 Tm: 60.152
Left primer sequence: **TGTGAAACTTCTGGCAAACG**
Position: 108 Length: 20 GC%: 45 Tm: 59.881
cDNA amplicon size:99 Estimated genomic amplicon size:2848

Gene Name: ***Il33***
Right primer sequence: **TCCTTGCTTGGCAGTATCCA**
Left primer sequence: **TGCTCAATGTGTCAACAGACG**

Gene Name: *Itgax* (CD11c)
Right primer sequence: **AAAATCTCCAACCCATGCTG**
Left primer sequence: **CACCACCAGGGTCTTCAAGT**

Gene Name: ***Lta*** RefSeq ID: NM_010735 Chromosome: chr17 Strand: -
Transcription: 33700679-33698658 Number of introns: 3
Right primer sequence: **CACCCTCAAGAGGTGGAGAC**
Position: 194 Length: 20 GC%: 60 Tm: 59.682
Left primer sequence: **TTTCTTGAGCCACAGCCTTT**
Position: 90 Length: 20 GC%: 45 Tm: 59.993
cDNA amplicon size:105 Estimated genomic amplicon size:473

Gene Name: ***Ltb*** RefSeq ID: NM_008518 Chromosome: chr17 Strand: +
Transcription: 33690219-33692000 Number of introns: 2
Right primer sequence: **CTTTTCTGAGCCTGTGCTCC**
Position: 190 Length: 20 GC%: 55 Tm: 60.134
Left primer sequence: **TATCACTGTCCTGGCTGTGC**
Position: 98 Length: 20 GC%: 55 Tm: 59.862
cDNA amplicon size:93 Estimated genomic amplicon size:459

Gene Name: ***Rpl19***
Right primer sequence: **GAAGGTCAAAGGGAATGTGTTCA**
Left primer sequence: CCTTGTCTGCCTTCAGCTTGT
Ref: (Bindels et al., 2012)

Gene Name: ***Tnf*** RefSeq ID: NM_013693 Chromosome: chr17 Strand: -
Transcription: 33697492-33694905 Number of introns: 3
Right primer sequence: **AGGGTCTGGGCCATAGAACT**
Position: 196 Length: 20 GC%: 55 Tm: 59.957
Left primer sequence: **CCACCACGCTCTTCTGTCTAC**
Position: 94 Length: 21 GC%: 57.143 Tm: 59.922
cDNA amplicon size:103 Estimated genomic amplicon size:619

2.8 Cell isolation

2.8.1 Spleen

Spleen was dissected into Hanks' buffered saline solution (HBSS) (Sigma) # cooled on ice. Spleens were transferred into gentleMACS C tube (Miltenyi Biotec #130-093-237) containing 4.9 ml of 10 mM 4-(2-hydroxyethyl)-1-piperazineethanesulfonic acid (HEPES) - sodium hydroxide (NaOH) pH 7.4, 150 mM Sodium Chloride (NaCl), 5 mM potassium chloride (KCl), 1 mM magnesium chloride ($MgCl_2$) and 1.8 mM calcium chloride ($CaCl_2$), hereafter referred to as HEPES buffer and 100 µl Collagenase D (Roche #11088866001) reconstituted to 100 mg / ml to produce a final concentration of 2 mg / ml. Tissue was disrupted using gentleMACS (Miltenyi Biotec) via automated program m_spleen_02, and incubated for 30 minutes at 37°C. DNase I (Roche #10104159001) was added to a final concentration of 100 units / ml (i.e. 50 µl). Sample was mixed and further disrupted on gentleMACS via program m_spleen_03. Sample was collected via centrifugation at 300 x *g* using a Labofuge 4R centrifuge (Hereaus Instruments) cooled at 4°C and supernatant discarded. Red blood cell lysis was performed using 1 ml Red Blood Cell Lysing Buffer (Sigma #R7757) mixed gently for 1 minute. Following lysis 15 ml HEPES buffer was added and unlysed cell were collected via centrifugation at 300 x *g* for 7 minutes at 4°C. Supernatant was discarded and cells were resuspended in 15 ml HEPES buffer and filtered into a sterile 50 ml falcon tube through a 100 µm pore size cell strainer (Fisher Scientific). Cells were re-centrifuged as above and resuspended in 1:20 MACS BSA Stock Solution (Miltenyi Biotec #130-091-376) and autoMACS Rinsing Solution (Miltenyi Biotec #130-091-222) hereafter referred to as PEB buffer, and filtered into a sterile 50 ml falcon tube through a 40 µm pore size cell strainer (Fisher Scientific #734-0002).

2.8.2 Intestine

Intestinal tissues were dissected and extraneous fat, mesenteric lymph node and Peyer's Patches excised. Tissue was split into equal lengths and luminal contents extruded using blunt forceps. Tissue was flushed with 15 ml CMF Buffer (Ca2+- and Mg2+ free HBSS supplemented with 1x HEPES Bicarbonate and 2% Fetal Bovine Serum) introduced via syringe, then longitudinally cut with scissors to open out the tissue into a sheet and cut laterally into ~0.5cm pieces. To extract intra-epithelial lymphocytes (IEL), tissues were washed with

CMF buffer and incubated for 1 hr at 37°C in CMF supplemented with 0.005M EDTA with agitation. Supernatants were pooled and IEL populations collected by centrifugation at 400 x g for 5 min at 4°C. IEL were resuspended in FC buffer, diluted to relevant cell concentrations and stained for analysis via flow-cytometry.

The remaining intestinal tissue pieces were washed via agitation in HBSS, and digested in 25 ml RPMI with 1.75 mg/ml Collagenase D (Roche #11088866001) and 0.05 mg/ml DNase I (Roche #10104159001) for 1 hour at 37°C with agitation. Filter into a clean 50 ml Falcon tube through a 100 µm cell strainer, washed with a further 10 ml RPMI buffer. Filter into a clean 50 ml Falcon tube through a 40 µm cell strainer. Centrifuge filtrate at 500 x *g* for 5 minutes at 4°C, discard supernate and resuspend cells in 50 ml PEB buffer as described above.

2.8.3 Lymph nodes and Peyer's patches

Tissues were dissected into Hanks' buffered saline solution (HBSS) (Sigma # cooled on ice. Tissue was macerated in a petri dish using a 22A scalpel and added to a 15 ml falcon tube. Tissue was digested with a 0.3 mg/ml collagenase/dispase mix for 20 minutes at ambient temperature. Digested tissue was strained through a 40 µm cell strainer with the aid of a plunger from a 1ml syringe and washing with HBSS.

2.9 Cell counting

To count cell density, 20 µl of cells suspended in relevant buffer was mixed with 180 µl Trypan blue solution for microscopy (Sigma #93595). Cell counts were taken from 10 µl sample using a haemocytometer. The number of live cells was counted in each corner and the central quadrant of the haemocytometer using E800 Microscope (Nikon).

2.10 Magnetic-activated cell sorting (MACS)

Cell populations from all tissues were enriched by magnetic-activated cell sorting. Cell suspension concentrations were calculated by cell counting as described above, centrifuged at 500x g for 5 minutes at 4°C and resuspended to produce a final concentration of 90 µl of PEB buffer per 5 x 10^6 cells. To isolate $CD11c^+$ cells, 10 µl CD11c microbeads (Miltenyi Biotec) were added per 5 x 10^6 cells and samples were incubated on ice for 20 minutes. Cells were

washed via centrifugation at 500x g for 5 minutes at 4°C and discarding supernate. Cells were resuspended in an equivalent volume of PEB buffer, and applied to a pre-washed MACS column. Columns were cleared of non-adherent cells using 3 separate washes of 3 ml PEB buffer, retaining flow through for further isolation of other cell types. CD11c positive cells were eluted from the column using 5 ml PEB buffer, cells were washed twice in RPMI buffer via centrifugation at 500x g for 5 minutes at 4°C. Following depletion of $CD11c^+$ cells, other cell populations were separated from the $CD11c^-$ flow through fraction using either anti-CD11b (Macrophages), anti-CD45RO-B220 (B cells) or anti-CD90.2 (T cells) microbeads.

2.11 Protein extraction

2.11.1 Brain

Brain tissues were homogenised in NP40 lysis buffer (1% NP40, 0.5% Sodium Deoxycholate, 150 mM Sodium Chloride, 50 mM TrisHCL [pH 7.5]) at 10% w/v, clarified by centrifugation at 16,000g for 20 min at 4°C and supernate stored at -70°C. For the detection of PrP^{Sc} homogenates were incubated at 37°C for 1 hour with 20 µg ml^{-1} proteinase K, digestions were halted by addition of 1 mM Phenylmethylsulfonyl fluoride (PMSF).

2.11.2 Scrapie-associated fibrils

For prion infected peripheral tissues such as Spleen, Scrapie-associated fibrils were purified using the following method. Tissues were homogenised in dounce glass/glass homogenisers in 1ml 0.2M KCL with 1mM NEM and 1 mM PMSF. Homogenate was centrifuged at 500g for 10 minutes at 4°C, and supernatant centrifuged at 100,000g for 30 min at 4°C. Pellets were re-homogenised in 0.2M TrisHCL [pH 7.4]. Samples were subject to 5µg/ml proteinase K for 1 hour at 37°C, following digestion samples were adjusted to 1% sarkosyl, 1mM PMSF and 0.001% 2-Mercaptoethanol before incubation for 1 hour at 37°C. Samples were overlayed onto 20% sucrose in 0.1M TrisHCL [pH 7.4] and centrifuged at 100,000g for 2 hours at 4°C. Pellets were air-dried overnight at 4°C and stored dry at -70°C. SAF were resolubilised in 2xSDS sample buffer for western blotting.

2.12 Western Blot

2.12.1 SDS polyacrylamide gel electrophoresis

Samples were prepared and separated on 12% Tris Glycine Polyacrylamide pre-cast gels (Nupage, Life Technologies) according to manufacturer's instructions. Briefly, samples were diluted 10-fold in 2x SDS sample buffer (Life Technologies), ultra-pure H_2O and 10x Reducing Agent (Life Technologies) and denatured for 10 minutes at 95°C. Samples were loaded into gels and run for 1 h 45 min at 125 V constant voltage in Towbin SDS-PAGE running buffer (25 mM Tris, 192 mM glycine, 0.1% SDS). Relative protein sizes in kDa were assessed using Seeblue and Seeblue Plus 2 pre-stained markers (Invitrogen).

2.12.2 Semi-dry Western blotting

Following SDS-PAGE, gels were removed from cassette. For blotting a stack of pre-cut filter paper (Whatmann 3MM) and PVDF membrane (Immobilon P, Millipore) was pre-soaked in Semi-Dry Transfer Buffer (Towbin buffer with 20% Methanol). Electroblotting was performed at 2 mA / cm^2 for 90 min, with a maximum voltage set at 25 V. Following electroblotting, PVDF membrane were washed in ultra-pure H_2O for 2 x 5 min to remove transfer buffer.

2.12.3 Protein immunodetection

Immunostaining of PVDF membranes were performed by washing in the following: 2 x 5 min in TBS (pH 7.5), 1 hour in 1x Western Block reagent diluted in TBS (Roche), overnight with primary antibody diluted to working concentration in 0.5x Western Block reagent diluted in TBS, 2 x 10 min washes with TBST (TBS with 0.01% Tween20), 2 x 10 min 0.5x Western Block reagent diluted in TBS, 45 min with HRP-conjugated species-specific secondary antibody (Jackson Immunoresearch) diluted as primary, 4 x 15 min TBST and finally 1 min in ultra-pure H_2O. For detection of PrP monoclonal antibody 7A12 was used at 1:20,000 dilution (Yin et al., 2007). Antibody binding was detected using BM Chemiluminescent substrate kit (Roche) and exposed to Lumifilm (Kodak) for various times determined empirically via initial 30 sec, 1 min and 3 min exposures.

2.13 Enzyme-linked immunosorbent assay (ELISA)

Maxisorp plates were coated with specific antigen diluted in carbonate-bicarbonate buffer via overnight incubation at 4°C. Plates were washed 3 times with Phosphate buffered saline with 0.5% Tween 20 between each incubation step. Plates were incubated with 5% Bovine serum albumen in PBS, pre-diluted mouse serum or control isotype antibody, Isotype specific biotinylated secondary antibody and avidin-horseradish peroxidase conjugate each for 1 hr at 37°C. Specific binding was detected with p-Nitrophenyl Phosphate (pNPP) and measured using an automated plate-reader to detect absorbance at 405 and 620 nm. Group mean and SEM were calculated for each serum dilution and plotted as standard curves.

Table 2.2 Antibodies used in ELISA

Target	Capture	Detection antibody
T. muris IgG1	E/S†	RMG1-1
T. muris IgG2a	E/S†	RMG2a-62

†Trichuris muris excretory/secretory antigen

2.14 Flow-cytometry

Cell suspensions were incubated with fluorescently conjugated antibodies and analysed using a Fortessa flow cytometer (BD Biosciences). Each of the cell type makers CD3, CD11c, CD11b or B220 were used alone or with anti-CXCR5 only.

Table 2.3 Antibodies used in flow cytometry

Target	Clone	Fluorophore conjugate
CD3	17A2	Pacific Blue
CD11c	N418	Alexa 488
CD11b	M1/70.15	Alexa 488
CD45RO-B220	RA3-6B2	Brilliant Violet 605
CXCR5	2G8	Allophycocyanin (APC)

2.15 Histology

2.15.1 Tissue collection and fixation

Tissues were collected into Periodate-Lysine-Paraformaldehyde (PLP) fixative (McLean and Nakane, 1974) and fixed for a minimum of 1hr and maximum 24 hr before trimming and processing.

2.15.2 Processing and embedding

Tissues were processed using a TP1050 Tissue Processor (Leica) using the following program before embedding into paraffin wax.

Table 2.4 Automated tissue-processing schedule

Reagent	Time
70% IMS*	30 mins
90% IMS	30 mins
95% IMS	30 mins
99% IMS	35 mins
99% IMS	35 mins
99% IMS	30 mins
Xylene	30 mins
Xylene	20 mins
Xylene	20 mins
Wax	10 mins
Wax	15 mins
Wax	15 mins

*IMS = Industrial methylated spirit

2.15.3 Sectioning

Paraffin-embedded tissue sections were cut at 6 µm using a microtome (Jung) and mounted onto superfrost plus slides (Menzel-Glaser). Sections were air-dried for 48 hrs at 55°C before storing at ambient conditions until use.

2.15.4 Lesion profiling

Lesion profiling was conducted on Haematoxylin and Eosin stained brain sections as described previously (Bruce et al., 2004). Briefly, nine grey matter and three white matter brain areas were scored for vacuolation on a scale of 0-5. Lesion profiles plots were constructed from a minimum group of N=6 mice, plotting the average vacuolation score and SEM.

2.15.5 Immunohistochemistry

To prepare cryosections, optimal cryotomy temperature (OCT) medium was removed by immersion of slides into distilled H_2O for 5 min. For paraffin embedded tissues, slides were de-paraffinized and rehydrated using xylene and a graded industrial methylated spirit (IMS)

series in a Leica Autostainer. For wholemount staining of gut or Peyer's patches, tissues were dissected, gut lumen exposed and pinned out as a flat sheet onto wax. Mucus was removed using vigorous pipetting and wash buffer was supplemented with 0.1% saponin. Samples were washed in either tris- or phosphate- buffered saline/0.1% bovine serum albumen buffer for 5 min and incubated with normal serum (Jackson Immunoresearch). Primary antibodies were used as detailed in table 5. Primary antibodies (except where directly fluorophore conjugated) were detected using appropriate species specific secondary antibodies (Jackson Immunoresearch). Anti-CD11c staining was enhanced using tryamide-Alexa fluorophore signal amplification kits (Invitrogen). Tissues were analysed and imaged for fluorescence on a LSM 5 Pascal confocal microscope (Carl Zeiss).

Table 2.5 Antibodies used in immunohistochemical analysis

Target	Species	Clone
CD8α	Rat	YTS105.18
CD45RO-B220	Rat	RA3-6B2
Complement C4	Rat	FDC-M2
CR1/2 [CD21/35]	Rat	7G6
CR1 [CD35]	Rat	8C12
CXCR5 [CD185]	Goat	[Santa Cruz]
F4/80	Rat	CI:A31
GFAP	Rabbit	[Dako]
Glycoprotein 2 [GP2]	Rat	2F11-C3
Iba1 [AIF1]	Rabbit	[Wako]
ITGAM [CD11b]	Rat	M1/70.15
ITGAX [CD11c]	Armenian Hamster	N418
Macrosialin [CD68]	Rat	FA-11
MAdCAM-1	Rat	MECA-367
MARCO	Rat	ED31
mPDCA1	Rat	JF05-1C2.4.1
PrP	Rabbit	1B3
PrP	Mouse	6H4
Sialoadhesin [CD169]	Rat	MOMA-1
SIGN-R1 [CD209b]	Armenian Hamster	22D1
SIGN-R1 [CD209b]	Rat	ER-TR9

2.15.6 Image analysis

Image analysis were performed using Zen and ImageJ software, a minimum of 6 animals per group and where applicable 6 non-overlapping fields of view at relevant magnification per animal were used. For area or colocalisation based analyses then counterstaining with relevant antibodies were undertaken to define cellular or regional localizations for analysis purposes.

2.16 Paraffin Embedded Tissue blot

Serial tissue sections were cut and mounted on nitrocellulose membrane. Paraffin Embedded Tissue (PET) blotting was performed as described previously (Schulz-Schaeffer et al., 2000). Briefly, membranes were de-paraffinized and sections rehydrated by washing in Xylene and a graded Isopropanol series at 100%, 95%, 70% and 50% before washing in 0.1% Tween20 in water. Further washes were performed in tris-buffered saline [pH 7.8] with 0.5% Tween20 (TBST). Sections were digested with 20ug/ml Proteinase K at 55°C overnight. Following TBST washes, sections were treated with 3M guanidine isothiocyanate for 10 min before further TBST washes. Sections were blocked for 30 min with 2% casein in TBST. PK-resistant PrP^{Sc} was detected using polyclonal antibody 1B3 and visualised using goat anti rabbit alkaline phosphatase conjugated secondary antibody and nitro-blue tetrazolium and 5-bromo-4-chloro-3'-indolyphosphate (NBT/BCIP) (Sigma). PET blots were imaged on a SteREO Lumar.V12 microscope using Zen software (Carl Zeiss).

2.17 Statistical analysis

Statistical analysis were performed using Excel (Microsoft) and Minitab 17 software (Minitab). Survival times after prion exposure and immunofluorescence analysis quantification data were tested for equal variances and analysed by two-sample t-test. Vacuolation profile data were analysed via analysis of variance and grouped via Tukey's post hoc testing. Elisa data were used to calculate mean relative titre at ½ maximal value and compared via two-sample T-test. Data are presented as mean ± SEM. P values of <0.05 were accepted as significant.

Chapter 3. Characterising CD11c and CSF1-R expression in the murine mononuclear phagocyte system

3.1 Abstract

The murine mononuclear phagocyte (MNP) system comprises a diverse population of cells, including monocytes, classical dendritic cells (cDC) and macrophages. Derived from the myeloid haematopoietic lineage, this group of cells express a variety of well characterised surface markers. Expression of CD11c (integrin alpha x subunit/Itgax) is commonly used to identify cDC, and similarly expression of CSF1-R (colony stimulating factor 1 receptor/CD115) to identify macrophages. In this chapter the expression of these markers was characterised using a variety of transgenic mouse models. CD11c expression was observed in anatomically defined subsets of MNP in secondary lymphoid organs, including all MNP identified within the germinal centre. The majority of MNP in the intestinal lamina propria are $CD11c^{+}$. All mucosal $CD11c^{+}$ cells are also $CSF1\text{-}R^{+}$ suggesting CSF1-dependent haematopoietic derivation. This double-positive population included germinal centre MNP. These data reveal that CD11c and CSF1-R do not specifically define cDC and macrophages. The use of CD11c-mediated transgenic expression systems, such as CD11cCre, targets particular functionally and anatomically distinct MNP populations that are dependent upon CSF1-R during haematopoiesis.

3.2 Introduction

The murine MNP system comprises a diverse group of cells including monocytes, macrophages and cDC. Originally defined as non-phagocytic cells specialised for presentation of antigen to naïve T cells, the functional distinction of cDC from macrophages has blurred considerably with time (Hume, 2008b, Hume et al., 2013). Terminally differentiated MNP are commonly defined by surface marker expression, function and anatomical localisation. Characterization and sub-setting of MNP has progressed apace with increasing marker recognition and available antibodies as well as transgenic reporter lines (Hume, 2011). Several markers have been proposed as cell type specific including the 'macrophages-specific' markers F4/80 (Hume et al., 1983), CD11b (Springer et al., 1979, Dziennis et al., 1995) and CD64 (Tamoutounour et al., 2012), the 'cDC-specific' marker CD11c (Metlay et al., 1990), the pan-cDC transcription factor zDC (Satpathy et al., 2012), and cDC subset transcription factors Batf3 (Edelson et al., 2010), IRF4 (Carreras et al., 2010) and IRF8 (Becker et al., 2012) as well as markers such as sialoadhesin that delineate MNP subsets in specific locations (Crocker and Gordon, 1986). Each marker on further investigation has been revealed to be expressed by distinct cell types or sub-populations but not to be unique identifiers (Hume, 2008a). In this chapter, using a variety of transgenic mouse models and techniques, we compared the expression of CD11c and CSF1-R.

CSF1-R is expressed on bone marrow precursors of $CD11c^+$ cells in lymphoid organs and major tissues (Onai et al., 2007, Auffray et al., 2009, Onai et al., 2010), and CSF1 controls the production of these cells (MacDonald et al., 2005). Administration of antibody against CSF1-R to mice leads to depletion of a subset of monocytes, and consequent depletion of all CSF1-R^+ cells in the gut wall and in many other organs (MacDonald et al., 2005). However, it remains possible that genuine $CD11c^+$ cDC, have lost expression of CSF1-R and/or are actually derived from a local source or from non-monocytic precursors. To determine whether there is a complete overlap between the CSF1-R and CD11c markers, we used the Tg(*Csf1r*-eGFP)1Hume (see 2.1.6) transgenic mouse model in which the *Csf1r* promoter drives expression of enhanced green fluorescent protein (hereafter referred to as *Csf1r*-eGFP mice) (Sasmono et al., 2003). In this line, eGFP is very stable and is retained even after *Csf1r* mRNA is depleted; for example when macrophages transdifferentiate into smooth muscle cells (Mooney et al., 2010). This transgene was combined by selective breeding with a transgenic mouse model in which the *Itgax* promoter drives expression of a simian diphtheria toxin receptor (hereafter referred to as CD11c-DTR mice – see 2.1.5) (Jung et al., 2002).

Treatment of *Csf1r*-eGFP:CD11c-DTR compound transgenic mice with diphtheria toxin temporarily ablates $CD11c^+$ cells with 85% loss at 24 hours and peak loss at day 2 after treatment and DC numbers recovering to pre-treatment levels by day 6 after treatment (Jung et al., 2002). The resultant loss of $eGFP^+$ cells was characterised in a variety of tissues, including secondary lymphoid organs such as spleen, lymph nodes and intestinal Peyer's patches as well as the mucosal surface of the small intestine. Our data indicate that all $CD11c^+$ cell populations had expressed CSF1-R and are presumably dependent upon, or influenced by, CSF1 signalling during haematopoiesis.

3.3 Results

3.3.1 Identification of CD11c$^+$ cells in the small intestine lamina propria

Within the intestinal lamina propria, two distinct subsets of MNP exist, those located within the lymphoid tissues such as Peyer's patches, isolated lymphoid follicles, cryptopatches and the remaining intraepithelial population within the villi, or sub-mucosal layers (Figure 3.1A to 3.1E). The lamina propria MNP have been sub-divided into the CD103$^+$ cDC (Annacker et al., 2005) and CX_3CR1^+ cDC (Del Rio et al., 2008) or macrophage (Schulz et al., 2009) and conventional macrophage subsets (Pavli et al., 1990). The relationship between these subsets remains somewhat obscure. Much earlier studies, isolating the lamina propria cDC on the strict definition of cells able to stimulate an allogeneic mixed lymphocyte reaction, indicated that activity was confined to non-phagocytic cells (Pavli et al., 1990). Here, *Csf1r*-eGFP eGFP:CD11c-DTR compound transgenic mice were given a single injection with diphtheria toxin to temporarily deplete their CD11c$^+$ cells (see 2.3.1). In this model all CSF1-R-dependent derived cells express eGFP and cells that express CD11c are sensitive to diphtheria toxin.

Following diphtheria toxin-mediated depletion of CD11c$^+$ cells, an almost complete loss of eGFP$^+$ cells was observed in the intraepithelial population (Figure 3.1F to 3.1J). These data clearly show that all intraepithelial and sub-mucosal MNP (including cDC and macrophages) within the small intestinal lamina propria express both CD11c and CSF1-R. Following diphtheria toxin-mediated depletion extremely rare isolated eGFP$^+$ cells were observed with random distribution (Figure 3.1G). These cells were subsequently found to be CD11c$^+$ by immunohistochemical methods (see 2.15.5 and Figure 3.1H) and most likely represent incomplete depletion of the totality of CD11c$^+$ cells due to limitations of the DTR system. In previous studies using the CD11c-DTR model a splenic reduction of ~ 60% was observed by flow cytometric analysis after a single diphtheria toxin treatment, which may be indicative of rapid replenishment or more sensitive, and therefore more accurate, assessment of cell loss than immunohistological assessment (Raymond et al., 2007). In the current study a highly sensitive tyramide-enhanced immunostaining protocol was used to detect CD11c$^+$ cells (see 2.15.5). Therefore it is plausible that these remaining cells may represent the lamina propria MNP previously identified as CD11b$^+$/CD11c$^-$ (via immunohistochemistry) that were shown in the same study to be CD11b$^+$/CD11c^{int} via flow cytometry (Jang et al., 2006). As such these

MNP may express much lower levels of DTR via the CD11c-DTR transgene and have a higher tolerance for diphtheria toxin.

The cellular sites of CD11c expression were also compared using CD11c-Cre:mTmG Cre-reporter transgenic (Muzumdar et al., 2007). In these mice, Cre expression is driven by the CD11c promoter so that $CD11c^+$ cells only express Cre. Membrane-targeted tomato fluorescent protein is expressed constitutively in the mTmG reporter (Figure 3.1K, red) except after Cre-mediated recombination when expression is switched to membrane targeted eGFP (Figure 3.1L, green). Therefore in the compound transgenic all cells should express tomato fluorescence except $CD11c^+$ cells which express eGFP. Consistent with data above, within the intestinal lamina propria only intraepithelial cells were observed to be eGFP+ in CD11c-Cre:mTmG mice (Figure 3.1L). The CD11c-promoted transgenic model systems provided comparable data regardless of the system type or reporter mechanism (i.e. DTR-diptheria toxin sensitivity or Cre-mediated genomic recombination). In conclusion, these data are both confirmatory and representative of the true pattern of CD11c expression as they were matched by direct immunohistological staining. The use of tyramide-enhanced immunostaining has clearly identified numerous MNP populations described previously as $CD11c^-$ but proven to be $CD11c^{int}$ or $CD11c^{lo}$ by flow cytometry, and shown to be diphtheria toxin-sensitive in the CD11c-DTR model. A concurrent loss of other markers found on $CD11c^+$ cells was also observed such as $mPDCA1^+$ (Figure 3.1D, 3.1I), plasmacytoid DCs (Krug et al., 2004, Barchet et al., 2005). CD8α staining (Figure 3.1E) was retained only on intraepithelial lymphocytes such as T cells after diphtheria toxin treatment (Figure 3.1J).

Figure 3.1 Characterization of CD11c expression in the small intestinal lamina propria

(A-E) MNP expressing eGFP from the Csf1r-eGFP transgene were detected using fluorescent microscopy (green). CD11c (C & H; red), mPDCA1 (D & I; red), CD8α (E & J; red) and actin (C & H; blue) expressing cells were detected by IHC. (F-J) DTX-mediated depletion of CD11c cells (via CD11c-DTR transgene) reveals an almost complete loss of eGFP+ MNP from the intraepithelial population. (H) Rare eGFP+ cells were observed to be immunoreactive to the CD11c antibody. (K & L) Analysis of CD11cCre expression using mTmG dual fluorescent reporter reveals eGFP expression (L, green/yellow) in intraepithelial cells only. No eGFP expression was detected in the absence of Cre (K).

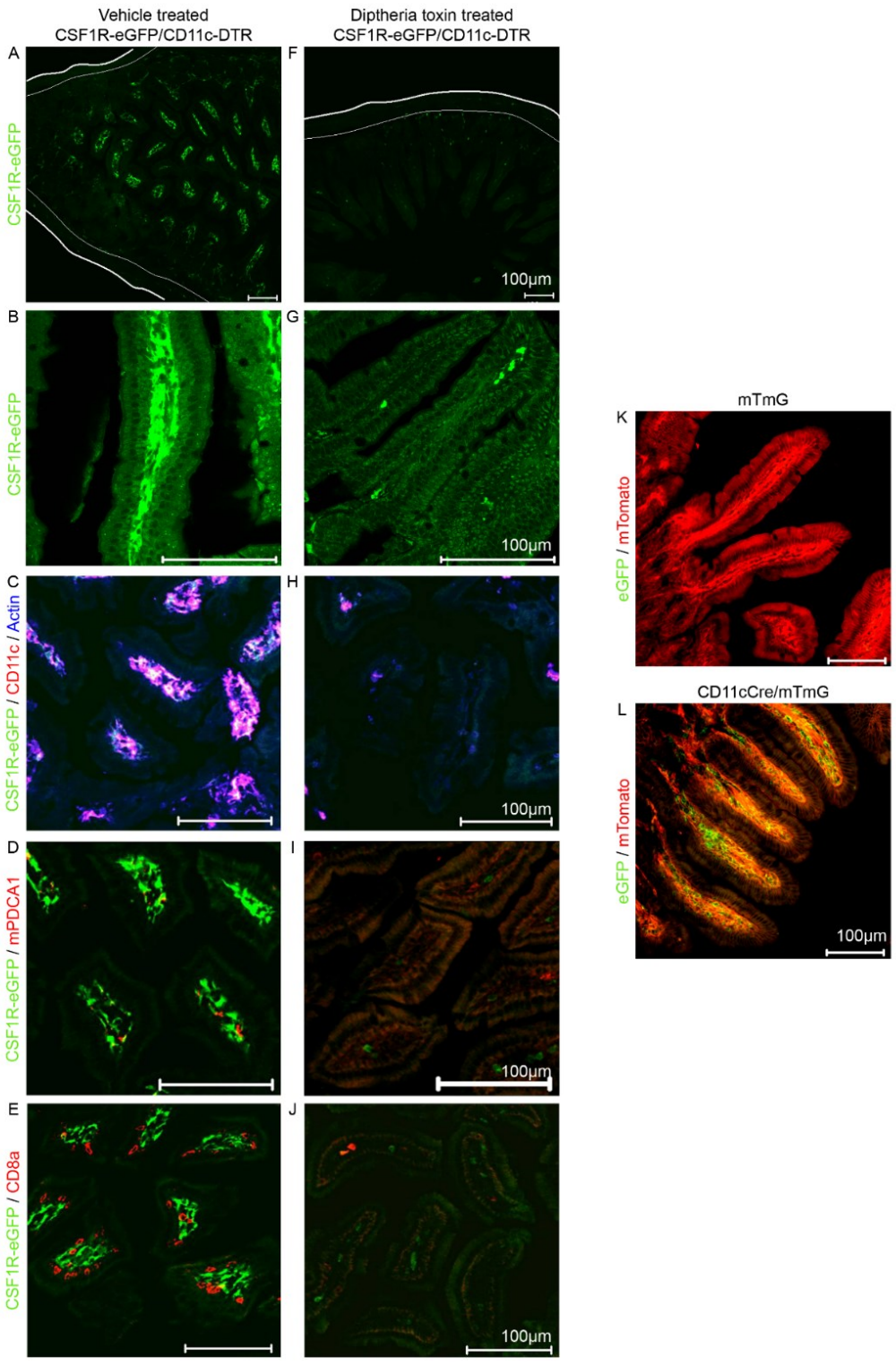
Vehicle treated
CSF1R-eGFP/CD11c-DTR
Diptheria toxin treated
CSF1R-eGFP/CD11c-DTR
A
F
CSF1R-eGFP
100μm
B
G
CSF1R-eGFP
100μm
C
H
CSF1R-eGFP / CD11c / Actin
100μm
D
I
CSF1R-eGFP / mPDCA1
100μm
E
J
CSF1R-eGFP / CD8a
100μm
mTmG
K
eGFP / mTomato
CD11cCre/mTmG
L
eGFP / mTomato
100μm

3.3.2 Identification of CD11c$^+$ cells in the small intestinal Peyer's Patches

Within Peyer's patches, MNP including both cDC and macrophages, are located in the sub-epithelial dome (SED; Figure 3.2A, B), inter-follicular region (IFR; Figure 3.2A, C), infrequently within the B cell rich marginal zone (MZ; Figure 3.3A) and rarely within the B cell follicle or germinal centre (GC; Figure 3.3D). Analysis of Peyer's patches from *Csf1r*-eGFP:CD11c-DTR compound transgenic mice confirmed each subset expressed eGFP (Figure 3.4A). Following diphtheria toxin treatment, specific subsets of eGFP$^+$ MNP remained in the sub-epithelial dome (Figure 3.3E and 3.3F) and IFR (Figure 3.3E and 3.3G) regions, whereas the loss of all germinal centre eGFP$^+$ cells was observed (Figure 3.3E and 3.3H). The MNP retained after diphtheria toxin treatment corresponded to the CD11c$^-$/ CD11b$^+$ MNP (Denning et al., 2007), as they revealed no CD11c immunoreactivity (Figure 3.3J). As such residual eGFP$^+$ MNP are found only in the sub-epithelial dome and inter-follicular regions of the Peyer's patch (Figure 3.3F and 3.3G). Analysis of plasmacytoid DC (pDC) using the marker mPDCA1 revealed large dendritic morphology cells present in the Peyer's patch (Figure 3.3K, arrow), however after diphtheria toxin-mediated depletion only small residual staining was observed (Figure 3.4L, arrow) most likely indicative of phagocytosed material.

CD11cCre expression was reported with eGFP expression in most regions of the Peyer's patch except perhaps the marginal zone region (Figure 3.3A). Large complex morphological MNP reported CD11cCre-mediated recombination particularly in the sub-epithelial dome (Figure 3.3B) and germinal centre (Figure 3.3C), confirming again that MNP observed within the germinal centre region express CD11c, and in the CD11cCre also display Cre activity as measured by the switch in fluorescent protein expression in the mTmG reporter.

Analysis of the preferential co-localisation of CD11b and CD11c suggest therefore that all CD11c$^+$ only or double-positive (CD11c$^+$/CD11b$^+$) cells were depleted. Analysis of differential integrin (CD11c/CD11b) expression by intestinal MNP reveals CD11b$^+$ only MNP in Peyer's patch regions (Figure 3.4A and 3.4B). In contrast all MNP within the lamina propria outwith mucosa associated lymphoid tissues (MALT) were observed to be double-positive CD11c$^+$/CD11b$^+$.

Figure 3.2 Characterization of CD11c expression in Peyer's patches.

(A-F) normal distribution of *Csf1r*-eGFP^{+} cells in vehicle treated *Csf1r*-eGFP:CD11c-DTR mice. (G-L) DTX-mediated depletion of CD11c^{+} cells from the Peyer's patches leaves a small population of eGFP^{+} cells particularly in the follicle associated epithelium (FAE) or sub-epithelial dome (SED) and interfollicular (IFR) regions, but not in the germinal centre (GC) or marginal zone (MZ) regions. (E, F, K & L) Co-expression of CD11c (red) and mPDCA1 (blue) was detected by IHC. Nuclei were detected with TOPRO3 (blue).

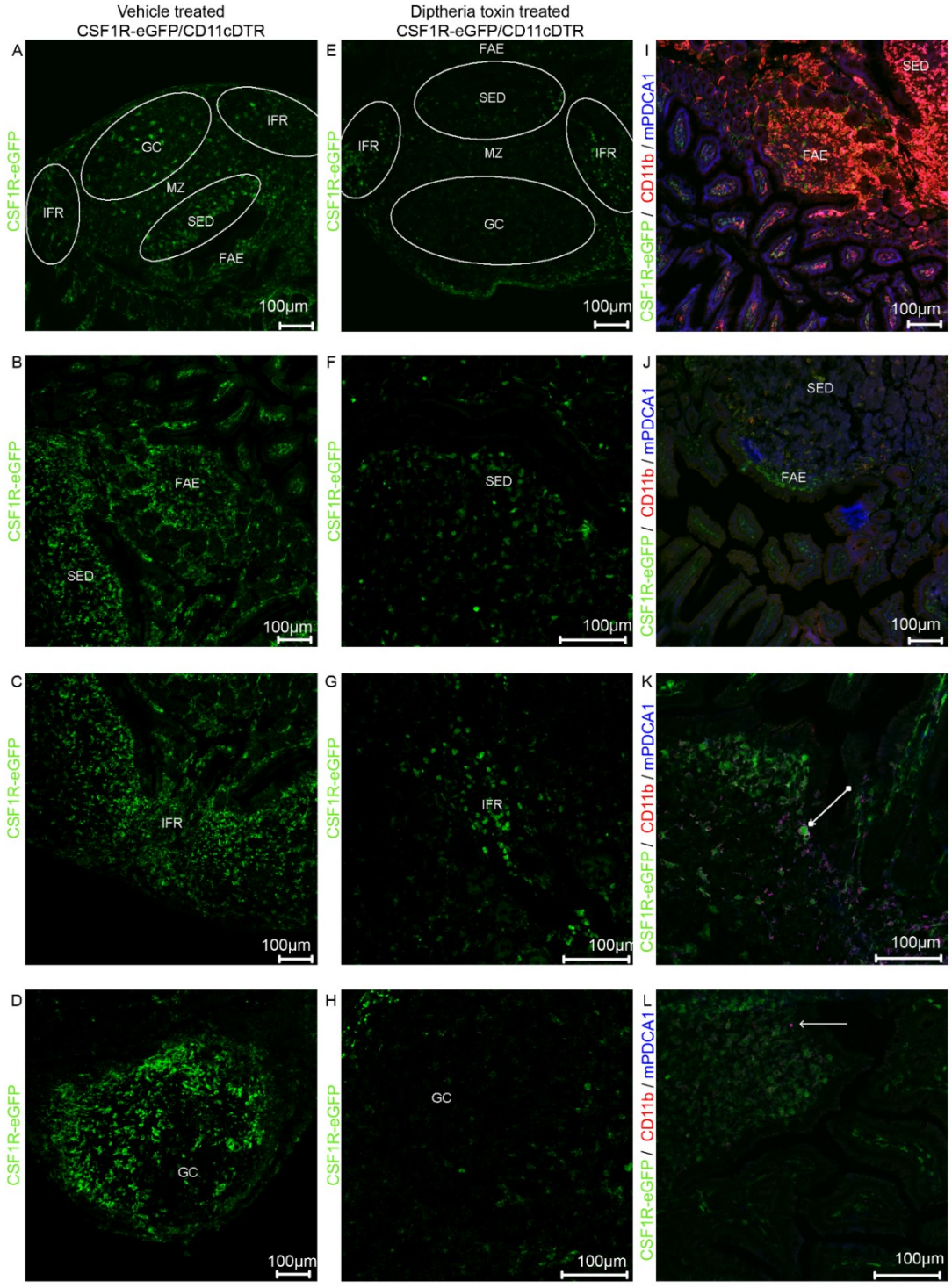

Figure 3.3 Analysis of CD11c-Cre expression in Peyer's patches using mTmG reporter mice.

Histological analysis of Peyer's patch tissue in mTmG and CD11cCre:mTmG reporter mice revealed GFP expression due to Cre-mediated recombination in MNP within all Peyer's patch regions except marginal zone (A). CD11c-mediated eGFP expression was observed in both sub-epithelial dome (B) and germinal centre (C; arrows), indicating the presence of $CD11c^{+}$ cells within these regions.

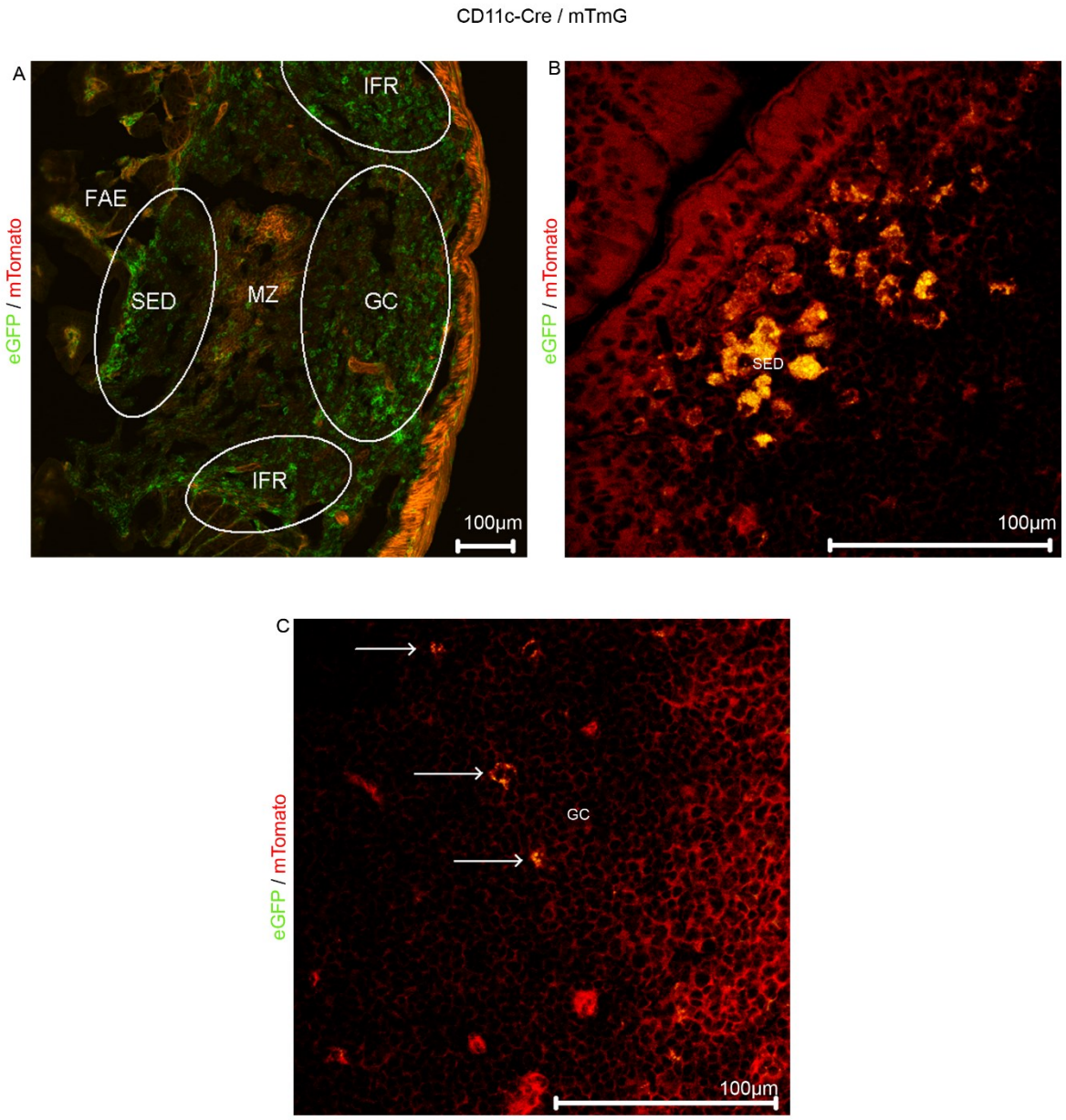

Figure 3.4 Immunohistochemical analysis of integrin expression within the small intestine.

Analysis of integrin CD11c and CD11b expression in Peyer's patch follicle-associated epithelium (FAE) (A), interfollicular region (IFR) (B) and surrounding small intestinal villi (C). C57Bl/6 mice reveal $CD11c^+$ only (A & B; green arrows), $CD11b^+$ only (A & B; red arrows), and $CD11c^+/CD11b^+$ (A, B and C; yellow arrows) cells present in Peyer's patches. The majority of intraepithelial MNP in small intestinal villi are $CD11c^+/CD11b^+$ (C, yellow arrows).

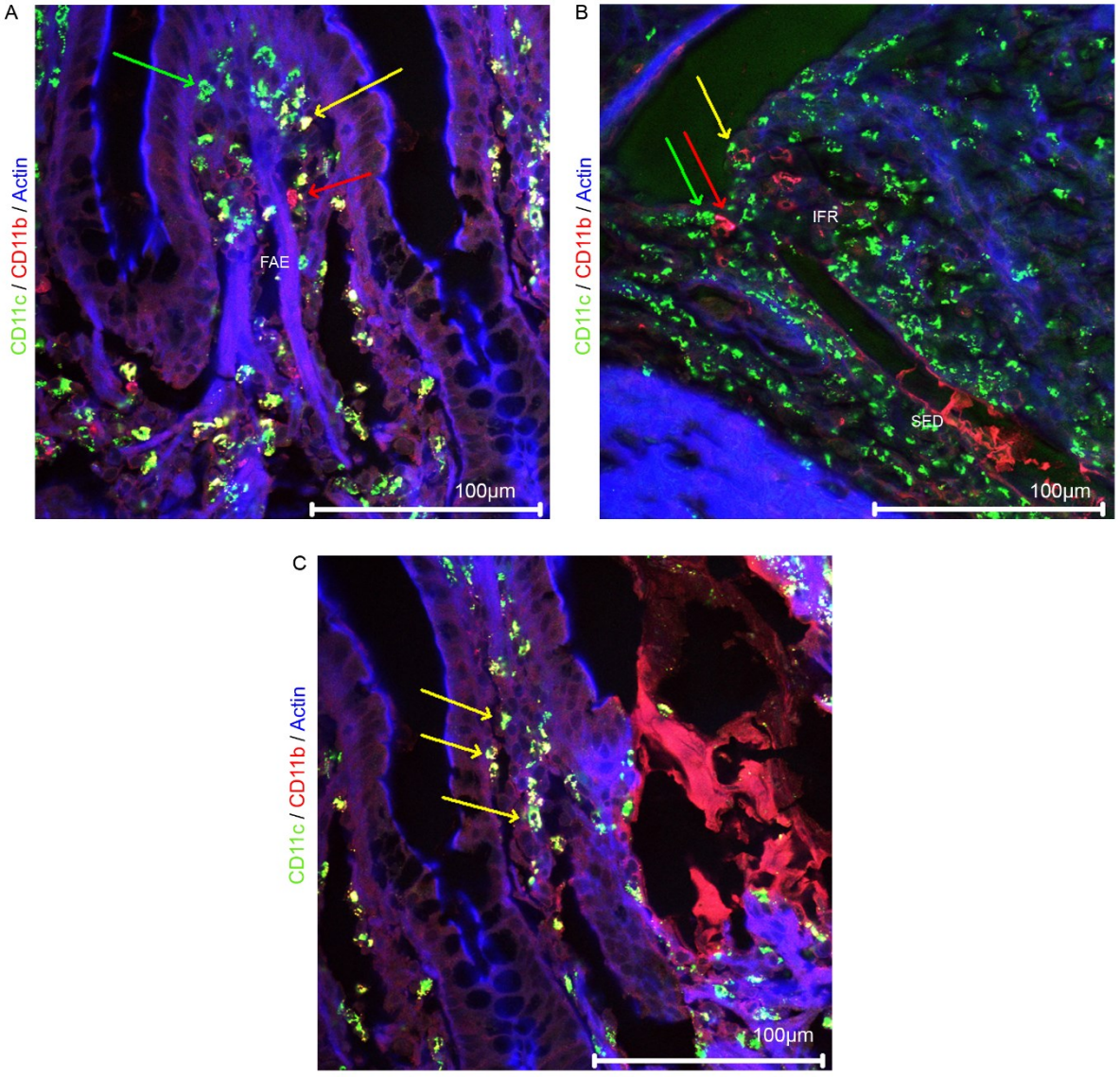

3.3.3 Identification of CD11c$^+$ cells in the mesenteric lymph nodes

Abundant eGFP$^+$ MNP were observed in the mesenteric lymph nodes (Figure 3.5A). Following diphtheria toxin treatment, sinusoidal cell and germinal centre populations were depleted from the lymph nodes and a reduction of eGFP$^+$ cells was observed from the cortex and paracortex regions (Figure 3.5D). Analysis of CD8α expression reveals numerous T cells and rare eGFP$^+$/CD8α$^+$ MNP (Figure 3.5B), however little to no CD8α expression co-localized with CSF1-R-eGFP after diphtheria toxin treatment (Figure 3.5E), suggesting MNP CD8α expression occurs mostly on CD11c$^+$ cells. Analysis of CD11c-Cre expression in lymph nodes revealed widespread recombination and eGFP expression in all regions (Figure 3.5F, green). Again individual MNP reported Cre expression within the germinal centre. Characterization of the CD11c$^+$ cells within the GC revealed large CD11c$^+$/CXCR5$^-$ cells likely to be tingible body macrophages (Red) and complex CXCR5$^+$/CD11c$^+$/Actin$^+$ (white) likely to be cDC (Figure 3.5G).

Figure 3.5 Characterization of CD11c expression in the mesenteric lymph nodes.

To characterize CD11c-expressing cells in the lymph node we used several transgenic mouse models. Diptheria toxin treatment of *Csf1r*-eGFP:CD11c-DTR mice resulted in a reduction in eGFP+ cells (A) normally observed in the lymph node cortex (B), indicating these cells are also CD11c$^+$. In the paracortical region, some eGFP+ cells were still observed indicating they are CD11c$^-$, however a concurrent loss of eGFP$^+$/CD8α$^+$ cells was observed (C) compared to vehicle treated control mice (D) revealing that eGFP$^+$/CD11c$^+$ cells also express CD8α. Cre-negative mTmG reporter mice display only dTomato (Red) expresison (E). Analysis of CD11c-Cre expression in CD11cCre:mTmG reporter mice revealed strong Cre-mediated GFP expression (Green) in the cortex and paracortex regions, with individual cells visible in the germinal centre (GC) regions (F), confirming the presence of CD11c$^+$ cells as observed in the *Csf1r*-eGFP:CD11c-DTR model. IHC characterisation of GC region CD11c$^+$ cells in C57Bl/6 mice reveals two distinct populations; a CD11c$^+$/CXCR5$^-$ population of resident tingible-body macrophages (red) and CD11c$^+$/F-actin^{Hi}/CXCR5$^+$ population, likely to be migratory cDC (white) (G).

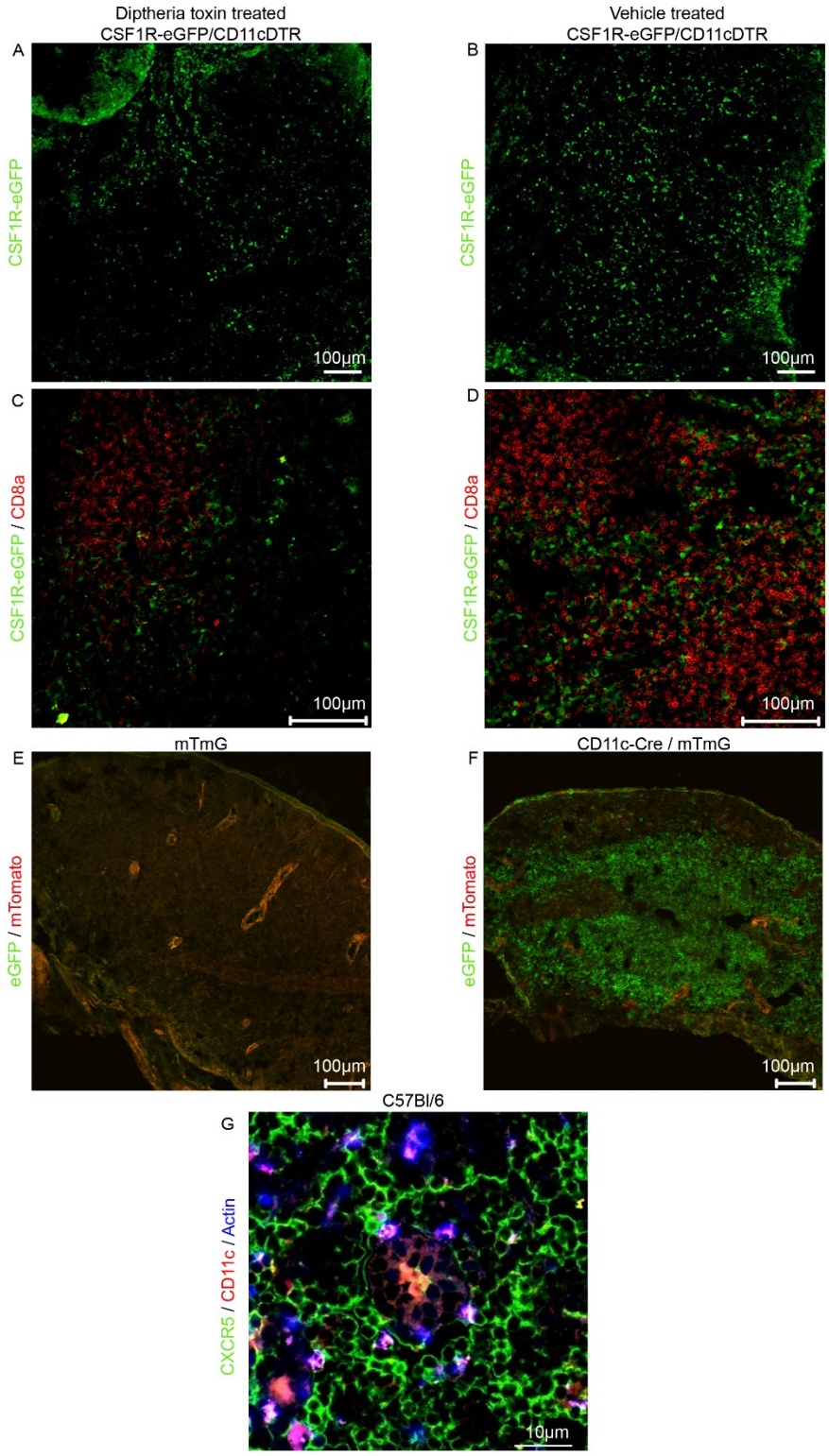
Diptheria toxin treated
CSF1R-eGFP/CD11cDTR
Vehicle treated
CSF1R-eGFP/CD11cDTR
A
B
CSF1R-eGFP
CSF1R-eGFP
100µm
100µm
C
D
CSF1R-eGFP / CD8a
CSF1R-eGFP / CD8a
100µm
100µm
mTmG
CD11c-Cre / mTmG
E
F
eGFP / mTomato
eGFP / mTomato
100µm
100µm
C57Bl/6
G
CXCR5 / CD11c / Actin
10µm

3.3.4 Identification of CD11c$^+$ cells in the spleen

Csf1r-eGFP expression was observed mainly in the red pulp of the spleen (Figure 3.6A, 3.6B), with fewer eGFP$^+$ cells observed in white pulp regions (Figure 3.6A, 3.6C). Following diphtheria toxin-mediated depletion of CD11c$^+$ cells, a significant number of the eGFP$^+$ cells within the red pulp were removed (RP; Figure 3.6F) and the majority of those from white pulp (WP; Figure 3.6G) regions. Peri-arteriolar eGFP$^+$ interdigitating cells within the T cell zone (Figure 3.6C) were also depleted following diphtheria toxin treatment (Figure 3.6H). Following diphtheria toxin-treatment, strong residual F4/80 (Figure 3.6I) and CD11b (Figure 3.6O) immunostaining was observed concurrent with retention of numerous eGFP$^+$ MNP cells within the red pulp. Within the marginal zone of the white pulp, the Sialoadhesin-positive metallophilic macrophages (Figure 3.6M) were observed to be CD11c$^+$ (Figure 3.6K) and CD11b$^+$ (Figure 3.6L) and were completely lost following diphtheria toxin treatment (Figure 3.6N-3.6P). These data indicate that splenic metallophilic macrophages and interdigitating cells co-express CD11c and CSF1-R. As observed in Peyer's patches, all eGFP$^+$ cells were completely absent from germinal centres following CD11c$^+$ cell depletion (Figure 3.6F, 3.6N-3.6P). Following diphtheria toxin-mediated depletion CD8α was observed only on T cells due to the loss of eGFP$^+$/ CD8α$^+$ MNP (Figure 3.6J).

Fig. 3.6 Characterization of CD11c expression in the spleen.

Spleen tissue from vehicle treated CSF1reGFP/CD11cDTR (A-E, K-M) or diptheria toxin treated CSF1reGFP/CD11cDTR (F-J, N-P) mice were analysed histologically. Morphologically complex (i.e. dendritic) eGFP$^+$ cells in both red pulp and peri-arteriolar white pulp regions (A, arrows in B & C) are depleted following diphtheria toxin treatment (G & H). Co-expression of F4/80 (D & I; red), CD8α (E & J; red), CD11c (K & N; red), CD11b (L & O; red), Sialoadhesin (M & P; red) and actin (blue) was detected by immunohistochemistry. Diptheria toxin-mediated depletion of CD11c$^+$ cells was concurrent with complete loss of expression of Sialoadhesin (P). These cells also expressed CD11b$^+$ indicative of metallophilic macrophages (O). Residual eGFP+ cells remaining in the red and white pulp after CD11c depletion are also CD11b$^+$ (O) and F4/80$^+$(I). WP, white pulp; RP, red pulp. A & F, Large ovals indicate boundary of the red pulp. C & H, small circles indicate central arterioles.

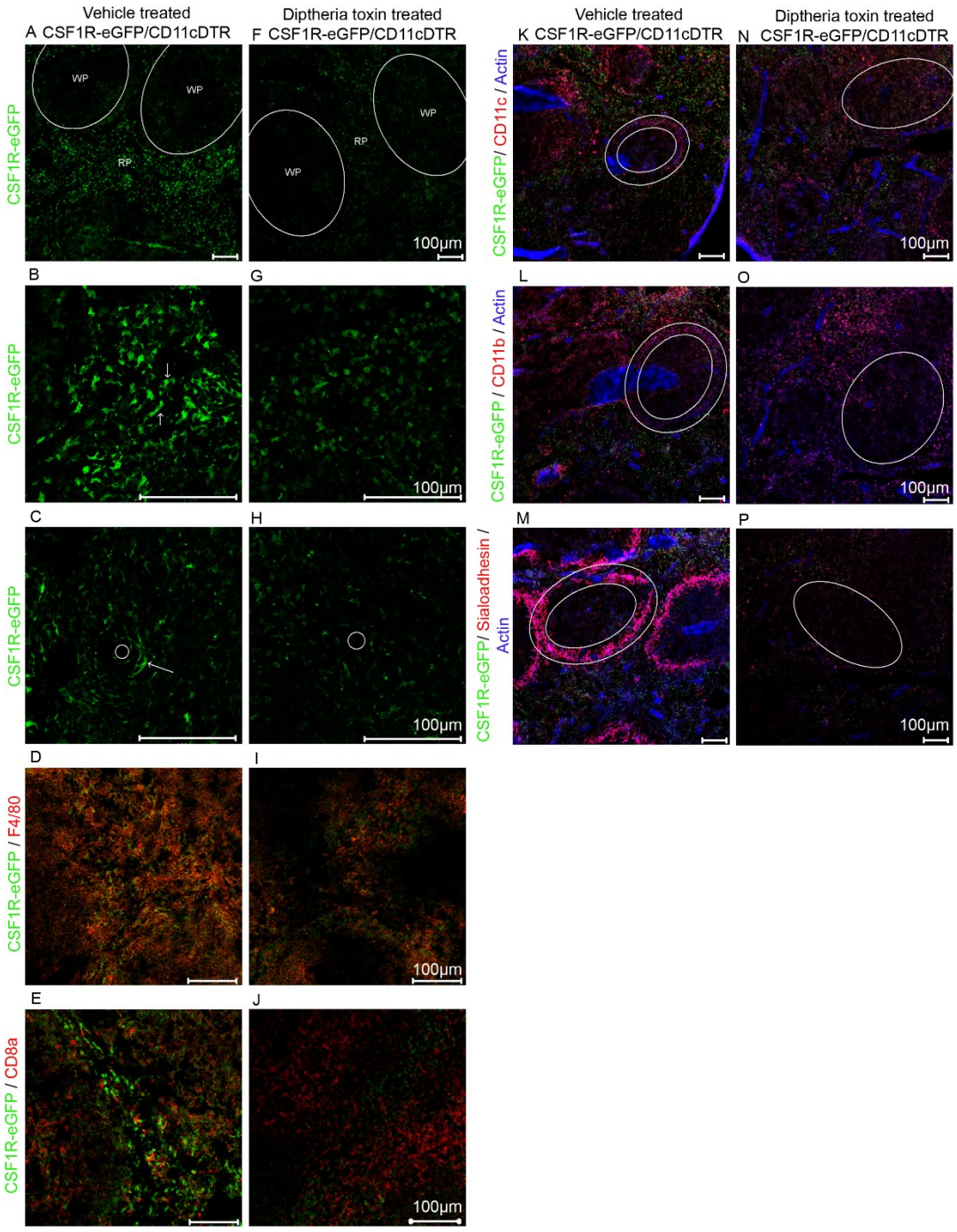
Vehicle treated
A CSF1R-eGFP/CD11cDTR
Diptheria toxin treated
F CSF1R-eGFP/CD11cDTR
Vehicle treated
K CSF1R-eGFP/CD11cDTR
Diptheria toxin treated
N CSF1R-eGFP/CD11cDTR
CSF1R-eGFP
CSF1R-eGFP/ CD11c / Actin
WP
RP
100µm
B
G
L
O
CSF1R-eGFP / CD11b / Actin
C
H
M
P
CSF1R-eGFP/ Sialoadhesin / Actin
D
I
CSF1R-eGFP / F4/80
E
J
CSF1R-eGFP / CD8a

3.4 Discussion

These data clearly demonstrate that all murine *Itgax* expressing cells can be detected with the *Csf1r*-eGFP transgene, which in turn overlaps completely with *Csf1r* expression (Sasmono et al., 2003). These data also suggest that all $CD11c^+$ cells derive from a precursor that is potentially CSF1 responsive. Accordingly, the complete depletion of $eGFP^+$ lamina propria cells seen in response to anti-CSF1-R treatment of CSF1-R-eGFP mice includes all "cDC" as identified using CD11c as a marker (MacDonald et al., 2010), demonstrating that in the CD11c-DTR transgenic model (Bar-On and Jung, 2010), all non-lymphoid intestinal lamina propria MNP identified by the transgene are depleted.

The *Itgax*-promoted transgenic model systems provided comparable data regardless of the system type or reporter mechanism (i.e. diphtheria toxin-DTX sensitivity or Cre-mediated genomic recombination). We therefore conclude that these data are both confirmatory and representative of the true pattern of CD11c expression as they were matched by direct immunohistological staining. In this study a highly sensitive immunostaining protocol was used to detect $CD11c^+$ cells. Our use of tyramide-enhanced immunostaining has clearly identified numerous MNP populations described previously as $CD11c^-$ but proven to be $CD11c^{int}$ or $CD11c^{lo}$ by flow cytometry, and shown to be diphtheria toxin-sensitive in the CD11c-DTR model. Therefore it is plausible that the remaining $CD11c^+$ cells observed after depletion may represent the lamina propria MNP previously identified as $CD11b^+/CD11c^-$ (via immunohistochemistry) that were shown in the same study to be $CD11b^+/CD11c^{int}$ via flow cytometry (Jang et al., 2006). As such these MNP may express much lower levels of DTR via the CD11c-DTR transgene and have a higher tolerance for diphtheria toxin.

The expression of CD11c by all MNP found within germinal centres suggests that MNP that are either resident to the germinal centre, or gain access to it, derive from the $CD11c^+$ population. Specialised stromal cells termed follicular dendritic cells within the germinal centre express high levels of the chemokine CXCL13, the ligand for the chemokine receptor CXCR5, whose expression by naïve B cells is important for their recruitment to B cell follicles (Gunn et al., 1998, Ansel et al., 2000). Further characterization of the MNP within the germinal centre confirmed these cells likewise express the chemokine receptor CXCR5, as has been previously reported for cDC (Yu et al., 2002). These data suggest that germinal centre-homing $CD11c^+$ MNP are responding to the chemokine CXCL13 produced by cells of the germinal centre (Carlsen et al., 2002). $CD11c^+$ cells have been hypothesised to aid in the formation of

Peyer's patches during embryogenesis (Veiga-Fernandes et al., 2007) and the development of isolated lymphoid follicles in the small intestine (McDonald et al., 2010). Depletion of these cells in adult mice however appeared to have had no impact on the maintenance of the germinal centre structure as has been shown with blockage of CXCL13-CXCR5 signalling (Henry and Kendall, 2010).

Despite these facts the expression of CD11c defines specific populations of MNP throughout the tissues known to be involved in prion pathogenesis and in the absence of unique markers for APC or cDC, CD11c-based transgenic models are the most well-characterised and applicable for the following studies. Based on these findings we determined that CD11cCre mice were the most appropriate model for the subsequent studies looking at the roles of trafficking and chemotaxis of antigen-presenting cells in the dissemination of prions and other infection models. Throughout all observations, MNP within germinal centres and proximal to FDC robustly displayed CD11c expression and within the CD11cCre model were also observed to report Cre activity. Therefore gene modification studies using CD11cCre mice should target our cells of interest.

Chapter 4. Conditional knockout of the chemokine receptor CXCR5

4.1 Abstract

Chemokines are small secreted proteins that induce strong chemotaxis in responsive cells possessing the relevant receptors. The chemokine receptor CXCR5 responds solely to the chemokine CXCL13 and is responsible for both the formation of lymphoid germinal centres and migration of cells to them. During lymphoid organogenesis immature stromal cells, and in established lymphoid tissues, mature stromal cells such as follicular dendritic cells (FDC) express the chemokine CXCL13. This chemokine expression organises the surrounding mobile leukocyte populations with those expressing CXCR5 being attracted to and retained within this CXCL13 rich environment. Complete transgenic knockout of either CXCR5 or CXCL13 results in loss of specific lymphoid tissues due to failed organogenic development. Lymphoid tissues that do develop have structural deficits such as loss of mature FDC as they require reciprocal lymphotoxin signalling from attracted CXCR5-expressing B cells for their maintenance. To surmount both the issue of failed development and maintenance of critical cell populations a conditional CXCR5 transgenic model is described in this chapter which allows specific cell-restricted knockout using Cre/*loxP* technology. This novel model is then used to generate a CD11c-mediated CXCR5 deletion which undergoes normal organogenesis with mature FDC present, however $CD11c^+$ cells are restricted from entering the B-cell follicle. This model thus allows the investigation of the role of $CXCR5^+$ $CD11c^+$ cells play in the transport of antigens and the subsequent immune responses elicited under various conditions such as prion and gastrointestinal helminth pathogen infection.

4.2 Introduction

The chemokine receptor CXCR5 mediates the chemotaxis of cells to its sole ligand CXCL13 (Gunn et al., 1998) and is involved in both lymphoid organogenesis and the localisation of immune cells into the B-cell follicle of mature lymphoid tissues (Forster et al., 1996). Lymphoid organogenesis is initiated during embryogenesis and progresses in discrete steps. This was visualised by the blockage of LTβ signalling during gestation using LTβR-Ig. Application of LTβR-Ig at specific embryonic stages prevented the development of specific lymphoid organs (Rennert et al., 1996). In the GALT, Peyer's patch structures are developmentally programmed and form in distinct steps by defined mechanisms (Adachi et al., 1997, Yoshida et al., 1999, Nishikawa et al., 2003). Isolated lymphoid follicles (ILF) and cryptopatches (CP) on the other hand are dynamic and reveal great plasticity, their formation can be induced by external stimuli such as gut microbiota (Pabst et al., 2005, Pabst et al., 2006). The visualisation of lymphoid tissue inducer (LTi) cells (phenotype: $CD4^+$ CD3- $\alpha4\beta7^+$ and $IL7R\alpha^+$) scattered along the developing small intestine at embryonic stage E15.5 (i.e. 15.5 days post conception) reveal the earliest signs of Peyer's patch development. Over the next 24-48 hours (to E17.5) these cells agglomerate in the Payer's patch anlage in response to signals and adhesion molecules such as mucosal vascular addressin cell adhesion molecule 1 (MadCAM1) and vascular cell adhesion molecule-1 (VCAM-1) expressed by stromal cells. Finally influx of T and B lymphocytes ($CD3^+$ and $CD45R^+$ [i.e. $B220^+$] cells) occurs in the final Peyer's patch formation stage at E18.5.

During lymphoid organogenesis $CXCR5^+$ cells, including cDC, are recruited by LTi cells in the early stages. This occurs via activation of expression of CXCL13 and establishes into a positive feedback loop (Müller and Lipp, 2003). The LTi cells themselves may be localised by innervation and subsequent neuronal production of retinoic acid. Once in the Peyer's patch anlagen LTi cells play a role in the establishment of distinct B-cell and T-cell zone architecture via differential expression of CXCR4 & CXCR5 or CCR7 (Nakagawa et al., 2013). cDC also possess ability to migrate towards retinoic acid which may also inhibit their IL-4 mediated differentiation (de Sousa-Canavez et al., 2009). CXCR5 or CXCL13 complete knockout mice fail to undergo correct lymphoid organogenesis, lacking various secondary lymphoid structures, both CXCR5-deficient and CXCL13-deficient mice lack most Peyer's patches and lymph nodes, and the lymphoid organs that do develop generally lack mature FDC (Forster et al., 1996, Ansel et al., 2000), furthermore they have impaired B cell homing, localization and antigen dependent and independent differentiation (Hopken et al., 2004). The absence of

specific GALT has a significant impact upon the susceptibility to oral prion infection (Glaysher and Mabbott, 2007, Donaldson et al., 2015).

In mature lymphoid tissues FDC express the CXCR5 chemokine ligand CXCL13 and regulate the formation of the B-cell follicle (Vermi et al., 2008, Wang et al., 2011). CXCR5 is found mainly on B cells and subsets of T cells that localise to the B-cell follicle (Figure 4.1), however specific cDC subsets have been reported that express CXCR5 (Saeki et al., 2000) and use CXCR5-mediated chemotaxis for migration to B-cell follicles (Ishikawa et al., 2001, Wu et al., 2001, Wu and Hwang, 2002). The maturation of FDC is critically regulated by reciprocal signalling between FDC and B cells, FDC attract mature $CXCR5^+$ B-cells into the follicular structure and in return B cells provide positive lymphotoxin signalling for the maintenance and function of mature FDC (Fu et al., 1997, Fu et al., 1998). In CXCR5- or CXCL13-deficient mice (Forster et al., 1996, Ansel et al., 2000) mature FDC develop aberrantly in T-cell regions (Voigt et al., 2000) resulting in enhanced prion pathogenesis due to the proximity of FDC to peripheral nerves (Prinz et al., 2003a). Blockade of lymphotoxin signalling induced dedifferentiation of FDC and drastic reduction in prion susceptibility (Mabbott et al., 2003) highlighting the significance of mature, correctly localised FDC in regulating prion pathogenesis. Therefore to investigate the role of $CXCR5^+$ cDC in prion pathogenesis and other infection models the use of complete CXCR5 knockout models is excluded.

Figure 4.1 Expression of CXCR5 and CD11c in major immune cell subsets.

Gene expression data for CXCR5 and CD11c in major immune cell subsets from Immgen.org (Heng et al., 2008). CXCR5 is most highly expressed in mature follicular-localising B-cell populations and T-cell subsets, whereas CD11c is most highly expressed upon cDC, NK cells and $CD8^+$ effector T cells in naïve mice.

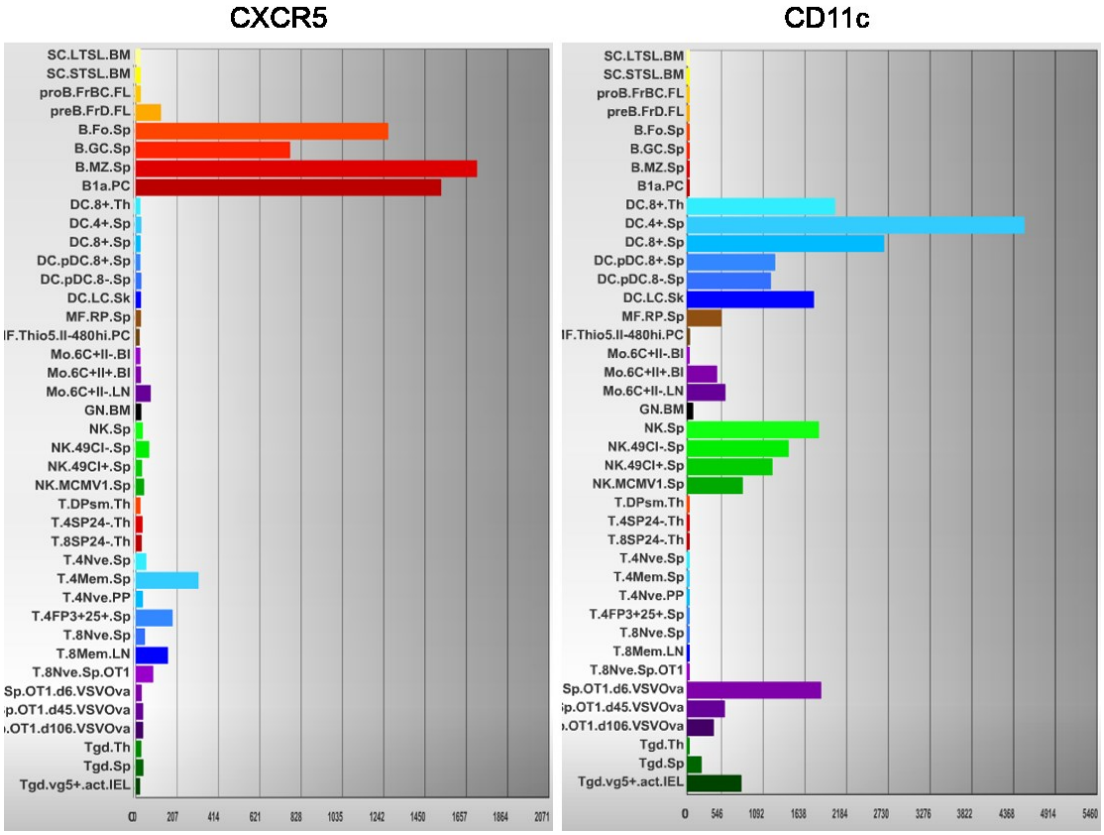

The murine *Cxcr5* gene, GenBank accession number(s) NM_007551, BC064059, is found on chromosome 9 (Dobner et al., 1992), and has two exons spread over ~ 15 kb with a coding sequence of 1125 nucleotides encoding a protein consisting of 374 amino acids (Figure 4.2). To bypass issues observed in complete CXCR5 knockout mice a conditional gene expression model system can be utilised such as the Cre/*loxP* system (Sauer and Henderson, 1988). By targeting *loxP* recognition sequences around exon 2 of the *Cxcr5* gene, expression of *Cxcr5* in the normal situation should be unaffected. However, introduction of the Cre recombinase should result in genomic recombination and loss of *Cxcr5* exon 2, thus functionally ablating the ability to express the mature CXCR5 chemokine receptor protein. Cell-restricted Cre expression should control the cell-specificity of *Cxcr5* knockout (Gu et al., 1994).

Figure 4.2 CXCR5 Nucleotide and amino acid sequence

Complete coding nucleotide sequence for murine *Cxcr5* gene and corresponding CXCR5 protein amino acid sequence translation, displaying exon1 (grey) and exon 2 (black).

C-X-C chemokine receptor type 5 [Mus musculus]
NCBI Reference Sequence: NP_031577.2

Nucleotide Sequence (1125 nucleotides):

```
1    ATGAACTACC CACTAACCCT GGACATGGGC TCCATCACAT ACAATATGGA
51   TGACCTGTAC AAGGAACTGG CCTTCTACAG TAACAGCACG GAGATTCCCC
101  TACAGGACAG TAACTTCTGC TCTACAGTCG AGGGACCCTT ACTGACGTCC
151  TTTAAGGCGG TATTCATGCC TGTGGCCTAC AGCCTCATCT TCCTCCTGGG
201  TATGATGGGA AACATCCTGG TGCTGGTAAT CCTGGAGAGG CACCGGCACA
251  CGCGGAGCTC AACCGAGACC TTCCTGTTCC ACCTCGCAGT AGCCGACCTT
301  CTCTTAGTCT TCATCCTGCC TTTTGCAGTG GCTGAGGGCT CTGTGGGTTG
351  GGTCCTAGGG ACCTTCCTCT GCAAAACTGT GATCGCTCTG CACAAGATCA
401  ATTTCTACTG CAGCAGCCTG CTGCTGGCCT GTATAGCTGT AGACCGGTAC
451  CTAGCCATCG TCCATGCTGT TCACGCCTAC CGCCGCCGTC GACTCCTCTC
501  CATCCACATC ACCTGCACGG CCATTTGGCT GGCCGGCTTC CTGTTCGCCT
551  TACCGGAACT CCTCTTTGCC AAGGTTGGCC AACCTCATAA CAACGACTCC
601  TTACCACAGT GCACCTTCTC CCAGGAAAAC GAAGCGGAAA CTAGAGCCTG
651  GTTCACCTCC CGTTTCCTCT ACCACATCGG GGGCTTCCTA CTACCGATGC
701  TTGTGATGGG ATGGTGTTAC GTGGGCGTGG TCCACAGGCT ACTGCAGGCC
751  CAGCGGCGCC CTCAGCGGCA GAAGGCGGTC AGGGTGGCCA TTTTAGTGAC
801  AAGCATTTTC TTCCTCTGCT GGTCGCCCTA CCACATTGTC ATCTTCCTAG
851  ATACACTGGA GAGGCTGAAG GCTGTGAATA GCAGCTGCGA GCTGAGTGGC
901  TATCTCTCTG TGGCCATCAC CTTGTGTGAA TTCCTGGGCC TGGCACACTG
951  CTGTCTCAAT CCCATGCTCT ACACCTTCGC TGGCGTAAAG TTCCGCAGTG
1001 ACCTCTCTCG GCTTCTGACC AAGCTGGGCT GTGCTGGCCC GGCCTCCCTT
1051 TGCCAACTTT TCCCCAACTG GCGCAAGAGT AGTCTCTCTG AGTCAGAGAA
1101 TGCTACTTCC CTCACCACCT TCTAG
```

Translation (374 amino acids):

```
1   MNYPLTLDMGSITYNMDDLYKELAFYSNSTEIPLQDSNFCSTVEGPLLTS
51  FKAVFMPVAYSLIFLLGMMGNILVLVILERHRHTRSSTETFLFHLAVADL
101 LLVFILPFAVAEGSVGWVLGTFLCKTVIALHKINFYCSSLLLACIAVDRY
151 LAIVHAVHAYRRRRLLSIHITCTAIWLAGFLFALPELLFAKVGQPHNNDS
201 LPQCTFSQENEAETRAWFTSRFLYHIGGFLLPMLVMGWCYVGVVHRLLQA
251 QRRPQRQKAVRVAILVTSIFFLCWSPYHIVIFLDTLERLKAVNSSCELSG
301 YLSVAITLCEFLGLAHCCLNPMLYTFAGVKFRSDLSRLLTKLGCAGPASL
351 CQLFPNWRKSSLSESENATSLTTF
```

The marker CD11c was previously investigated in Chapter 3 and despite its failure to represent a unique marker of cDC, all GC localising MNP were identified as $CD11c^+$ (See also Figure 4.1). The findings in chapter 3 validate the use therefore of CD11c-based transgenic mouse models for investigating follicle homing cDC. Mice that express the Cre recombinase enzyme via the CD11c promoter, display high Cre expression in specific cDC subsets (> 90% of cells) except plasmacytoid (86%) and dendritic cell progenitor (51%) subsets (Caton et al., 2007). Cre expression was also reported in 12% of natural killer ($DK5^+$) cells, 6% of T ($CD3^+$) cells, 5% of B ($CD19^+$) cells and 0.6% of granulocyte cells extracted from spleen. (Caton et al., 2007). Combining CD11cCre mice with novel conditional CXCR5 mice, subsequent transgenic model mice produced will specifically lack CXCR5 in $CD11c^+$ cells and be tested for their hypothesised lack of ability of cDC to transport prions and other antigens to B cell follicles and FDC. However, as a cautionary note some LTi cells and specific B-cell subsets may express CD11c (Ebisawa et al., 2011, Nakagawa et al., 2013, Rubtsov et al., 2015) and potentially require CXCR5 expression for their normal localisation and function. Therefore generation of a CD11c-mediated CXCR5 conditional knockout model will require careful examination in order to determine that lymphoid organogenesis and lymphoid microarchitecture develop correctly in these mice and validating their use to investigate the role of follicle-homing cDC.

4.3 Results

4.3.1 Generation of CXCR5^{fl} mice

To generate a conditional CXCR5 allele, *loxP* sites were introduced flanking the complete CXCR5 coding sequence (CDS) in exon 2 via homologous recombination. A 5' homology arm including the PGK-Neo-pA-SD-IS (Ozgene) standard selection cassette, *loxP* arm including the entire CDS and 3' homology arm were constructed via PCR. The 5' and 3' homology arms were approximately 5-6 kb in length and generated from C57BL/6 genomic DNA. The completed targeting vector was constructed using these three fragments and the plasmid FSniper (Ozgene).

The 5' homology arm was amplified from C57BL/6 genomic DNA using the primers P1149_05 and P1149_06, generating a 6571 bp fragment cloned upstream of the Frt-flanked PGK-Neo-pA-SD-IS selection cassette in the FSniper plasmid. The *loxP* homology arm containing the entire CXCR5 CDS was amplified from C57BL/6 genomic DNA using the primers P1149_07 and P1149_08, generating a 2620 bp fragment with 5' *loxP* site proceeding the entire CXCR5 CDS, cloned downstream of the Frt-flanked PGK-Neo-pA-SD-IS selection cassette in the FSniper plasmid. The 3' homology arm was amplified from C57BL/6 genomic DNA using the primers P1149_09 and P1149_10, generating a 5842 bp fragment containing a 5' *loxP* site and the remainder of CXCR5 exon 2, i.e. the 3' untranslated region (3' UTR) cloned downstream of the *loxP* arm in the FSniper plasmid.

Figure 4.3 Oligonucleotide primers for the construction of the CXCR5 floxed transgene

Oligonucleotide primer sequences used to amplify C57Bl/6 genomic DNA during the construction of the CXCR5^{fl} transgene. Restriction enzyme sites colour denoted, *loxP* sequences in red and sequences homologous to CXCR5 genomic DNA are underlined

5' Homology arm primers

P1149_05

5' AGTTTAAACTGGTTCAGAGGGTAAAGGTGCTTG 3'

PmeI site Homology

P1149_06

5' TGGCGCGCCGGATCCGGGAATGGTTGAGTGCTGATGTAGC 3'

AscI site BamHI site Homology

***loxP* arm primers**

P1149_07

5' TATCGAT**ATAACTTCGTATAGCATACATTATACGAAGTTAT***TAATTAA*

ClaI site ***loxP* site** ***Pac*I** site

CATCAGCACTCAACCATTCCCCAC 3'

Homology

P1149_08

5' TATCGATAACCTTCTGGAACTTGCCCTCAGTC 3'

ClaI site Homology

3' Homology arm primers

P1149_09

5' AGGCGCGCCATCGAT**ATAACTTCGTATAGCATACATTATACGAAGTTAT**

AscI ClaI ***loxP* site**

GATATCACTAGTAATATTACTGAGGGCAAGTTCCAGAAGGTTC 3'

EcoRV SpeI SspI Homology

P1149_10

5' TGTTTAAACGGCGCGCCATACAGGCTCATCGACAGATGGACC 3'

PmeI AscI Homology

Once completed the entire construct was excised and electroporated into manipulated embryonic stem (ES) cells. ES cells were screened for inclusion of the modified CXCR5 allele including the neomycin resistance selection cassette due to homologous recombination events using neomycin. $CXCR5^{fl}$ positive ES cells were injected into C57Bl/6N albino blastocysts to generate chimeric offspring, with ES cell contribution observed as black coat-colouring. Chimaeric mice were subsequently bred with C57Bl/6N albino mice again using black coat coloration to detect germline transmission. All positive offspring were screened by Southern blotting to confirm the presence of the $CXCR5^{fl}$ transgene. Cloning, ES work, and chimaera generation and germline transmission and screening were all performed by Ozgene Pty Ltd. Finally $CXCR5^{fl}$ positive offspring were crossbred with enhanced flipase (FLPe) FLP-deleter mice on a C57Bl/6 genetic background and resultant offspring shipped to the Roslin institute. The $CXCR5^{fl}$ mice (genotype $CXCR5^{fl/wt}$:$FLPe^{+/-}$) were interbred to generate $CXCR5^{fl/fl}$ homozygotes. All mice were screened for FLPe and at each generation a negative selection criteria for $FLPe^{+}$ was animals put in place to establish the line $CXCR5^{fl/fl}$:$FLPe^{-/-}$ (termed $CXCR5^{fl}$). This line was maintained in-house via standard breeding practices and used in subsequent breeding programs for Cre-mediated deletion of the $CXCR5^{fl}$ allele.

Figure 4.4 CXCR5^{fl} transgene construct

The three homology arms were cloned to surround the selection cassette in the FSniper plasmid to generate the final gene-targeting construct. After selection of positive ES cells and generation of chimeric mice F1 generation offspring were crossbred with FLPe mice on C57Bl/6 background to remove the selection cassette via in vivo FLP activity and generating the final CXCR5fl transgene. Screening of this transgene in offspring was performed by a PCR amplicon containing the 5' *loxP* (or not in wt animals) using primers that matched the genomic DNA sequence.

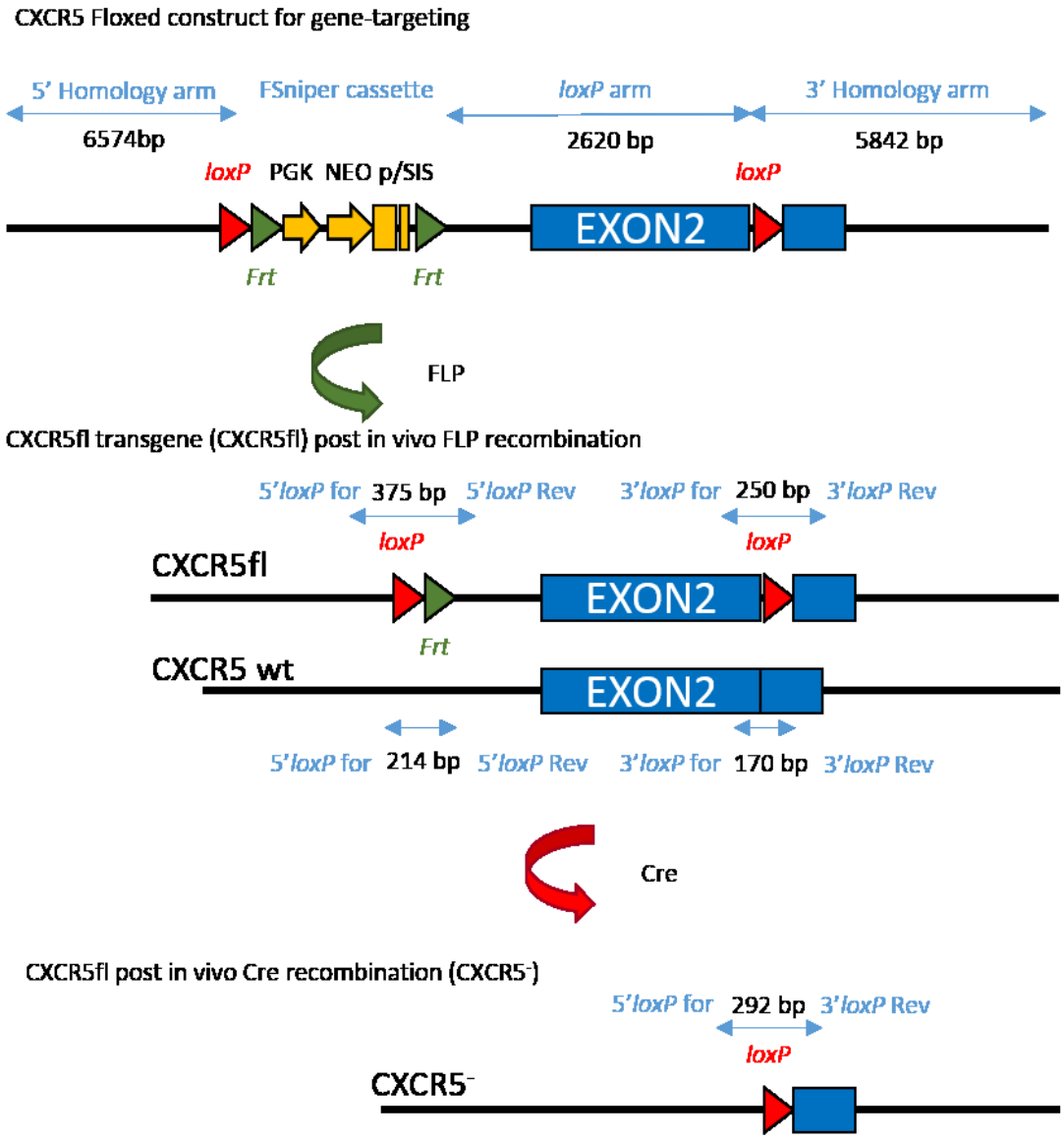

4.3.2 Genotyping analysis of conditional CXCR5^{fl} transgenic mice

For breeding and experimental use of CXCR5^{fl} conditional transgenic mice oligonucleotide sequences were designed to span either the 5' or 3' *loxP* insert regions (see figure 4.3 and Table 2.1), such that CXCR5^{fl} alleles produced a larger fragment size (Figure 4.5A & 4.5B lane 3) than wild type CXCR5 alleles (Figure 4.5A & 4.5B lane 2) allowing simple selection of homozygotes. Inclusion of the 3' *loxP* reverse primer into the 5' *loxP* mix allowed the visualisation of Cre-mediated recombined (CXCR5^{-}) alleles (Figure 4.5A, lane 4). The presence of a 203bp fragment of the CXCR5 coding sequence within Exon2 was detectable in both wild type (Figure 4.5C lane 2) and CXCR5^{fl} homozygotes (Figure 4.5C lane 3) but was undetectable following Cre-mediated recombination (Figure 4.5C lane 4), indicating that following Cre-mediated recombination of CXCR5^{fl} alleles, exon 2 of CXCR5 was successfully removed.

Figure 4.5 Genotyping of CXCR5^{fl} transgenic mice

Using primers generated against the genomic CXCR5 gene sequence that spanned the *loxP* inclusion sites both the presence of the CXCR5^{fl} allele and its status were determined (A & B). Inclusion of the *loxP* sequences at both 5' (A) and 3' (B) location produced larger fragment sizes than the corresponding genomic sequence in wild type mice. Cre-mediated recombination resulted in a loss of product due to loss of the internal primer site (B), therefore a combination of 5' l*oxP* forward and reverse primers supplemented with the 3'*loxP* reverse primer were used for all routine screening as this allowed the detection of Cre-recombined (i.e. CXCR5 null) alleles in the offspring (A). Similarly CXCR5 exon2 sequence were confirmed in floxed alleles but were undetectable following cre-mediated recombination (C). 1kb = 1 KB plus DNA ladder, fragment sizes indicated in base pairs.

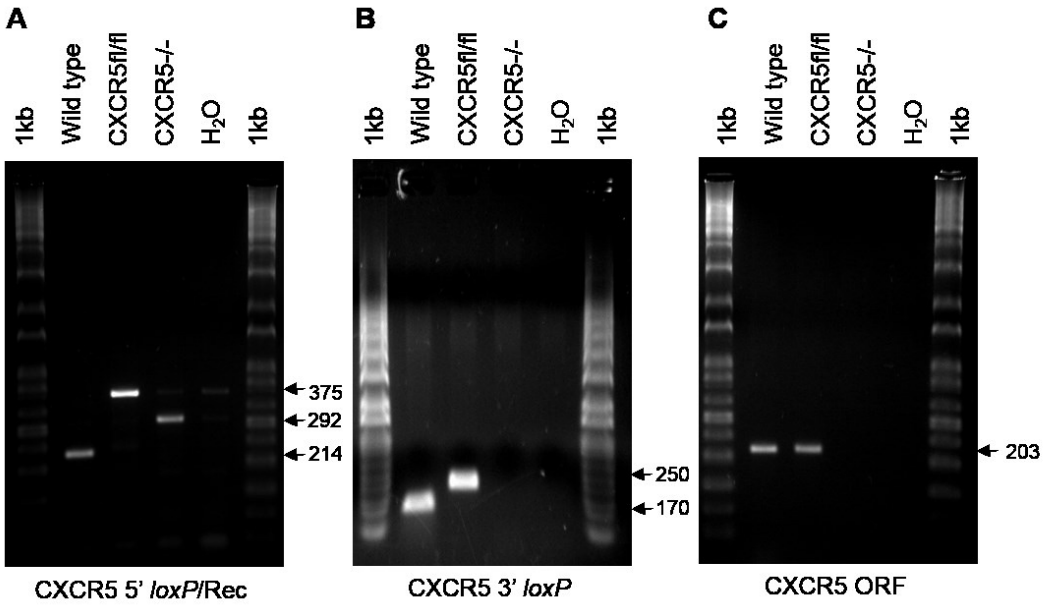

4.3.3 Generation of cell-specific CXCR5 knockout

To generate cell-specific CXCR5 knockout, the $CXCR5^{fl}$ transgene was crossbred onto mice expressing Cre under the control of specific gene promoters. Cre expression within these mice occurs within the same cells and tissues as the gene whose promoter is used to drive Cre, hence Cre-mediated deletion of the $CXCR5^{fl}$ allele only occurred within cell types that specifically express the gene used to drive Cre expression. Where possible cell-specific gene promoters can be selected as models for driving Cre expression, however careful analysis (i.e. as performed in Chapter 3 for the CD11c gene *Itgax*) must be undertaken to truly determine in which cell types the gene is expressed.

4.3.4 CD11cCre mediated CXCR5 knockout

To generate the study mice for the following chapters, $CXCR5^{fl}$ mice were crossbred with CD11cCre mice (Caton et al., 2007) to produce a final genotype of $CD11cCre^{+/-}$: $CXCR5^{fl/fl}$ (termed CD11cCre:$CXCR5^{fl}$) compound transgenic mice. Subsequent generations were produced by backcrossing these mice with $CXCR5^{fl}$ mice. All offspring were genotyped for both $CXCR5^{fl}$ and CD11cCre (see Chapter 2 and figure 4.5 for details). All mice were $CXCR5^{fl}$ homozygotes (Figure 4.6A) regardless of the presence or absence of CD11cCre (Figure 4.6B) no recombination of the $CXCR5^{fl}$ allele was detectable in genomic DNA samples extracted from ear snip material for the purposes of genotyping these mice. The production of a CXCR5-deficient transgenic mouse was possible in some instances due to cre-mediated recombination of the $CXCR5^{fl}$ allele. A Cre^{-}/$CXCR5^{-}$ inbred line (termed $CXCR5^{-}$) was generated and used for comparison purposes against $CXCR5^{fl}$ and CD11cCre:$CXCR5^{fl}$ mice.

4.3.5 Cellular characterisation of CD11cCre mediated CXCR5 knockout.

Investigation of total splenocytes (see 2.8.1) extracted from either $CXCR5^{fl}$ or CD11cCre:$CXCR5^{fl}$ mice revealed only $CXCR5^{fl}$ allele fragments via PCR analysis of genomic DNA (Figure 4.6). Using magnetic-activated cell sorting (see 2.10), splenocytes from CD11cCre:$CXCR5^{fl}$ mice were isolated into a $CD11c^{+}$ population (i.e. cDC) and the $CD11c^{-}$ population were further sorted on the expression on CD11b, B220 and CD90.2 to broadly represent macrophages, B cells and T cells respectively. Using RTPCR analysis a 196bp

fragment of the Cre coding sequence was barely detectable in total splenocytes from CD11cCre:CXCR5^{fl} mice (Figure 4.6C lane 3). From sorted cell populations expression of Cre was only detectable within the CD11c^{+} cells (Figure 4.6C lane 4). Analysis of the genomic DNA from these same cell populations revealed cre-mediated recombination of the CXCR5^{fl} allele had only occurred in CD11c^{+} cells of CD11cCre:CXCR5^{fl} mice (Figure 4.6D lane 4) , thus confirming CD11c restricted CXCR5 knockout.

Figure 4.6 Genetic analysis of CD11cCre:CXCR5^{fl} compound transgenic mice

Transgenic mice were produced under standard breeding conditions to be CXCR5^{fl} homozygote (A) either with or without CD11cCre transgene (B). Expression analysis by reverse-transcriptase PCR of Cre recombinase sequence revealed it was barely detectable in CD11cCre:CXCR5^{fl} total splenocytes however following MACS sorting of cell populations Cre was detectable in CD11c^{+} cell populations, but not CD11c^{-}/CD11b^{+}, CD11c^{-}/B220^{+} or CD11c^{-}/CD90.2^{+} (C). Investigation of genomic DNA from these same cell populations confirmed Cre activity only in CD11c^{+} cells with complete recombination of the CXCR5^{fl} allele (D).

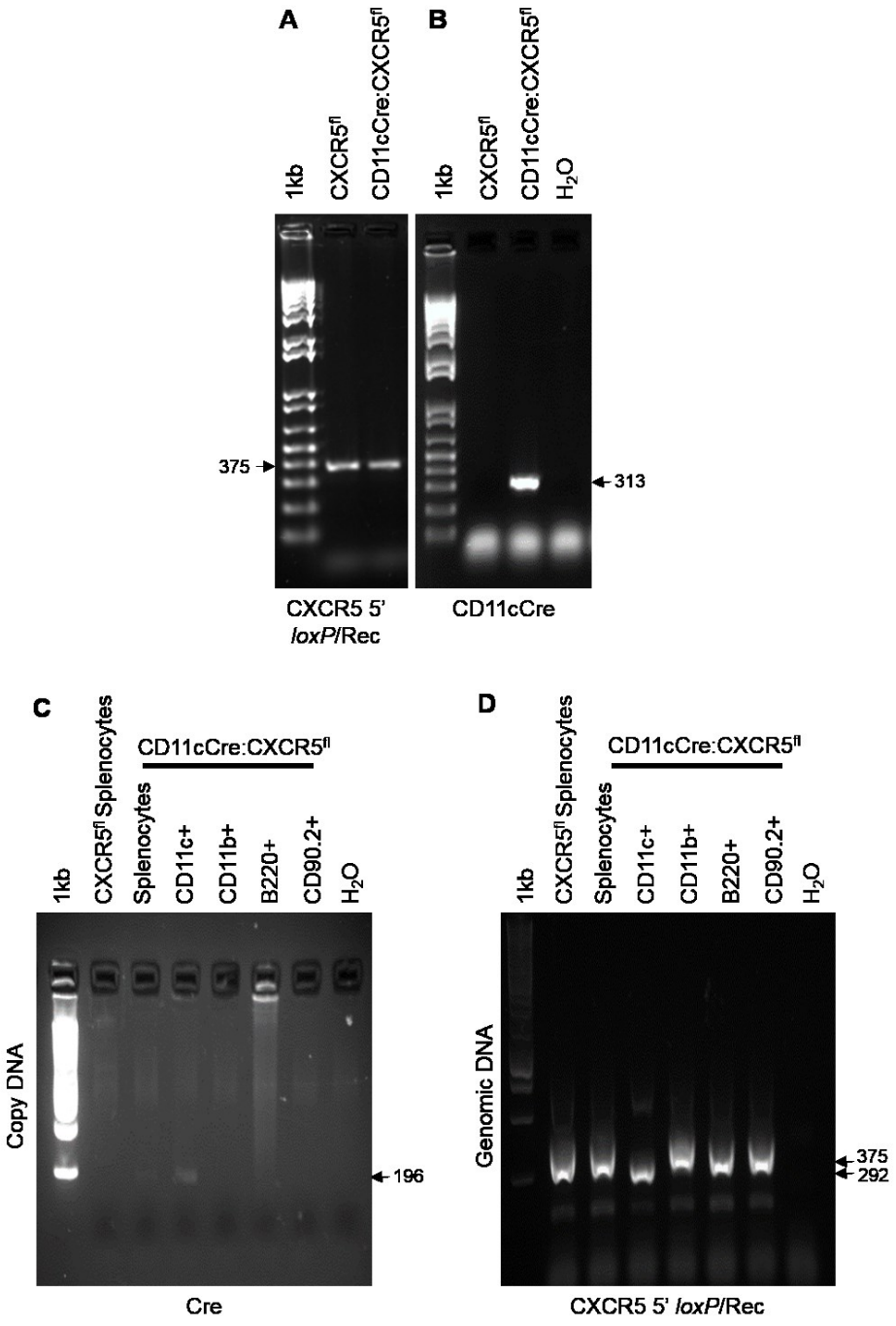

4.3.6 Anatomical characterisation of lymphoid tissues in CD11cCre:CXCR5^{fl} mice

Many lymphoid tissue structures are small and difficult to locate and identify macro-anatomically due to their positioning in fat deposits and similarity in colour to surrounding tissue. To perform anatomical characterisation of lymphoid tissues, mice of genotypes CXCR5^{fl}, CD1Cre:CXCR5^{fl} and CXCR5^{-} were injected with Chicago Sky Blue 6B ink and sacrificed 1 week later (see 2.3.6). Sequestration of Chicago Sky Blue 6B ink allowed more accurate identification and counting of both nodes and in some tissues the number of follicular structures within them, e.g. caecal patch (Table 4.1).

The majority of lymphoid structures develop consistently, however lumbar aortic lymph nodes and lateral iliac lymph nodes are known to develop inconsistently. Within our analysis some constant developing lymph nodes were not always identified but this is more likely due to failure of recognition of these structures rather than a failure of their development. Overall CXCR5^{fl} mice develop lymphoid structures with the same incidence and frequency of follicular structures (Table 4.2) as has been reported for wild type (i.e. non-transgenic) mice (Van den Broeck et al., 2006). Furthermore investigation of CD11cCre:CXCR5^{fl} mice revealed indistinguishable incidence and frequency of lymphoid structures developing when compared to CXCR5^{fl} mice (Table 4.2). These data suggest that despite CD11c-mediated CXCR5 knockout within CD11cCre:CXCR5^{fl} mice there has been no impact upon the induction of lymphoid organogenesis despite reports of Peyer's patch LTi cells expressing CD11c. Importantly CD11cCre:CXCR5^{fl} mice develop intestinal Peyer's patches, mesenteric lymph nodes and spleen structures and are therefore applicable for use in further studies within this thesis.

Table 4.2 Assessment of lymphoid organogenesis in CXCR5^{fl}, CD11cCre:CXCR5^{fl} and CXCR5-deficient mice

Incidence as expressed by the number of times positively identified/number of mice investigated and mean number of follicles or nodes and range (where variable) of follicle or node number were counted at the macroscopic level following sequestration of Chicago Sky Blue 6B ink. ln. = lymph node. *reported inconstant.

Lymphoid structure	CXCR5^{fl} Incidence	CXCR5^{fl} number (range)	CD11cCre: CXCR5^{fl} Incidence	CD11cCre CXCR5^{fl} number (range)	CXCR5- Incidence
Spleen	6/6	1	8/8	1	8/8
Mandibular ln.	6/6	2	8/8	2	8/8
Accessory mandibular ln.	6/6	2	8/8	2	8/8
Superficial parotid ln	6/6	2	8/8	2	8/8
Cranial deep cervical ln.	6/6	2	8/8	2	8/8
Proper axillary ln. (Brachial)	6/6	5 (4-6)	8/8	5 (4-6)	0/8
Accessory axillary ln.	6/6	5 (2-7)	8/8	5 (3-6)	0/8
Subiliac ln. (Inguinal)	6/6	2	8/8	2	1/8
Sciatic ln.	6/6	2	8/8	2	8/8
Popliteal ln.	6/6	2	8/8	2	8/8
Cranial mediastinal ln.	6/6	4	7/8	4	8/8
Tracheobronchal ln.	6/6	1	8/8	1	8/8
Caudal mediastinal ln.	6/6	1	8/8	1	8/8
Gastric ln.	6/6	1	7/8	1 (0-1)	8/8
Pancreaticoduodenal ln.	6/6	1	7/8	1 (0-1)	8/8
Jejunal ln. (Mesenteric)	6/6	5 (4-6)	8/8	5 (5-6)	8/8
Colic ln.	5/6	1 (0-2)	7/8	1 (0-3)	5/8
Caudal mesenteric ln.	6/6	1	8/8	1	0/8
Renal ln.	6/6	2 (1-3)	8/8	2	8/8
Lumbar aortic ln. *	4/6	2 (0-2)	1/8	1 (0-1)	2/8
Lateral iliac ln. *	5/6	1 (0-1)	2/8	1 (0-1)	4/8
Medial iliac ln.	6/6	2 (1-2)	8/8	2	0/8
External iliac ln.	2/6	1 (0-1)	6/8	1 (0-1)	2/8
Peyer's patches	6/6	6 (5-9)	8/8	6 (5-7)	0/8
Caecal patch (follicles)	6/6	5 (3-8)	7/8	2 (0-5)	8/8

Similar to previous reports of CXCR5-deficient mice (Müller et al., 2003), our novel cre-mediated CXCR5$^-$ mice revealed a complete absence of intestinal Peyer's patches and lack of certain specific lymph nodes (Table 4.2). CXCR5$^-$ mice also displayed complete absence of axillary (brachial), caudal mesenteric ln., medial iliac ln. and almost complete absence of subiliac ln. (inguinal) lymph nodes (1 of 8 mice examined had a single inguinal lymph node on the right side, but was lacking the left side inguinal node). Previous reports of CXCR5-deficient mice suggest invariant presence of Peyer's patches, presence of brachial lymph nodes and only rare loss of inguinal lymph nodes which are in contrast to our findings.

4.3.7 Flow cytometric analysis of CD11cCre:CXCR5^{fl} mice

Investigation of expression of CXCR5 on various cell populations was performed via flow cytometric analysis (see 2.14). In CXCR5^{fl} mice CD11c$^+$ cells revealed CXCR5$^-$ and CXCR5$^+$ subpopulations, with the CXCR5$^+$ cells representing ~ 75% of the CD11c$^+$ cell population in Peyer's patch (Figure 4.7A), but only ~20% of the total population in MLN (Figure 4.7B) and in spleen (Figure 4.7C). CXCR5 was also expressed highly on a subpopulation of CD11b$^+$ cells, especially in MLN (Figure 4.7E) and most B220$^+$ cells (Figure 4.7G-I). Most CD3$^+$ cells are CXCR5$^-$ except for a small population of follicular helper T cells (Figure 4.7J-L). In all CD11cCre:CXCR5^{fl} mice a reduction in CXCR5 expression by CD11c$^+$ cells was observed in all tissues investigated as expected (Figure 4.7A-C). Within Peyer's patches CXCR5 was observed with an approximately 10-fold reduction in mean fluorescence intensity on CD11c$^+$ cells in CD11cCre:CXCR5^{fl} mice than CXCR5^{fl} mice (Figure 4.7A, N=6, P<0.0001 via two-sample T-test), in lymph node and spleen CD11c$^+$CXCR5^{Hi} populations were reduced (Figure 4.7B & 4.7C). A reduction in CXCR5$^+$/CD11b$^+$ cells was also observed in the Peyer's patch (Figure 4.7D) and MLN (Figure 4.7E) most likely due to overlapping expression of CD11c & CD11b upon MNP in these tissues, no alteration to CXCR5$^+$/CD11b$^+$ were observed in the spleen (Figure 4.7F). Within mesenteric lymph nodes of CD11cCre:CXCR5^{fl} mice the majority of the B220$^+$ population has reduced CXCR5 (Figure 4.7H), possibly due to altered B-cell follicular structure (see Figure 4.11). Furthermore the loss of CD3$^+$/CXCR5$^+$ follicular helper T cells in mesenteric lymph node of CD11cCre:CXCR5^{fl} mice (Figure 4.7K) but not spleen or Peyer's patch also indicates altered follicular integrity within the lymph node, as these cells are not known to express CD11c. In the spleen of CD11cCre:CXCR5^{fl} mice a subpopulation of B220$^+$ cells had reduced CXCR5$^+$ (Figure 4.7I), most likely those known to express CD11c (Rubtsov et al., 2015).

Investigation of total cell populations within lymphoid tissues were also investigated via flow cytometry (Figure 4.8). There were no statistically significant differences observed between any of the cell populations investigated in either Peyer's Patches (Figure 4.8A), mesenteric lymph nodes (Figure 4.8B) or spleen (Figure 4.8C). Within Peyer's patches and mesenteric lymph nodes there was a trend for a slight reduction in frequency of $CD11c^+$ and $CD11b^+$ cells. In spleen there was a trend for a slight reduction in $CXCR5^+$ cells, possibly due to the loss of CXCR5 on some B cells (Figure 4.7I). These data suggest that not only are lymphoid tissues undergoing normal organogenesis, there are also no deficits in various key immune cell types localising to and populating these structures.

Figure 4.7 Flow cytometry analysis of CD11c-mediated CXCR5 knockout

CXCR5 expression was measured on cell populations gated for expression of CD11c (A –C), CD11b (D-F), B220 (G-I) and CD3 (J-L) in Peyer's patch, mesenteric lymph node and spleen of CXCR5^{fl} and CD11cCre:CXCR5^{fl} mice.

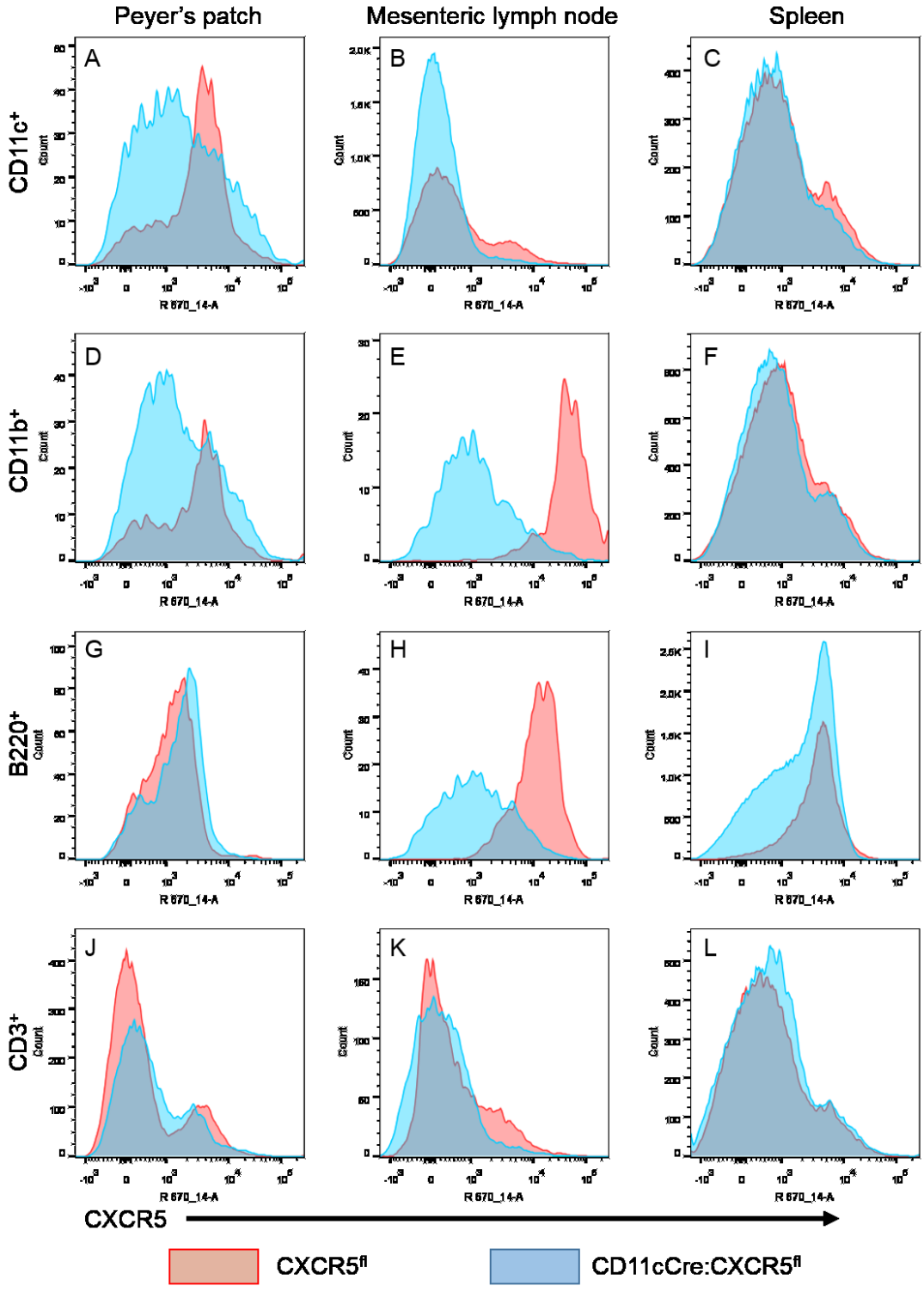

Figure 4.8 Relative cell frequencies in lymphoid tissue of CXCR5^{fl} and CD11cCre:CXCR5^{fl} mice

Cell populations of Peyer's patch (A), mesenteric lymph nodes (B) or spleen (C) were enumerated sing standard flow-cytometric techniques. The relative amounts of CD11c^{+}, CD11b^{+}, B220^{+} and CD3^{+} cells and total CXCR5^{+} cells are displayed expressed as mean percentage of total cells ±SEM.

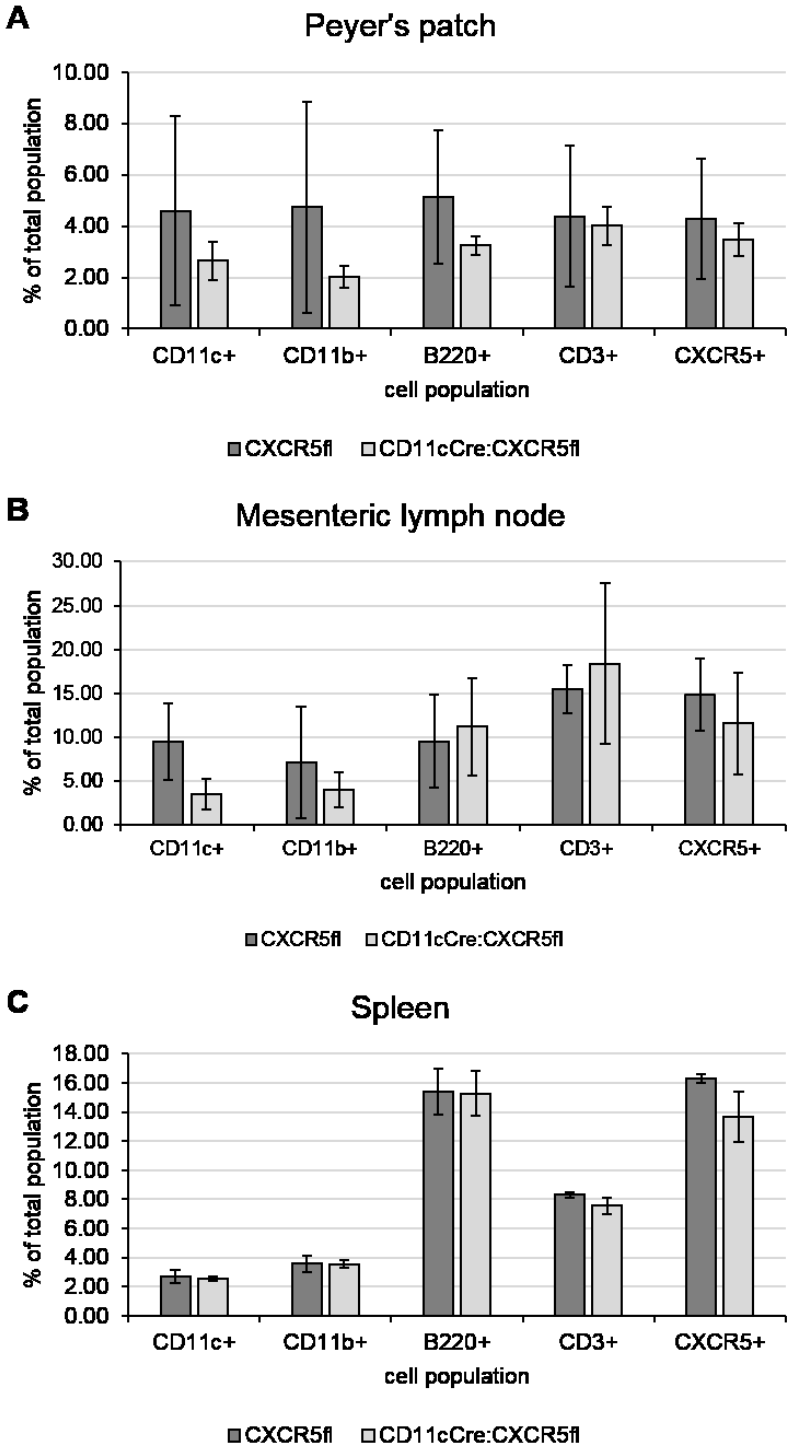

4.3.8 Peyer's patch microarchitecture in CD11cCre:CXCR5^{fl} mice

Within the small intestine in CXCR5^{fl} mice, CD11c^{+} cells were observed within the intestinal lamina propria and Peyer's patches (Figure 4.9A see also 3.3.1 and 3.3.2). Furthermore the presence of follicular dendritic cells (FDC) expressing CD35 (Figure 4.9C) and PrP (Figure 4.9E) were confirmed within Peyer's patch structures (Figure 4.9G). In CD11cCre:CXCR5^{fl} mice, investigation of the lymphoid microarchitecture no difference in the lamina propria localization of CD11c^{+} cells were observed between CD11cCre:CXCR5^{fl} and CXCR5^{fl} mice. However, an altered localisation of CD11c^{+} cells to para-follicular regions such as the interfollicular T-cell region was detectable within the Peyer's patch (Figure 4.9B & 4.9H yellow arrows). Despite this altered localization of CD11c^{+} cells in CD11cCre:CXCR5^{fl} Peyer's patches, FDC expressing CD35 (Figure 4.9D) and PrP (Figure 4.9F) were observed in all Peyer's patches from all mice examined. These data suggest that Peyer's patch structures develop with normal follicles containing mature FDC in CD11cCre:CXCR5^{fl} mice, however CD11c^{+} cells are unable to traffic to them effectively and mislocate to areas known to be regulated by CCR7-CCL19/21 signalling (Cyster, 2000).

As M-cells are critical for the uptake of prions following oral infection (Heppner et al., 2001a, Donaldson et al., 2012) and their development is potentially regulated by CD11c^{+} B cells (Ebisawa et al., 2011) it was therefore important to check M-cell status in CD11cCreCXCR5^{fl} mice. Utilising wholemount staining of intestinal Peyer's patches with anti-glycoprotein-2 and the lectin *Ulex Europaeus* agglutinin 1 to identify the presence of mature M-cells . Mature M-cells were detectable in the follicle-associated epithelium of Peyer's patches examined from both CD11cCre:CXCR5^{fl} and CXCR5^{fl} mice (Figure 4.10). CXCR5^{fl} mice possessed on average 84±3 M-cells per follicle (N=17) and CD11cCre:CXCR5^{fl} mice possessed on average 83±2 M-cells per follicle (N=31), showing no difference in their frequency between CXCR5^{fl} and CD11cCre:CXCR5^{fl} mice (P = 0.696, CI 95% via two sample T-test). These data suggest M-cells develop normally upon Peyer's patch structures in CD11cCre:CXCR5^{fl} mice.

Figure 4.9 Peyer's patch microarchitecture

Immunohistochemical analysis of Peyer's patches from CXCR5fl and CD11cCre:CXCR5fl mice. Detection of CD11c (A, B), CD35 (C, D) and PrP (E,F) in intestinal Peyer's patches reveals aberrant extra-follicular localization of $CD11c^{+}$ cell accumulations in $CD11cCre:CXCR5^{fl}$ mice only (B, yellow arrows) apparently unable to traffic to $CD35^{+}/PrP^{+}$ FDC (F).

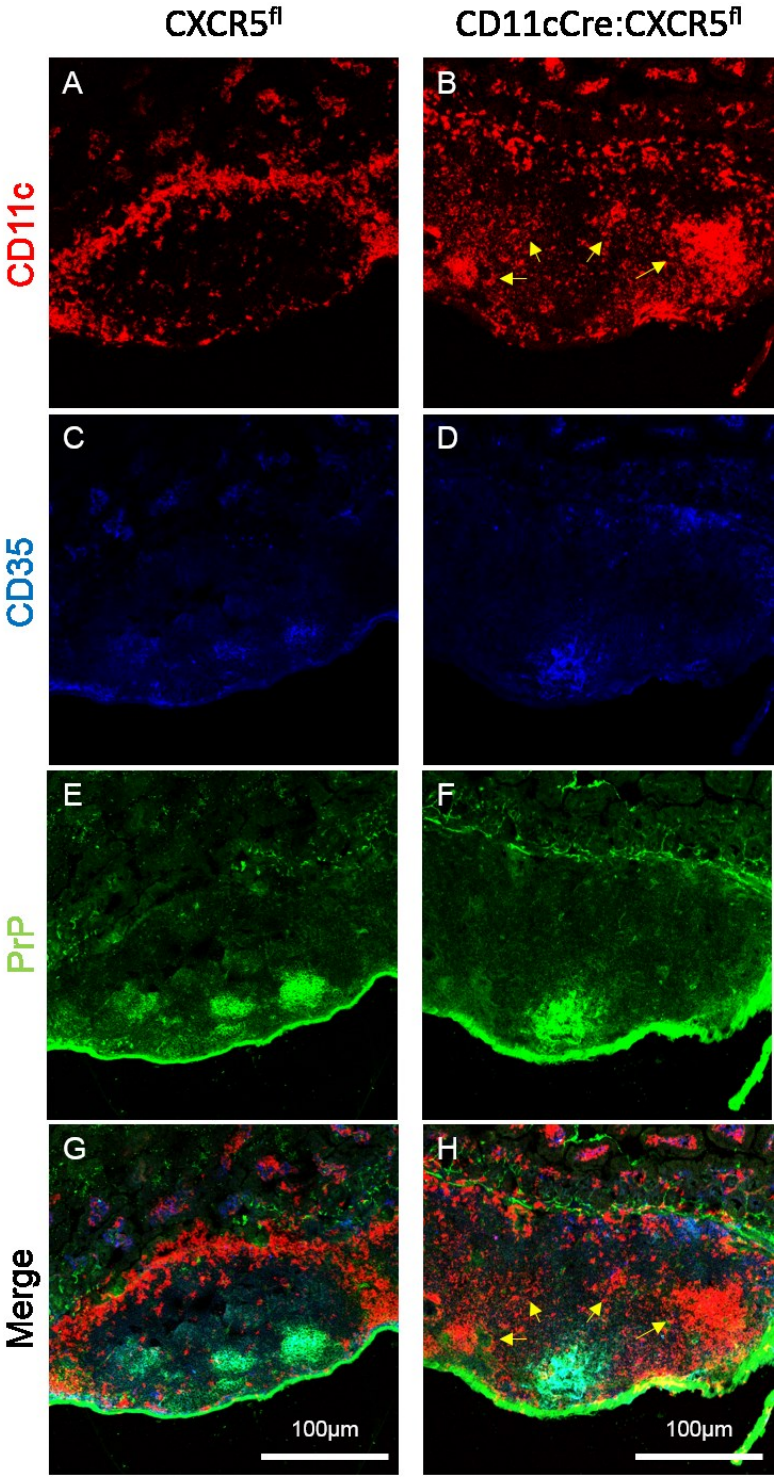

Figure 4.10 Development and localisation of Peyer's patch M-cells

Wholemount immunostaining for M-cell marker Glycoprotein-2 and with the lectin *Ulex Europaeus* agglutinin 1 (UAE-1), reveals M-cells localised to the FAE of Peyer's patches in both CXCR5^{fl} (A) and CD11cCre:CXCR5^{fl} mice (B).

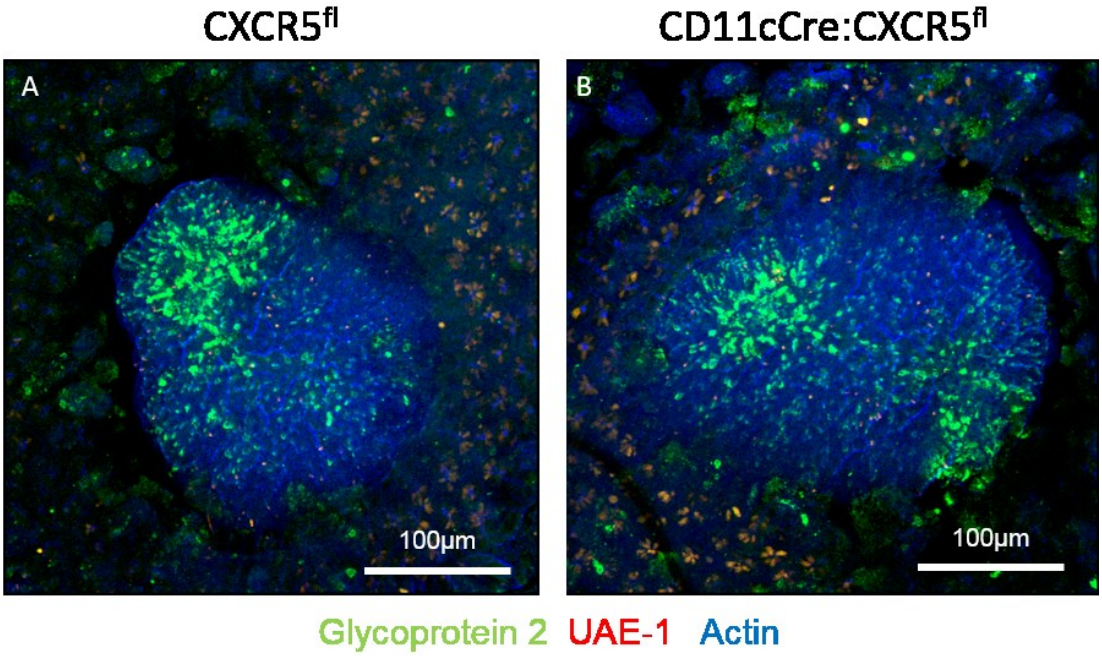

4.3.9 Mesenteric lymph node microarchitecture in CD11cCre:CXCR5^{fl} mice

Investigation of lymphoid microarchitecture in mesenteric lymph nodes revealed a normal distribution of CD11c^{+} (green) cells to cortical regions with IgM^{+} (red) B-cell follicles containing PrP expressing (blue) FDC in CXCR5^{fl} mice (Figure 4.11A see also 3.3.3). Investigation of CD11c^{+} cell localisation revealed them mostly surrounding the B-cell follicles with occasional cells in proximity to CD35^{+}/PrP^{+} FDC (Figure 4.11C). Mesenteric lymph nodes of CD11cCre:CXCR5fl mice however appeared to be slightly disrupted, with an over-abundance of CD11c^{+} cells within the cortex (Figure 4.11B) and surrounding the FDC containing follicles (Figure 4.11D). Less defined B-cell regions were identifiable expressing IgM (Figure 4.11B), however mature CD35^{+}/PrP^{+} FDC were still present (Figure 4.11D). These data suggest that mesenteric lymph node structures develop normally in CD11cCre:CXCR5^{fl} mice with mature FDC, however the follicular structure is not as well-defined and increased CD11c^{+} cells are observed in both cortical and peri-follicular regions.

Figure 4.11 Lymph node microarchitecture in CXCR5^{fl} and CD11cCre:CXCR5^{fl} mice

Detection of CD11c, IgM and PrP (A, B) and CD11c, CD35 and PrP (C, D) in mesenteric lymph nodes reveals increased cortical and extra-follicular build-up of CD11c^{+} cell and altered IgM^{+} B-cell follicular structures in CD11cCre:CXCR5^{fl} mice despite the presence of mature CD35^{+}/PrP^{+} FDC. Scale bars = 100 µm

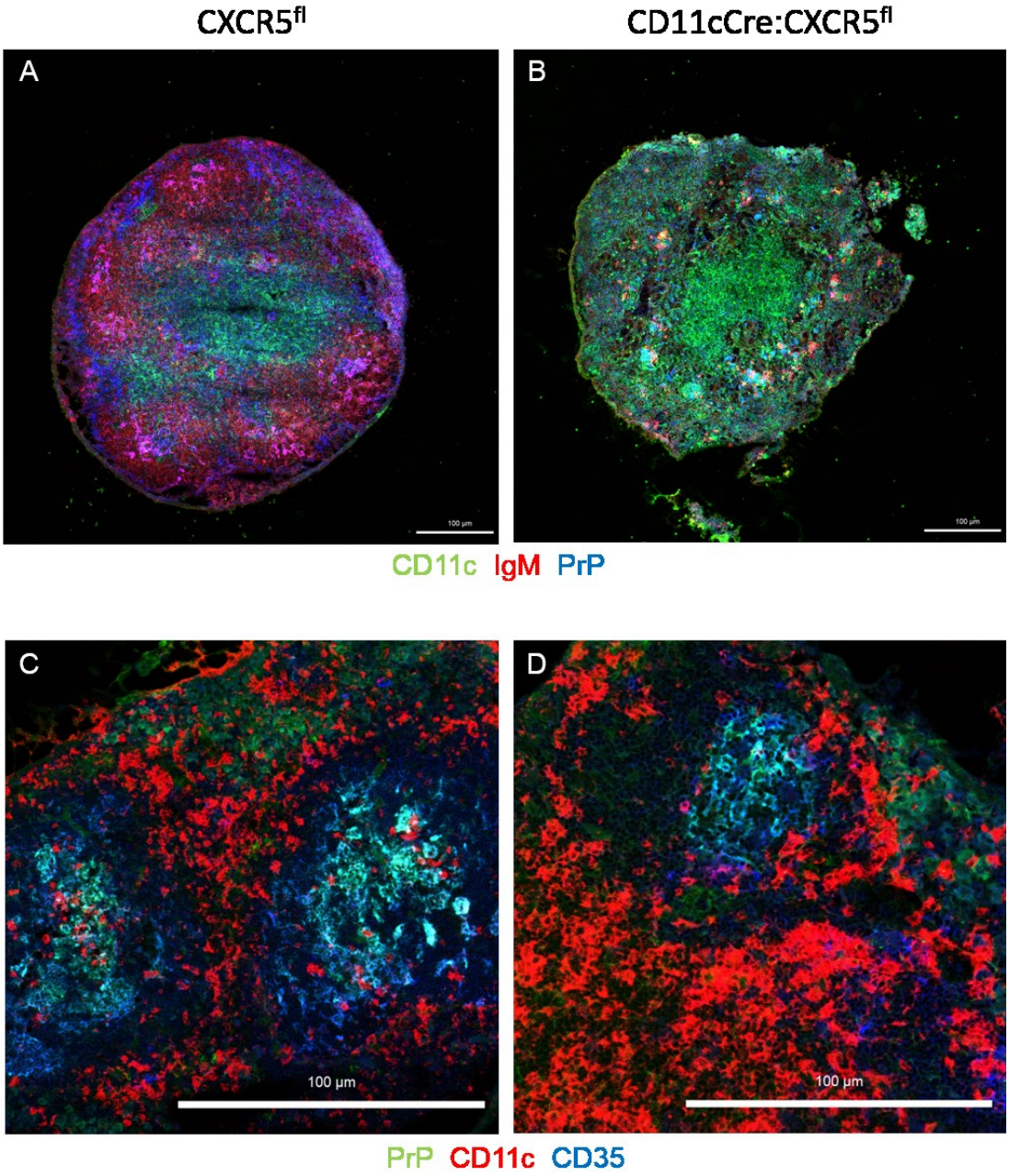

4.3.10 Spleen microarchitecture in CD11cCre:CXCR5^{fl} mice

Investigation of lymphoid microarchitecture in spleen revealed CD11c^{+} cells mostly localised to the red pulp and marginal zone regions in CXCR5^{fl} mice (Figure 4.12A, see also 3.3.4). In contrast in CD11cCre:CXCR5^{fl} mice an increase in CD11c^{+} cells were observed within the splenic white pulp region localised to the T-cell zone surrounding the central arteriole (Figure 4.12B). Mature CD35^{+}/PrP^{+} FDC were observed within follicles of both CXCR5^{fl} and CD11cCre:CXCR5^{fl} (Figure 4.12C & 4.12D). Investigation of the surface marker molecules sialoadhesin (investigated further in Chapter 7) and SIGN-R1 (investigated further in Chapter 8), revealed no differences between CXCR5^{fl} and CD11cCre:CXCR5^{fl} mice indicative of no alteration to resident marginal zone MNP that are also CD11c^{+} (Figure 4.12E & 4.12F). These data suggest that splenic microarchitecture develops normally with B-cell follicles forming containing functional FDC. Similar to Peyer's patches aberrant localisation of CD11c^{+} cells occurs with over-representation of them within the CCR7-CCL19/21 organised T-cell regions (Figure 4.12B & D), implying that CD11c^{+} cells are unable to correctly localise to B-cell follicles.

Figure 4.12 Splenic follicular microarchitecture in CXCR5^{fl} and CD11cCre:CXCR5^{fl} mice

Detection of CD21/35 and CD11c reveals mostly marginal zone CD11c^{+} cells in CXCR5^{fl} spleen (A) but an aberrant buildup of CD11c^{+} cells in T-cell regions of the white pulp (B). Detection of CD11c, CD35 and PrP reveals mature FDC in both CXCR5^{fl} (C) and CD11cCre:CXCR5^{fl} (D) mice. Investigation of resident CD11c^{+} marginal zone macrophage markers SIGN-R1 and sialoadhesin revealed no differences between CXCR5^{fl} (E) and CD11cCre:CXCR5^{fl} mice (F).

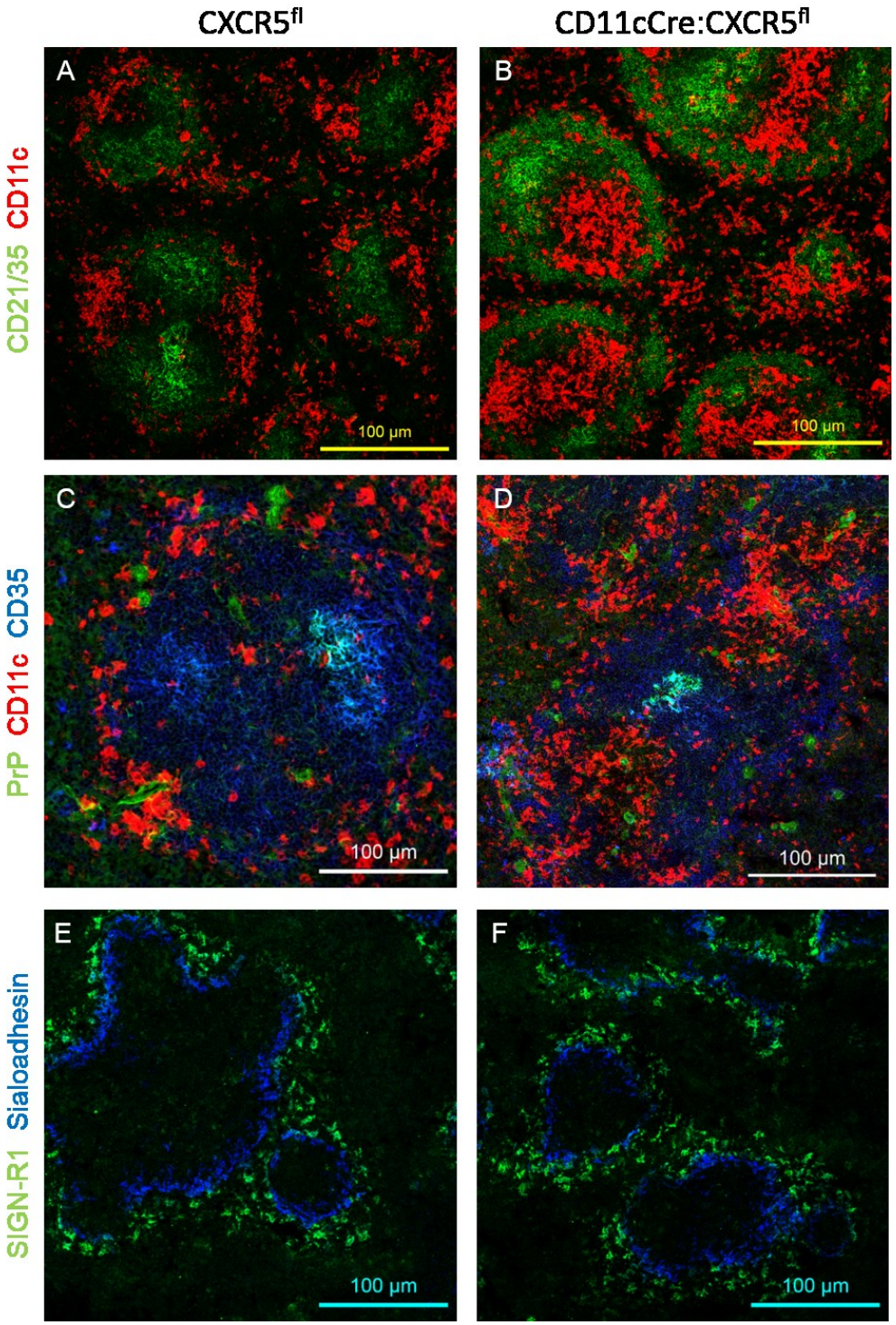

4.4 Discussion

The expression of the chemokine receptor CXCR5 mediates chemotaxis to the chemokine CXCL13. The expression of this receptor-ligand pair is important for the generation (lymphoid organogenesis) and maintenance of the B-cell follicular structure in lymphoid organs and the trafficking of specific cells (e.g. B cells, T_{FH} and cDC) to these structures. The effect of CXCR5 expression upon specific cell types has been investigated utilising both CXCR5-deficient transgenic mouse models and complex bone-marrow reconstituted models. To circumvent the complications and caveats of using such models the Cre/*loxP* targeted transgenic technology was used here. Introduction of *loxP* sites around the major coding portion of the CXCR5 gene did not interrupt CXCR5 expression unless in the presence of Cre recombinase. Cre-mediated recombination resulted in expected recombination of the $CXCR5^{fl}$ allele and loss of CXCR5. Using a well-characterised CD11c mediated Cre-expressing model (Caton et al., 2007) we have successfully deleted CXCR5 in $CD11c^+$ cells and observed the resultant phenotype.

In CD11cCre:$CXCR5^{fl}$ mice, all observations suggest that lymphoid organogenesis occurs normally as all major gross anatomical lymphoid structures were present at similar frequency to that observed in $CXCR5^{fl}$ mice (Table 4.2). Furthermore investigation of intestinal Peyer's patch, mesenteric lymph node and spleen revealed normal lymphoid microarchitecture with defined B and T cell regions and the presence of mature ($CD35^+/PrP^C$ expressing) FDC within B-cell follicles (Figures 4.8, 4.10 & 4.11). Migratory $CD11c^+$ populations (i.e. cDC) are normally only rarely observable in lymphoid organs (Figures 4.8, 4.10 & 4.11). This is likely due to their function as antigen presenting cells (APC), during which they travel from exposure sites to present antigen to cognate T, B or possibly FDC cells and following a short period of immunological synapse formation, priming and educating effector cells with co-stimulatory molecule signalling, cDC are typically deleted via apoptosis following successful antigen presentation (Chen and Wang, 2010). In CD11cCre: $CXCR5^{fl}$ mice however an increase in $CD11c^+$ cells was observed within T cell regions of lymphoid organs (e.g. in splenic white pulp Figure 4.11B). These data suggest that migratory $CD11c^+$ cells can enter the T cell region, but their failure to exit into the B-cell follicle due to the lack of CXCR5 expression may delay completion of their life-cycle. Maturation of cDC has been described by the switch from expression of the chemokine receptors CCR6 to CCR7, initiating their traffic to T cell regions of lymphoid organs (Dieu et al., 1998). By definition the $CD11c^+$ cells building up within secondary lymphoid organs of CD11cCre:$CXCR5^{fl}$ mice must be mature (i.e. $CCR7^+$) but due

to their inability to express CXCR5 or interact with relevant effector cells (i.e. B cells, FDC or cognate T cells) in CD11cCre:CXCR5^{fl} mice they fail to undergo deletion via apoptosis.

The generation of novel Cre-mediated CXCR5-deficient mice allowed the confirmation that the observed genetic recombination of the CXCR5^{fl} allele results in functional loss of CXCR5. Complete removing of all CXCR5 expression resulted in a severe deficit in lymphoid organogenesis with mice lacking several defined lymph node structure and complete loss of intestinal Peyer's patches similar to standard CXCR5 knockout mice reported previously (Müller et al., 2003). CD11c-mediated deletion of CXCR5 failed to alter localisation of resident CD11c^{+} cell populations within lymphoid organs with effective splenic marginal zones and lymph node subcapsular sinus populations appearing intact and expressing relevant markers. Furthermore the presence of CD11c^{+} tingible body macrophages was unaltered in CD11cCre:CXCR5^{fl} mice suggesting that for resident CD11c^{+} populations the expression of CXCR5 is not critical for the correct localisation either within the follicle or localised to the follicular marginal zone. It is likely that CXCR4 regulates the positioning of these cell populations as signalling via its ligand CXCL12 also provides MNP differentiation and pro-survival signals necessary for long lived resident cells (Sánchez-Martín et al., 2011). CXCR4 is also critical along with CXCR5 for the establishment of the germinal centre dark zone and light zone respectively during the germinal centre reaction (Allen et al., 2004). Tingible body macrophages are hypothesised to be one of the major sources of CXCL12 (Barone et al., 2008).

These data further suggest that normal lymphoid organogenesis and microarchitecture is established as normal in CD11cCre:CXCR5^{fl} mice. No differences were observed in the presence and follicular size of any of the lymphoid structures investigated in CD11cCre:CXCR5^{fl} mice when compared to CXCR5^{fl} mice proving there were no deficits in lymphoid organogenesis. Furthermore B-cell follicular structure developed sufficiently to allow the differentiation and maintenance of mature and correctly localised FDC. The major phenotypic impact of CD11c-mediated CXCR5 deletion appears to be restricted to preventing follicular-homing of CD11c^{+} cDC and their subsequent deletion whilst performing antigen presenting functions. As such this model represents a tractable and usable model for the investigation of follicular-homing of cDC. For example in the following chapters CD11cCre:CXCR5^{fl} mice are investigated in infection models such as prion disease (Chapter 5) or gastrointestinal helminth infection (Chapter 6) in order to test the hypotheses that

$CXCR5^+$ cDC play critical roles in the transport of prions to FDC or antigens to the B-cell follicle.

Chapter 5. Effect of CD11c-mediated CXCR5 knockout on peripheral prion pathogenesis

5.1 Abstract

Prion diseases are protein-misfolding neurodegenerative disorders of the central nervous system, many of which can naturally spread via oral exposure. Following oral exposure, early prion replication upon follicular dendritic cells (FDC) in Peyer's patches is obligatory for the efficient spread of disease to the brain (termed neuroinvasion). M-cells appear critical for the uptake of prions from the gut but how prions are transported from M-cells to FDC is currently unknown. $CD11c^+$ cells have been suggested to play an important role in the initial uptake and transfer of prions to FDC since their depletion has previously been shown to reduce susceptibility to oral prion infection. FDC are non-mobile cells of stromal origin which reside within B cell follicles and secrete the chemokine CXCL13. CXCL13 stimulates chemotactic movement of cells expressing the cognate receptor CXCR5 towards the chemokine source. To understand further how prions are transported to FDC in lymphoid tissues such as Peyer's patches, lymph nodes and spleen, we generated a conditional Cre/*loxP* gene knockout mouse model in which $CD11c^+$ cells were unable to express the chemokine receptor CXCR5. Following oral exposure, CD11cCre:$CXCR5^{fl}$ mice displayed inefficient transfer of prions to FDC in lymphoid tissues such as Peyer's patches. CD11cCre:$CXCR5^{fl}$ mice are statistically significantly less susceptible to oral prion infection than $CXCR5^{fl}$ control mice which express CXCR5 normally. These data reveal that CXCR5-mediated chemotaxis by $CD11c^+$ cells constitutes an efficient mechanism for the delivery of prions to FDC. Blocking this mechanism of prion transport alters pathogenesis and reduces susceptibility to oral prion infection.

5.2 Introduction

The most common likely form of prion exposure is via dietary consumption of infected material as evidenced by the propagation of bovine spongiform encephalopathy (BSE) within the UK cattle population via meat and bone meal supplements and to other animals and humans via the food chain. Following oral challenge the infectious prions must pass from the gut lumen across the epithelial gut wall to cause infection. The most likely mechanisms may involve either direct transcytosis through gut epithelial cells, uptake via microfold cells (M-cells), or uptake by lumenal-antigen sampling dendritic cells. M-cells are specialised for the transport of antigen across the epithelial barrier (Neutra et al., 1996). For this purpose, M-cells are localised to the follicle-associated epithelium (FAE) structures covering secondary lymphoid organs of the gut-associated lymphoid tissue (GALT), e.g. Peyer's patches. M-cells function to sample antigens in the gut lumen and allow rapid presentation to the resident lymphoid cells situated immediately against their basal aspect. Depletion of M-cells prior to oral prion infection blocked pathogenesis (Donaldson et al., 2012) indicative of M-cells constituting the most efficient route of prion uptake, though other non M-cell routes of prion uptake have been observed (Kujala et al., 2011).

For the efficient transmission of prions to the central nervous system (CNS) after peripheral exposure (a process termed neuroinvasion), the replication of prions within secondary lymphoid tissues is crucial (Donaldson et al., 2015). Following oral exposure, the uptake and replication of prions in intestinal Peyer's patches is critical for infection (Prinz et al., 2003c). Within lymphoid tissues such as Peyer's patches, prions replicate upon stromal-derived follicular dendritic cells (FDC) located within the B cell follicles (Mabbott et al., 2000, Montrasio et al., 2000, McCulloch et al., 2011). Unlike other infections prions disseminate throughout the lymphoreticular system and are observed to spread from the site of infection to draining then non-draining lymph nodes and finally the spleen (Brown et al., 2000). Following their replication and amplification upon FDC, the prions subsequently spread along neurones of the sympathetic and parasympathetic nervous systems, accessing the CNS wherein they ultimately cause neurodegeneration resulting in the death of the host (Beekes and McBride, 2000, Glatzel et al., 2001, McBride et al., 2001, Kujala et al., 2011).

Mononuclear phagocytes (MNP) arise from haematopoietic precursor cells within the bone marrow and are a heterogeneous population of monocytes, macrophages, and dendritic cells (Mabbott et al., 2010, Bradford et al., 2011, Hume et al., 2013) (see also Chapter 3). These

cells are abundant throughout the body and possess a diverse range of functions based on the anatomic locations they occupy. For example, some MNP are strategically situated at exposure sites such as the skin or intestinal lamina propria to provide a first line of defence against pathogens by phagocytosing and destroying them in their phagolysosomal compartments. Others, such as conventional dendritic cells (cDC), are potent antigen presenting cells and provide an important link between the innate and adaptive immune systems. These MNP are located to efficiently sample host tissues and fluids for pathogens and their antigens (see Chapter 3). The immature cDC at these sites are highly phagocytic. Following the uptake of pathogens or antigens, these cells typically undergo maturation and migrate via the lymphatics to the draining (regional) lymphoid tissue, such as the mesenteric lymph nodes associated with the intestine (Houston et al., 2015), where they present the antigens to lymphocytes to initiate an antigen-specific (adaptive) immune response or induce tolerance (Banchereau et al., 2000). Other MNP populations appear to play an important role within lymphoid tissues in the transfer of intact antigens to B cells (Wykes et al., 1998, Phan et al., 2009). Viable commensal bacteria can be recovered from cDC migrating from the intestine (Macpherson and Uhr, 2004) and some pathogenic microorganisms may exploit cDC as an efficient way to infect host tissues (Steinman et al., 2003). In the transient absence of $CD11c^+$ cells at the time of peripheral exposure, the early accumulation of prions in the draining lymphoid tissue was blocked and disease susceptibility reduced (Raymond et al., 2007, Sethi et al., 2007, Cordier-Dirikoc and Chabry, 2008).

Migratory, bone marrow-derived cDC (Banchereau et al., 2000) are entirely distinct from the stromal derived FDC (Mabbott et al., 2011, Krautler et al., 2012) which have been shown to be the critical sites of prion replication in lymphoid tissues (McCulloch et al., 2011). The FDC, in contrast, are localized within B cell follicles of lymphoid tissues, derive from ubiquitous perivascular precursor cells (Krautler et al., 2012), are tissue fixed and non-phagocytic. FDC are long-lived cells which can retain native antigens on their surfaces for long periods (Nossal et al., 1965, Chen et al., 1978, Mandels et al., 1980, Heesters et al., 2014). FDC also play a role in organizing B cell follicles via expression of the chemokine ligand CXCL13 (Vermi et al., 2008, Wang et al., 2011), recognised by its cognate receptor CXCR5 (Forster et al., 1996). CXCR5 is expressed mostly on B cells but also on other follicle-homing cell subtypes such as follicular B helper T cells 'T_{FH}' (Breitfeld et al., 2000) and MNP subsets (Saeki et al., 2000, Ishikawa et al., 2001, Yu et al., 2002).

In this chapter the hypothesis that the transport of prions from the initial exposure/uptake site directly to FDC within B cell follicles occurs via CXCR5-mediated chemotaxis of $CD11c^+$ cells is tested. An oral prion challenge using the well-characterized ME7 mouse-adapted scrapie prion strain was performed on transgenic model $CXCR5^{fl}$ mice which express CXCR5 normally and CD11cCre:$CXCR5^{fl}$ mice which specifically lack CXCR5 expression on $CD11c^+$ cells. Following analysis of disease pathogenesis in these models, CD11cCre:$CXCR5^{fl}$ mice revealed impaired peripheral prion pathogenesis following oral prion exposure and a statistically significant relative resistance to oral prion infection when compared to $CXCR5^{fl}$ mice. These data highlight the crucial role of $CXCR5^+$ $CD11c^+$ cells in the efficient trafficking of prions following oral infection.

5.3 Experimental design

Using standard breeding methods, groups of CXCR5^{fl} mice were generated that either possessed or were devoid of the CD11cCre transgene (see Chapter 4) as confirmed by PCR genotyping of genomic DNA derived from ear snip material (see 2.4 & 2.5). Groups of mice were assigned for either oral or intracerebral (i.c.) ME7 mouse-adapted scrapie challenge (see 2.3.4). Following oral exposure, sub-groups were sacrificed at 35, 70 and 105 days post exposure and lymphoid tissues harvested (see 2.15.1) to analyse prion pathogenesis by immunohistochemical (IHC) techniques. In the case of spleens from 70 and 105 day mice bioassay of prion infectivity were performed by i.c. inoculation of spleen homogenate into Tga20 prion indicator mice. All remaining orally exposed mice were monitored for clinical signs of infection or sacrificed at 500 days post exposure. Mice challenged i.c. were monitored for clinical signs of infection, clinically negative Tga20 mice (see 2.1.8) were sacrificed 200 days post challenge. Group mean incubation periods were calculated as the average time between challenge and sacrifice due to confirmed positive clinical signs of prion infection. Relative susceptibilities were calculated as number of mice showing clinical signs / total mice challenged (Figure 5.1).

Figure 5.1 Experimental design

Groups of 24x CXCR5^{fl} or CD11cCre:CXCR5^{fl} mice were orally exposed to ME7. To study sequential pathogenesis, groups were sacrificed at 35, 70 and 105 days post exposure for histological analysis. Spleens from 70 and 105 days were also assessed for prion infectivity by bioassay into groups of Tga20 indicator mice. Groups of 6x 24x CXCR5^{fl} or CD11cCre:CXCR5^{fl} mice were also infected intracerebrally with ME7 prions to assess CNS pathogenesis.

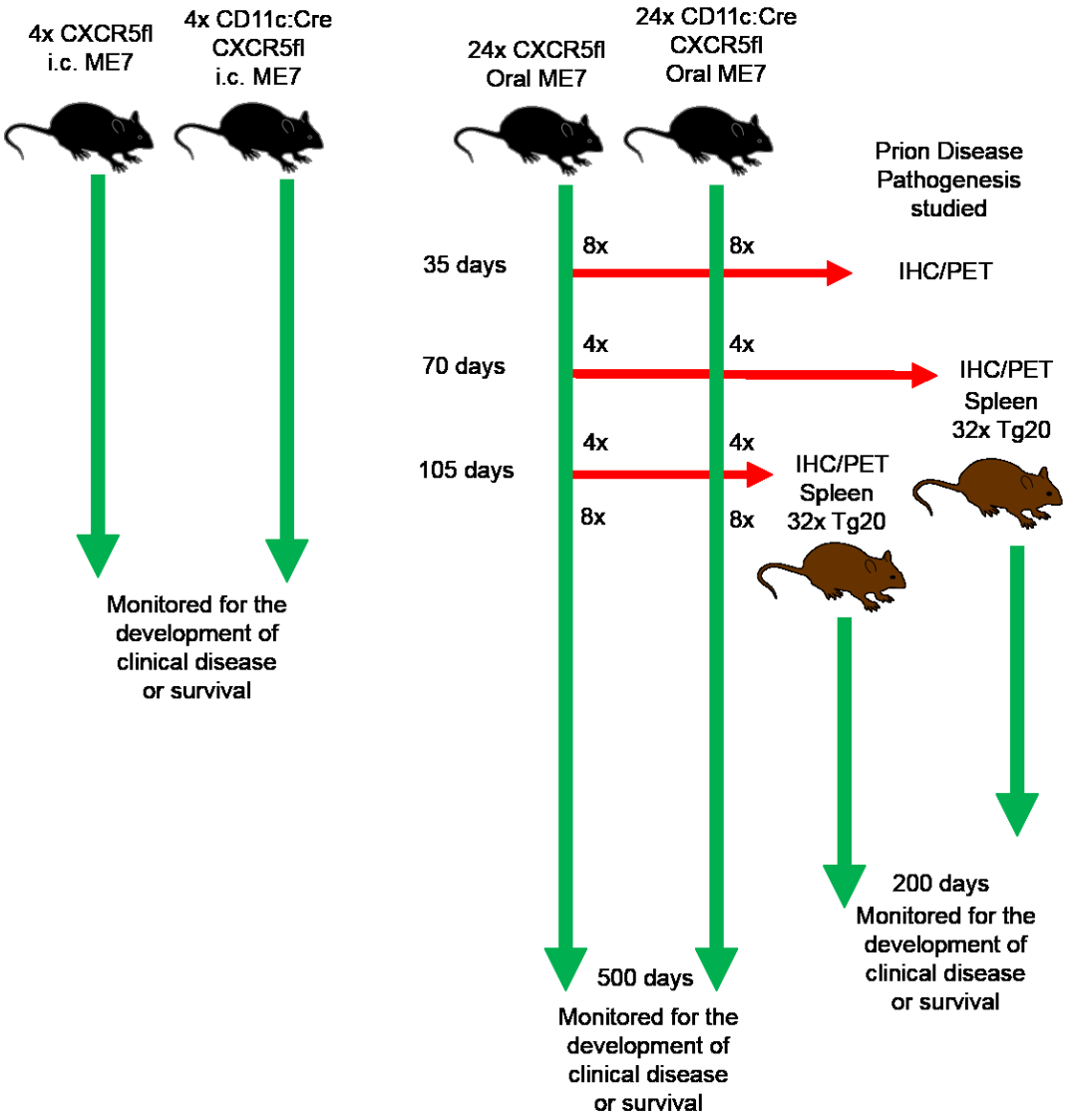

5.4 Results

5.4.1 Peripheral prion pathogenesis in CD11cCre:CXCR5^{fl} mice

To determine the role of CXCR5^{+} CD11c^{+} cells in oral prion disease pathogenesis, groups of CD11cCre:CXCR5^{fl} and CXCR5^{fl} control mice were orally exposed to ME7 scrapie prions (see 2.3.4). At 35, 70 and 105 days post challenge mice were sacrificed and the presence of disease specific PrP (PrP^{d}) accumulation determined in intestinal Peyer's patches, mesenteric lymph nodes and spleen by IHC analysis (see 2.15.5). Confirmatory PET analysis (see 2.16) were performed on serial paraffin sections to identify the accumulation of proteinase K (PK) –resistant scrapie prions (PrP^{Sc}). Observation of both PrP^{d} and PrP^{Sc} were required within a given tissue to confirm prion accumulation.

Following oral ME7 exposure, prion accumulation was analysed in intestinal Peyer's patches at 35 (Figure 5.2), 70 (Figure 5.3) or 105 (Figure 5.4) d.p.i.. Within CXCR5^{fl} mice IHC and PET-blot confirmed prion-positive patches occurred at relatively high frequency within all positively affected mice at all time points studied. Indeed by 105 days post exposure all CXCR5^{fl} Peyer's patches examined were positive for prion accumulation in all 4 mice (i.e. 100%) (Figure 5.4). In contrast CD11cCre:CXCR5^{fl} mice revealed reduced frequency of prion-accumulation within Peyer's patches. In contrast to CXCR5^{fl} mice only 1/4 CD11cCre:CXCR5^{fl} was observed to have prion accumulation in all patches studied. Furthermore prion accumulation in CD11cCre:CXCR5^{fl} Peyer's patches often had a more basal distribution of prions (Figure 5.2H & 5.3H) unlike CXCR5^{fl} mice which revealed prions distributed all across their FDC network (Figure 5.2D & 5.3D).

Figure 5.2 Oral ME7 pathogenesis in intestinal Peyer's patches at 35 d.p.i.

Immunohistochemical analysis of intestinal Peyer's patches following oral exposure to ME7. At 35 days post oral ME7 infection, CXCR5fl Peyer's patches were observed to be either negative (A) or positive (B) for disease-associated prion deposition (PrP^{d}). The absence (C) or presence (D) of protease resistant prions (PrP^{Sc}) was confirmed by PET immunoblotting and treatment with PK. prions were detected with anti-PrP antibody 1B3. Analysis of Peyer's patches from CD11cCre:CXCR5fl mice revealed immunohistochemically negative (E) and positive (F) deposition of prions upon FDC, with PET analysis confirmation (G, H) the frequency of observed positive patches was reduced in CD11cCre:CXCR5fl mice when compared to CXCR5fl mice (I). Scale bars = 100µm, error bars = SD.

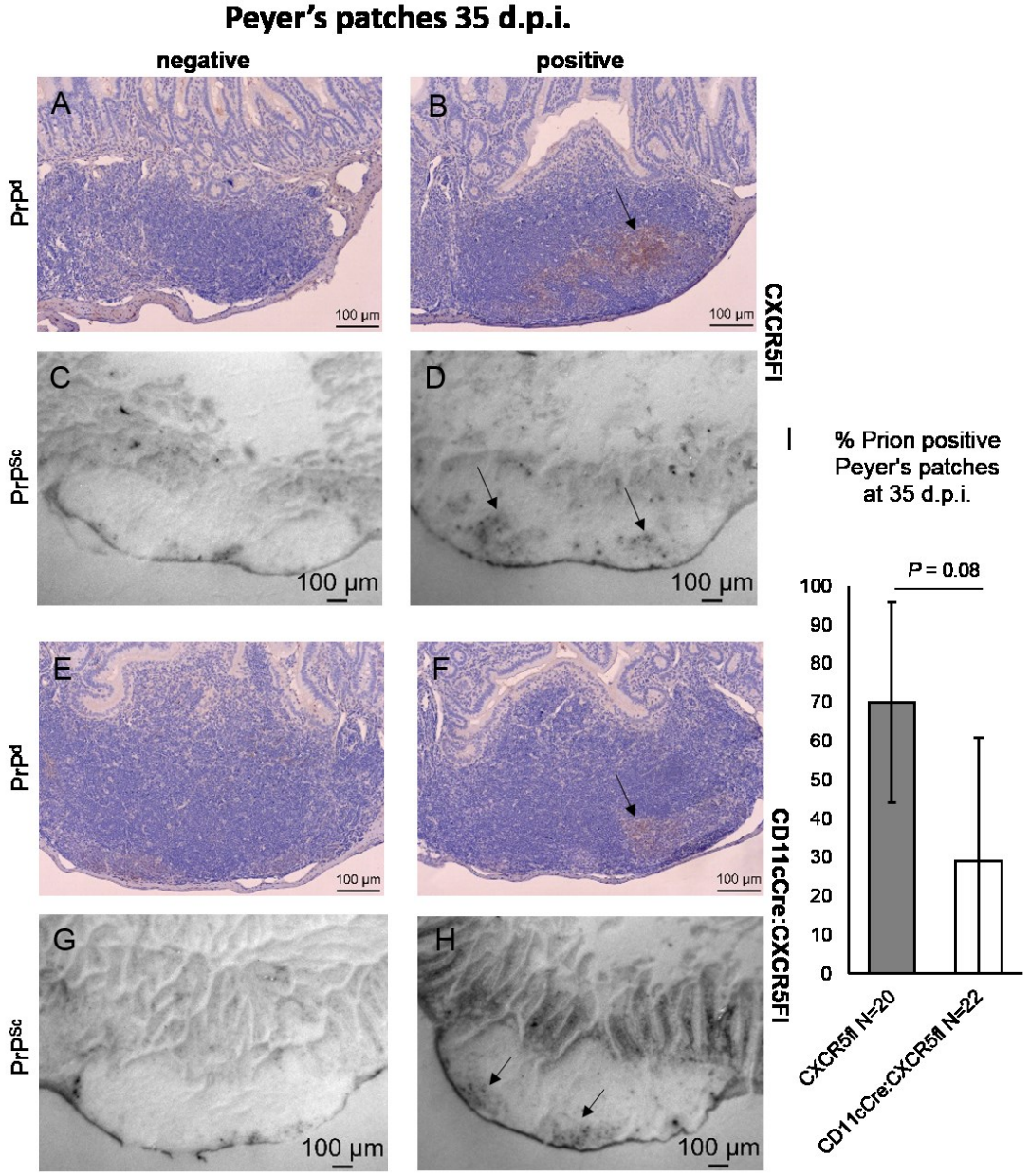

Figure 5.3 Oral ME7 pathogenesis in intestinal Peyer's patches at 70 d.p.i.

Immunohistochemical analysis of intestinal Peyer's patches following oral exposure to ME7. At 70 days post oral ME7 infection, CXCR5fl Peyer's patches were observed to be either negative (A) or positive (B) for disease-associated prion deposition (PrP^d). The absence (C) or presence (D) of protease resistant prions (PrP^{Sc}) was confirmed by PET immunoblotting and treatment with PK. Prions were detected with anti-PrP antibody 1B3. Analysis of Peyer's patches from CD11cCre:CXCR5fl mice revealed immunohistochemically negative (E) and positive (F) deposition of prions upon FDC, with PET analysis confirmation (G, H) the frequency of observed positive patches was reduced in CD11cCre:CXCR5fl mice when compared to CXCR5fl mice (I). Scale bars = 100µm, error bars = SD.

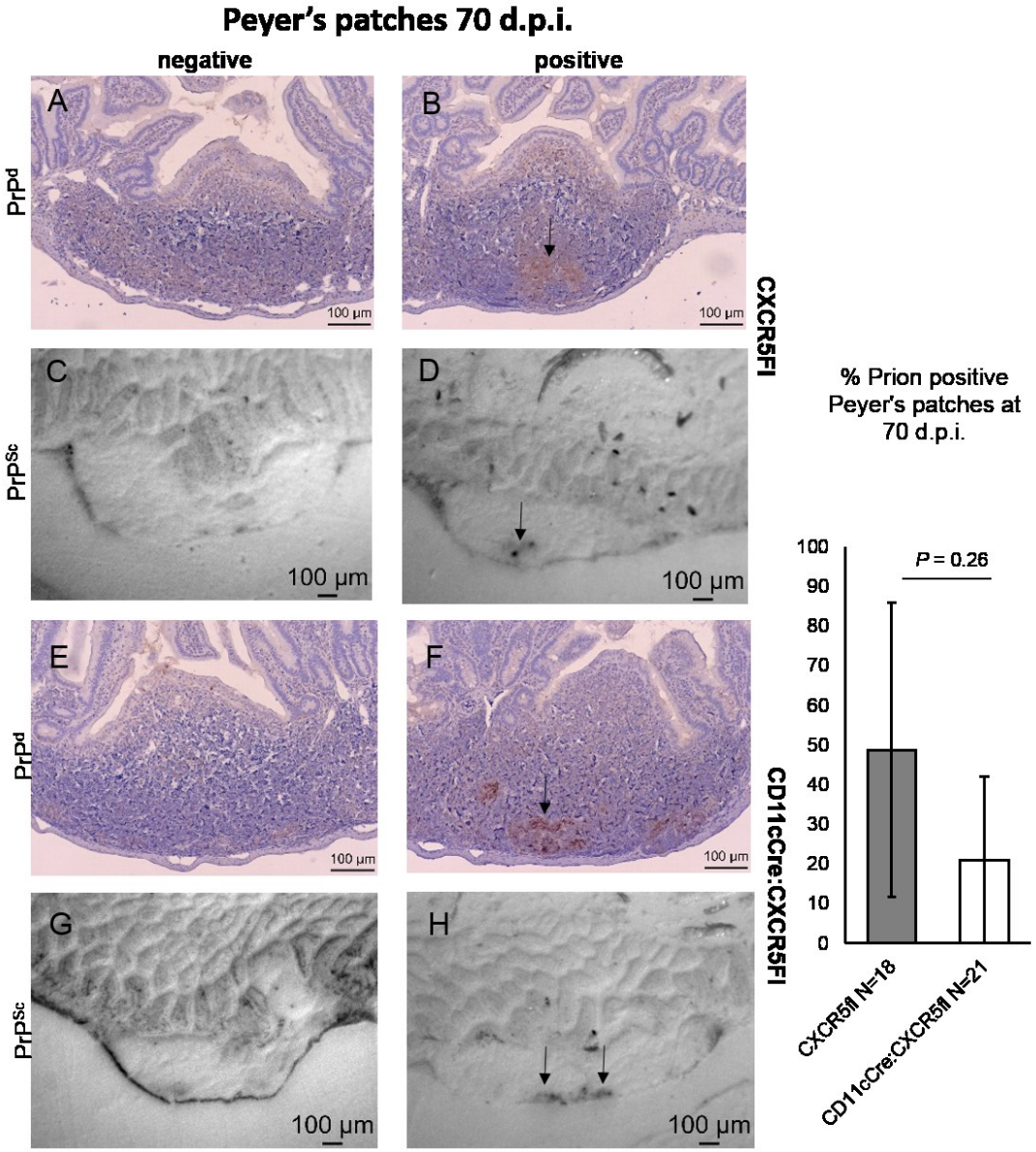

Figure 5.4 Oral ME7 pathogenesis in intestinal Peyer's patches at 105 d.p.i.

Immunohistochemical analysis of intestinal Peyer's patches following oral exposure to ME7. At 105 days post oral ME7 infection, CXCR5fl Peyer's patches were observed to be either negative (A) or positive (B) for disease-associated prion deposition (PrP^d). The absence (C) or presence (D) of protease resistant prions (PrP^{Sc}) was confirmed by PET immunoblotting and treatment with PK. Prions were detected with anti-PrP antibody 1B3. Analysis of Peyer's patches from CD11cCre:CXCR5fl mice revealed immunohistochemically negative (E) and positive (F) deposition of prions upon FDC, with PET analysis confirmation (G, H) the frequency of observed positive patches was reduced in CD11cCre:CXCR5fl mice when compared to CXCR5fl mice (I). Scale bars = 100µm, error bars = SD.

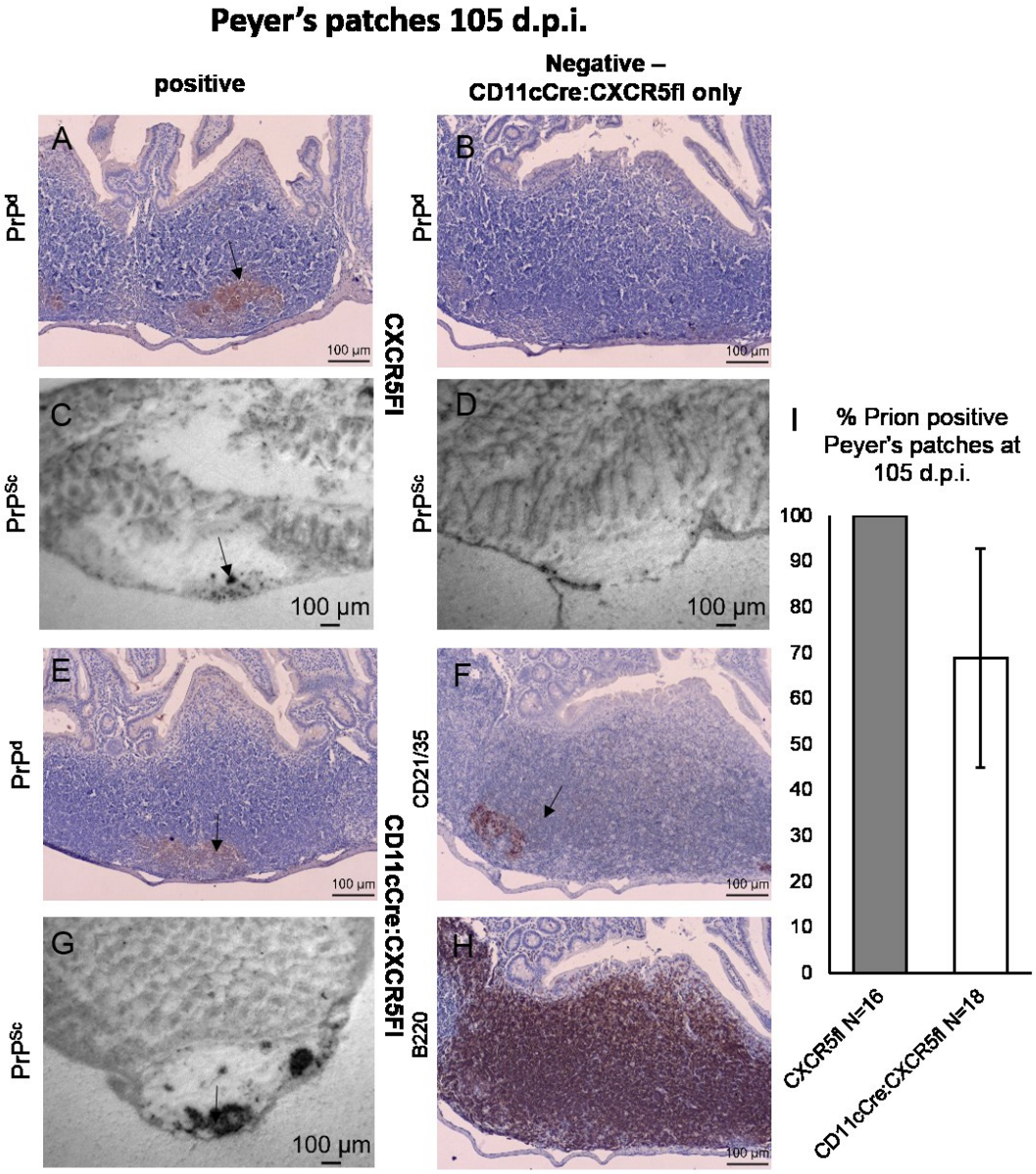

Peyer's patches from all mice were analysed in sequential order collected along the gastrointestinal tract. The appearance of prion accumulation was distributed across patches along the length of the intestine, with no preference for proximal or distal patch location. These observations suggest a stochastic uptake of prions in which location along the intestinal tract did not influence the probability of prion accumulation within a given Peyer's patch.

Figure 5.5 Oral ME7 pathogenesis in mesenteric lymph nodes

Immunohistochemical and paraffin-embedded tissue blot analysis of mesenteric lymph nodes at 35 d.p.i. (A-D), 70 d.p.i. (E-H) and 105 d.p.i. (I-L) post oral exposure to ME7. FDC presence in B cell follicles were confirmed in serial sections via IHC staining for CD21/35 (M, N) and B220 (O, P) respectively. PrP^{d} (IHC) or PrP^{Sc} (PET) were detected with anti-PrP antibody 1B3. Scale bars = 100µm.

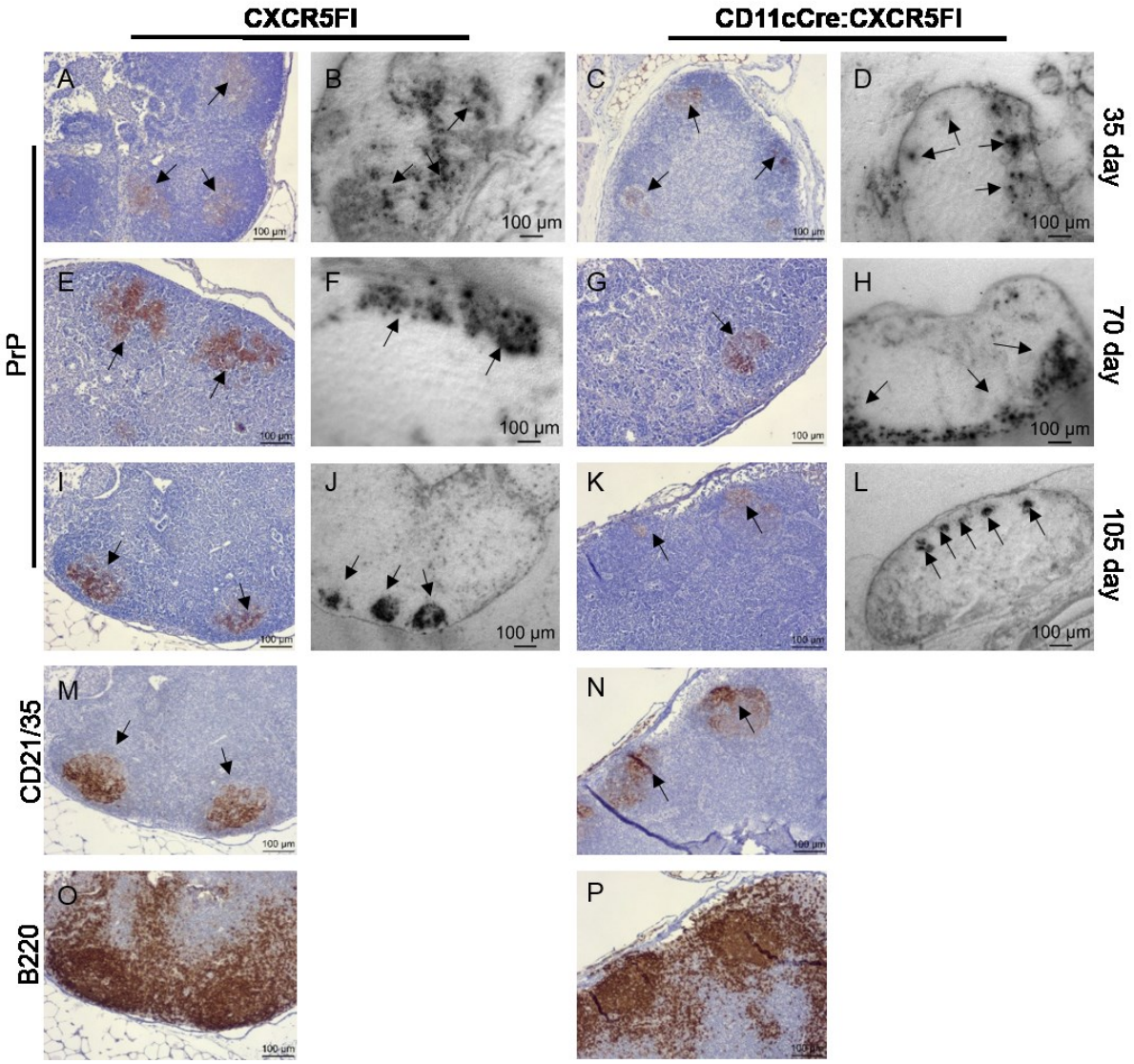

Within the mesenteric lymph nodes, presence of PrP^d was detected weakly at 5 weeks post oral infection in mice of both genotypes (Figure 5.5A-D). Lymph nodes from $CXCR5^{fl}$ mice at 10 (Figure 5.5E-H) and 15 (Figure 5.5I-L) weeks post infection displayed increased staining and patterning of FDC networks, as confirmed by CD21/35 labelling (Figure 5.5M & 5.5N) within B cell follicles (Figure 5.5O & 5.5P). CD11cCre:$CXCR5^{fl}$ mice also showed mildly reduced intensity and smaller foci of PrP^d staining (Figure 5.5C, 5.5G & 5.5K) when compared to $CXCR5^{fl}$ mice at the same time points (Figure 5.5A, 5.5E & 5.5I).

Following oral infection, confirmation of PrP^d staining was absent from all spleen samples at 35 days post exposure (Figure 5.6A-D) and was not observed until a minimum of 10 weeks post infection (Figure 5.6E-H). In $CXCR5^{fl}$ mice numerous FDC networks within splenic follicles were affected (Figure 5.6E), however in CD11cCre:$CXCR5^{fl}$ mice only rare (1-2 per spleen section studied) follicles were observed as positive for PrP^d staining (Figure 5.6G). Furthermore at 15 weeks almost all FDC networks/follicles in $CXCR5^{fl}$ mice displayed strong prion-staining (Figure 5.6I) whereas CD11cCre:$CXCR5^{fl}$ mice displayed prion-staining only in tingible-body macrophages around the central arterioles within the T cell region (Figure 5.6K) despite the presence of nearby FDC (Figure 5.6M) within B cell regions (Figure 5.6O). These data are further suggestive of impaired trafficking of prions both to and within splenic follicles in orally ME7 exposed CD11cCre:$CXCR5^{fl}$ mice when compared to $CXCR5^{fl}$ mice.

Figure 5.6 Oral ME7 pathogenesis in spleen

Immunohistochemical and paraffin-embedded tissue blot analysis of spleen at at 35 d.p.i. (A-D), 70 d.p.i. (E-H) and 105 d.p.i. (I-L) post oral exposure to ME7. PrP^{d} (IHC) or PrP^{Sc} (PET) were detected with anti-PrP antibody 1B3. FDC presence in B cell follicles were confirmed in serial sections via IHC staining for CD21/35 (M, N) and B220 (O, P) respectively. Scale bars = 100µm.

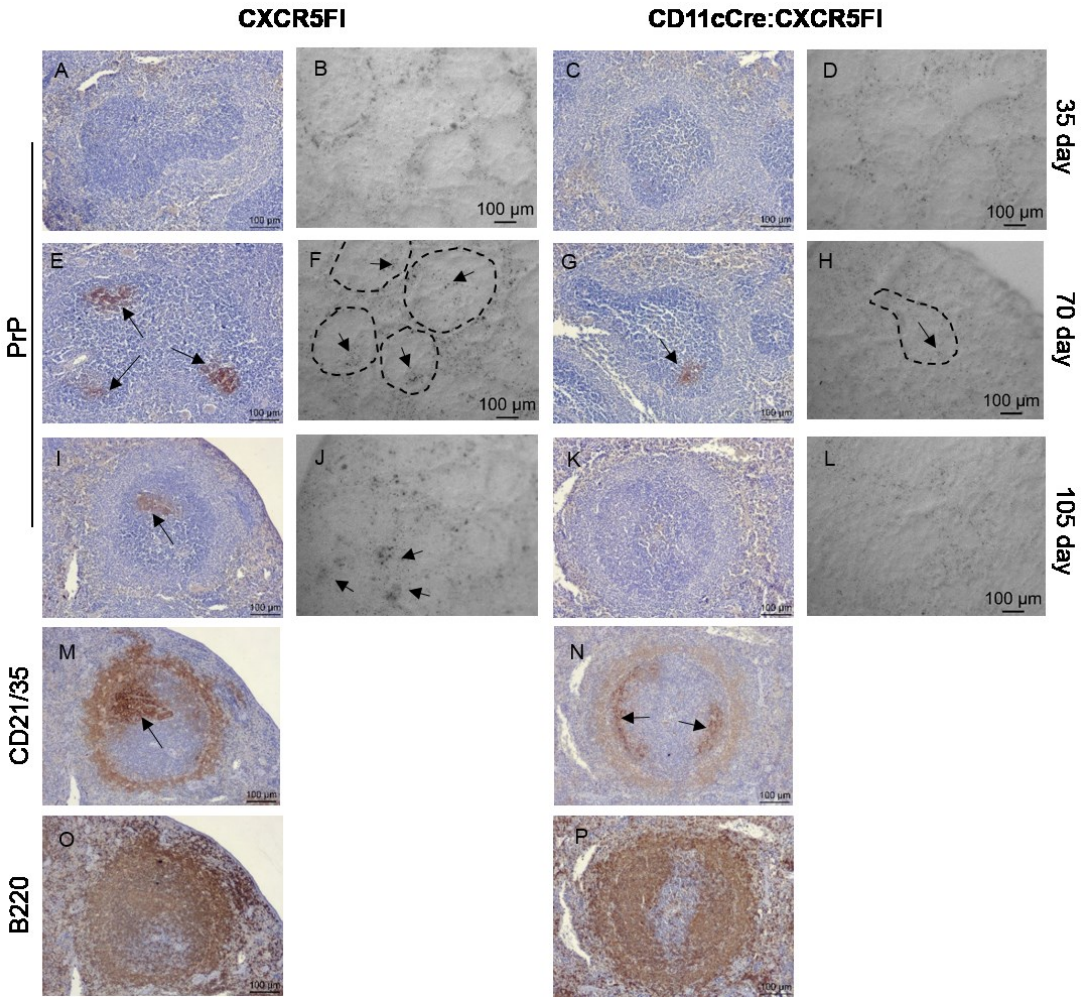

5.4.2 Bioassay of splenic prion load in Tga20 indicator mice

To assess accumulation of prion infectivity in spleen, spleen samples were homogenized at 0.1% (weight/volume) and sterilized via exposure to 28 kGy gamma irradiation. Groups of four tga20 indicator mice were injected i.c. with 20 µl of each homogenate. The scrapie titer in each sample was determined from the mean incubation period in the indicator mice, by reference to a dose/incubation period response curve for ME7 scrapie-infected spleen tissue serially titrated in tga20 mice using the relationship: $y = 9.4533 - 0.0595x$ (where y is log ID50 U/20 µl of homogenate, and x is the incubation period; $R2 = 0.9562$). As the expression level of cellular PrP^c controls the TSE disease incubation period, Tga20 mice overexpressing PrP^c are extremely useful as indicator mice in scrapie agent infectivity bioassays as they succumb to disease with much shorter incubation times than conventional mouse strains (Fischer et al., 1996).Using both attack rate and incubation period we robustly observed higher levels of prion infectivity within $CXCR5^{fl}$ spleens at both 10 and 15 weeks post infection when compared to spleens from CD11cCre:$CXCR5^{fl}$. The incidence of disease in Tga20 mice was reduced and the prion infectious load within CD11cCre:$CXCR5^{fl}$ mouse spleens was ~ 1-2 $Log_{10}ID_{50}$/g less (where detectable) than in $CXCR5^{fl}$ mice at equivalent time-points (Figure 5.7). These results suggest a reduction in the uptake and transport of prions to the spleen in CD11cCre:$CXCR5^{fl}$ mice following oral prion infection.

Figure 5.7 Bioassay in Tg20 indicator mice results

Using the incidence of infection in groups of 4 Tg20 indicator mice per spleen sample the Scrapie agent infectivity $Log_{10}ID_{50}/g$ were calculated via comparison to previously generated titration data of ME7 infection in Tg20 mice.

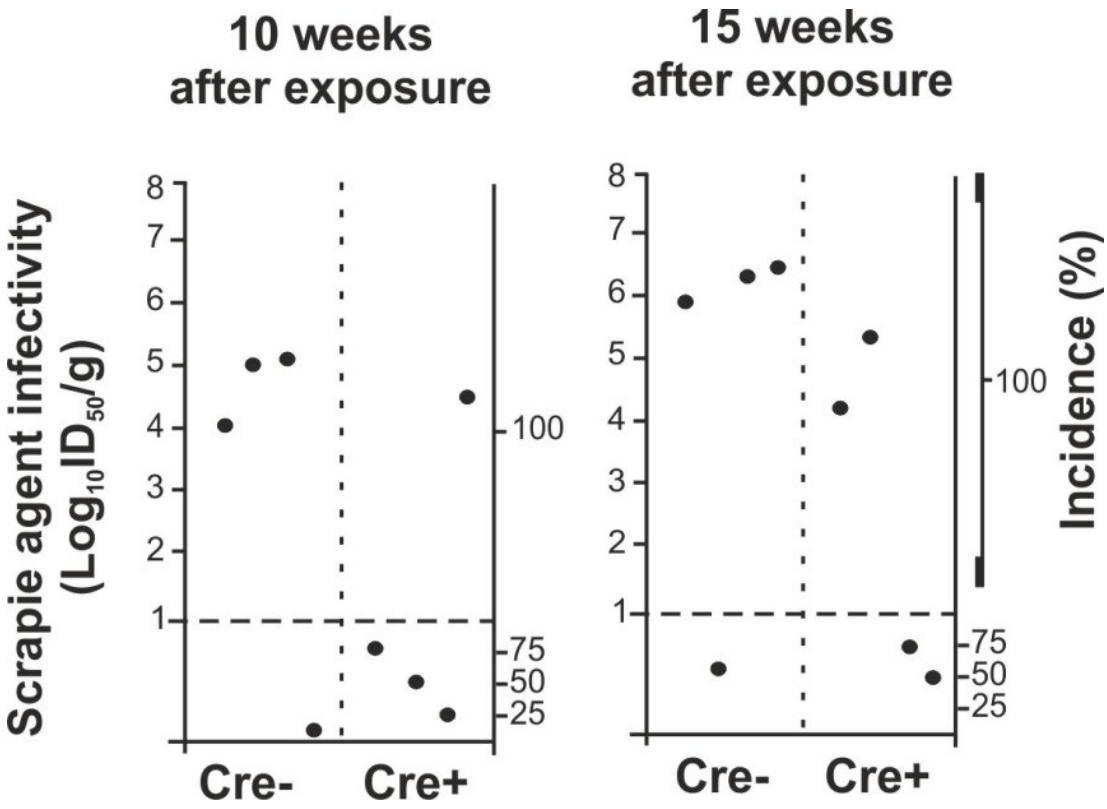

5.4.3 Oral prion susceptibility of CD11cCre:CXCR5^{fl} mice

To determine the effects of CD11c-mediated CXCR5 knockout on susceptibility to oral prion infection, groups of 8 CXCR5^{fl} or CD11cCre:CXCR5^{fl} mice were orally challenged with terminal ME7 mouse-adapted scrapie brain homogenate diluted 10^{-3}. A statistically significant difference in attack rate was observed between CXCR5^{fl} and CD11cCre:CXCR5^{fl} mice (P-value = 0.023 at 95% CI, Fisher's exact test), with CD11c-mediated CXCR5 knockout mice displaying much higher resistance to prion infection (Figure 5.8 and Table 5.1).

Figure 5.8 Survival curve analysis post oral ME7

Survival curve analysis reveals a reduced susceptibility to oral prion infection in CD11cCre:CXCR5^{fl} mice when compared to CXCR5^{fl} control. Experiment was terminated at 500 days post exposure and survivors sacrificed for analysis. N = 8 mice per gentoype group, Fisher's exact test: P-Value = 0.023.

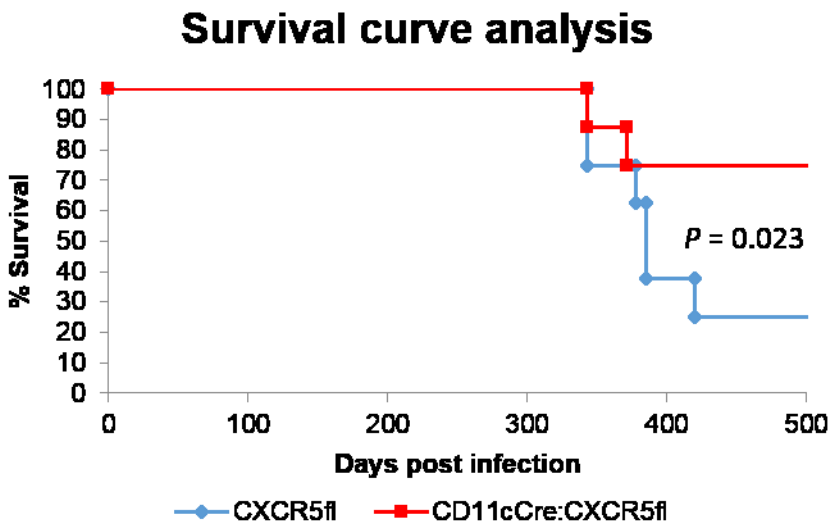

Table 5.1 Mean incubation period post oral ME7.

Group	Mean Incubation period (days ± S.E.M.)	Incidence of clinical disease
CXCR5^{fl}	375 ± 30	6/8
CD11cCre:CXCR5^{fl}	343, 371	2/8

Figure 5.9 Neuropathological analysis of prion-exposed CD11cCre:CXCR5^{fl} and CXCR5^{fl} mice.

Immunohistochemical staining for PrP (A-D), GFAP (E-H), Iba1 (I-L) or haematoxylin and eosin histological staining (M-P) of coronal brain sections from terminal mice either sacrificed 500 days post prion infection and displaying no clinical signs or sacrificed due to positive clinical symptoms of prion disease. Mice sacrificed at 500 days post injection with no clinical presence of prion disease revealed no PrP deposition (A, C), minimal astrocyte activation (E, G) and resting microglia (I, K). Mice sacrificed with positive clinical signs of prion disease revealed characteristic PrP deposition (B, D), Astrogliosis (F, H) and microgliosis (J, L). Prion-specific vacuolation scoring were performed on haematoxylin and eosin stained sections (M, N, O & P). Scale bar = 100µm.

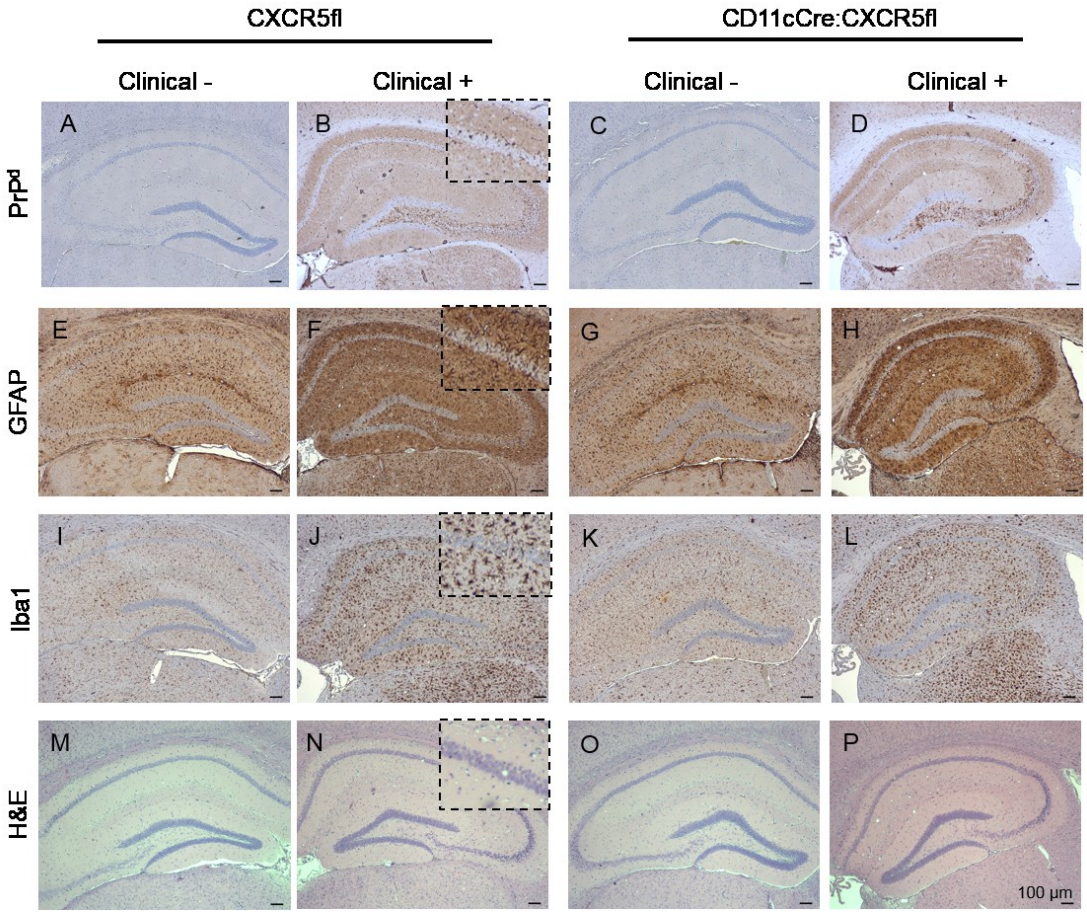

Clinically and confirmed pathologically positive $CXCR5^{fl}$ mice succumbed to oral ME7 infection with a mean incubation period of 375 days (range 343-420 days), whereas only 2 CD11cCre:$CXCR5^{fl}$ mice succumbed at 343 and 371 days post infection, i.e. within a similar time period (see figure 5.8 & table 5.1). Histopathological and IHC analysis of the brains from these mice revealed characteristic changes associated with terminal oral ME7 neuropathology; including PrP^{d} deposition, astro- and micro-gliosis (Figure 5.9).

Following oral ME7 infection, clinically positive $CXCR5^{fl}$ mice revealed vacuolar lesion profiles similar to those previously observed in terminal oral ME7 infected wild-type mice (Figure 5.10A). Insufficient CD11cCre:$CXCR5^{fl}$ mice succumbed to oral ME7 infection to allow an accurate lesion profile to be calculated. However, two clinically positive CD11cCre:$CXCR5^{fl}$ mice revealed sufficient levels of disease-specific vacuolation within specific brain areas to confirm a pathological diagnosis of terminal prion infection (Figure 5.10A). All clinically negative mice, regardless of genotype, revealed no prion-specific vacuolation (i.e. scoring zero) for all brain regions studied (Figure 5.10A).

Western blot analysis (see 2.12) of terminal clinically positive brain samples revealed high levels of accumulation of PK-resistant PrP^{Sc}, as expected from the IHC assessment of the same brain samples (see figure 5.9B & 5.9D). No differences in total PrP levels were observed between $CXCR5^{fl}$ and CD11cCre:$CXCR5^{fl}$ clinically positive samples (Figure 5.10B & 5.10C). Similarly all clinically negative brain samples from mice surviving to 500 days post exposure revealed no difference in total PrP^{C} and no presence of PK-resistant PrP^{Sc} (Figure 5.10B & 5.10C), again as expected from the corresponding absence of PrP^{d} staining during IHC analysis of the same brain samples (see Figure 5.9A & 5.9C)

Following oral exposure, high levels of prion accumulation are maintained for the duration of infections and evidence of prion accumulation in peripheral lymphoid tissues was readily observed in terminal clinically positive animals. Investigation of clinically negative animals however revealed no evidence of prion accumulation (Figure 5.11), confirming that these individuals were not sub-clinical or harbouring prion disease.

Figure 5.10 Lesion profile and western blot analysis post oral ME7

(A) Lesion profile analysis from terminal oral ME7 exposed animals. CXCR5^{fl} (N=6) mice reveal standard oral ME7 lesion profile, clinically positive CD11cCre:CXCR5^{fl} mice (N=2) reveal similar vacuolation profile, confirming diagnosis of prion disease. Clinically negative mice of CXCR5^{fl} (N=2) or CD11cCre:CXCR5^{fl} (N=6) genotypes revealed no vacuolation upon post-mortem examination. Vacuolation was scored on a scale of 0 – 5 in the following grey (1 – 9) and white (1 – 3) matter areas: Grey: 1, dorsal medulla; 2, cerebellar cortex; 3, superior colliculus; 4, hypothalamus; 5, thalamus; 6, hippocampus; 7, septum; 8, retrosplenial and adjacent motor cortex; 9, cingulate and adjacent motor cortex; White: 1, inferior and middle cerebellar peduncles; 2, decussation of superior cerebellar peduncles; and 3, cerebellar peduncles. Western blot analysis of terminal clinically positive or clinically negative (sacrificed at 500 days post exposure) brain samples using anti-PrP antibody 7A12 (B). Clinically negative survivors revealed no PK-resistant PrP within brain (C).

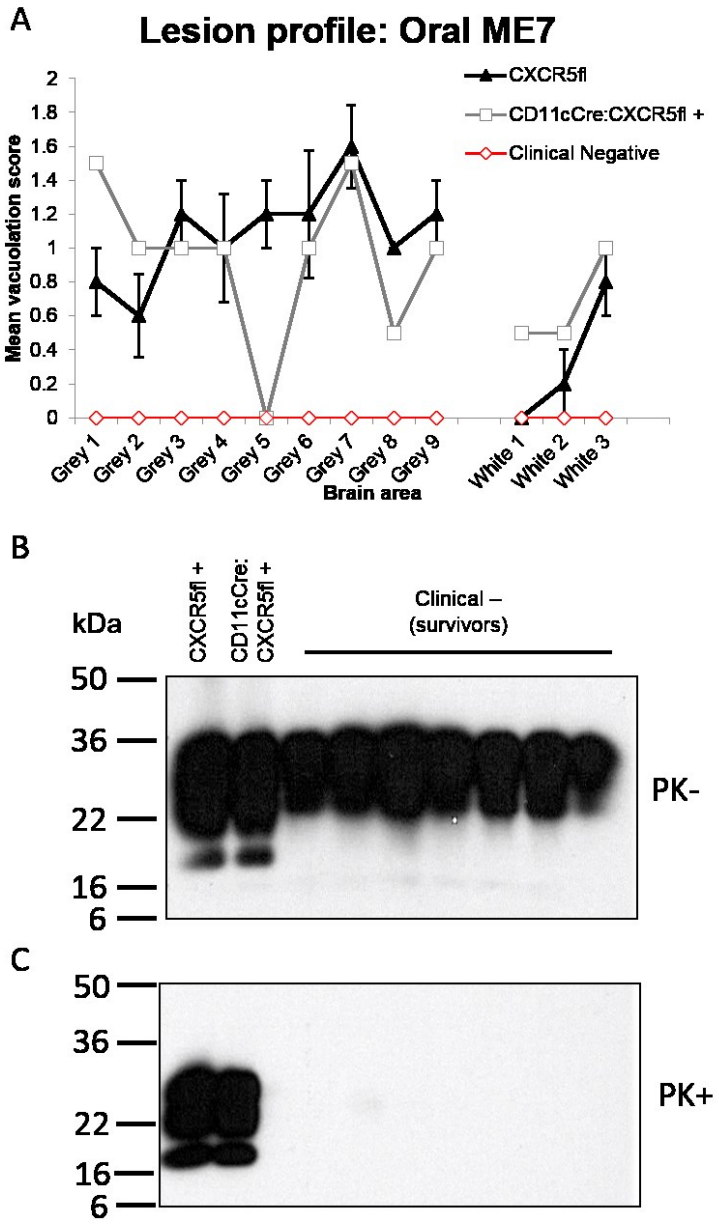

Figure 5.11 analysis of lymphoid tissue post oral ME7

Immunohistochemical staining and paraffin-embedded tissue blot analysis of Peyer's patches (A-H) mesenteric lymph nodes (I-P) and spleen (Q-X) of clinically positive or clinically negative mice of confirmed genotype CXCR5fl or CD11cCre:CXCR5fl post oral ME7 exposure. PrP^{d} (IHC) or PrP^{Sc} (PET) were detected with anti-PrP antibody 1B3. Scale bars = 100 µm.

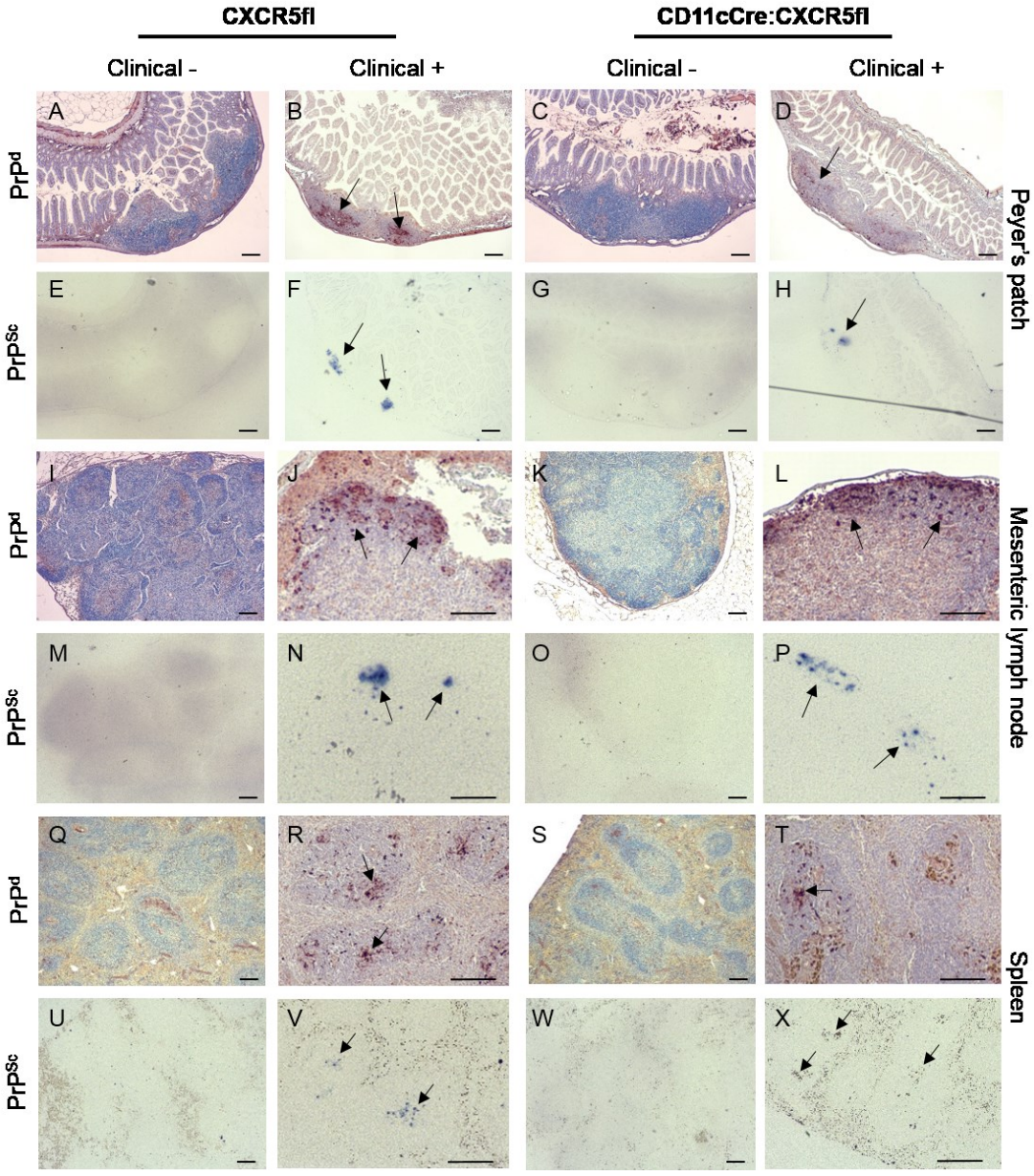

5.4.4 Intracerebral prion challenge of CD11cCre:CXCR5^{fl} mice

To determine the ability of the brains of CD11cCre:CXCR5^{fl} mice to support prion infection a direct intracerebral delivery of prions to the CNS was undertaken. Following intracerebral ME7 challenge of CD11cCre:CXCR5^{fl} and CXCR5^{fl} control group mice, no statistically significant difference in disease incubation period was observed (Table 5.2). Incubation periods observed were comparable to archival data of numerous intracerebral ME7 challenges in C57Bl/6 strain mice.

Table 5.2 Mean incubation period post intracerebral ME7.

Group mean incubation period and incidence of clinical disease in intracerebral infected mice of confirmed genotype CXCR5fl or CD11cCre:CXCR5fl. T-test of difference, p = 0.302 at 95% CI.

Group	Mean Incubation period (days ± S.E.M.)	Incidence of clinical disease
CXCR5^{fl}	162 ± 3	4/4
CD11cCre:CXCR5^{fl}	157 ± 3	4/4

Histopathological analysis of the brains from these mice revealed characteristic changes associated with terminal intracerebral ME7 neuropathology; including PrP deposition, astro- and micro-gliosis (Figure 5.12). Neuropathological changes in CD11cCre:CXCR5^{fl} were indistinguishable from those observed in CXCR5^{fl} mice.

TSE vacuolation scoring and lesion profile analysis revealed no statistically significant differences between terminal ME7 challenged CD11cCre:CXCR5^{fl} and CXCR5^{fl} brains (Figure 5.13A). Western blot analysis of all intracerebrally ME7 challenged terminal brain samples revealed the presence of PK-resistant PrP^{Sc} regardless of genotype (Figure 5.13B).

Figure 5.12 Neuropathological analysis of i.c. ME7 challenged CD11cCre:CXCR5^{fl} and CXCR5^{fl} mice.

Immunohistochemical staining reveals characteristic PrP^{d} deposition (A, B), Astrogliosis (C, D) and microgliosis (E, F). TSE-specific vacuolation scoring were performed on haematoxylin and eosin stained sections (G, H). Scale bar = 100µm.

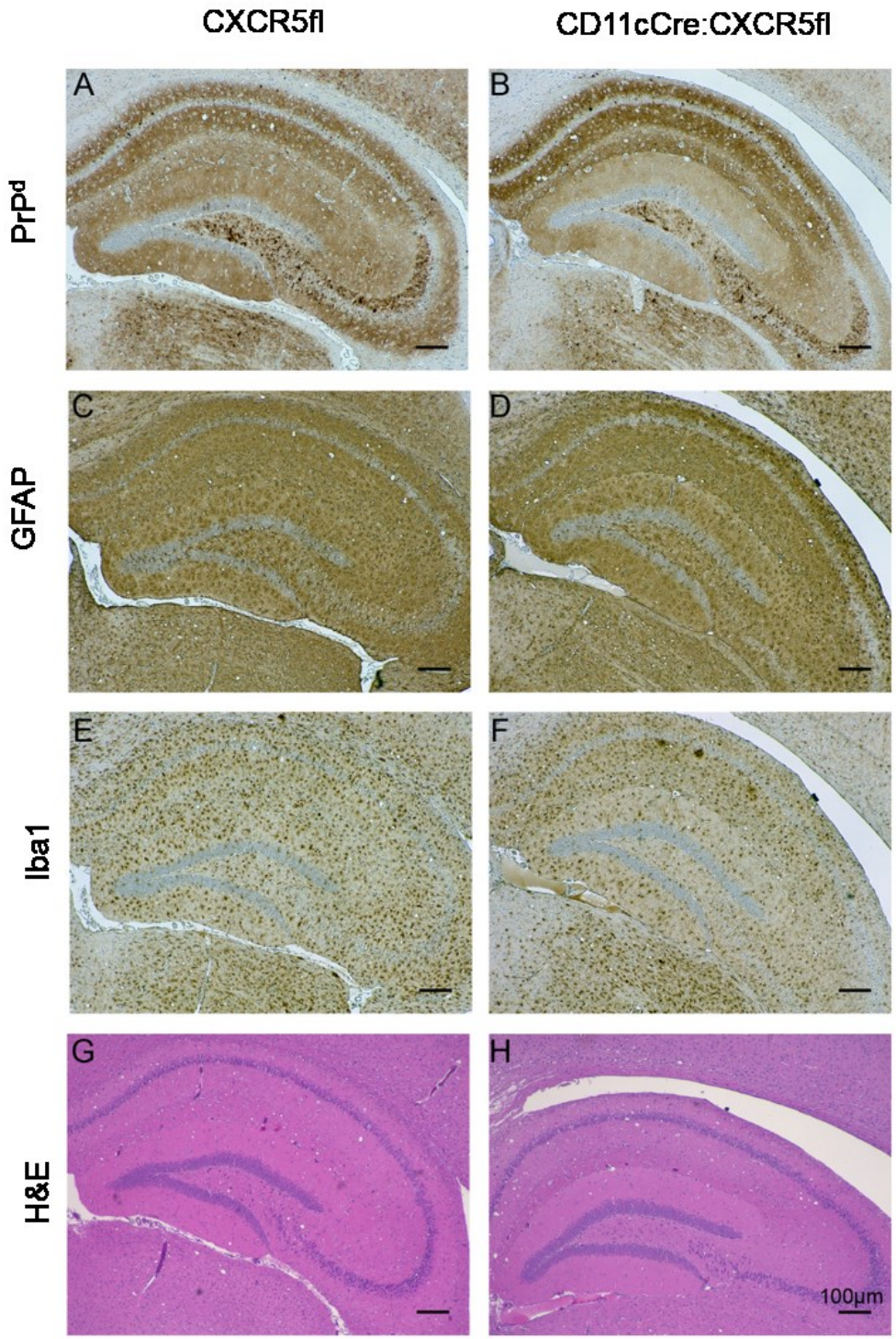

Figure 5.13 Lesion profile and Western blot analysis post i.c. ME7

(A) Lesion profile analysis from terminal i.c. ME7 infected brains. Scores for each brain area were analysed by ANOVA. No statistically significant differences were observed in TSE-specific vacuolation between CXCR5^{fl} and CD11c:CXCR5^{fl} mice. Vacuolation was scored on a scale of 0 – 5 in the following grey (1 – 9) and white (1 – 3) matter areas: Grey: 1, dorsal medulla; 2, cerebellar cortex; 3, superior colliculus; 4, hypothalamus; 5, thalamus; 6, hippocampus; 7, septum; 8, retrosplenial and adjacent motor cortex; 9, cingulate and adjacent motor cortex; White: 1, inferior and middle cerebellar peduncles; 2, decussation of superior cerebellar peduncles; and 3, cerebellar peduncles (B) Western blot analysis of terminal i.c. ME7 infected brains revealed proteinase K (PK) -resistant PrP using anti-PrP antibody 7A12.

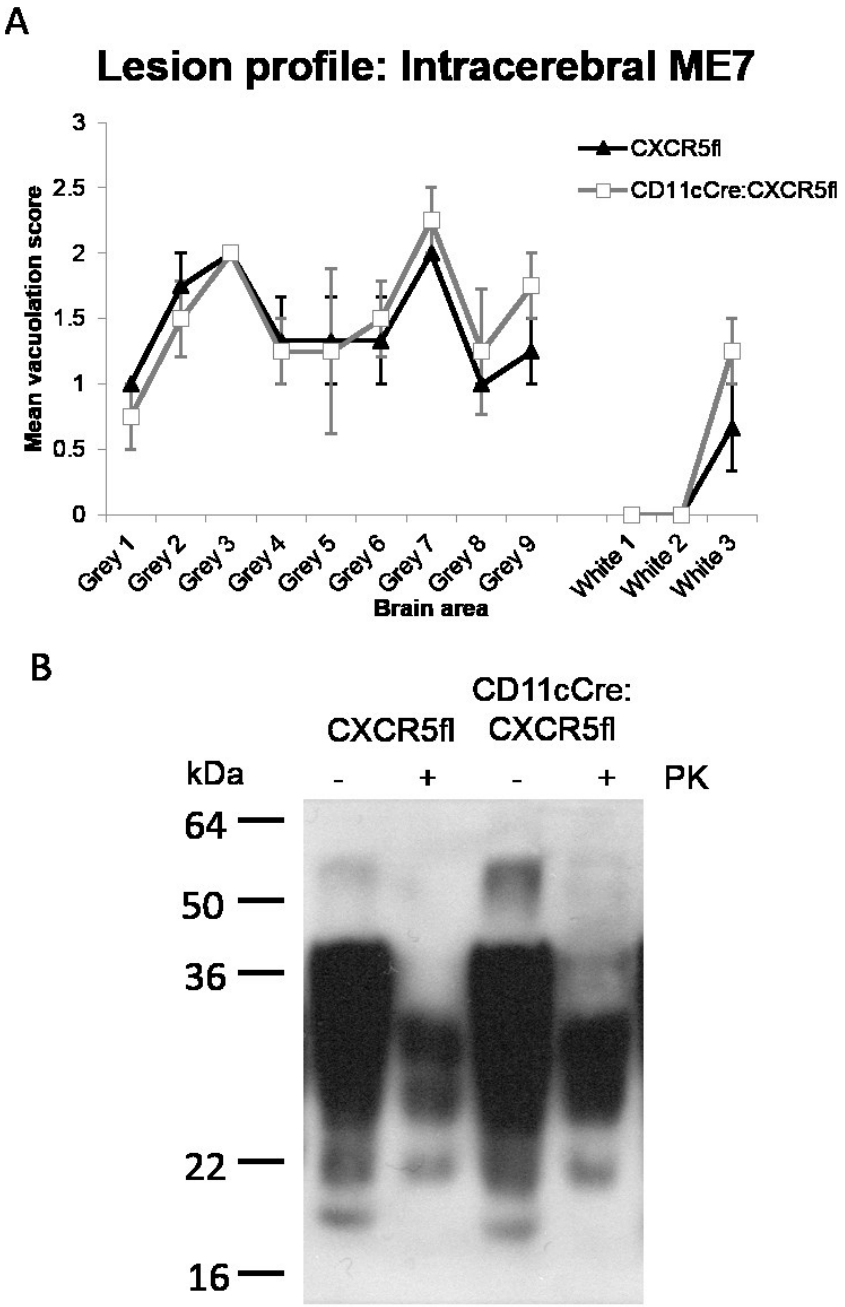

5.5 Discussion

The mechanism of uptake and trafficking of prions from the site of exposure to secondary lymphoid organs is poorly defined. Both cell-free and cell-mediated mechanisms of trafficking have been reported (Michel et al., 2012) and in previous studies the role of $CD11c^+$ cells shown to be critical for effective prion transport (Raymond et al., 2007). Looking at early pathogenesis events, a relative reduction in prion uptake and replication upon FDC within intestinal Peyer's patches was observed in CD11cCre:$CXCR5^{fl}$ mice at all time-points studied post oral exposure. Prion dissemination to the mesenteric lymph nodes appeared unaltered in CD11cCre:$CXCR5^{fl}$ mice, whereas transit to the spleen was impaired similar to observations within the Peyer's patches. Reduced levels of infective prions were detected even at 15 weeks post infection in the spleens of CD11cCre:$CXCR5^{fl}$ mice when compared to $CXCR5^{fl}$ mice. In fact CD11cCre:$CXCR5^{fl}$ mice revealed only 20% attack rate to oral prion infection, similar to results obtained via complete ablation of all $CD11c^+$ cells using the CD11c-DTR transgenic mice (Raymond et al., 2007). These complementary data reveal that not only are $CD11c^+$ cells necessary for effective uptake and transport of prions to FDC in secondary lymphoid organs, but transport via CXCR5-CXCL13 is critical to this process.

CD11c is expressed mainly upon myeloid cells such as monocytes, macrophages and myeloid dendritic cells as well as a small subset of lymphocytes including a specific T/B border B-cell subset, moderate to low level of CD11c expression has also been reported on NK cells, granulocytes and neutrophils (see Figure 4.1). The use of CD11c-cre mice to drive targeted knockout of CXCR5 is assumed to have been most effective in this particular study in leukocytes whose primary purpose is to migrate from exposure sites to lymphoid tissues during their role as antigen-presenting cells. While many cell types may act as APC, dendritic cells are most specialized towards both antigen-presentation and this specific migratory pathway. The majority of other CD11c-expressing cells (excluding the B-cell subset, perhaps) migrate to the exposure site following activation, either from the blood or resident within tissues, in order to undertake their primary functions. Therefore the use of the marker CD11c in this study is concurrent with the concept that the major cell type involved in the trafficking of prions from exposure sites to FDC in B-cell follicles are cDC functioning as APC. The possibility cannot be excluded that traffic by other CD11c+ cell types may also play a role in trafficking of prions as they will have experienced genetic knockout of CXCR5 equally. However with the notable exception of B-cells there is little evidence to suggest expression of CXCR5 within these other immune cell populations.

The observation of some prion transport even in the presence of CD11c-mediated CXCR5 depletion (similar to the CD11c-cell depletion model) suggests that alternative mechanisms or routes of transport occur which are potentially less efficient. Within the Peyer's patches prion accumulation on FDC of CD11cCre:CXCR5^{fl} mice was observed to occur proximal to the basal area of the FDC network as opposed to FDC in CXCR5^{fl} mice where prion accumulation on FDC was first observed proximal to the FAE. These data suggest a circuitous transfer of prions, possibly by CD11c^{+} cells unable to enter the B cell area and trafficking alternatively into the interfollicular (IFR) region of the Peyer's patch, likely by CCR7-CCL19/21 mediated chemotaxis. Prion build-up in the IFR or basal area immediately proximal to FDC networks may have occurred to a critical mass or concentration enough to effect final transit to the nearby FDC. Similarly cell-free transit of prions should be unaltered in our model, therefore any prions evading collection by either CD11c^{+} or degradative MNP has a chance to percolate through the follicle to the FDC, though our data suggest clearly this is much more inefficient than CXCR5-directed delivery by CD11c^{+} cells.

No differences were observed between CD11cCre:CXCR5^{fl} and CXCR5^{fl} mice in the ability to transport prions from the gut to mesenteric lymph nodes. The extra-follicular uptake of prions via villi endothelium and transport by lamina-propria resident CD11c^{+} cells will occur to the lymph node medulla via the lymphatic system (Cerovic et al., 2013). Again direct transition of CD11c^{+} cells into CXCL13 organised B cell follicles will have been restricted in CD11cCre:CXCR5^{fl} mice, however prion build-up within the medullary region may have reached levels sufficient to infect nearby FDC. CXCR5 expression within Peyer's patches and mesenteric lymph nodes has also been reported at high-endothelial venules (Okada et al., 2002), as an entry site for re-circulating B cells and activated CD4^{+} T cells into these structures (Miyasaka and Tanaka, 2004). Similarly the likelihood of transport of prions by recirculating B cells (Mok et al., 2012) should be unaltered in this model, however transport by recirculating B cells would be as effective to spleen as it is the MLN and a distinct difference in splenic transport of prions was observed in CD11cCre:CXCR5^{fl} mice refuting this hypothesis.

Transport to splenic follicles appeared impaired in CD11cCre:CXCR5^{fl} mice at 70 days post exposure and by 105 days any prions within CD11cCre:CXCR5^{fl} spleens appeared to be proximal to the central arterioles within the T cell region or sequestered by tingible-body macrophages. These observations are similar to the results observed in mice devoid of PrP

upon their FDC (McCulloch et al., 2011). Together these data suggest that in the circumstance of prions reaching the spleen but failing to gain access to FDC directly, or in the presence of PrP-deficient FDC, then these prions are not sequestered or retained upon the FDC surface but instead are processed for degradation by tingible-body macrophages. This alternative processing results in a failure for prions to transition between lymphoreticular cells and the peripheral nervous system, thus underlying the basis of resistance to prion infection within these models.

Following intracerebral prion infection CD11cCre:CXCR5^{fl} mice were unimpaired in their ability to propagate prions within the CNS and succumbed to prion disease similar to CXCR5^{fl} mice. The relative resistance to infection in CD11cCre:CXCR5^{fl} mice therefore does not stem from any inability of prions to propagate within the CNS. CD11cCre:CXCR5^{fl} mice surviving oral prion infection also revealed no prion accumulation within their peripheral tissues. In conclusion, these data reveal that CXCR5-mediated chemotaxis by CD11c^{+} cells constitutes the effective mechanism of prion transport from the exposure site to FDC in Peyer's patches and thereby directly influence subsequent prion pathogenesis and susceptibility.

Chapter 6. Effect of CD11c-mediated CXCR5 knockout on oral *T. muris* infection

6.1 Abstract

The expression of CXCR5 on antigen presenting cells (APC) facilitates their migration into the B-cell follicles of lymphoid tissues. A specific role of CXCR5 expressing APC was discovered in the generation of interleukin-4 producing T-helper type 2 (T_H2) cells. For the efficient generation of T_H2 cells, lymphotoxin expressing B cells, CXCL13 expression and CXCR5 expression upon conventional dendritic cells (cDC) and T cells are postulated requirements. CD11cCre:CXCR5^{fl} mice specifically lack the ability to express CXCR5 on CD11c$^+$ cells and therefore cDC are unable to traffic into B-cell follicles and present antigen here. To test the hypothesis that CXCR5$^+$ CD11c$^+$ cells are the critical antigen-presenting cells for the stimulation of a T_H2 response we utilised a natural gastrointestinal pathogen *Trichuris muris* which when delivered at high dosage can promote a strong, protective T_H2 response in C57Bl/6 mice. In this chapter we describe how high dose *T. muris* infection in CD11cCre:CXCR5^{fl} mice leads to persistent infection and a 'susceptible' T_H1 dominated response. These data reveal that preventing transport of CD11c$^+$ cells to B-cell follicles during infection impairs the formation of appropriate protective T_H2 responses to *T. muris* infection. These data further suggest that the critical homing location of antigen presenting cells such as cDC are capable of modifying the bias of generated helper T cell responses, the ability to alter cDC homing may prove beneficial for example promoting resistance to helminth infection or preventing inappropriate allergic responses to antigens.

6.2 Introduction

The gastrointestinal endoparasite *Trichuris muris* is a natural pathogen of mice and has in recent decades been used as a model of *Trichuris trichiuria* in humans. Soil transmitted helminth infections, mainly trichuriasis, ascariasis and hookworm, affect around 1 billion people worldwide. Unfortunately, host immune responses to helminth infections occur over a wide spectrum. The T_H1/T_H2 paradigm is based upon the stimulation of naïve $CD4^+$ helper T cells (T_H0) into prolific cytokine-producing effector cells. The cytokines they produce are broadly classed into proinflammatory (T_H1) e.g. interferon gamma for killing intracellular parasites and perpetuating autoimmune responses or anti-inflammatory (T_H2) e.g. interleukins 4, 5 and 13 which promote IgE production and eosinophilic responses. T_H0 cells possess specific T cell receptors (TCR) which drive their stimulation upon recognition of their cognate antigen, usually presented by antigen presenting cells (APC) along with signals from co-stimulatory molecules and receptors expressed upon each of these cell types. The generation of a T_H1 maturation by naïve (T_H0) CD4-positive T cells is driven by expression of the cytokine interleukin-12 (IL-12) from the antigen-presenting cell. No specific cytokine has been identified for driving T_H2 maturation, leading to the 'default' hypothesis. This hypothesis states that naïve CD4-positive T cells have in inbuilt tendency towards T_H2 maturation in the absence of IL-12. This may be partly due to their own ability to generate T_H2-type cytokines such as IL-4. Other possibilities include exogenous IL-4 or IL-13 (potentially driven by either IL33 or IL25), direction by T-follicular helper cells or already primed T_H2 cells via modulatory or feedback cytokine loops. The paradigm established of a susceptibility-associated T_H1 versus a resistance-associated T_H2-type response is currently being supplemented with knowledge of the differing roles played by host immune cell types and the responses they are capable of (Klementowicz et al., 2012).

The common hypothesis states that antigen-presenting cells interact with naïve T cells in the T cell zone of secondary lymphoid organs (Cyster, 2000) via expression of CCL19 within this region and of the cognate chemokine receptor CCR7 on both cell types (Forster et al., 2008). However mice with the plt (paucity of lymph node T cells) mutation lack the CCR7 ligands CCL19 and CCL21a but are capable of generating effective T cell responses (Mori et al., 2001). Subsequently it has been shown that T cell responses may be generated within the B-cell follicle. The B-cell follicle is organised by expression of the chemokine CXCL13 by stromal cells such as FDC (Vermi et al., 2008, Wang et al., 2011) and its cognate receptor CXCR5 upon follicle homing cells e.g. B cells and follicular helper T cells. The formation of

T-cell responses within the B-cell follicles is due to the required upregulated CXCR5-expression on both antigen presenting cells and CD4-positive T cells. Furthermore this localisation is critical for the generation of T_H2-type responses (Leon et al., 2012). In this study the authors observed altered cDC localization within secondary lymphoid organs dependent upon the type of infection, with influenza-virus infected mice displaying a classical localization of cDC to T-cell regions whereas infection with the intestinal nematode *Heligmosomoides polygyrus* resulted in increased CXCR5-expression and altered localisation of cDC to the T/B border region. Blocking this response either with anti-CXCL13 antibody or mixed bone marrow chimeras to generate DC-CXCR5-negative mice blocked the generation of T_H2-type responses.

Infection with *T. muris* occurs by ingestion of infective embryonated eggs that accumulate within the caecum. The first larvae (L1) hatch around 90 minutes after ingestion following interaction with the host gut microflora which induce parasite hatching. Following hatching the L1 larvae penetrate the caecum and proximal colon epithelial wall in which they reside and undergo 3 larval moults to L2 (9–11 days p.i.), L3 (17 days p.i.) and L4 stage (22 days p.i.). During these moults the larvae extend from within the epithelium wall out into the lumen of the caecum or colon, however the anterior part remains buried in parasite-modified epithelial tunnels. Dioecious adult worms may be observed by 32 days p.i. which may produce eggs which leave via the faeces and require 2 months to embyonate and become infective (Klementowicz et al., 2012). The time between moults may be regulated by the host mouse strain, with more resistant mouse strains displaying retardation of *T. muris* development through larval stages. Similar to human infections, various mice strains display differing responses following *T. muris* infection. Mice of strain C57Bl/6 display a resistant T_H2-type response phenotype when infected with a high dose of eggs, leading to expulsion and clearance (Bancroft et al., 1994). The C57Bl/6 strain however also displays a susceptible T_H1-type response when infected with a low dose of eggs, leading to persistent helminth infection (Bancroft et al., 2001). In this chapter we test the hypothesis that CD11cCre:CXCR5^{fl} mice should be unable to generate protective T_H2-type responses to a high dose *T. muris* infection.

6.3 Results

6.3.1 Effects of CD11c-mediated CXCR5 knockout on *T. muris* infection

To determine the effects of CD11c-mediated CXCR5 knockout on intestinal helminth infection groups of 12 $CXCR5^{fl}$ and $CD11cCre:CXCR5^{fl}$ mice were orally inoculated with ~250 embryonated *T. muris* eggs (see 2.3.5). To determine the response to oral infection, 4 mice from each group were sacrificed at 2 weeks and the remaining mice sacrificed at 30 days post inoculation. At 2 weeks post infection the inflammatory macro-anatomy of the caecum and proximal colon was confirmed visually and presence of larval stage L2 was confirmed within the caecum in all mice investigated, indicative of successful oral *T. muris* infection. At 30 days post infection, of the $CXCR5^{fl}$ mice infected, 3 had no detectable worms, 4 had only 1 adult worm present (residing in the caecum in one mouse, within the colon in two of the mice and 1 found in faecal intestinal contents), additionally 1 mouse was found to have 16 adult worms within the caecum. On average 2.5 worms per mouse were observed within the $CXCR5^{fl}$ genotype group indicative of a successful infection that was in the latter stages of clearance. In contrast $CD11cCre:CXCR5^{fl}$ mice possessed from 55 to 175 adult worms within the caecum with further worms observed both within the large intestine and large intestinal contents (figure 6.1) indicative of persistent worm infection. In conclusion $CD11cCre:CXCR5^{fl}$ mice had statistically significantly more *T. muris* present within their caecum, large intestine and faecal contents at 30 days post infection than $CXCR5^{fl}$ mice (T-test of difference $P = 0.038$).

Figure 6.1 Worm burden at 30 days post infection with ~250 *T. muris* embryonated eggs.
Error bars represent the standard error of the mean for total number of *T. muris* observed per mouse (faeces, colon and caecum combined). T-test of difference *P* = 0.038.

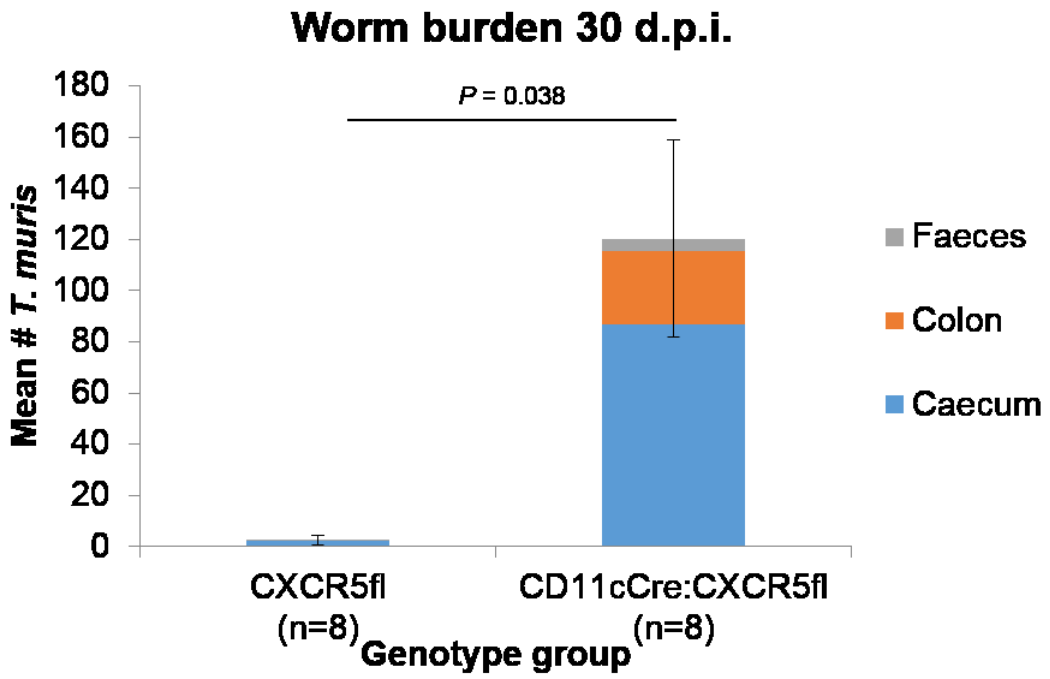

Further histopathological investigation (see 2.15) of the large intestine revealed evidence of persistent infection in CD11cCre:CXCR5^{fl} mice. Haematoxylin and eosin stained sections of large intestine from CXCR5fl mice 30 days post *T. muris* infection were indistinguishable from uninfected mice, suggesting any pathological changes had resolved following worm expulsion (Figure 6.2A). In contrast the large intestines from infected CD11cCre:CXCR5^{fl} mice revealed inflammatory expansion of the submucosa, lengthening of the crypts and visible damage to the intestinal epithelial layer (Figure 6.2B). In CXCR5^{fl} mice lymphocytes (B220^{+} B cells) and (CD11c^{+}/CD11b^{+}) mononuclear phagocytes appeared evenly distributed within the intestinal lamina propria (Figure 6.2C). In contrast infected CD11cCre:CXCR5^{fl} mice revealed focal aggregation of CD11c^{+}/CD11b^{+} monocytes/macrophages aggregating around areas of damage.

Figure 6.2 Histopathological alterations to the large intestine following *T. muris* infection

Orally *T. muris* infected CXCR5^{fl} mice revealed no alteration to large intestine at 30 days post infection (A) however infected CD11cCre:CXCR5^{fl} mice revealed inflammatory expansion of the submucosa (black arrows), crypt expansion (yellow arrows) and epithelial damage (Blue arrowheads) upon histological examination (B). CXCR5^{fl} mice revealed even distribution of leucocytes (C) whilst CD11cCre:CXCR5^{fl} mice revealed aggregation of CD11c+/CD11b+ macrophage around damaged areas of epithelium (D) scale bars = 100 µm

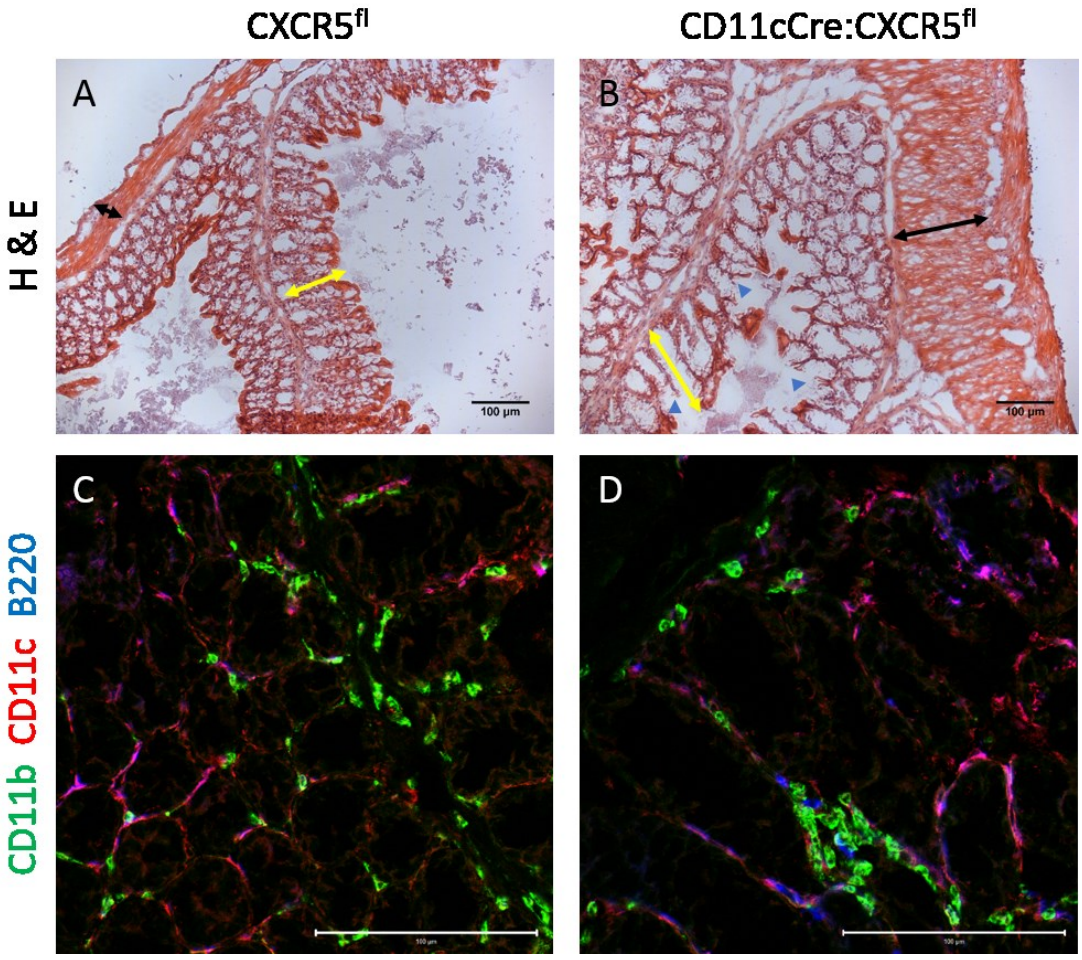

6.3.2 Alteration of antibody responses to *T. muris* in CD11cCre:CXCR5^{fl} mice

Antibody responses to *T. muris* were measured in sera of CD11cCre:CXCR5^{fl} and CXCR5^{fl} mice 30 days post infection via ELISA (see 2.13 and table 2.2). Using a dilution series, measurement of *T. muris* excretory/secretory (E/S) product reactive antibody binding were measured for both IgG1 and IgG2A antibody subtypes in naïve and *T. muris* infected CD11cCre:CXCR5^{fl} and CXCR5^{fl} mice. As expected, naïve mice of both genotype revealed no antibodies to *T. muris* E/S product. CXCR5^{fl} mice infected with *T. muris* revealed relatively high levels of *T. muris* E/S product specific IgG1 and low levels of *T. muris* E/S product specific IgG2A in an IgG1/IgG2A ratio of 5:1, indicative of the generation of a protective T_H2-biased response. In contrast *T. muris* infected CD11cCre:CXCR5^{fl} mice revealed low levels of *T. muris* E/S product specific IgG1 and low *T. muris* E/S product specific IgG2A in an IgG1/IgG2A ratio of 1:1 (Figure 6.3) associated with an inappropriate T_H1-biased response and confirmatory of their persistently infected status. Comparatively in CXCR5^{fl} mice twice the amount of *T. muris* E/S product specific IgG1 and half the amount of *T. muris* E/S product specific IgG2A were detectable in sera compared to CD11cCre:CXCR5^{fl} mice following infection (Figure 6.3).

Figure 6.3 Antibody subtype responses to *T. muris* antigen in CD11cCre:CXCR5^{fl} mice

ELISA plates coated with *T. muris* E/S product were used to capture specific antibodies from sera of 30 d.p.i, *T. muris* infected CXCR5^{fl} (n=8) or CD11cCre:CXCR5^{fl} (n=8) mice. Naïve mice of both genotypes were used as controls, revealing the presence of no *T. muris*-specific antibodies. Using subtype specific detection antibodies, levels of IgG1 (A) and IgG2A (B) were measured and group mean responses calculated for various sera dilutions. (C) Relative mean titre values were calculated at ½ maximal response and compared via 2-sample T-test. Error bars = SEM.

A

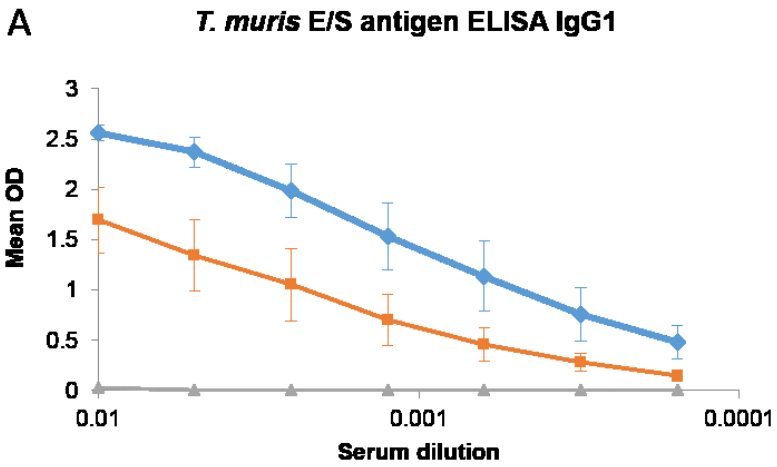

B

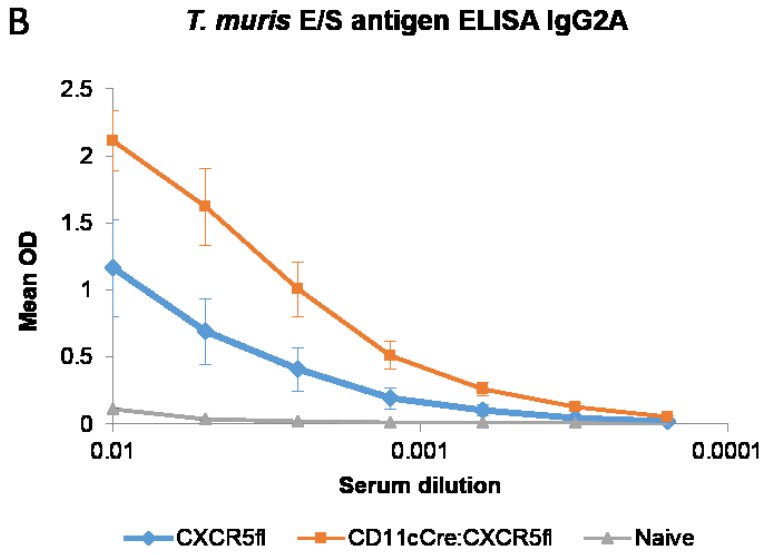

C

Group	Mean relative titre	SEM	P=
CXCR5fl IgG1	1.2917	0.024	0.002
CD11cCre:CXCR5fl IgG1	0.754	0.11	
CXCR5fl IgG2A	0.558	0.11	0.002
CD11cCre:CXCR5fl IgG2A	1.095	0.072	

6.3.3 Alteration of cytokine responses to *T. muris* in CD11cCre:CXCR5^{fl} mice

To assess the cytokine responses to *T. muris* infection, mesenteric lymph nodes were collected and total RNA extracted (see 2.7.1). cDNAs were synthesised (see 2.7.2) and real-time PCR performed with specific oligonucleotide primer sets for various cytokines (see 2.7.3 for primer details and targets). In the initial screen, cytokines and genes identified as relevant to *T. muris* infection were assessed (Table 6.1). Following this assessment, genes which displayed robust alteration between genotypes or are known to have an essential role in the response to infection were re-analysed in both naïve and infected mice of both genotypes for further statistical analysis (Figure 6.4).

Assessment of gene expression in the mesenteric lymph nodes of either naïve or 30 day post *T. muris* infected CD11cCre:CXCR5^{fl} or CXCR5^{fl} mice revealed a stark contrast in responses to infection. CXCR5^{fl} mice revealed statistically significant high levels of the protective T_H2-associated cytokines *Il4* (Figure 6.5A), *Il13* (Figure 6.5B) and *Il5* (Figure 6.5C) in response to infection. In addition, easily detectable levels of *Il9* (Table 6.1) were observed. Furthermore inflammatory *Il1b* and T_H1-associated cytokines such as *Ifng* (Figure 6.5E), *Il1b* (Figure 6.5F) and *Il6* (Figure 6.5G) were not upregulated in *T. muris* infected CXCR5^{fl} mice.

Figure 6.4 Cytokine responses to *T. muris* infection

Investigation of cytokine mRNA expression in mesenteric lymph node. Mesenteric lymph nodes from either naïve or 30 days post high dose *T. muris* infected mice of confirmed genotype CXCR5fl or CD11cCre:CXCR5fl (N=8 per group) were harvested and RNA extracted and translated into cDNA. Using cytokine-specific oligonucleotides the relative expression levels of *Il4* (A), *Il13* (B), *Il5* (C), *Blr1* (D), *Il1b* (E), *Ifng* (F), *Il6* (G) and *Itgax* (H) were calculated against the control gene *Rpl19* using the ΔΔCT method and resultant data were analysed by ANOVA and Tukey's comparison. Error bars = SEM. Increases in cytokine levels within groups are indicated at <0.05 (*), <0.005 (**), <0.001 (***) or <0.0001(****) levels of statistical significance.

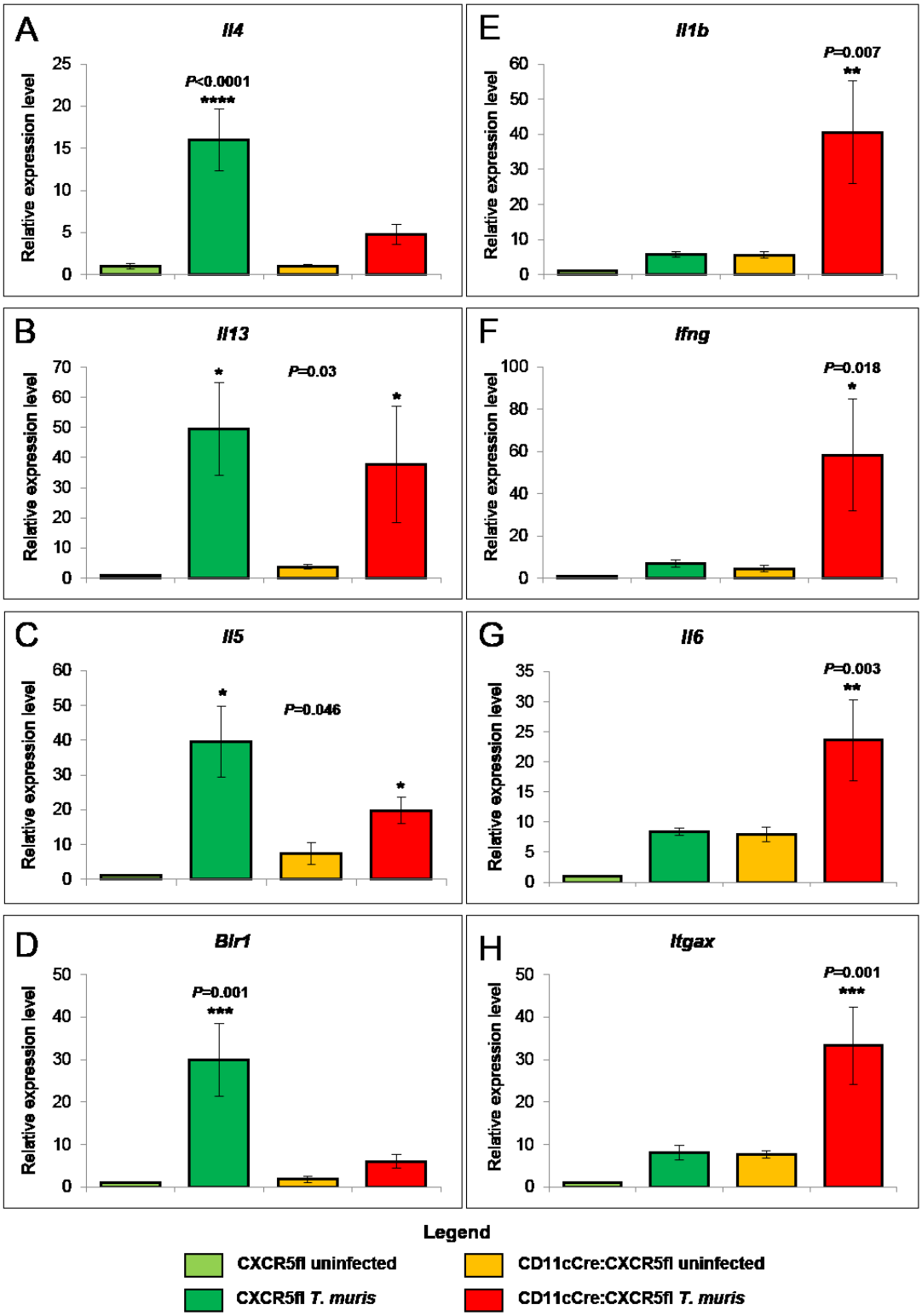
A
Il4
Relative expression level
P<0.0001
****
B
Il13
P=0.03
C
Il5
P=0.046
D
Blr1
P=0.001
***
E
Il1b
P=0.007
**
F
Ifng
P=0.018
G
Il6
P=0.003
H
Itgax
P=0.001
Legend
CXCR5fl uninfected
CXCR5fl T. muris
CD11cCre:CXCR5fl uninfected
CD11cCre:CXCR5fl T. muris

In contrast *T. muris* infected CD11cCre:CXCR5^{fl} mice displayed no statistically significant increase in *Il4* (Figure 6.4A), but significant increases in both *Il13* (Figure 6.4B) and *Il5* (Figure 6.4C) occurred over naïve mice, but at reduced but not statistically significantly different levels to infected CXCR5^{fl} mice. A significant increase in *Blr1* (CXCR5) was observed in *T. muris* infected CXCR5^{fl} mice, in contrast *T. muris* infected CD11cCre:CXCR5^{fl} mice revealed *Blr1* expression indistinguishable from naïve mice. In contrast an extreme upregulation of the cDC marker *Itgax* (CD11c) occurred in the mesenteric lymph nodes of *T. muris* infected CD11cCre:CXCR5^{fl} mice, which was not observed in the lymph nodes of infected CXCR5^{fl} mice.

Table 6.1 relative cytokine gene expression following *T. muris* infection

QPCR CT data normalised to *T. muris* infected CXCR5^{fl} mice at 30 days post infection. * $p<0.05$ statistically significant difference in CD11cCre:CXCR5^{fl} mice. Relative increase (▲), decrease (▼) or no change indicated (◄). SEM = standard error of the mean.

Gene of interest	CXCR5^{fl} Normalised expression level	SEM	CD11cCre:CXCR5^{fl} Relative expression level	SEM	P =
Il2	1.00	0.15	1.59 ▲	0.37	0.174
Il9	1.00	0.00	No CT ▼	n/a	0.116
Il10	1.00	0.05	1.73 ▲	0.29	0.814
Il12a	1.00	0.24	1.49 ▲	0.29	0.217
Il12b	1.00	0.34	1.40 ▲	0.37	0.436
Il17	1.00	0.17	0.67 ▼	0.49	0.240
Il18	1.00	0.32	1.31 ▲	0.61	0.676
Il17e	1.00	0.32	0.51 ▼	0.10	0.179
9230117N10Rik	1.00	0.09	1.42 ▲	0.25	0.191
Lta	1.00	0.48	1.08 ◄	0.44	0.909
Ltb	1.00	0.15	0.73 ▼	0.08	0.144
Tnfa	1.00	0.34	0.98 ◄	0.19	0.961

Investigation of other cytokine gene expression changes in the mesenteric lymph nodes of *T. muris* infected CXCR5^{fl} and CD11cCre:CXCR5^{fl} mice revealed no statistically significant differences in their responses. Trends for an increase in cytokines such as *Il2*, *Il12*, *Il18* and decrease in *Il17* were observed which may assist T_H1-maturation. Also trends in a reduction in T_H2-associated *Il9* and *Il17e* (Il-25) were observed. In the case of *Il9* it was readily and variably detectable in *T. muris* infected CXCR5^{fl} mice but below the limit of detection in naïve mice of both genotypes and *T. muris* infected CD11cCre:CXCR5^{fl} mice, suggesting that no substantial increase in *Il9* expression had occurred in CD11cCre:CXCR5^{fl} mice following *T. muris* infection. Considering the critical role IL9 plays in worm expulsion these data are not surprising as CD11cCre:CXCR5^{fl} mice were persistently colonised following high dose *T. muris* infection. A trend toward increased levels of the T_H1 restricting *Il10* and the T_H2 promoting *9230117N10Rik* (Il-33) in *T. muris* infected CD11cCre:CXCR5^{fl} mice when compared to *T. muris* infected CXCR5^{fl} mice revealed the mixed nature of response (Table 6.1).

Investigation of changes in chemokine and chemoreceptor gene expression in mesenteric lymph nodes of *T. muris* infected mice revealed a statistically significant increase in *Ccr2* in CD11cCre:CXCR5^{fl} mice compared to CXCR5^{fl} mice. Further trends in increased *Ccr1*, *Ccr5*, *Ccr7* and *Cxcr4* and decreased *Ccr3* and *Ccr4* were observed in CD11cCre:CXCR5^{fl} mice.

Table 6.2 relative chemokine and chemoreceptor gene expression following *T. muris* infection

QPCR CT data normalised to *T. muris* infected CXCR5^{fl} mice at 30 days post infection. * $p<0.05$ statistically significant difference in CD11cCre:CXCR5^{fl} mice. Relative increase (▲), decrease (▼) or no change indicated (◄). SEM = standard error of the mean.

Gene of interest	CXCR5^{fl} Normalised expression level	SEM	CD11cCre:CXCR5^{fl} Relative expression level	SEM	P =
Ccl5	1.00	0.12	1.00 ◄	0.41	0.997
Ccl11	1.00	0.12	1.03 ◄	0.29	0.934
Ccr1	1.00	0.13	3.31 ▲	1.62	0.186
Ccr2	1.00	0.23	2.07 ▲	0.38	0.037*
Ccr3	1.00	0.18	0.59 ▼	0.10	0.074
Ccr4	1.00	0.19	0.79 ▼	0.14	0.393
Ccr5	1.00	0.27	3.42 ▲	1.34	0.106
Ccr7	1.00	0.24	1.25 ▲	0.33	0.551
Cxcr4	1.00	0.27	1.46 ▲	0.52	0.452

Investigation of gene expression changes of other cellular receptors and markers revealed a statistically significant decrease of *Il27ra* in CD11cCre:CXCR5^{fl} mice compared to CXCR5^{fl} mice. Further trends in increased *Cd4* (T cell), *Cd80* and *Cd86* (DC co-stimulatory molecules) and Il-12 receptor subunits *Il12b1* associated with T_H2 maturation and *Il12b2* associated with T_H1 maturation respectively.

Table 6.3 relative cellular marker gene expression following *T. muris* infection

QPCR CT data normalised to *T. muris* infected CXCR5^{fl} mice at 30 days post infection. * $p<0.05$ statistically significant difference in CD11cCre:CXCR5^{fl} mice. Relative increase (▲) or decrease (▼) indicated SEM = standard error of the mean.

Gene of interest	CXCR5^{fl} Normalised expression level	SEM	CD11cCre:CXCR5^{fl} Relative expression level	SEM	P =
Cd4	1.00	0.31	1.33 ▲	0.60	0.633
Cd80	1.00	0.09	1.45 ▲	0.33	0.220
Cd86	1.00	0.12	1.39 ▲	0.30	0.262
Il12rb1	1.00	0.29	2.08 ▲	0.62	0.143
Il12rb2	1.00	0.23	4.34 ▲	1.67	0.075
Il27ra	1.00	0.13	0.58 ▼	0.07	0.048*
Prnp	1.00	0.35	0.40 ▼	0.15	0.142

6.4 Discussion

Expression of the chemokine receptor CXCR5 and the localisation towards B cell follicles by APC is critical for the generation of protective T_H2-biased responses to intestinal helminth infection (Leon et al., 2012). However, the use of blocking antibodies to the chemokine CXCL13 or the generation of mixed bone marrow chimeras to generate dendritic cells lacking CXCR5 may both have accessory effects on the microarchitecture of secondary lymphoid organs. To further confirm the dependence of CXCR5 expression by dendritic cells in the induction of T_H2-type responses to helminth infection we infected CD11cCre:CXCR5^{fl} mice generated on a C57Bl/6 background with a high dose of *T. muris* embryonated eggs. Control CXCR5^{fl} infected mice developed an appropriate and protective T_H2 response and were clear of infection by 30 days. However, CD11cCre:CXCR5^{fl} mice became persistently infected with *T. muris* and revealed alterations to both cytokine and antibody isotype responses indicative of a failure to generate a protective T_H2 response. Instead a mixed helper T immune response was observed which was dominated by T_H1-associated cytokines.

The expression of CXCR5 by DCs has previously been suggested to regulate antibody-specific immune responses (Wu and Hwang, 2002). Following *T. muris* infection the generation of antibody responses by B cells has been suggested to be involved in the protection to infection (Blackwell and Else, 2001). Furthermore differences in the production of antibody subtypes have been identified between resistant and susceptible animals, with resistance associated with high levels of parasite-specific IgG1 production and susceptibility associated with high levels of parasite-specific IgG2A production (Koyama et al.). B cells and antibody production had been considered as a requirement for expulsion of *T. muris*. Adoptive transfer of B cells restored resistance to the *T. muris* susceptible B cell deficient μMT mice, as did administration of IgG from infected mice (Blackwell and Else, 2001). However adoptive transfer of CD4$^+$ T cells into the *T. muris* susceptible SCID mice also results in worm expulsion, revealing antibody-independent mechanisms (Else and Grencis, 1996).

In this study, we observed as anticipated that CXCR5^{fl} control mice were resistant to high dose *T. muris* infection and generated a parasite-specific IgG1-dominated antibody response. In contrast CD11cCre:CXCR5^{fl} mice were susceptible to infection and generated a parasite-specific IgG2A-dominated antibody response, however this response may not account for their failure to expel the parasite. The role of cDC during *T. muris* infection has previously been questioned, with a suggestion that basophils may act as the APC driving protective T_H2

responses (Perrigoue et al., 2009). However following infection with helminths such as *Schistosoma mansoni, Heligmosomoides polygyrus* and *Nippostrongylus brasiliensis,* depletion of $CD11c^+$ cells has been shown to directly abrogate T_H2 induction and development (Phythian-Adams et al., 2010, Smith et al., 2012). Following *T. muris* infection in $CXCR5^{fl}$ control mice a classic T_H2 response was observed in the cytokine gene expression profile of MLN, indicative of protection and clearance of infection.

Cytokines associated with resistance to *T. muris* usually trigger expulsion mechanisms such as increased epithelial cell turnover (Cliffe et al., 2007) increased mucin production by goblet cells (Hasnain et al., 2010) both likely dependent upon IL-13 and down-regulated by IFNγ, and increased hypercontractility of the intestinal smooth muscle (Khan et al., 2003) potentiated by IL-9, and lead to clearance of the parasite. IL-4 and IL-13 are the two major cytokines associated with resistance to infection (Grencis, 2001). We observed increased expression of both corresponding genes *Il4* and *Il13* as well as *Il5* in *T. muris* infected $CXCR5^{fl}$ mice. Cytokines associated with susceptibility to *T. muris* lead to chronic infection and are associated with T_H1-responses (Cliffe and Grencis, 2004), included IFNγ (Bradley et al., 1996), IL-12 (Hsieh et al., 1993, Manetti et al., 1993, Seder et al., 1993, Wu et al., 1993, Manetti et al., 1994) and IL-18 (Dinarello, 1999). In *T. muris* infected $CXCR5^{fl}$ control mice we observed no difference in *Ifng* between naïve and infected mice, whereas *Il12* and *Il18* expression levels were comparatively lower than in *T. muris* infected CD11cCre:$CXCR5^{fl}$ mice though this was a non-significant trend due to the variation within each group. Furthermore we observed easily detectable levels of *Il9* produced in *T. muris* infected $CXCR5^{fl}$ mice, previously associated with parasite expulsion (Faulkner et al., 1998) but were levels in naïve mice and *T. muris* infected CD11cCre:$CXCR5^{fl}$ mice were below the level of detection, indicating negligible amounts of IL-9 were expressed in these groups.

Investigation of *T. muris* infected CD11cCre:$CXCR5^{fl}$ mice revealed no statistically significant increase in *Il4* gene expression over levels expressed in naïve mice, but did reveal a statistically significant increase in *Il13* expression level which was indistinguishable from the increased expression level observed in *T. muris* infected $CXCR5^{fl}$ control mice. Previous studies have revealed that IL-13 restores resistance to infection in IL-4 knockout mice (Bancroft et al., 2000), yet CD11cCre:$CXCR5^{fl}$ mice revealed chronic infection. We observed a large increase in expression of *Ifng* in *T. muris* infected CD11cCre:$CXCR5^{fl}$ mice shown to be critical for susceptibility (Else et al., 1994). Other evidence of a T_H1-dominanted response

including grossly elevated levels of *Il1b* (Chizzolini et al., 1997) and *Il6* (Yamamoto et al., 2000) were also observed in *T. muris* infected CD11cCre:CXCR5^{fl} mice. A statistically significant reduction in *Il27ra* was also observed, linked with the induction of chronic infection (Bancroft et al., 2004), however these mice were already persistently infected at the time of sampling. IL-27RA is a negative regulatory receptor for DC antigen-presenting function and DC-mediated T_H1-maturation of CD4 T cells (Wang et al., 2007, Mascanfroni et al., 2013), suggesting therefore that in CD11cCre:CXCR5^{fl} mice decreased expression of *Il27ra* would increase capacity for DC antigen presentation to-, and bias towards- T_H1-maturation in CD4$^+$ T cells. Conversely the comparatively high *Il27ra* expression level in CXCR5^{fl} mice should restrict T_H1-maturation.

The prevention of follicle-homing of CD11c$^+$ cells in *T. muris* infected CD11cCre:CXCR5^{fl} mice due to CD11c-mediated knockout of the chemokine receptor CXCR5 resulted in a mixed helper T immune response. While some protective cytokines were observed to be upregulated similar to levels observed in CXCR5^{fl} control mice, a large T_H1-dominated susceptible response was generated in the absence of IL-4. This resulted in a chronic *T. muris* infection in CD11cCre:CXCR5^{fl} mice which were persistently infected. In conclusion the inability for CD11cCre:CXCR5^{fl} mice to clear *T. muris* infection demonstrate the critical role that follicle-homing cDC play during *T. muris* infection. The failure to present *T. muris* antigens to T cells (and B cells) within the B-cell follicle switched the response to *T. muris* infection from resistance as observed in CXCR5^{fl} control mice to complete susceptibility and chronic infection. These data suggest that efficient polarisation of T_H2 responses requires cDC capable of expressing CXCR5. The reason for this requirement appears to be so that the cDC APC capacity must occur to naïve T-cells within the B-cell follicular environment, suggesting a tripartite cellular relationship. The migration of CD4 T-cells into the B-cell follicle is regulated by interaction with cDC and is dependent upon CD40-dependent maturation of cDC as it does not occur in CD40-deficient mice (Fillatreau and Gray, 2003). Regulatory B-cells are capable of engaging T-cells via CD40/CD40L and producing IL10, a cytokine that not only promotes T_H2 maturation but inhibits production of T_H1 stimulating cytokines such as IL2 (Fillatreau et al., 2008). Studies have revealed that B-cell-cDC interaction can lead to cDC maturation which favours T_H2 polarisation due to cDC secretion of IL-4, -5 and -13 and expression of OX40L, a CD-40-dependent event. This interaction occurs between cDC and activated B-cells via CD69 and BAFF-R and more importantly is contact-dependent thus requiring cDC and B-cells

to co-localise effectively (Maddur et al., 2014), a process which appears highly likely if both cells express CXCR5 and reside or migrate to the CXCL13-organised B-cell follicle .

These findings further reinforce the observations of Leon et al. and display using an elegant model of genetic deletion that $CD11c^{+}$ cells expressing CXCR5 are a requirement for the generation of protective T_H2 responses to infection by gastrointestinal parasites such as *T. muris* and *H. polygyrus* and potentially underlie the formation of protective responses to the majority of gastrointestinal nematode parasites.

Chapter 7. Sialoadhesin and peripheral prion pathogenesis

7.1 Abstract

An intact splenic marginal zone is important for the efficient delivery of prions into the B cell follicles where they subsequently replicate upon follicular dendritic cells before infecting the nervous system. Sialoadhesin is a mononuclear phagocyte-restricted cell adhesion molecule that binds sialylated glycoproteins and is constitutively expressed upon splenic marginal zone metallophilic and lymph node sub-capsular sinus macrophage populations. Sialoadhesin binds sialylated glycoproteins, pathogens and exosomes in the blood and lymph via recognition of terminal sialic acid residues. The expression of sialoadhesin on marginal zone and subcapsular sinus macrophage populations enables these cells to screen the blood and lymph for sialylated glycoproteins and facilitate their capture and possible uptake or further processing. Since the prion glycoprotein is highly sialylated, in this chapter the hypothesis that sialoadhesin may influence prion disease pathogenesis was explored. After peripheral exposure, prion pathogenesis was observed to be unaltered in sialoadhesin-deficient mice; revealing that lymphoid sequestration of prions is not mediated via sialoadhesin. Thus although an intact marginal zone is important for the efficient uptake and delivery of prions into the B cell follicles of the spleen, this is not influenced by sialoadhesin expression by the MNP within it.

7.2 Introduction

The precise mode by which infectious prions are initially conveyed from the site of exposure to follicular dendritic cells (FDC) within the B-cell follicles was uncertain (see Chapter 1.1.5), however a number of cellular and molecular components of the innate immune system have been shown to be involved. Data presented in Chapter 5 reveal that $CD11c^+$ cells deliver prions to FDC via CXCR5-mediated chemotaxis, however ablation of CXCR5 specifically from $CD11c^+$ cells did not completely block prion transport or generate complete resistance to prion infection. FDC characteristically trap and retain native antigen on their surfaces in the form of immune complexes, consisting of antigen-antibody and/or opsonizing complement components. FDC appear to initially trap and retain prions on their surfaces in the form of complement-bound complexes (Klein et al., 2001, Mabbott et al., 2001, Zabel et al., 2007). In addition to these molecular factors, migratory cells such as integrin alpha x-expressing (Itgax/CD11c) mononuclear phagocytes (MNP) may also play an important role in the initial uptake and transport of prions since their depletion prior to peripheral exposure blocked prion accumulation upon FDC and reduced disease susceptibility (Raymond et al., 2007, Cordier-Dirikoc and Chabry, 2008). Complement components may also aid the initial uptake of prions by MNP (Flores-Langarica et al., 2009).

The splenic marginal zone surrounding the white pulp comprises a marginal sinus with a network of sinus-lining cells and reticular cells through which the blood percolates on its way to the red pulp. Attached to this network are specific populations of MNP and B cells which enable the continual surveillance and clearance of pathogens, antigens and apoptotic cells from the blood-stream. The positioning of these cells in the splenic marginal zone enables them to regulate the clearance of blood-borne immune-complexes and proteoglycans into the FDC-containing B-cell follicles (Aichele et al., 2003, Cinamon et al., 2008). For example, in lymph nodes sub-capsular sinus macrophages capture immune complexes on their surfaces, and pass them to follicular B cells for delivery to FDC in the B-cell follicles (Phan et al., 2009). An intact splenic marginal zone also plays an important role in the efficient delivery of complement-bound prions to FDC (Brown et al., 2012, Brown and Mabbott, 2014).

Treatments which block the early accumulation and replication of prions in the spleen can block or substantially reduce disease susceptibility (Mabbott et al., 2000, Montrasio et al., 2000, Mabbott et al., 2001, Raymond et al., 2007). Therefore, identification of the cellular and molecular factors which influence the initial accumulation of prions in secondary lymphoid

tissues may reveal novel targets for therapeutic intervention. Sialic acids are a large family of nine-carbon sugars that are normally found at the terminal, exposed positions of glycans at the cell surface and on secreted proteins. Sialoadhesin can bind to sialic acid residues expressed on the surface of some important pathogens such as porcine reproductive and respiratory syndrome virus (PRSSV), HIV-1, *Trypanosoma cruzi*, *Neisseria meningitides* and *Campylobacter jejuni* (Klaas and Crocker, 2012).

Host-encoded sialic acid binding Ig-like lectin (siglec) proteins are expressed by various MNP subsets under steady-state or induced during inflammatory conditions and act as cell-cell and cell-pathogen recognition and endocytic internalization receptors (Crocker, 2002). Sialoadhesin (siglec-1/CD169) binds sialylated glycan end chains (Crocker et al., 1991) and specifically recognises N-acetylneuraminic acid (Neu5Ac), the predominant sialic acid found in mammalian cells (Klaas and Crocker, 2012). The prion protein is variably glycosylated and extensively sialylated (Stimson et al., 1999) and undergoes altered sialylation during disease-associated accumulation in the CNS (Zomosa-Signoret et al., 2011) and in secondary lymphoid organs (Srivastava et al., 2015). Since marginal zone metallophilic macrophages (and subcapsular sinus macrophages in lymph nodes) are characterized by their constitutive expression of sialoadhesin (Crocker and Gordon, 1986), in this chapter the hypothesis that sialoadhesin plays an important role in regulating the initial delivery of prions to FDC within the B cell follicles was explored.

7.3 Results

7.3.1 Effect of sialoadhesin-deficiency on follicular dendritic cell status and function

To determine the effect of sialoadhesin-deficiency on the status and function of FDC, spleens of wild type and sialoadhesin-deficient mice (see 2.1.7) were investigated via immunohistochemistry (see 2.15.5) in naïve mice and in mice subject to passive immunizations (see 2.3.3). In the spleens of wild type mice, high levels of sialoadhesin expression were detected only in association with the inner marginal zone metallophilic macrophages surrounding the white pulp (Figure 7.1A) and their counterparts, the subcapsular sinus macrophages, in lymph nodes (Figure 7.1C) via immunohistochemistry (see 2.15.5). As anticipated these MNP populations lacked sialoadhesin expression in tissues from sialoadhesin-deficient mice (Figure 7.1B & 7.1D). Since prion replication upon PrP^C-expressing FDC is important for efficient neuroinvasion, FDC status and function were characterized in sialoadhesin-deficient mice. FDC characteristically express high levels of complement receptor 1 (CR1/CD35) on their surfaces. Immunohistochemical (IHC) analysis suggested that sialoadhesin-deficiency had no observable effect on the expression of complement receptor 1 by splenic FDC (Figure 7.1E & 7.1F). Morphometric analysis also suggested that size of the FDC networks was similar in the spleens of mice from each group (Figure 7.1G, $n = 6$ mice per group, $P = 0.257$). These data are consistent with the expression of negligible levels of the *Siglec1* gene (which encodes sialoadhesin) by FDC in contrast to MNP (Figure 7.2).

Figure 7.1 Effect of sialoadhesin-deficiency on FDC status.

Splenic marginal zone macrophages (green) (A) in wild-type (WT) mice but is undetectable in splenic marginal zone of sialoadhesin-deficient (Sn-/-) mice (B). Spleen sections were also immunostained to detect B cells (B220+ cells, blue A, B). In lymph node, subcapsular sinus macrophages express high levels of sialoadhesin in WT mice (C) absent in Sn-/- mice (D). Immunostaining with anti-CD35 (E & F, red) revealed that sialoadhesin-deficiency had no effect on FDC network size when compared to WT mice (G). Comparison of sialoadhesin (blue), complement component C4 (green) and PrP^C-expression (red) in the spleens of WT (H) and Sn-/- (I) mice. In the spleens of Sn-/- mice, morphometric analysis revealed significant increases in the level of complement component C4 on the surfaces of FDC (J) and their expression of PrP^C (K) when compared to WT mice. *, $P < 0.001$; **, $P < 0.0001$.

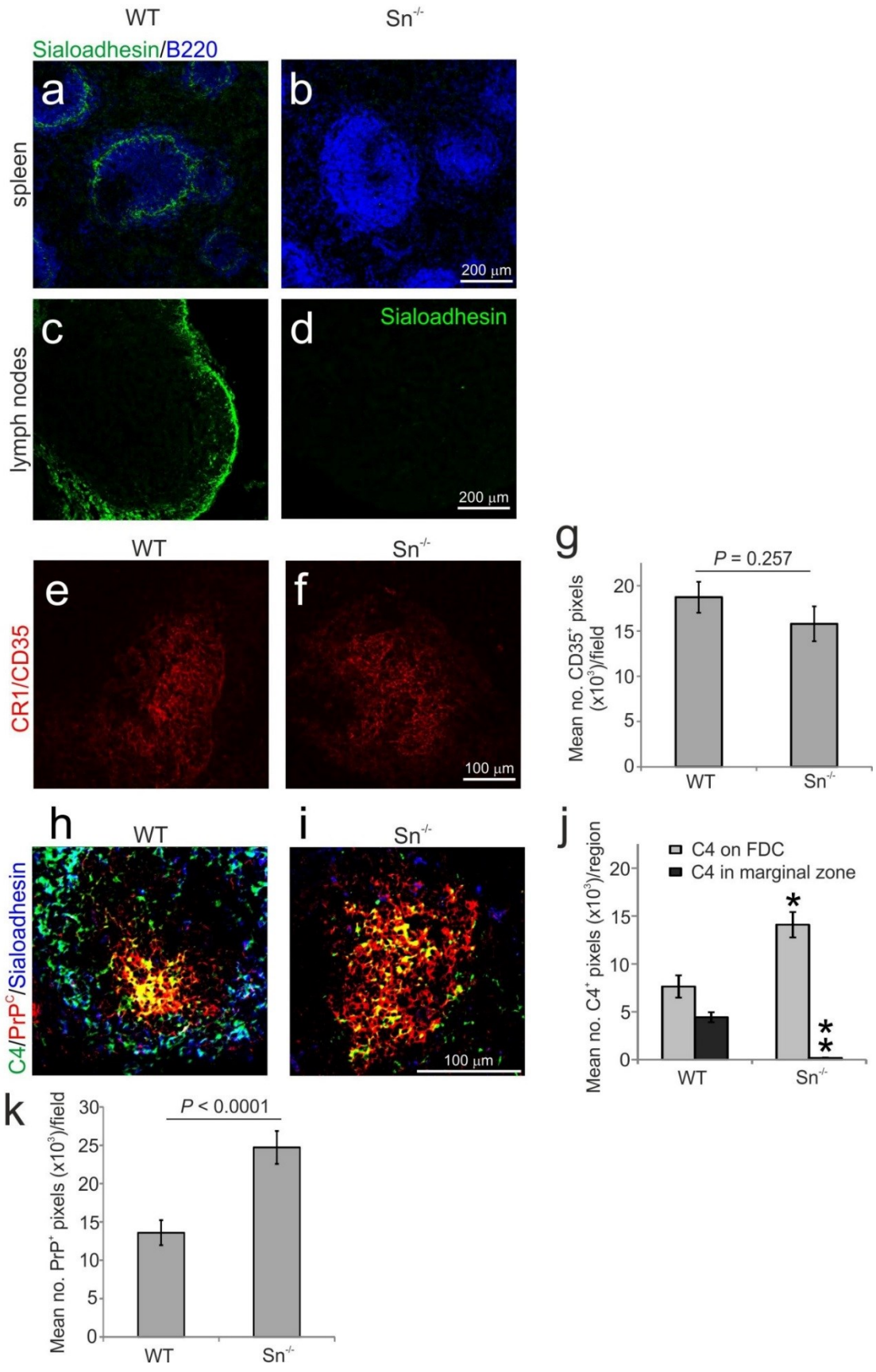
WT
Sn-/-
Sialoadhesin/B220
a
b
spleen
200 µm
c
d
Sialoadhesin
lymph nodes
200 µm
WT
Sn-/-
e
f
CR1/CD35
100 µm
g
P = 0.257
Mean no. CD35+ pixels (x10³)/field
20
15
10
5
0
WT
Sn-/-
h
WT
i
Sn-/-
C4/PrPC/Sialoadhesin
100 µm
j
C4 on FDC
C4 in marginal zone
Mean no. C4+ pixels (x10³)/region
20
15
10
5
0
*
**
WT
Sn-/-
k
P < 0.0001
Mean no. PrP+ pixels (x10³)/field
30
25
20
15
10
5
0
WT
Sn-/-

FDC trap and retain complement component C4 on their surfaces and express high levels of cellular PrP^C (Figure 7.1H). These characteristics are important for the retention and replication of prions upon the surfaces of FDC (Klein et al., 2001, Mabbott et al., 2001, Zabel et al., 2007, McCulloch et al., 2011). IHC analysis revealed that significantly more complement component C4 was detected on the surfaces of FDC in the spleens of sialoadhesin-deficient mice when compared to wild type controls (Figure 7.1I & 7.1J; $n = 6$ per group, $P < 0.001$). This coincided with a significant reduction in the ability of cells in the marginal zone of sialoadhesin-deficient mice to trap complement component C4 (Figure 7.1I & 7.1J, $n = 6$ mice per group, $P < 0.0001$). Data suggest that the trapping of immune complexes by FDC upregulates their expression of PrP^C (Lötscher et al., 2003). Here, the increased association of C4 on the surfaces of FDC in the spleens of sialoadhesin-deficient mice coincided with a significant increase in the expression of PrP^C upon their surfaces (Fig. 7.1K; $n = 6$ mice per group, $P < 0.0001$) implying a similar relationship.

Figure 7.2 Comparison of *Siglec1* mRNA expression in murine tissues and cells.

(A) Expression profile of *Siglec1* (which encodes sialoadhesin/CD169; Affymetrix probe set ID 1422161_at) across a wide range of microarray data sets representing 95 distinct mouse tissues and cell-lineages. All sample analysis was performed on the Affymetrix MOE430 2.0 expression array. Data were analysed using the GNF1M Mouse tissue atlas (http://biogps.gnf.org). Detailed conditions of the cell and tissue preparation and treatment are available in the above study. The normalised, mean gene expression level data for each tissue and cell type are shown. These data show that in the steady-state sialoadhesin is not expressed by microglia (blue box), Neuro2a neuroblastoma cells (green box) or in the brain (red box). (B) Subcapsular sinus macrophages, in contrast to FDC, express high levels of *Siglec1* mRNA in the steady state. Comparison of *Siglec1* expression levels (Affymetrix probe set 1422161_at) by subcapsular sinus (SCS) macrophages, microglia, FL-Y cells (a follicular dendritic cell (FDC)-like cell-line) (Nishikawa et al., 2006), Peyer's patches (PP) FDC, astrocytes and neuro2a cells. Publicly available gene expression data sets performed on Affymetrix MOE430 2.0 expression arrays were download and normalised using RMA (Affymetrix, Santa Clara, CA). The chip identification accession numbers for each data set are indicated: SCS macrophages, GSM395738, GSM395739, GSM395740; microglia, GSM258721, GSM258722; FL-Y-cells, RMLNDC002001, RMLNDC003001; PP-FDC, GSM481976, GSM481977; astrocytes, GSM241898; neuro2a cells, GSM258727, GSM258728.

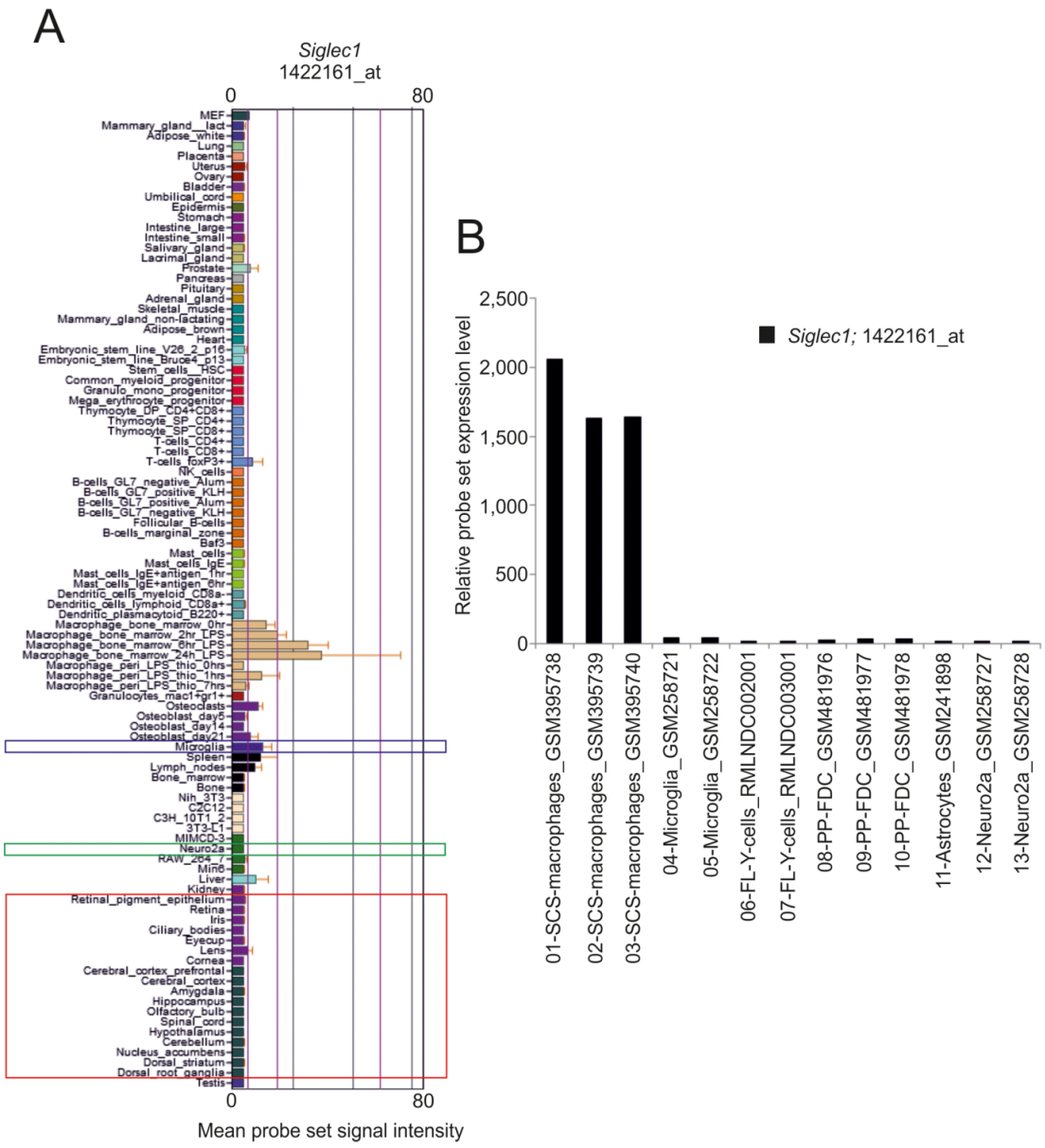
A
Siglec1
1422161_at
0
80
MEF
Mammary_gland__lact
Adipose_white
Lung
Placenta
Uterus
Ovary
Bladder
Umbilical_cord
Epidermis
Stomach
Intestine_large
Intestine_small
Salivary_gland
Lacrimal_gland
Prostate
Pancreas
Pituitary
Adrenal_gland
Skeletal_muscle
Mammary_gland_non-lactating
Adipose_brown
Heart
Embryonic_stem_line_V26.2_p16
Embryonic_stem_line_Bruce4_p13
Stem_cells_HSC
Common_myeloid_progenitor
Granulo_mono_progenitor
Mega_erythrocyte_progenitor
Thymocyte_DP_CD4+CD8+
Thymocyte_SP_CD4+
Thymocyte_SP_CD8+
T-cells_CD4+
T-cells_CD8+
T-cells_FoxP3+
NK_cells
B-cells_GL7_negative_Alum
B-cells_GL7_positive_KLH
B-cells_GL7_positive_Alum
B-cells_GL7_negative_KLH
Follicular_B-cells
B-cells_marginal_zone
Baf3
Mast_cells
Mast_cells_IgE
Mast_cells_IgE+antigen_1hr
Mast_cells_IgE+antigen_6hr
Dendritic_cells_myeloid_CD8a-
Dendritic_cells_lymphoid_CD8a+
Dendritic_plasmacytoid_B220+
Macrophage_bone_marrow_0hr
Macrophage_bone_marrow_2hr_LPS
Macrophage_bone_marrow_6hr_LPS
Macrophage_bone_marrow_24h_LPS
Macrophage_peri_LPS_thio_0hrs
Macrophage_peri_LPS_thio_1hrs
Macrophage_peri_LPS_thio_7hrs
Granulocytes_mac1+gr1+
Osteoclasts
Osteoblast_day5
Osteoblast_day14
Osteoblast_day21
Microglia
Spleen
Lymph_nodes
Bone_marrow
Bone
Nih_3T3
C2C12
C3H_10T1_2
3T3-L1
MIMCD-3
Neuro2a
RAW_264_7
Min6
Liver
Kidney
Retinal_pigment_epithelium
Retina
Iris
Ciliary_bodies
Eyecup
Lens
Cornea
Cerebral_cortex_prefrontal
Cerebral_cortex
Amygdala
Hippocampus
Olfactory_bulb
Spinal_cord
Hypothalamus
Cerebellum
Nucleus_accumbens
Dorsal_striatum
Dorsal_root_ganglia
Testis
0
80
Mean probe set signal intensity
B
Relative probe set expression level
2,500
2,000
1,500
1,000
500
0
Siglec1; 1422161_at
01-SCS-macrophages_GSM395738
02-SCS-macrophages_GSM395739
03-SCS-macrophages_GSM395740
04-Microglia_GSM258721
05-Microglia_GSM258722
06-FL-Y-cells_RMLNDC002001
07-FL-Y-cells_RMLNDC003001
08-PP-FDC_GSM481976
09-PP-FDC_GSM481977
10-PP-FDC_GSM481978
11-Astrocytes_GSM241898
12-Neuro2a_GSM258727
13-Neuro2a_GSM258728

To determine whether sialoadhesin-deficiency influenced the trapping and retention of immunoglobulin/antigen-containing immune complexes by FDC, mice from each group were passively immunized with preformed peroxidase-anti peroxidase immune complexes (see 2.3.3), and 24 h later, the presence of follicular dendritic cell-associated immune complexes identified by IHC (Figure 7.3A). Although FDC from each group captured and retained high levels of preformed immune complexes, a small but significant reduction was observed in the spleens of sialoadhesin-deficient mice (Figure 7.3B; $n = 6$ mice per group, $P = 0.032$).

Figure 7.3 Effect of sialoadhesin deficiency on passive immune complex trapping upon FDC and lectin mediated endocytic uptake in the MZ.

(A & B) Effect of sialoadhesin-deficiency on the ability of FDC to trap preformed peroxidase anti-peroxidase (PAP) immune complexes. Sections were immunostained to detect FDC ($CD35^+$ cells, red) and PAP (rabbit IgG, green). (C & D) The trapping of dextran:FITC within the splenic MZ is unaltered in sialoadhesin-deficient ($Sn^{-/-}$) mice.

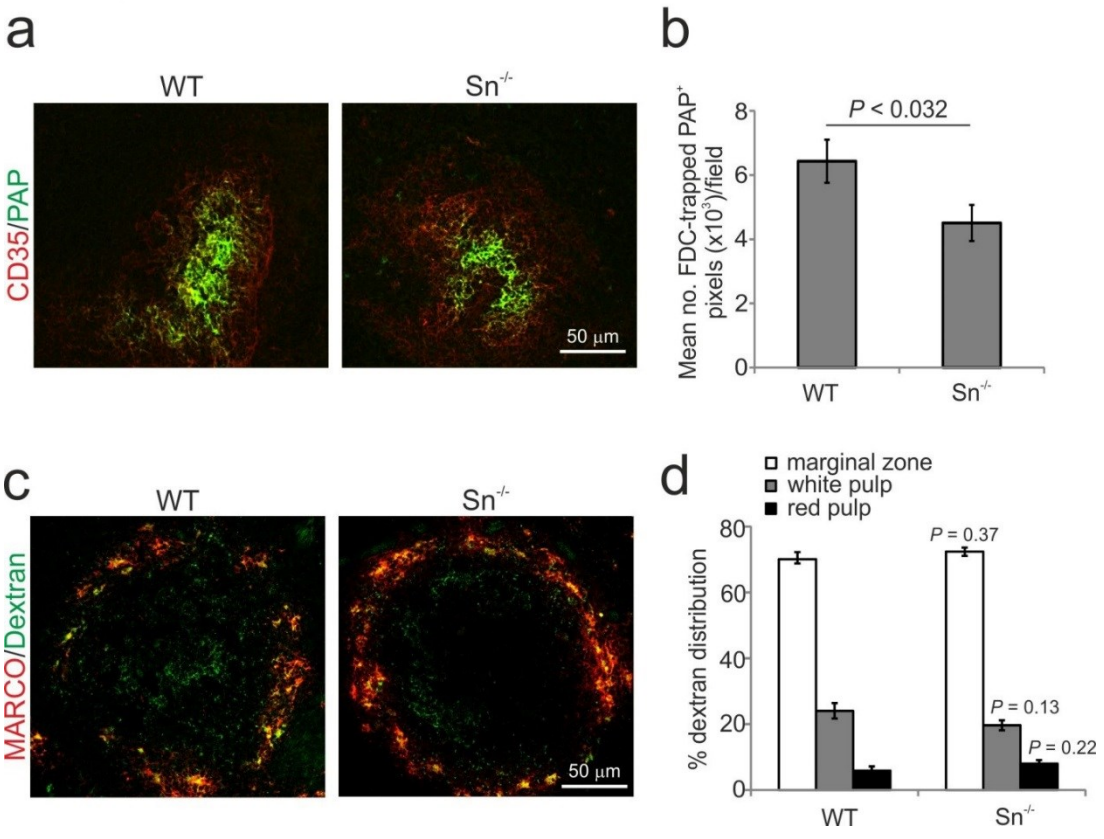

7.3.2 Effect of sialoadhesin-deficiency on the lectin-mediated endocytic uptake of polysaccharides by marginal zone macrophages

MNP in the splenic marginal zone play important roles in the uptake and clearance of particulate antigens from the blood-stream. Situated within the outer layer of the marginal zone are a ring of macrophage receptor with collagenous structure positive ($MARCO^+$) MZ macrophages, whereas the sialoadhesin-expressing marginal zone metallophilic macrophages form a continuous inner ring close to the white pulp. $MARCO^+$ marginal zone macrophages also express an array of scavenger receptors including scavenger receptor-A (SR-A) and the C-type lectin SIGNR1 (Aichele et al., 2003) which recognize specific carbohydrate structures such as bacterial capsular polysaccharides. Next it was determined whether the phagocytosis of polysaccharide antigens by $MARCO^+$ marginal zone macrophages was influenced by sialoadhesin deficiency. Mice from each group were passively immunized with fluorescently-labelled dextran particles (dextran:FITC) and spleens analysed 1 h later by IHC (see 2.3.3). No differences in MARCO expression by marginal zone macrophages and their ability to endocytose dextran within the marginal zone were observed between spleens of wild type and sialoadhesin-deficient mice (Figure 7.3C). In spleens from each mouse group the majority of the dextran:FITC was typically colocalized with $MARCO^+$ macrophages within the outer layer of the marginal zone (Figure 7.2D) with lesser amounts being observed within the red pulp and occasionally within follicular B cell areas as was described previously (Kang et al., 2003). These data demonstrate that sialoadhesin-deficiency does not affect the ability of $MARCO^+$ marginal zone macrophages to clear blood-borne dextran particles (Figure 7.3D).

7.3.3 Effect of sialoadhesin-deficiency on the early accumulation of PrP^{Sc} in the spleen

To determine the effect of sialoadhesin-deficiency upon peripheral prion pathogenesis, groups of C57Bl/6 or sialoadhesin-deficient mice were infected intraperitoneally with ME7 mouse-adapted scrapie prions (see 2.3.4). Within weeks after peripheral exposure, prions accumulate first upon FDC in the secondary lymphoid organs and are maintained at high levels for the duration of the disease. The effect of sialoadhesin-deficiency on the initial accumulation of prions upon FDC in the spleen was determined. ME7 scrapie prions were injected into the peritoneal cavity of mice, which were then sacrificed at various intervals after exposure and tissues were collected for analysis (see 2.15). Heavy accumulations of disease-associated PrP (PrP^{d}), consistent with localisation upon FDC, were detected by IHC analysis in the spleens of all wild type mice at 5 weeks after prion exposure (Figure 7.4A). By 10 and 15 weeks after intraperitoneal injection with prions, the levels of PrP^{d} upon the surfaces of FDC appeared to have increased, and were maintained for the duration of the disease. Paraffin-embedded tissue (see 2.16) immunoblot analysis of adjacent tissue sections (Fig. 7.4B) and western immunoblot (see 2.12) analysis of tissue homogenates (Fig. 7.4C) confirmed that the PrP^{d} detected in these tissues was prion disease-specific PrP^{Sc}. Similarly, high levels of PrP^{Sc} also were detected in association with FDC in the spleens of sialoadhesin-deficient mice analysed at the same times after prion exposures (Figure 7.4). These data show that sialoadhesin-deficiency did not impair the early accumulation of PrP^{Sc} upon FDC.

Figure 7.4 Effect of sialoadhesin deficiency on prion accumulation in the spleen.

(A) IHC detection of prion-specific abnormal PrP (PrP^{d}, brown, arrows) upon FDC in the spleens of wild-type (WT) and sialoadhesin-deficient ($Sn^{-/-}$) mice. Sections counterstained with haematoxylin (blue). dpi, days post injection with prion. (B) PET-blot analysis confirmed the presence of prion-specific, PK-resistant PrP^{Sc} (black) upon FDC (arrows). (C) Immunoblot analysis of PK-treated spleen tissue homogenates confirmed the accumulation of high levels of prion-specific, PK-resistant PrP^{Sc}. After PK-treatment, a typical three-band pattern was observed between molecular mass values of 20-30 kDa, representing unglycosylated, monoglycosylated and diglycosylated isomers of PrP (in order of increasing molecular mass). Approximate molecular weight markers indicated. (D & E) Analysis of spleen sections from Alexa-PrP^{Sc}-injected mice suggested that the PrP^{Sc} (red) was mostly associated with $SIGNR1^{+}$ marginal zone (MZ) macrophages (D, blue, arrows), and occasionally in the red pulp (RP) and white pulp (WP; D, arrow-heads) in regions in close association with $CR1/CD35^{+}$ (green) FDC (E, arrows). No apparent differences were observed between tissues from WT or $Sn^{-/-}$ mice. Dashed lines indicate the border of the MZ. WP, white pulp; RP, red pulp.

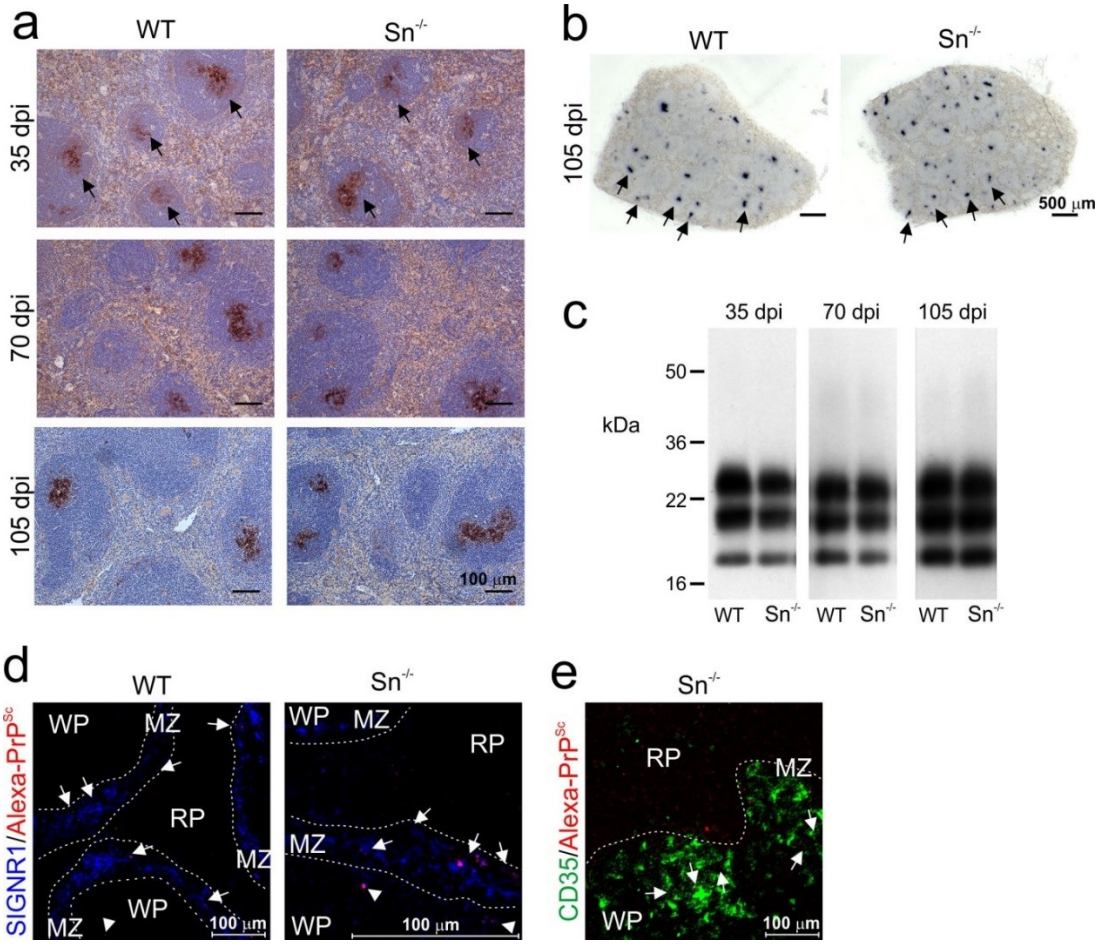

A parallel experiment was also performed to determine whether sialoadhesin-deficiency influenced the accumulation of prion-specific PrP^{Sc} within the spleen. Highly PrP^{Sc}-enriched, scrapie-associated fibrils were isolated from the brains of clinical prion disease-affected mice and fluorescently labelled as described (Gousset et al., 2009, Wathne et al., 2012). This labelling enabled the visualisation of Alexa-PrP^{Sc} in tissues by immunofluorescent confocal microscopy (Gousset et al., 2009, Wathne et al., 2012). Mice from each group were injected intravenously with Alexa-PrP^{Sc}; spleens were collected 1 h later and immunostained to detect the SIGN-$R1^{+}$ MZ macrophages. No differences in SIGN-R1 expression by marginal zone macrophages and the anatomical localization of Alexa-PrP^{Sc} between spleens of wild type and sialoadhesin-deficient mice were observed. The majority of the Alexa-PrP^{Sc} was observed within the marginal zone (Figure 7.3D, arrows), but small amounts were observed in the white pulp (Figure 7.4D, arrow-heads) occasionally in close-association with FDC (Figure 7.4E, arrows).

7.3.4 Effect of sialoadhesin-deficiency on prion disease susceptibility

To determine whether sialoadhesin deficiency influenced prion neuroinvasion or disease susceptibility, wild type or sialoadhesin-deficient mice were exposed to prions. Our data show that sialoadhesin-deficiency had no significant effect on the spread of prions to the brain after intraperitoneal injection as all wild type and sialoadhesin-deficient mice succumbed to clinical prion disease with similar incubation periods (Table 7.1, $P = 0.130$). Similarly, when wild type and sialoadhesin-deficient mice were injected with prions directly into the central nervous system by intracranial injection, they developed clinical prion disease with similar incubation periods (Table 7.1, $P = 0.717$). Histopathological analysis confirmed that brains from all clinically-affected wild type and sialoadhesin-deficient mice displayed the characteristic spongiform pathology, astrocytosis, microgliosis and PrP^{d} accumulation typically associated with terminal infection with ME7 scrapie prions (Figure 7.5). Together, these data reveal no significant effect of sialoadhesin-deficiency on prion neuroinvasion or disease susceptibility.

Table 7.1. Effect of sialoadhesin-deficiency on prion disease susceptibility.

* Number of mice affected/injected with prions.

	Route of prion exposure			
	Intracerebral		Intraperitoneal	
Mouse strain	Incidence of clinical disease*	Mean incubation period (Days) ± SEM	Incidence of clinical disease*	Mean incubation period (Days) ± SEM
Wild type C57Bl/6J	5/5	153 ± 4	8/8	241 ± 7
Sialoadhesin-knockout	6/6	151 ± 4	6/6	256 ± 6

Figure 7.5 Effect of sialoadhesin-deficiency on the neuropathology in the brains of prion-infected mice.

(A) Sialoadhesin-deficiency had no observable effect on disease specific vacuolation, PrP^{d} deposition, or reactive glial responses in the brains of the clinically-affected, peripheral prion infected mice. High levels of spongiform pathology (haematoxylin and eosin (H & E), top row), heavy accumulations of disease-specific prion protein (PrP) (brown, second row), reactive astrocytes expressing glial fibrillary acidic protein (GFAP) (brown, third row), and active microglia expressing Iba1 (brown, bottom row) were detected in the brains of all clinically prion disease-affected wild-type (WT) mice (left-hand column) and sialoadhesin-deficient ($Sn^{-/-}$) mice (right-hand column). (B) Pathological assessment of the spongiform change (vacuolation) in brains from terminally prion-affected WT (blue line) and $Sn^{-/-}$ (red line) mice. Vacuolation was scored on a scale of 0 – 5 in the following gray (G1 – G9) and white (W1 – W3) matter areas: G1, dorsal medulla; G2, cerebellar cortex; G3, superior colliculus; G4, hypothalamus; G5, thalamus; G6, hippocampus; G7, septum; G8, retrosplenial and adjacent motor cortex; G9, cingulate and adjacent motor cortex; W1, inferior and middle cerebellar peduncles; W2, decussation of superior cerebellar peduncles; and W3, cerebellar peduncles.

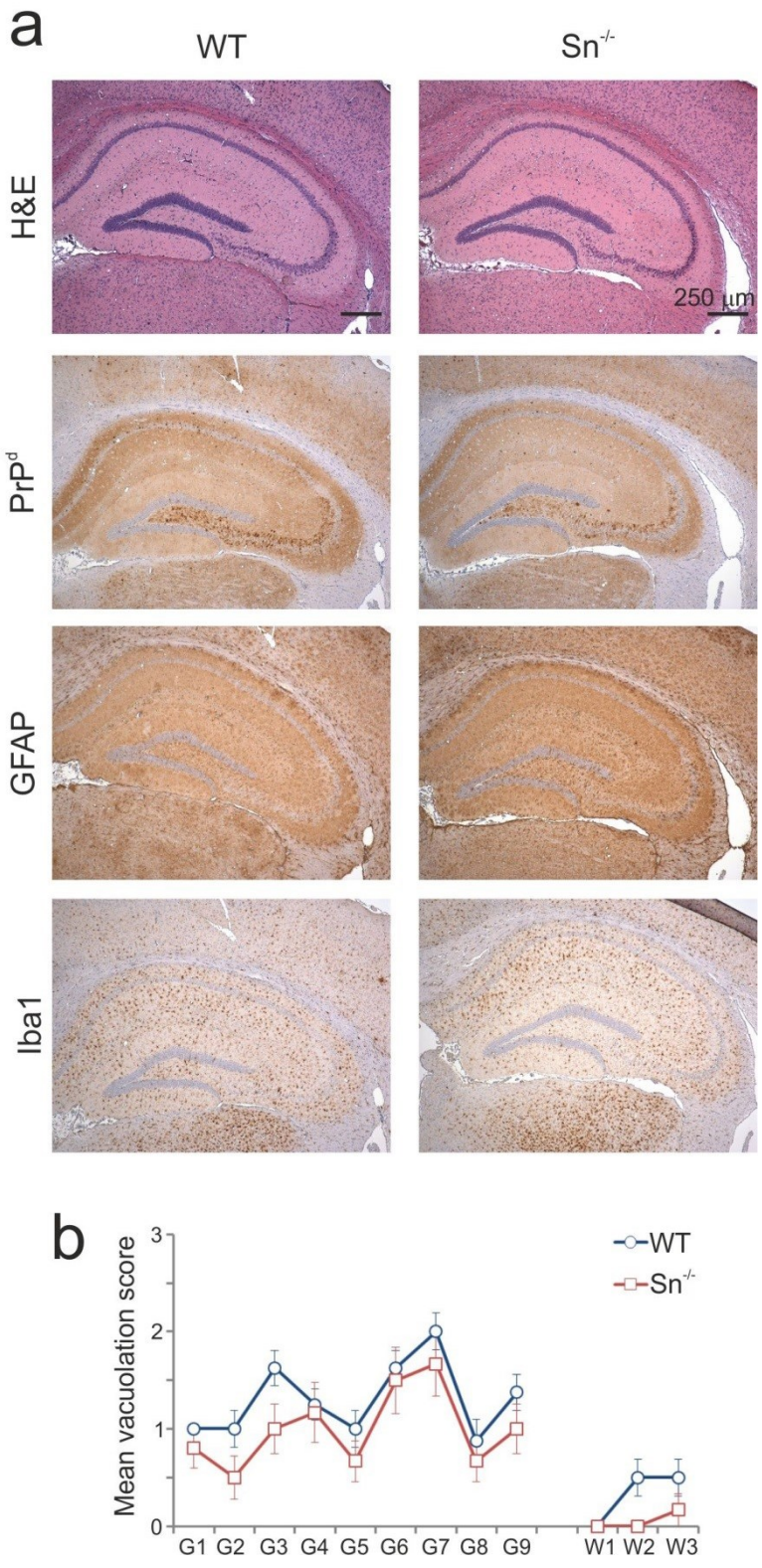
a
WT
Sn-/-
H&E
PrPd
GFAP
Iba1
250 μm
b
Mean vacuolation score
0
1
2
3
WT
Sn-/-
G1 G2 G3 G4 G5 G6 G7 G8 G9
W1 W2 W3

7.4 Discussion

Prion replication upon FDC in secondary lymphoid organs is critical for their efficient neuroinvasion (Mabbott et al., 2000, Montrasio et al., 2000, McCulloch et al., 2011). However, as FDC are non-motile, stromal-derived cells which form networks in the B cell follicles (Mabbott et al., 2011, Krautler et al., 2012) it is uncertain how prions are first conveyed to secondary lymphoid tissues and transferred to FDC. Cell-associated and cell-free mechanisms of prion transport have both been suggested (Klein et al., 2001, Mabbott et al., 2001, Zabel et al., 2007, Michel et al., 2012). The splenic marginal zone is a specialised microenvironment that plays an important role in the capture and clearance of blood-borne pathogens/antigens. Specific populations of MNP within the marginal zone (and subcapsular sinus of lymph nodes) have also been shown to capture immune complexes and present them to follicular B cells for delivery to FDC (Phan et al., 2007, Cinamon et al., 2008, Phan et al., 2009). The opsonisation of prions with complement components is important for their retention by FDC (Klein et al., 2001, Mabbott et al., 2001, Zabel et al., 2007). In studies elsewhere we have also shown that an intact marginal zone is also important for the initial localization of prions upon FDC (Brown et al., 2012, Brown and Mabbott, 2014). These data imply that a similar cellular relay may shuttle complement-opsonized prions to FDC.

The prion protein is highly sialylated (Stimson et al., 1999), and marginal zone metallophilic macrophages in the spleen, and the subcapsular sinus macrophages in the lymph nodes, constitutively express high levels of sialoadhesin which binds to sialylated glycoproteins (Crocker and Gordon, 1986). Prions may also be released from infected cells in association with exosomes and play an important role in their cell-to-cell transmission (Fevrier et al., 2004, Kujala et al., 2011). A role for MNP-expressed sialoadhesin in the capture of B cell-derived exosomes in the spleen and lymph nodes via surface expressed sialic acids has also been described (Saunderson et al., 2014). The identification of molecular factors which influence the initial accumulation of prions in secondary lymphoid tissues may reveal novel targets for therapeutic intervention. Therefore, in the current study sialoadhesin-deficient mice were used to test the hypothesis that sialoadhesin-expressing MNP in the marginal zone play an important role in the initial uptake of prions in the spleen. Data presented here show that after peripheral prion disease exposure the early accumulation of PrP^{Sc} on FDC, subsequent neuroinvasion and disease susceptibility were unimpaired and unaltered in sialoadhesin-deficient mice. Thus, these data show that the efficient delivery of prions to FDC in the spleen is not influenced by sialoadhesin-expression by marginal zone metallophilic MNP. These data do not preclude the

possibility that marginal zone metallophilic macrophages may be involved in prion uptake and transfer into the B cell follicles, only that sialoadhesin itself is non-essential for this process.

In wild type mice high levels of activated complement component C4 were detected in association with FDC indicative of the retention of complement-opsonized immune complexes on their surfaces (Taylor et al., 2002). However, low levels were also detected in association with the splenic marginal zone. Studies elsewhere show that in the absence of effective immune-complex shuttling from the marginal zone to FDC, marginal zone B cells appear unable to "off-load" their complement-opsonized antigens resulting in their increased accumulation of complement component C4 (Pasparakis et al., 2000, Voigt et al., 2000, Cinamon et al., 2008). In the spleens of sialoadhesin-deficient mice the marginal zone localization of complement component C4 was significantly reduced. Furthermore, this coincided with a significant increase in complement component C4 upon FDC in the spleens of sialoadhesin-deficient mice (Fig. 7.1). Glycan profiling of complement component C4 has revealed that it carries a mixture of both oligomannose and complex biantennary glycans with varying amounts of sialylation (Ritchie et al., 2002). These data suggest sialoadhesin may play an important role in the initial uptake and sequestration of blood-borne complement-opsonized immune complexes by marginal zone metallophilic macrophages via terminal sialic acid residues on the glycans on complement component C4. Our data also suggest that in the absence of this activity in sialoadhesin-deficient mice, less complement component C4 is sequestered by MNP in the marginal zone enabling more to be shuttled to FDC. The retention of immune complexes on FDC promotes the ability of naïve IgM^+ B cells to mature and class switch to high affinity IgG (Aydar et al., 2005). Whether the significantly reduced IgM titre in the serum of sialoadhesin-deficient mice (Oetke et al., 2006) is a consequence of the effects of sialoadhesin-deficiency on complement component C4 retention is uncertain.

The expression of PrP^C by FDC has been shown to be stimulated by their retention of complement-opsonized immune complexes, and this upregulation in PrP^C-expression is blocked in mice deficient in complement component C1q (Lötscher et al., 2003). Conversely, the dramatically impaired retention of immune complexes by FDC in aged mice coincides with substantially reduced levels of PrP^C expression (Brown et al., 2009, Brown et al., 2012, Brown and Mabbott, 2014). In the current study, coincident with the increased accumulation of complement component C4, the level of PrP^C expressed by FDC was also significantly increased implying complement-mediated upregulation of PrP^C-expression by FDC.

Prions are considered to be initially acquired by FDC as complement-opsonized immune complexes (Klein et al., 2001, Mabbott et al., 2001, Zabel et al., 2007, McCulloch et al., 2011). In the absence of sialoadhesin expression by metallophilic macrophages the retention of complement component C4 upon FDC was increased. Thus it is plausible that in the spleens of sialoadhesin-deficient mice fewer complement-opsonized prions were sequestered by MNP in the marginal zone enabling them to be shuttled more efficiently to FDC.

Despite the important role of sialoadhesin in the binding of sialylated antigens (Crocker et al., 1991, Crocker, 2002, Klaas and Crocker, 2012, Klaas et al., 2012) and exosomes (Saunderson et al., 2014) our data show that after peripheral prion exposure sialoadhesin expression by metallophilic macrophages in the inner ring of the splenic marginal zone is not required for the efficient transport of prions to FDC and the subsequent spread of disease to the central nervous system. Treatments which block the early accumulation of prions upon FDC can block or substantially reduce disease susceptibility (Mabbott et al., 2000, Montrasio et al., 2000, Mabbott et al., 2001, Raymond et al., 2007). Therefore, identification of the cellular and molecular factors which influence the initial delivery of prions to FDC in the B cell follicles of secondary lymphoid tissues may reveal novel targets for therapeutic intervention in peripherally acquired infections, or factors which influence disease susceptibility.

Chapter 8. SIGN-R1 and peripheral prion pathogenesis

8.1 Abstract

The specific intercellular adhesion molecule-3-grabbing non-integrin related 1 (SIGN-R1) is the product of one of the five identified mouse genes that are homologous to human dendritic cell-specific intercellular adhesion molecule-3-grabbing non-integrin (DC-SIGN) and encodes a single, external, C-terminal C-type lectin domain. SIGN-R1 is expressed by specialized macrophages that reside within the follicular marginal zone and lymph node medullary region and functions to enhance the clearance of apoptotic cells via interaction with complement component C1q. C1q has been shown to bind to prions and aid in the uptake of infectious prions into cells. Recent data also show that an intact splenic marginal zone is important for the efficient delivery of prions to FDC within the B-cell follicles where they subsequently replicate before infecting the nervous system. A marked reduction in prion susceptibility and pathogenesis was observed in aged individuals, concurrent with a significant disruption of the splenic marginal zone and reduction of SIGN-R1. The hypothesis that SIGN-R1 may influence prion disease by facilitating the capture and uptake of free or C1q-bound prions in secondary lymphoid organs was therefore tested by downregulating SIGN-R1 prior to prion infection. Downregulation of SIGN-R1 prior to intravenous exposure of prions had no effect on the accumulation of prions upon FDC within lymphoid follicles and subsequent prion pathogenesis. These data reveal that SIGN-R1 is not required for lymphoid sequestration of prions and therefore, the loss of SIGN-R1 expression in aged individuals is not directly responsible for their increased resistance to prion infection.

8.2 Introduction

The specific intercellular adhesion molecule-3-grabbing non-integrin related 1 (SIGN-R1/CD209b) receptor is part of the array of receptors expressed by marginal zone macrophages, others include scavenger receptor A (SR-A) and macrophage receptor with collagenous structure (MARCO). SIGN-R1 functions to enhance the uptake and the clearance of apoptotic cells via the complement deposition pathway, specifically interacting with C1q in the spleen (Prabagar et al., 2013). Prion protein (PrP) has been shown to be directly bound by C1q and Factor H (Mitchell et al., 2007) and this binding occurs specifically when PrP is conformationally modified to represent the conversion to the disease-associated isoform PrP^{Sc} (Blanquet-Grossard et al., 2005). SIGN-R1 also mediates uptake of polysaccharides such as dextran (Kang et al., 2003) and the capsular polysaccharide of *Streptococcus pneumoniae* (Kang et al., 2004) in splenic marginal zone and influenza virus in lymph nodes (Gonzalez et al., 2010), playing an important role in mediating humoral immunity to these pathogens. SIGN-R1 is the murine homologue of dendritic cell-specific intercellular adhesion molecule-3-grabbing non-integrin (DC-SIGN or CD209) in humans, a receptor famous for its role in facilitating human immunodeficiency virus (HIV) infection (Geijtenbeek and van Kooyk, 2003). DC-SIGN also acts as a receptor or ligand for peanut *Arachis hypogaea* (Shreffler et al., 2006) and house dust mite allergens (Emara et al., 2012), viruses such as Ebola (Simmons et al., 2003), dengue (Tassaneetrithep et al., 2003), measles (de Witte et al., 2008), Junin [Hemorrhagic fever] arenavirus (Martinez et al., 2013), Marburg and severe acute respiratory syndrome (SARS) coronavirus (Marzi et al., 2004), mycobacteria such as *Mycobacterium tuberculosis* and *Mycobacterium leprae* (Geijtenbeek et al., 2003), *Helicobacter pylori* (Bergman et al., 2004), *Schistosoma mansoni* (van Liempt et al., 2007) and *Leishmania* parasites (Colmenares et al., 2002, Zhao et al., 2005).

The precise mode by which infectious prions are initially conveyed from the site of exposure to follicular dendritic cells (FDC) within the B-cell follicles was uncertain, however a number of cellular and molecular components of the innate immune system have been shown to be involved. FDC characteristically trap and retain native antigen on their surfaces in the form of immune complexes, consisting of antigen-antibody and/or opsonizing complement components. In addition to these molecular factors, migratory cells such as integrin alpha x-expressing (Itgax/CD11c) mononuclear phagocytes (MNP) may also play an important role in the initial uptake and transport of prions since their depletion prior to peripheral exposure blocked prion accumulation upon FDC and reduced disease susceptibility (Raymond et al.,

2007, Cordier-Dirikoc and Chabry, 2008). Data presented in Chapter 5 reveal that transport of prions to FDC by $CXCR5^+$ $CD11c^+$ cells constitutes the most efficient mechanism of prion transport to FDC following prion infection.

The splenic marginal zone surrounding the white pulp comprises a marginal sinus with a network of sinus-lining cells and reticular cells through which the blood percolates on its way to the red pulp. Attached to this network are specific populations of MNP and B cells, which enable the continual surveillance and clearance of pathogens, antigens, and apoptotic cells from the blood stream. The positioning of these cells in the marginal zone enables them to regulate the entry of blood-borne immune-complexes and proteoglycans into the FDC-containing B-cell follicles (Aichele et al., 2003, Cinamon et al., 2008). In the lymph node for example, sub-capsular sinus macrophages capture immune complexes on their surfaces, and pass them to follicular B cells for delivery to FDC in the B-cell follicles (Phan et al., 2009).

An intact splenic marginal zone also plays an important role in the efficient delivery of complement-bound prions to FDC, with disruption associated with increased resistance to prion infection in aged individuals (Brown et al., 2012, Brown and Mabbott, 2014). Complement components may also aid the initial uptake of prions by MNP, with component C1q possibly responsible for the binding and aiding uptake of infectious prions in conventional dendritic cells (Flores-Langarica et al., 2009). Prion uptake onto FDC has been linked to both C3 and C1q complement components as depletion of either impact upon early prion replication upon FDC and delays prion pathogenesis (Heppner et al., 2001b, Mabbott and Bruce, 2001). Interaction of C1q with SIGN-R1 has also been shown to be important in the release of captured opsonized antigens by MNP for their subsequent capture by FDC (Kang et al., 2006). Due to the role of SIGN-R1 specifically in binding C1q and aiding the uptake and clearance of pathogens, the hypothesis that SIGN-R1 may influence prion disease by facilitating the capture and uptake of free or C1q-bound prions in secondary lymphoid organs was therefore tested by downregulating SIGN-R1 prior to intravenous prion infection. The intravenous route of infection was used as it allows direct observation of the uptake of prions from the blood as it passes through and is filtered by the splenic marginal zone. This route of infection is also clinically relevant as secondary variantCJD infections have been reported within the human population following blood transfusion (Llewelyn et al., 2004, Wroe et al., 2006)

8.3 Results

8.3.1 Selective downregulation of SIGN-R1 and effect on marginal zone macrophage function

To selectively downregulate SIGN-R1 groups of mice were administered either the SIGN-R1-specific antibody clone 22D1 or an isotype control hamster antibody via tail vein (intravenous) infection (see 2.3.2). Mice were examined 24 hours after antibody administration and spleens were investigated by immunohistochemistry (see 2.15.5) for efficacy of treatment. Marginal zone macrophages were detectable with anti-SIGN-R1 (Figure 8.1A) and anti-MARCO (Figure 8.1B) antibodies revealing strong colocalisation of these markers (Figure 8.1C) in control antibody treated mice. SIGN-R1$^+$ MARCO$^+$ macrophages were localised in the outer marginal zone when compared to sialoadhesin (CD169) expressing marginal zone metallophilic macrophages (Figure 8.1D). In contrast, mice treated with anti-SIGN-R1 (clone 22D1) antibody still displayed MARCO expression on their marginal zone macrophages (Figure 8.1F) but SIGN-R1 was no longer detectable even when using anti-SIGN-R1 antibody clone ER-TR9 (Figure 8.1E & 8.1H). To assess the functional deficit following anti-SIGN-R1 downregulation, mice were treated with intravenous injection of fluorescein isothiocyanate (FITC)-labelled dextran. Control antibody treated mice were able to trap dextran within the marginal zone identified by MARCO$^+$ macrophages and transfer dextran into the white pulp (Figure 8.1 I-K), unlike anti-SIGN-R1 treated mice where the majority of dextran was localised to splenic red pulp regions (Figure 8.1 L-N).

Figure 8.1 Selective SIGN-R1-downregulation and effect on marginal zone macrophage function

Splenic marginal zone macrophages express either SIGN-R1, MARCO (A-C) or Sialoadhesin (D), expression of these is unaffected following treatment with hamster control antibody. Following anti-SIGN-R1 treatment SIGN-R1 is downregulated (E) while MARCO (F) and Sialoadhesin (H) are unaltered. FITC-labelled dextran is taken up into the splenic marginal zone and white pulp (I) as identified by relative distribution to and high frequency of colocalisation with MARCO+ marginal zone macrophages (J, K) in control antibody treated mice. Reduced splenic FITC-dextran (L) was observed distributed mostly in the red-pulp outwith MARCO+ macrophage bound regions (dashed white line) of anti-SIGN-R1 treated mice (N).

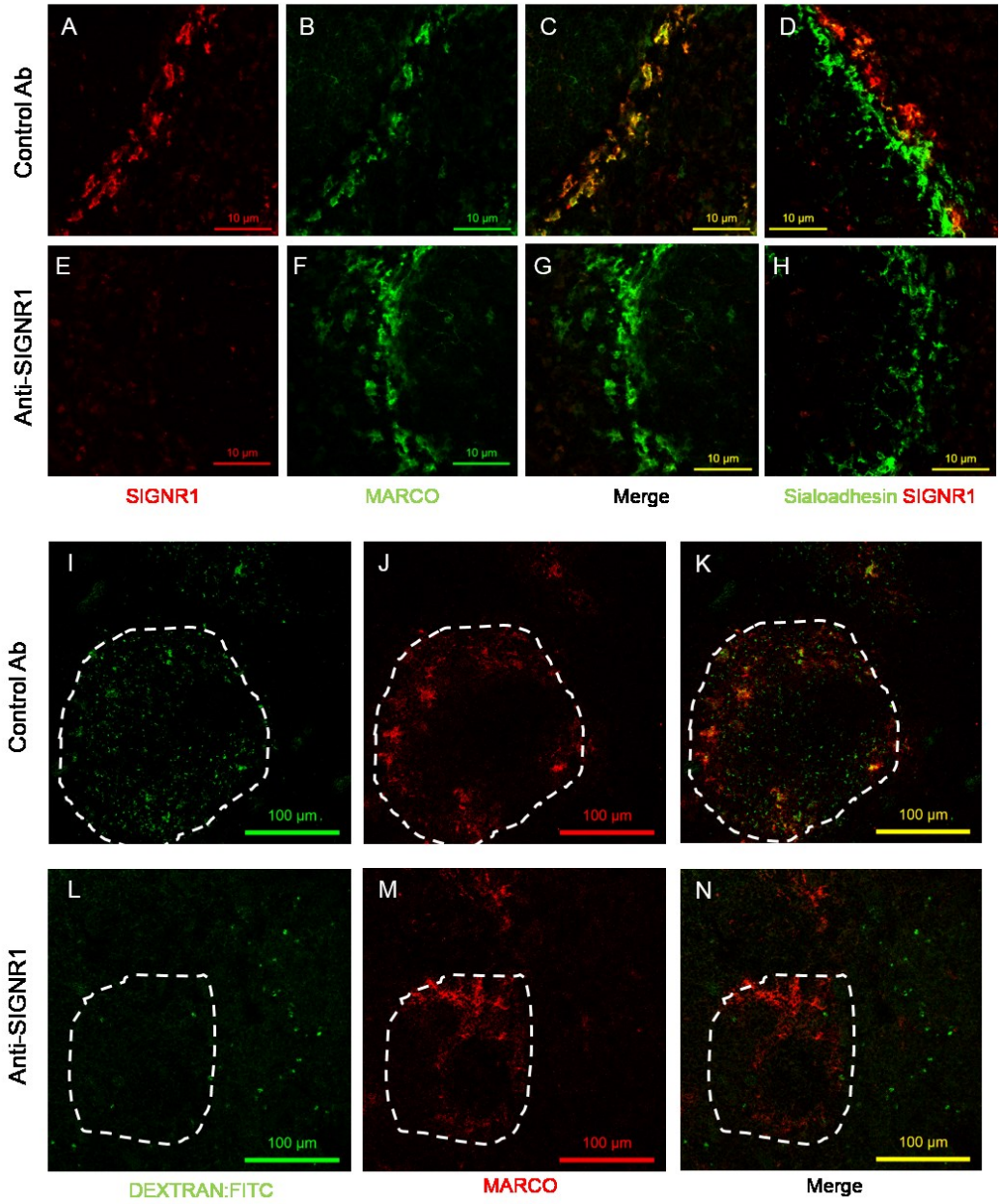

8.3.2 Effect of SIGN-R1 downregulation on FDC status and function

To assess the effect of antibody-mediated SIGN-R1 downregulation on FDC status and function, mice were treated with intravenous injection of preformed immune complexes in a passive immunization assay (see 2.3.3) 24 hours after antibody administration. Preformed rabbit peroxidase-anti-peroxidase complexes were detectable within the white pulp of splenic follicles, identified by staining for $MARCO^+$ marginal zone macrophages, in both control antibody and anti-SIGN-R1 treated mice (Figure 8.2A & 8.2C). Co-localization of PAP with FDC was confirmed using CD35 (Figure 8.2B & 8.D). Following anti-SIGN-R1 treatment a 1.5 fold increase in trapped preformed immune complexes was observed upon FDC networks (P<0.0001 Two-sample T-test 95% CI, N=36 per treatment group), despite no significant alteration observable in FDC network size (Figure 8.2B & 8.2D).

Figure 8.2 Altered immune complex trapping following SIGNR1-downregulation

Preformed peroxidase anti-peroxidase (PAP) immune complexes were detectable within the white pulp region ringed by MARCO$^+$ marginal zone macrophages of both control treated (A) and anti-SIGN-R1 treated (B) mice. PAP trapped to and colocalized with CD35$^+$ FDC (C) was increased following anti-SIGN-R1 treatment (D) despite no difference (N.D.) in FDC network size (E). Scale bars = 100 μm. N = 36 images per group.

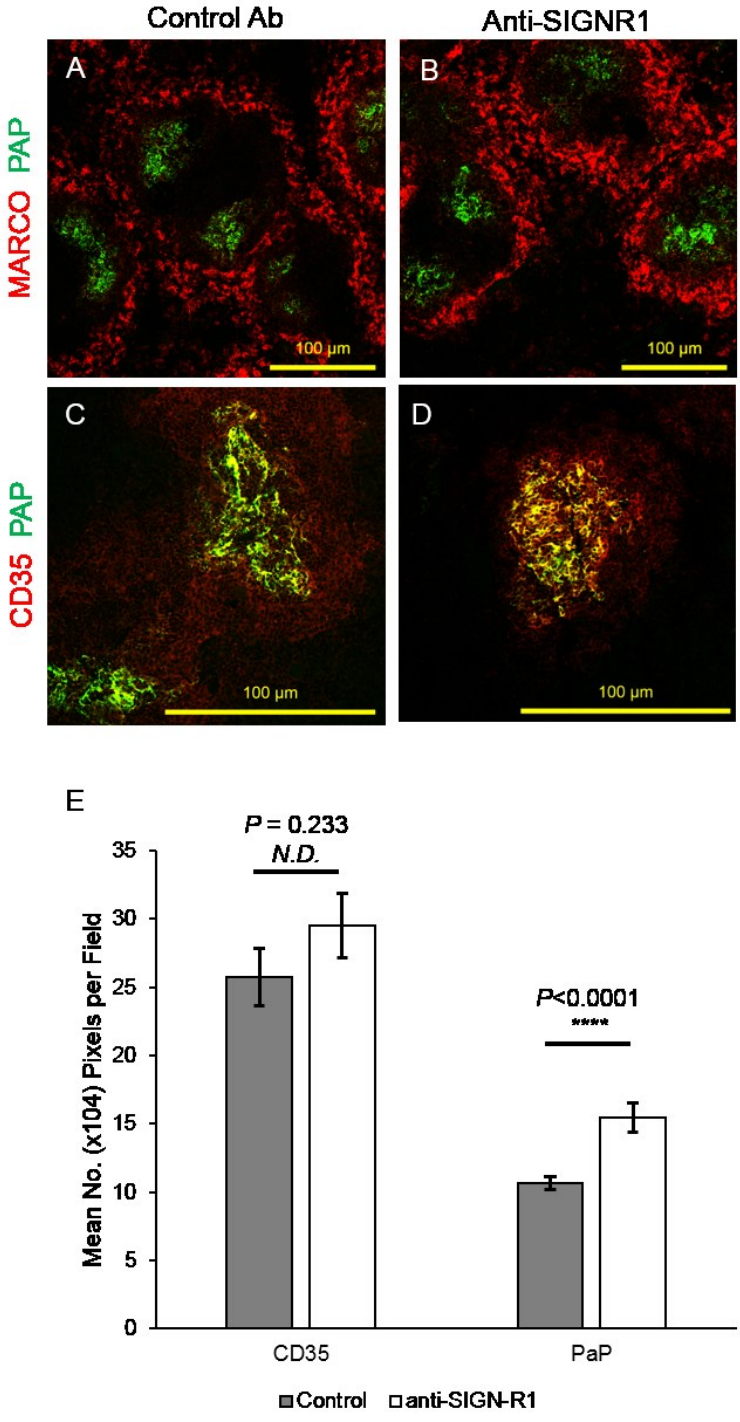

8.3.3 Effect of SIGN-R1 downregulation on prion accumulation in the spleen

To determine the effect of downregulation of SIGN-R1 on the early accumulation of PrP^{Sc} in the spleen, control antibody or anti-SIGN-R1 treated mice were intravenously injected with 20 µl of 0.01% w/v terminal ME7 brain homogenate 24 hours after antibody treatment (see 2.3.4). At 5 weeks post inoculation mice were sacrificed and spleen tissue harvested. Analysis of these spleen tissues revealed light PrP^{d} accumulation at 35 days post intravenous infection upon FDC networks within B-cell follicles of both control antibody (Figure 8.3 A) and anti-SIGN-R1 treated mice (Figure 8.3B). Further characterisation by PET immunoblotting (see 2.15.6) revealed corresponding small PrP^{Sc} deposits in numerous splenic follicles from mice of both groups (Figure 8.3C, 8.3D). Investigation of terminal tissues revealed much stronger PrP^{d} staining upon splenic FDC in both control antibody (Figure 8.3 E) and anti-SIGN-R1 treated mice (Figure 8.3F) again numerous confirmatory follicular PrP^{Sc} deposits were observed in mice of both groups (Figure 8.3G, 8.3H). No differences in the frequency or amount of PrP^{d} or PrP^{Sc} were observed between control antibody and anti-SIGN-R1 treated mice at each timepoint.

Figure 8.3 Effect of SIGN-R1 downregulation on peripheral prion pathogenesis.

Immunohistochemical and paraffin-embedded tissue blot analysis of spleen from 35 day post intravenous ME7 exposure or terminal clinically positive mice. PrP^{d} (IHC) counterstained with haematoxylin or PrP^{Sc} (PET) were detected with anti-PrP antibody 1B3.

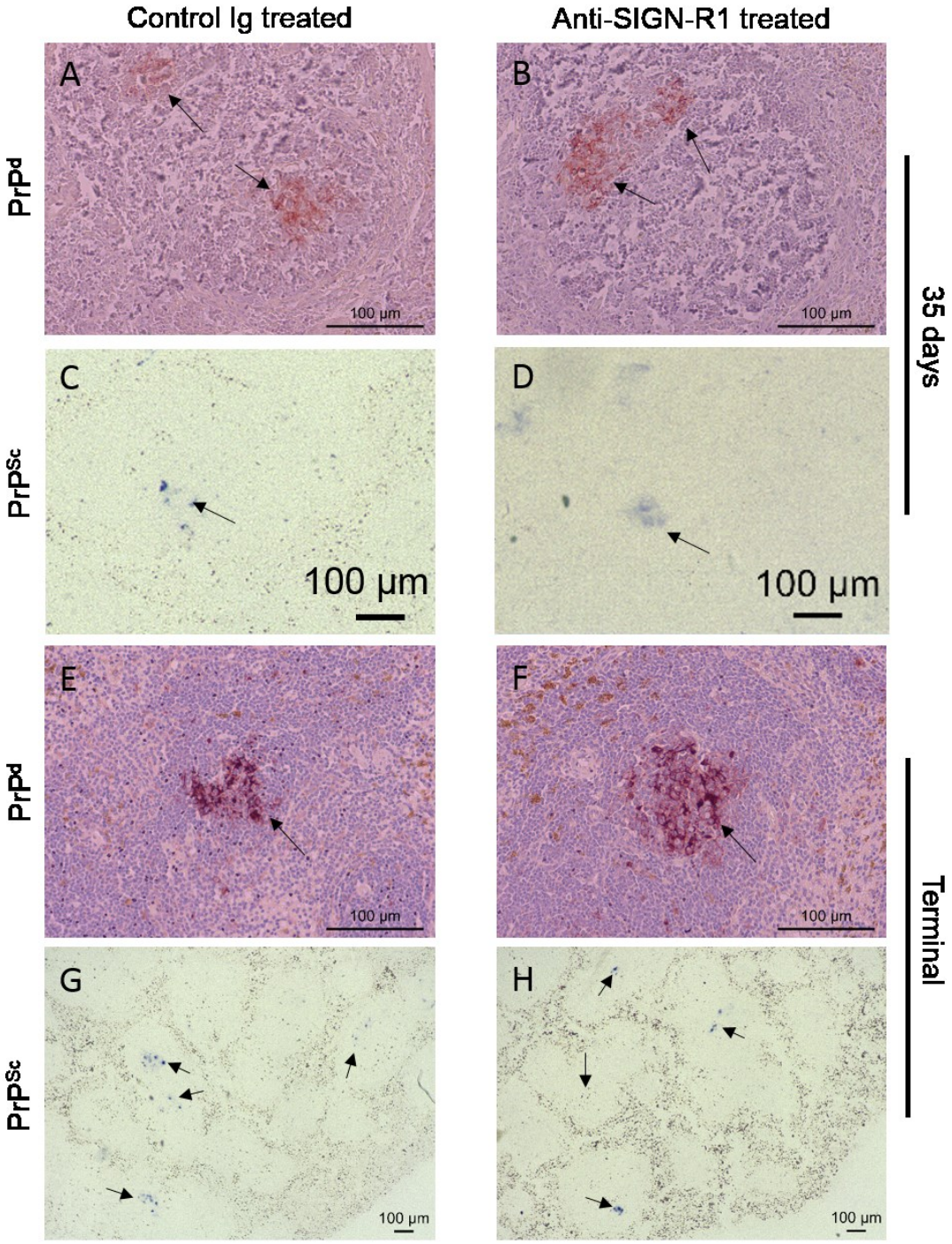

8.3.4 Effect of SIGN-R1 downregulation on prion disease susceptibility and survival time

Following intravenous prion inoculation into groups of control antibody or anti-SIGN-R1 treated mice, animals were monitored for the clinical signs of prion disease. Most mice in each treatment group succumbed to clinical prion disease with similar survival times. From previous studies using intravenous ME7 in C57Bl/6 mice it appears that treatment with control antibody had no effect on prion susceptibility or survival time, similarly in this experiment downregulating SIGN-R1 prior to infection with anti-SIGN-R1 treatment also had no effect on prion disease susceptibility or survival time (Figure 8.4 and Table 8.1).

Figure 8.4 Survival curve following intravenous ME7 infection

Survival curve plots from time of intravenous injection to assessment of positive clinical signs of prion disease in control treated or anti-SIGN-R1 treated mice. T-test of difference *P*=0.902 at 95% CI

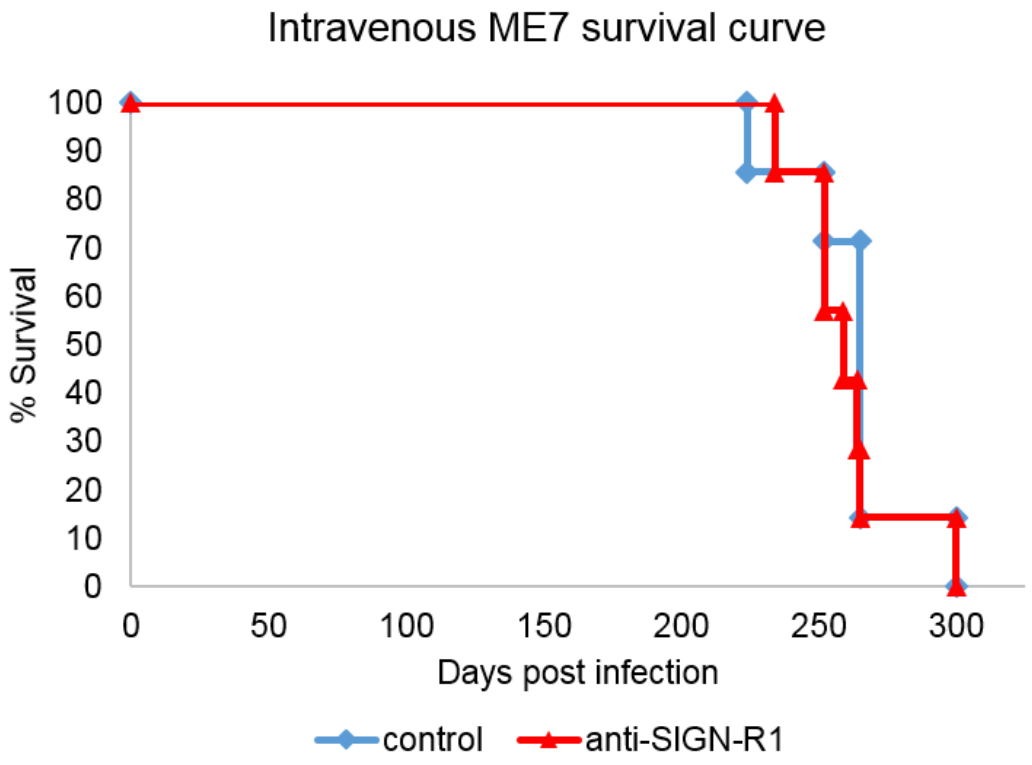

Table 8.1. Effect of SIGN-R1 downregulation on prion disease incubation period

Following intravenous injection of ME7 scrapie prions into groups of 8 control antibody or anti-SIGN-R1 treated mice, 7 mice from each group (susceptibility of 87.5%) succumbed to clinical prion disease with similar mean incubation periods. Sole clinically negative survivors from each group were culled for other reasons, survival times noted in brackets.

Treatment	Incidence of clinical disease	Mean incubation period (Days) ± SEM
C57Bl/6J Control antibody	7/8 (332 days)	262 ± 7
C57Bl/6J Anti-SIGN-R1	7/8 (339 days)	261 ± 7

8.3.5 Effect of SIGN-R1 downregulation on terminal prion neuropathology

Terminal neuropathological investigation of control antibody or anti-SIGN-R1 treated mice revealed no differences. Regardless of treatment, all clinically affected mice displayed classic terminal prion-associated neuropathological features such as deposits of PrP^{d} (Fig. 8.5A & 8.5B), reactive astrocytosis (Fig. 8.5C & 8.5D) and microgliosis (Fig. 8.5E & 8.5F) within the brain, with no differences observed between treatment groups.

Lesion profile assessment of vacuolar degeneration revealed a similar severity in standardized 9 grey matter and 3 white matter brain areas regardless of treatment (Figure 8.6A) (Fraser and Dickinson, 1968, Fraser and Dickinson, 1973). Western blot analysis (see 2.12) revealed equivalent levels of PK-resistant PrP (PrP^{Sc}) deposited in terminal i.v. ME7 infected brain samples regardless of pre-treatment with control antibody or anti-SIGN-R1 prior to prion challenge (Figure 8.6B). Therefore, in all standard prion neuropathological assessments control antibody and anti-SIGN-R1 treated mice were indistinguishable in their responses to prion infection.

Figure 8.5 Neuropathological analysis of terminal i.v. ME7 prion infected mice

Immunohistochemical staining reveals characteristic PrP deposition (A, B), Astrogliosis (C, D) and microgliosis (E, F) visualised with DAB (brown) lightly counterstained with Haematoxylin. Prion specific vacuolation scoring were performed on haematoxylin and eosin stained sections (G, H).

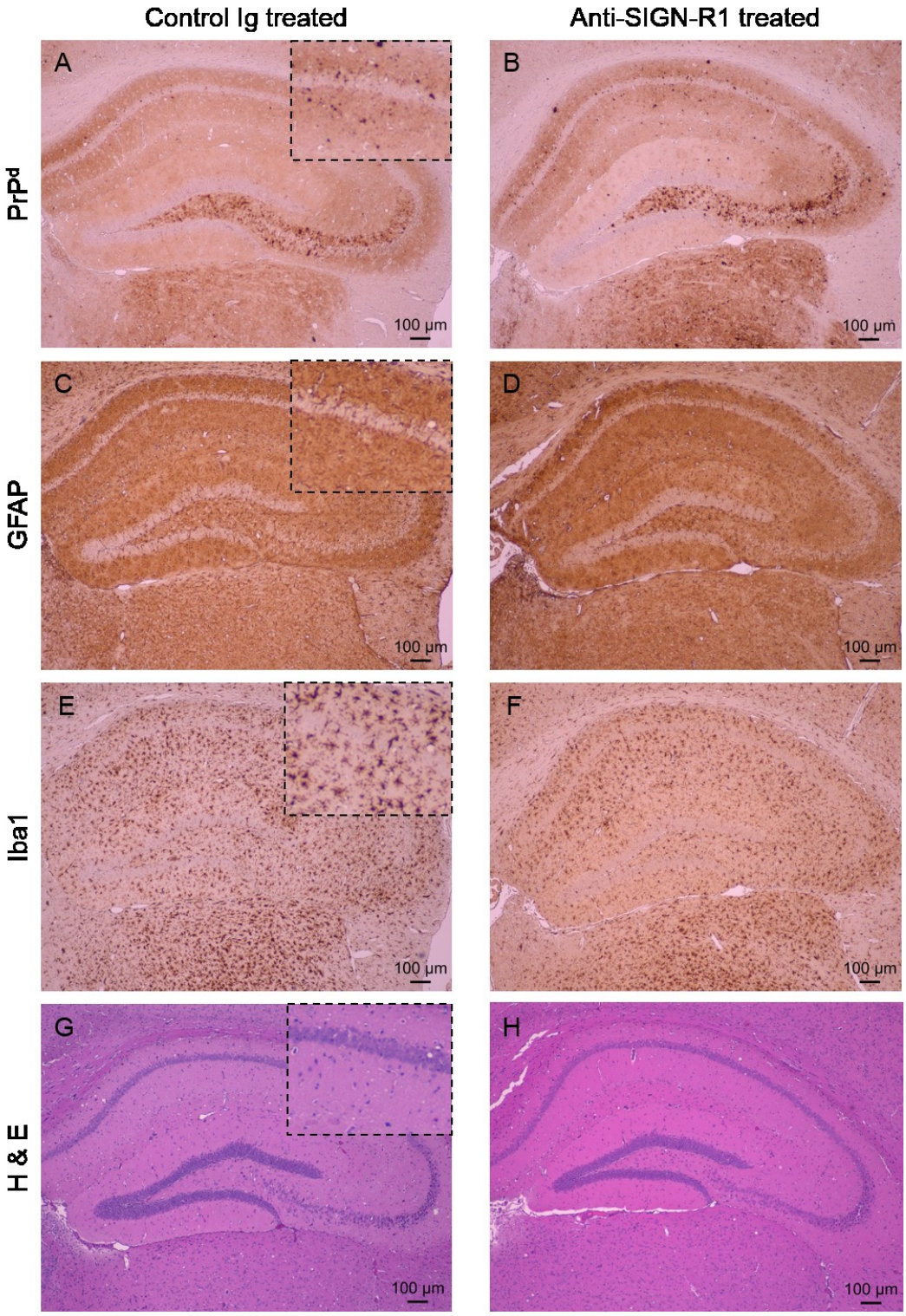

Figure 8.6 Lesion profile and Western blot analysis following intravenous ME7 infection

(A) Lesion profile analysis from terminal i.v. ME7 infected brains. Scores for each brain area were analysed by ANOVA. No statistically significant differences were observed in prion-specific vacuolation between control antibody and anti-SIGN-R1 treated mice. Vacuolation was scored on a scale of 0 – 5 in the following grey (G1 – G9) and white (W1 – W3) matter areas: Grey: 1, dorsal medulla; 2, cerebellar cortex; 3, superior colliculus; 4, hypothalamus; 5, thalamus; 6, hippocampus; 7, septum; 8, retrosplenial and adjacent motor cortex; 9, cingulate and adjacent motor cortex; White: 1, inferior and middle cerebellar peduncles; 2, decussation of superior cerebellar peduncles; and 3, cerebellar peduncles (B) Western blot analysis of terminal i.v. ME7 infected brains revealed proteinase K (PK) -resistant PrP using anti-PrP antibody 7A12.

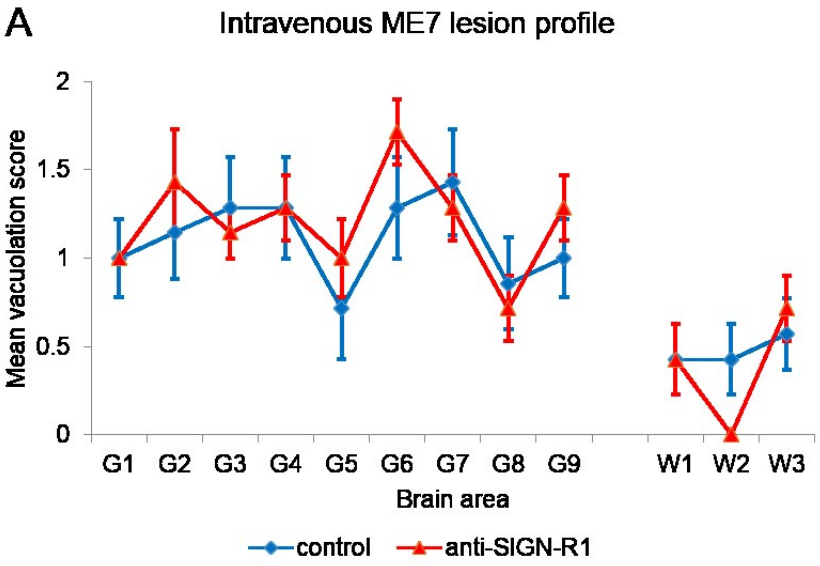

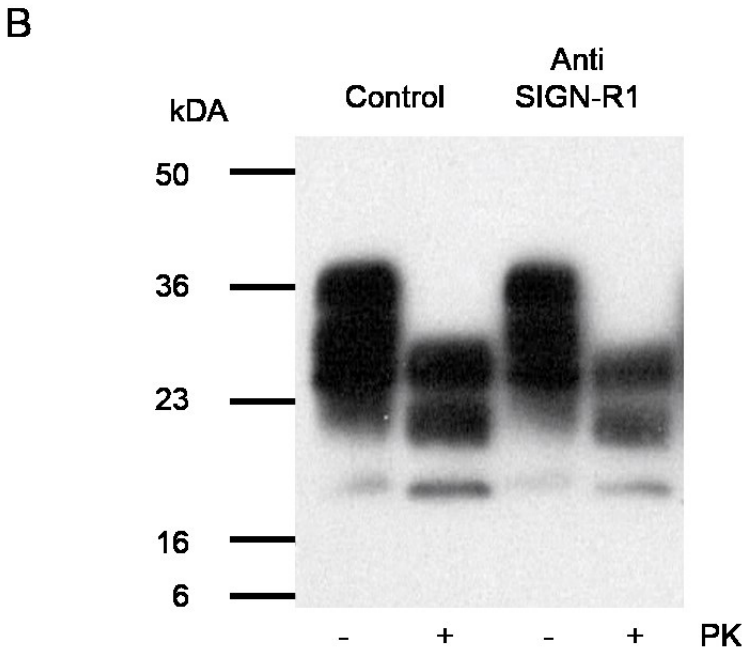

8.4 Discussion

In this chapter, the hypothesis that the specific loss of the receptor SIGN-R1 was responsible for the decreased susceptibility to prions in aged mice was tested. Using a well-characterised antibody-mediated method (Kang et al., 2003, Kang et al., 2004, Gonzalez et al., 2010), SIGN-R1 was downregulated in young mice and they were subsequently exposed to prions via intravenous infection. These mice revealed a decreased ability to capture dextran within splenic marginal zone macrophages and an enhanced ability for preformed immune-complex capture by FDC. This enhanced immune-complex capture by FDC may be due to a reduced uptake or processing of these complexes by marginal zone macrophages specifically lacking SIGN-R1. In the absence of FDC loading with material relayed from marginal zone macrophages by SIGN-R1-mediated complement activation, FDC ability to capture preformed immune complexes directly may have been enhanced.

Prion accumulation upon splenic FDC following intravenous prion infection occurred unaltered in the absence of SIGN-R1. Subsequent prion neuroinvasion occurred resulting in unaltered disease susceptibility, incubation period or terminal neuropathology when comparing anti-SIGN-R1 and control antibody treated mice. Despite the important role of SIGN-R1 in the binding and uptake of C1q opsonized pathogens and debris from apoptotic cells within the splenic marginal zone, these data suggest this mechanism is not critical to the uptake of prions and their subsequent relay to FDC during prion infection. Furthermore, the enhanced ability of FDC to trap and retain immune-complexes following SIGN-R1 downregulation also did not alter prion pathogenesis, again suggesting that this step is not rate limiting under standard experimental infection conditions. The possibility that under low dose infection conditions (a scenario that may better mimic the oral exposure of the general UK population to prions in the food-chain), this enhanced ability of FDC to trap immune-complexes under the condition of SIGN-R1 downregulation may represent an enhanced susceptibility to infection via increased trapping of prions to FDC. However, this hypothesis is clearly counter to the finding that in the aged population a loss of SIGN-R1 coincides with either a reduced susceptibility to infection/ reduced incidence of disease (i.e. variant CJD). Further evidence then that within the aged population it is likely that alterations to splenic microarchitecture other than the specific loss of SIGN-R1 from marginal zone macrophage are responsible for the observed reduced susceptibility to prion infection.

Immunosenescence or the decline of the immune system with ageing has been implicated in the resistance to prion infection. Despite the likely equivalent levels of exposure to both young and aged individuals, the zoonotic transmission of BSE to the human population as variant CJD occurred unusually in younger individuals (mean age 28.5 years) unlike other human prion diseases traditionally associated with ageing and dementia. Using mouse models it has been observed that older mice are more resistant to peripheral prion infection, despite their same ability to incubate prion disease following direct intracerebral infection (Brown and Mabbott, 2014). Specific alterations to secondary lymphoid organ structure and microarchitecture were observed in aged mice, which restrict the uptake and transport of prions from the site of infection to FDC. Alteration to the splenic marginal zone and specific and marked loss of the c-type lectin SIGN-R1 were observed in aged mice concurrent with their reduced susceptibility to peripheral prion infection.

Therefore, in aged individuals the nature of their resistance to prion infection is most likely due to other factors or changes in secondary lymphoid organ microarchitecture. For example changes to complement component C1q or C3 availability (Mabbott et al., 2001), FDC maturation state (Mabbott et al., 2002) or FDC proximity to peripheral nerves (Glatzel et al., 2001) have been shown to be critical in facilitating prion infection. Concurrent with my studies on sialoadhesin (Chapter 7) these combined data suggest that the expression of these receptors upon splenic marginal zone macrophages play a non-critical or minor role in any uptake and transport of prions to FDC following prion infection. These data further support the results in Chapter 5 that cell-mediated delivery of prions by $CXCR5^{+}$ $CD11c^{+}$ cells constitute the most effective transport, i.e. rate limiting during infection, of prions to FDC.

Chapter 9. General Discussion

9.1 Introduction

Prion diseases are fatal, infectious neurodegenerative diseases that affect humans and animals. Some prion diseases are zoonotic and can be spread by oral consumption of prion-infected material within the food-chain. Following prion infection a long lag phase occurs during which time the infectious prions are usually sequestered to the lymphoid tissues and replicate upon follicular dendritic cells prior to neuroinvasion and ultimate clinical outcome. The spread of prions throughout the body has been linked to particular critical cell types such as M-cells within the gut for prion uptake (Heppner et al., 2001a, Donaldson et al., 2012), FDC in lymphoid tissues (Bruce et al., 2000) which allow prion replication due to their expression of PrP^C (McCulloch et al., 2011) and similarly neurons of the peripheral and central nervous system (Glatzel and Aguzzi, 2000, Mallucci et al., 2003). During peripheral prion infection $CD11c^+$ cells of the mononuclear phagocyte system have been proven to be a requirement for efficient oral prion pathogenesis (Raymond et al., 2007). The exact role these cells play was not clear as they constitute wide and varied populations of cells in numerous tissues (Bradford et al., 2011) see also Chapter 3. Initially it was hypothesised that the expression of PrP^C was a requirement for each participant in this chain of cells (Payne and Krakauer, 1998). $CD11c^+$ cells however do not all express high levels of PrP^C (see Figure 1.1) and little evidence for replication of prions upon or within them has been described (Huang et al., 2002, Huang and MacPherson, 2004). In fact, $CD11c^+$ cells have a remarkable capacity for the degradation of infectious prions and appear to be one of the few cells identified capable of performing this apparently protective function (Luhr et al., 2002, Luhr et al., 2004).

The aims of this thesis were to investigate the various roles that cells of the mononuclear phagocyte system play during prion pathogenesis. The mononuclear phagocyte system contains a variety of cell types including macrophages, dendritic cells and monocytes, which undertake a vast array of roles dependent upon their differentiation state and localisation amongst other factors (Geissmann et al., 2010). MNP are acutely sensitive to their environment and respond accordingly befitting of innate immune cell types, constituting the first line of defence against infection or injury. However, following oral prion infection the uptake of prions is critically performed by M-cells that are localised to the follicle-associated epithelium of lymphoid structures of the gut such as Peyer's patches (Heppner et al., 2001a, Donaldson et al., 2012). Following uptake by M-cells, infectious prions are 'processed' by $CD11c^+$ cells of the MNP system (Raymond et al., 2007) and next appear to replicate upon follicular dendritic cells within the B-cell follicle. The most likely mechanism for the relocation of

infectious prions from the FAE to FDC are by either cell-mediated or cell-free mechanisms. The chemotaxis of mature $CD11c^+$ cells functioning as specialised antigen-presenting cells, would likely require their expression of the follicle-homing chemokine receptor CXCR5 to effectively undertake cell-mediated transport. Using a CD11c-mediated CXCR5 knockout model this precise transport mechanism could be isolated and prevented in order to determine the impact upon prion transport. Furthermore, the physiological role these $CXCR5^+/CD11c^+$ cells play in antigen-presentation were also investigated in the gastrointestinal pathogen infection model *T. muris*. *T. muris* infection is capable of generating both helper T cell type 1 (T_H1) and type 2 (T_H2) biased responses under various specific conditions. The mechanisms governing this bias were also elucidated using the novel CD11c-mediated CXCR5 knockout model, revealing further the functional implications of preventing follicle-homing of $CD11c^+$ cells. Investigating the role of resident (non-motile) $CD11c^+$ mononuclear phagocytes, their ability to identify and collect cell-free prions was altered via specific depletion or downregulation of the receptors sialoadhesin and SIGN-R1. The progress of prion pathogenesis was monitored in the absence of these receptors to determine their potential role in prion uptake and relay to FDC within lymphoid tissues.

9.2 Is CD11c a good marker of conventional dendritic cells?

Several studies have addressed the pathways of MNP differentiation, and defined "committed" progenitors including the macrophage and conventional dendritic cell (cDC) precursor (MDP), the common DC precursor (CDP) or bone marrow committed precursor of cDC (BM Pre-cDC) (Geissmann et al., 2010). Each of these identified precursors has been characterized independently; they share expression of the common markers cKit, Flt3, CX_3CR1 and the CSF1R and the distinction and relationship between them is unclear. The CSF1R-eGFP transgene provides a marker that is shared between all of these cells and their progeny (Sasmono et al., 2003). The lamina propria MNPs have been sub-divided into the $CD103^+$ cDC (Annacker et al., 2005) and CX_3CR1^+ cDC (Del Rio et al., 2008) or CX_3CR1^+ macrophage (Schulz et al., 2009) and CX_3CR1^- conventional macrophage subsets (Pavli et al., 1990). The relationship between these subsets remains somewhat obscure. Much earlier studies, isolating the lamina propria cDC on the strict definition of cells able to stimulate an allogeneic mixed lymphocyte reaction, indicated that activity was confined to non-phagocytic cells (Pavli et al., 1990). Since the large majority of these cells possess the surface marker

F4/80, and are actively phagocytic, this finding further illustrates the difficulty with considering CD11c as cDC-specific, and undermines the interpretation of studies using the CD11c-DTR system. The Flt3 receptor binds its ligand Flt3l and has recently been shown to regulate the homeostasis of specific MNP populations such as lymphoid organ $CD11c^+$ cDC (Liu et al., 2009). Data from bone marrow reconstitution experiments using *Cx3cr1*-GFP transgenic mouse models (Auffray et al., 2009) have led to the suggestion that *Cx3cr1* expression represents a unique marker of all MNPs. Expression of *Cx3cr1* has also been postulated as defining the anatomical localisation of differentiated MNPs in particular to the terminal ileum where the highest levels of its ligand *Cx3cl1* were observed (Niess et al., 2005). The *Cx3cr1*-GFP transgenic model also aided in the re-classification of ileal MNP that extend processes and sample lumenal antigens (Niess et al., 2005) into macrophages due to their non-migratory behaviour (Schulz et al., 2009). Data in the current study imply that CSF1-R is in fact the true marker of the universal precursor population.

The functional relevance of the differential expression of the alpha integrin subunits CD11c and CD11b are not known, however evidence exists that they are differentially regulated (Ammon et al., 2000) and must compete to form functional dimers as they both signal through the beta integrin tail subunit *Itgb2*/CD18 (Mazzone and Ricevuti, 1995). The alpha integrin subunit functions as the external pattern recognition element of the integrin dimer (Lu et al., 2001). The specific ligands recognized by CD11c remain cryptic due to the lack of antibodies that definitively block the binding site, but are hypothesized to include the inactive cleavage product of complement component C3b (iC3b) (Myones et al., 1988, Bilsland et al., 1994) and fibrinogen (Wright et al., 1988). CD11b has a better defined ligand repertoire which includes ICAM-1 (Diamond et al., 1990), iC3b, Factor X (Altieri and Edgington, 1988) and lipopolysaccharide (LPS) (Wright and Jong, 1986, Bullock and Wright, 1987). The differential expression of CD11c and CD11b alpha integrin subunits would therefore offer differential adhesion capacities to those cells expressing them. From data presented in chapter 3 in this thesis it appears that differential expression of CD11c and CD11b is either facilitated by or regulates the specific localisation of MNP as CD11c expression correlates well with subsets of MNP that have the capacity to populate specific location niches within lymphoid structures. Furthermore MNP that populate exposure sites such as the lamina propria of the gut or intraepithelium of the lung and whose function is primarily to act as a migratory antigen presenting cell appear to be associated with a predominance of CD11c expression. The sub-setting of MNPs will continue to use the readily available surface markers such as integrins,

lectins and G-protein coupled receptors. However, many are actually markers of derivation and localisation and may not represent the functional capacity of these cells. Further sub-setting of MNPs using major histocompatibility complex-class molecules, lysosomal enzymes, activation status markers, chemokine receptors and toll-like receptors, in conjunction with biological properties such as ability to stimulate naïve T cells, may in fact give better indication of the various status and predominant abilities of specific MNP populations.

Data presented in Chapter 3 adds to the argument that there is a distinct lack of absolutely unique cellular markers in the MNP system. The identification of the pan-cDC transcription factor *zbtb46* or 'zDC' (Satpathy et al., 2012) possibly presents a cDC marker more applicable to this study. The transcription factor *Zbtb46* (BTBD4) is expressed in all cDC subsets but not pDC, monocytes, macrophages or other lymphoid or myeloid lineage cells. The interferon regulatory factors (IRF) 4 and 8 are necessary for the development of distinct cDC subsets and their functional diversity (Tamura et al., 2005). During the inception of this study the functional relevance of these subsets was not known, however the transcription factor *Irf4* has subsequently been shown to be essential for driving T_H2 responses by cDC (Williams et al., 2013). With this knowledge it is plausible that the $CXCR5^+$ cDC altered in the studies presented in this thesis correspond to the *Irf4*-dependent cDC subset, however further work would need to be undertaken to confirm or deny this hypothesis. These discoveries were made after the commencement of the studies presented in this thesis and transgenic models had yet to be produced or validated e.g. a Cre-expressing transgene driven by the *Zbtb46* or *Irf4* promoter. Despite these facts the expression of *Itgax*/CD11c defines specific populations of MNP throughout the tissues known to be involved in prion pathogenesis and in the absence of unique markers for APC or cDC, CD11c-based transgenic models are the most well-characterised and applicable for the studies undertaken within this thesis. Based on these findings it was determined that CD11cCre mice were the most appropriate model for the subsequent studies looking at the roles of trafficking and chemotaxis of antigen-presenting cells in the dissemination of prions and other infection models. Throughout all observations, MNP within germinal centres and proximal to FDC robustly displayed CD11c expression and within the CD11c-Cre model were also observed to report Cre activity. Therefore gene modification studies using CD11cCre mice should target relevant cells of interest.

9.3 Assessment of conditional CXCR5 knockout transgenic mice

The generation and use of conditional CXCR5 expressing transgenic mice was crucial to this study. Following their construction and breeding $CXCR5^{fl}$ homozygote mice were indistinguishable from their parental background strain C57Bl/6 mice indicating that inclusion of the inserted *loxP* sequences had an undetectable impact upon the normal expression and function of CXCR5. The ability to genetically recombine the $CXCR5^{fl}$ transgene utilising Cre recombinase was observed to proceed as expected (Sauer and Henderson, 1988) resulting in a specific recombination event that excised CXCR5 exon 2 from the genome. Furthermore by generating Cre-mediated CXCR5-deficient mice the total loss of CXCR5 exon 2 was easily visualised indicating that 100% efficiency could be achieved. Regardless of this fact these mice also revealed severe phenotypic differences that proved a functional loss of CXCR5 had occurred due to the failed organogenic development of several key lymphoid structure, further proving the validity of the Cre/*loxP* conditional transgenesis approach. With the knowledge that the $CXCR5^{fl}$ transgenic construct behaved exactly as predicted, a cell-restricted knockout was produced using the well-characterized CD11cCre transgenic mouse (Caton et al., 2007). Despite the potential issues with using CD11c as a marker for a specific cell population (as discussed above), the population of interest had been confirmed as $CD11c^{+}$ as these cells are both critical for prion pathogenesis (Raymond et al., 2007, Cordier-Dirikoc and Chabry, 2008) and for the formation of T_H2 responses (Leon et al., 2012).

Investigation of CD11c-mediated CXCR5 knockout revealed surprisingly little alteration to lymphoid organogenesis. Despite reports that the Peyer's patch anlagen is established by $CD11c^{+}$ lymphoid tissue inducer (LTi) cells that express CXCR5 (Fukuyama and Kiyono, 2007, Veiga-Fernandes et al., 2007) no deficit in Peyer's patch development and maturation were observed in CD11cCre:$CXCR5^{fl}$ mice. Indeed it is CXCR5 and CCR7 that regulate the migration of LTi allowing them to colonize presumptive lymphoid organ sites (Forster et al., 1996, Honda et al., 2001, Luther et al., 2003, Mebius, 2003, Ferreira et al., 2012). Data presented in Chapter 4 suggest that either not all LTi express CD11c or that $CD11c^{+}$ LTi do not require CXCR5, i.e. can utilise CCR7 alone, to localise and instigate lymphoid organogenesis within for example intestinal Peyer's patches. Regardless of these observations it was important for further use of CD11cCre:$CXCR5^{fl}$ mice that lymphoid organogenesis was unimpaired so that investigation or prion and other pathogen infections could proceed without the added complication of loss or functional impairment of critical lymphoid tissues.

9.4 The role of follicular-homing CD11c$^+$ cells during infection

The trafficking of antigenic material from exposure sites to lymphoid effector sites is performed by antigen presenting cells (APC). Whilst numerous leucocytes are capable of performing the function of antigen presenting cells such as macrophages and B cells, conventional dendritic cells (cDC) are considered to be the experts (Kambayashi and Laufer, 2014). cDC have been shown to possess the ability to stimulate naïve T cells, and they can do so very effectively (Steinman and Witmer, 1978) though not all cDC possess this ability (Yewdall et al., 2010). However this ability is not unique to cDC as other subsets of cells including macrophages can also perform this function (Hume, 2008b). Furthermore cDC are migratory cells and are capable of maturing and altering chemokine receptor expression (Dieu et al., 1998, Lin et al., 1998) and are sensitive to other factors regulating their migration (Randolph, 2001, Sozzani, 2005) in order to traffic from the exposure site to lymphoid effector sites. The traditional view of cDC as APC is based on their upregulation of CCR7 during maturation in order to traffic to T-cell regions of lymphoid tissues in order to interact directly with T cells (Saeki et al., 1999). A specific migratory population of cDC was identified in the skin however which expressed CXCR5 and homed to B-cell follicles of lymphoid tissues (Saeki et al., 2000). Experiments using CXCR5-transduced bone-marrow derived DC subsequently suggested a possible role for CXCR5$^+$ cDC in modifying antigen-specific immune responses (Wu and Hwang, 2002). However a definitive role for CXCR5$^+$ cDC was not determined until their potential role in the formation of T_H2 responses was reported (Leon et al., 2012).

During prion infection, infectious prions are sequestered to follicular dendritic cells in B-cell follicles of lymphoid tissues. This is most apparent at the initial phase of oral prion infection, where following their uptake by M-cells (Donaldson et al., 2012), prions are first observed within Peyer's patches and lymph nodes suggesting that direct trafficking between FAE and FDC may occur (Beekes and McBride, 2000). In the transient absence of CD11c$^+$ cells at the time of peripheral exposure, the early accumulation of prions in the draining lymphoid tissue was blocked and disease susceptibility reduced following oral exposure (Raymond et al., 2007), however following intraperitoneal exposure these effects were reduced (Cordier-Dirikoc and Chabry, 2008). Conversely ablation of the CD8$^+$ cDC subset had a greater impact upon intraperitoneal and no effect on oral prion pathogenesis (Sethi et al., 2007). These findings imply that following oral prion infection CD11c$^+$/CD8$^-$ cDC are strong candidates for the transport of infectious prions to FDC. The fact that FDC strongly express the chemokine

CXCL13 and regulate follicular organisation with this chemokine (Vermi et al., 2008, Wang et al., 2011) also suggests that these cDC must also require CXCR5 expression to deliver prions to FDC.

In Chapter 4 we observed that CD11cCre:CXCR5^{fl} mice develop Peyer's patches which include CD11c^{+} cDC and mature PrP-expressing FDC, requirements for prion pathogenesis (Raymond et al., 2007, McCulloch et al., 2011) and FAE localised M-cells, required for prion uptake (Donaldson et al., 2012). However, in Chapter 5 we observed a reduced susceptibility to prion infection and impaired trafficking of prions to FDC in CD11cCre:CXCR5^{fl} mice. These data suggest that in the presence of M-cells, CD11c^{+} cells and FDC, the specific knockout of CXCR5 upon CD11c^{+} cells is directly responsible for the reduced efficiency in trafficking prions from the FAE to the FDC. The likelihood is that prions taken up by M-cell within CD11cCre:CXCR5^{fl} mice are possibly collected by cDC but trafficked aberrantly to peri-follicular T-cell regions such as the interfollicular region (IFR) of Peyer's patches. No deficit in transport of prions to the lymph nodal FDC were observed in CD11cCre:CXCR5^{fl} mice, possibly due to the over-abundance of mislocalised cDC within this structure and the altered B-follicular structure. Transport of prions to splenic FDC however was also reduced in orally infected CD11cCre:CXCR5^{fl} mice again despite the presence of PrP-expressing FDC and CD11c^{+} cells. These data suggest that CXCR5^{+} cDC constitute a more refined target for anti-prion therapeutic or preventative intervention strategies.

During gastrointestinal helminth infection, CXCR5^{+} cDC are critical for the formation of protective T_H2 responses due to antigen-presentation to follicular-homing T cells and the B-cell follicular environment. The pathogen *Trichuris muris* (*T. muris*) is capable of producing mixed responses in C57Bl/6 mice similar to the spectrum of human responses to helminth infections. In Chapter 6, following high dose *T. muris* infection of CD11cCre:CXCR5^{fl} mice we observed a failure to generate a protective T_H2 response and mice became persistently infected. Again in this model all relevant lymphoid structures have developed and contain the relevant immune system cellular components to generate a correctly T_H-biased response. The lack of the appropriate response and the aberrant and large T_H1 cytokine responses observed are directly attributable to the failure of CD11c^{+} cells to home to the B-cell follicle due to their lack of CXCR5.

Therefore in both prion and *T.muris* infection models we observed an altered response to infection in CD11cCre:CXCR5^{fl} mice. These altered responses can be directly attributed to the specific loss of CXCR5 on CD11c^{+} cells resulting in their altered trafficking and non-follicular homing. These observations advance the knowledge on both the hijacking of trafficking cDC by the prion infectious agent and also the targeted delivery of helminth antigen to effector immune cells following *T. muris* infection and therefore the specific role that CXCR5^{+} cDC play in the pathogenesis of both of these infections. Furthermore the potential exists that CXCR5^{+} cDC play a similar role in the formation of immune status in which aberrant T_H2 biased responses are generated, such as allergy. CD11cCre:CXCR5^{fl} mice represent a valuable and tractable model to further investigate the formation of allergic responses and also other infection models.

9.5 The role of receptors on resident CD11c^{+} cells during prion pathogenesis

Although the most efficient transport of prions to FDC during infection is attributable to CXCR5^{+} CD11c^{+} cells (Chapter 5), we did not observe a complete resistance to prion infection in CD11cCre:CXCR5^{fl} mice. The effect of CXCR5-knockout on CD11c and the complete ablation of CD11c^{+} cells produced strikingly similar responses to oral prion infection (Raymond et al., 2007), despite in the CD11c^{+} ablation model the loss of resident CD11c^{+} cells such as sialoadhesin^{+} marginal zone macrophages. Both cell-mediated and cell-free transport of prions has been observed in lymph (Michel et al., 2012) and the potential exists for the role of antigen presenting cells other than cDC in prion pathogenesis. Free prion infectious agent arriving at lymphoid structures such as lymph nodes or spleen would need to be captured and processed for delivery to FDC. Marginal zone macrophages function to screen the lymph and blood arriving at these tissues and capture antigenic material with an array of receptors.

The prion protein is highly sialylated (Stimson et al., 1999), and marginal zone metallophilic macrophages in the spleen, and the subcapsular sinus macrophages in the lymph nodes, constitutively express high levels of sialoadhesin which binds to sialylated glycoproteins (Crocker and Gordon, 1986). Similarly the receptor SIGN-R1 is expressed by outer marginal zone macrophages and functions to uptake complement C1q opsonized material and subsequently releasing such material for specific redirection to FDC (Kang et al., 2006). The enhanced uptake of prions into APC via C1q has been reported (Flores-Langarica et al., 2009)

and depletion of C1q significantly delays prion pathogenesis (Mabbott et al., 2001). Using both genetic knockout (Chapter 7 sialoadhesin-deficient mice) and antibody-mediated downregulation (Chapter 8 anti-SIGN-R1 treatment) the effect of the absence of each of these receptors upon prion pathogenesis were investigated independently. Following peripheral prion infection neither sialoadhesin-deficient nor SIGN-R1-downregulated mice displayed any alteration to prion susceptibility, pathogenesis or survival time. These data suggest that if resident $CD11c^+$ cells do play a role in prion pathogenesis then the receptors sialoadhesin and SIGN-R1 are not integral to that function. These data further confirm that cell-mediated prion delivery to FDC via $CXCR5^+$ $CD11c^+$ cells constitutes the major physiologically relevant and most efficient prion transport mechanism during prion infection.

Figure 9.1 Summary of the role of CXCR5 expression in CD11c$^+$ antigen presentation and responses to infection

Following prion infection CD11c$^+$ cells transport prions from the exposure site to the T-cell region of lymphoid tissues via the chemokine receptor CCR7. For efficient prion neuroinvasion to occur the expression of the chemokine receptor CXCR5 is required on CD11c$^+$ cells to transport prions into the B-cell follicle and potentially directly to follicular dendritic cells (FDC). In the absence of expression (i.e. in CD11cCre:CXCR5^{fl} transgenic mice) a decreased susceptibility to prion infection was observed. Altering expression of SIGN-R1 or Sialoadhesin on lymphoid resident marginal zone (MZ) or marginal zone metallophilic (MZM) CD11c$^+$ macrophages had no impact on prion neuroinvasion, further highlighting the importance of chemotactic trafficking of prions by mobile CD11c$^+$ cells. Conversely following gastrointestinal helminth infections such as *T. muris*, the trafficking of antigen into T-cell regions of lymphoid follicles allows effective T_H1-biased maturation resulting in susceptibility and persistent infection in CD11cCre:CXCR5^{fl} transgenic mice. In this case expression of CXCR5 by CD11c$^+$ antigen presenting cells facilitates the migration of both APC and naïve T-cells into the B-cell follicle, allowing CD40-CD40L dependent & B-cell-cDC contact mediated T_H2 polarised maturation of naïve T-cells. This B-cell dependent T_H2 biased response leads to worm expulsion and resistance. Therefore the regulation of CXCR5-mediated chemotaxis by CD11c$^+$ cells may be utilised for therapeutic potential in both preventing neuroinvasion of prion disease and generating resistance to gastrointestinal pathogens as demonstrated in infection studies within this thesis.

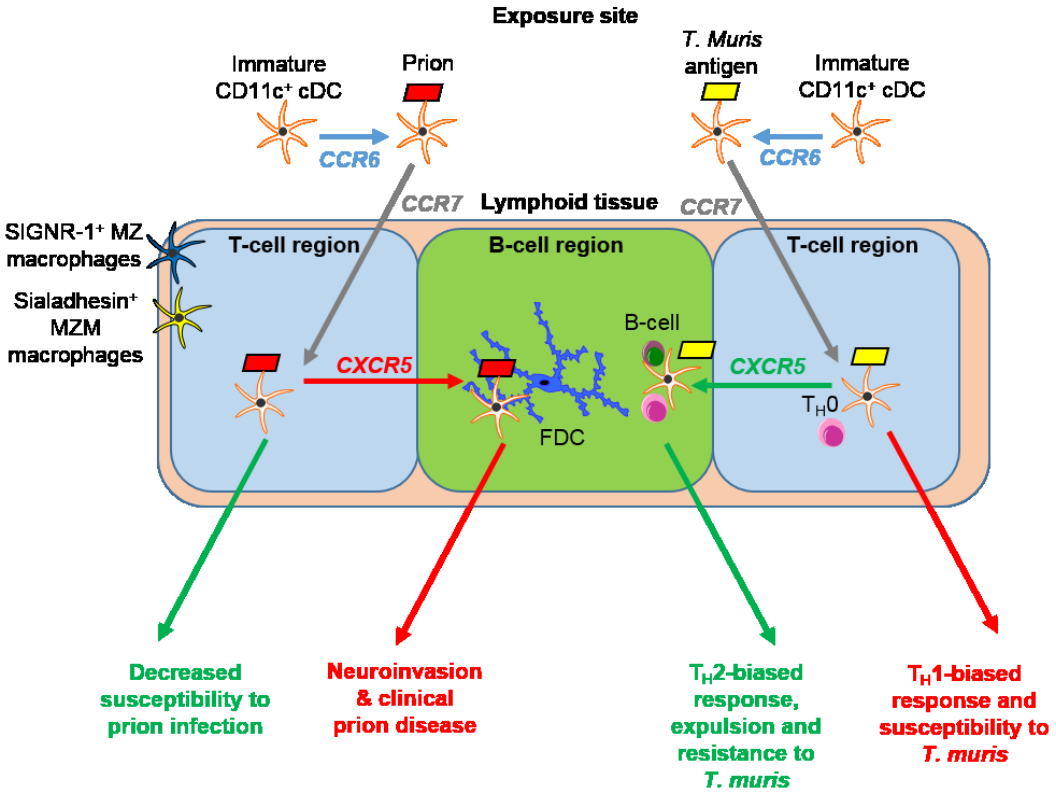

9.6 Future work

Following on from these studies the mechanisms and signalling pathways driving CXCR5 expression in CD11c-expressing cells represent viable targets for modulating the response to pathogens. Therefore understanding how and why $CD11c^+$ cells express CXCR5, and if this expression can be modulated by pathogens for the purposes of immune-evasion represent interesting fields of study. Furthermore the investigation of the role of CXCR5 expressing $CD11c^+$ cells in the inappropriate generation of T_H2 responses to allergens needs to be investigated. If allergic responses are generated via the same cell trafficking then our ability to modulate antigen-presentation may prove beneficial in combating allergy.

Bibliography

ADACHI, S., YOSHIDA, H., KATAOKA, H. & NISHIKAWA, S. 1997. Three distinctive steps in Peyer's patch formation of murine embryo. *International Immunology,* 9(4), 507-514.

AICHELE, P., ZINKE, J., GRODE, L., SCHWENDENER, R. A., KAUFMANN, S. H. E. & SEILER, P. 2003. Macrophages of the splenic marginal zone are essential for trapping of blood-borne particulate antigen but dispensable for induction of specific T cell responses. *Journal of Immunology,* 171(3), 1148-1155.

ALLEN, C. D. C., ANSEL, K. M., LOW, C., LESLEY, R., TAMAMURA, H., FUJII, N. & CYSTER, J. G. 2004. Germinal center dark and light zone organization is mediated by CXCR4 and CXCR5. *Nature Immunology,* 5(9), 943-952.

ALPER, T., CRAMP, W. A., HAIG, D. A. & CLARKE, M. C. 1967. Does the agent of scrapie replicate without nucleic acid ? *Nature,* 214(5090), 764-766.

ALPER, T., HAIG, D. A. & CLARKE, M. C. 1966. The exceptionally small size of the scrapie agent. *Biochemical and Biophysical Research Communications,* 22(3), 278-284.

ALTIERI, D. C. & EDGINGTON, T. S. 1988. The saturable high affinity association of factor X to ADP-stimulated monocytes defines a novel function of the Mac-1 receptor. *Journal of Biological Chemistry,* 263(15), 7007-7015.

AMMON, C., MEYER, S. P., SCHWARZFISCHER, L., KRAUSE, S. W., ANDREESEN, R. & KREUTZ, M. 2000. Comparative analysis of integrin expression on monocyte-derived macrophages and monocyte-derived dendritic cells. *Immunology,* 100(3), 364-369.

ANDREOLETTI, O., BERTHON, P., MARC, D., SARRADIN, P., GROSCLAUDE, J., VAN KEULEN, L., SCHELCHER, F., ELSEN, J.-M. & LANTIER, F. 2000. Early accumulation of PrP^{Sc} in gut-associated lymphoid and nervous tissues of susceptible sheep from a Romanov flock with natural scrapie. *Journal of General Virology,* 81(12), 3115-3126.

ANDRIAN, U. H. V. 2003. Introduction: chemokines--regulation of immune cell trafficking and lymphoid organ architecture. *Seminars in Immunology,* 15(5), 239-241.

ANNACKER, O., COOMBES, J. L., MALMSTROM, V., UHLIG, H. H., BOURNE, T., JOHANSSON-LINDBOM, B., AGACE, W. W., PARKER, C. M. & POWRIE, F. 2005. Essential role for CD103 in the T cell-mediated regulation of experimental colitis. *Journal of Experimental Medicine,* 202(8), 1051-1061.

ANSEL, K. M. & CYSTER, J. G. 2001. Chemokines in lymphopoiesis and lymphoid organ development. *Current Opinion in Immunology,* 13(2), 172-179.

ANSEL, K. M., NGO, V. N., HYMAN, P. L., LUTHER, S. A., FORSTER, R., SEDGWICK, J. D., BROWNING, J. L., LIPP, M. & CYSTER, J. G. 2000. A chemokine-driven positive feedback loop organizes lymphoid follicles. *Nature,* 406(6793), 309-314.

AUCOUTURIER, P., GEISSMANN, F., DAMOTTE, D., SABORIO, G. P., MEEKER, H. C., KASCSAK, R., KASCSAK, R., CARP, R. I. & WISNIEWSKI, T. 2001. Infected splenic dendritic cells are sufficient for prion transmission to the CNS in mouse scrapie. *Journal of Clinical Investigation,* 108(5), 703-708.

AUFFRAY, C., FOGG, D. K., NARNI-MANCINELLI, E., SENECHAL, B., TROUILLET, C., SAEDERUP, N., LEEMPUT, J., BIGOT, K., CAMPISI, L., ABITBOL, M., MOLINA, T., CHARO, I., HUME, D. A., CUMANO, A., LAUVAU, G. & GEISSMANN, F. 2009. CX_3CR1^+ $CD115^+$ $CD135^+$ common macrophage/DC precursors and the role of CX_3CR1 in their response to inflammation. *Journal of Experimental Medicine,* 206(3), 595-606.

AYDAR, Y., SUKUMAR, S., SZAKAL, A. K. & TEW, J. G. 2005. The influence of immune complex-bearing follicular dendritic cells on the IgM response, Ig class switching, and production of high affinity IgG. *Journal of Immunology,* 174(9), 5358-5366.

AYERS, J. I., KINCAID, A. E. & BARTZ, J. C. 2009. Prion strain targeting independent of strain-specific neuronal tropism. *Journal of Virology,* 83(1), 81-87.

BAKKEBØ, M. K., MOUILLET-RICHARD, S., ESPENES, A. E., GOLDMANN, W., TATZELT, J. & TRANULIS, M. A. 2015. The cellular prion protein: a player in immunological quiescence. *Frontiers in Immunology,* 6), 450.

BALLERINI, C., GOURDAIN, P., BACHY, V., BLANCHARD, N., LEVAVASSEUR, E., GRÉGOIRE, S., FONTES, P., AUCOUTURIER, P., HIVROZ, C. & CARNAUD, C. 2006. Functional implication of cellular prion protein in antigen-driven interactions between T cells and dendritic cells. *Journal of Immunology,* 176(12), 7254-7262.

BANCHEREAU, J., BRIERE, F., CAUX, C., DAVOUST, J., LEBECQUE, S., LIU, Y.-J., PULENDRAN, B. & PALUCKA, K. 2000. Immunobiology of dendritic cells. *Annual Review of Immunology,* 18(1), 767-811.

BANCROFT, A. J., ARTIS, D., DONALDSON, D. D., SYPEK, J. P. & GRENCIS, R. K. 2000. Gastrointestinal nematode expulsion in IL-4 knockout mice is IL-13 dependent. *European Journal of Immunology,* 30(7), 2083-2091.

BANCROFT, A. J., ELSE, K. J. & GRENCIS, R. K. 1994. Low-level infection with Trichuris muris significantly affects the polarization of the CD4 response. *European Journal of Immunology,* 24(12), 3113-3118.

BANCROFT, A. J., ELSE, K. J., HUMPHREYS, N. E. & GRENCIS, R. K. 2001. The effect of challenge and trickle Trichuris muris infections on the polarisation of the immune response. *International Journal for Parasitology,* 31(14), 1627-1637.

BANCROFT, A. J., HUMPHREYS, N. E., WORTHINGTON, J. J., YOSHIDA, H. & GRENCIS, R. K. 2004. WSX-1: a key role in induction of chronic intestinal nematode infection. *Journal of Immunology,* 172(12), 7635-7641.

BAR-ON, L. & JUNG, S. 2010. Defining in vivo dendritic cell functions using CD11c-DTR transgenic mice.595: Methods in Molecular Biology: Dendritic Cell Protocols 2nd edition. New York: Shalin H Naik, 2010. Vol 595: 429.

BARCHET, W., KRUG, A., CELLA, M., NEWBY, C., FISCHER, J. A. A., DZIONEK, A., PEKOSZ, A. & COLONNA, M. 2005. Dendritic cells respond to influenza virus through TLR7- and PKR-independent pathways. *European Journal of Immunology,* 35(1), 236-242.

BARONE, F., BOMBARDIERI, M., ROSADO, M. M., MORGAN, P. R., CHALLACOMBE, S. J., DE VITA, S., CARSETTI, R., SPENCER, J., VALESINI, G. & PITZALIS, C. 2008. CXCL13, CCL21, and CXCL12 expression in salivary glands of patients with Sjögren's syndrome and MALT lymphoma: association with reactive and malignant areas of lymphoid organization. *Journal of Immunology,* 180(7), 5130-5140.

BARTZ, J. C., KINCAID, A. E. & BESSEN, R. A. 2002. Retrograde transport of transmissible mink encephalopathy within descending motor tracts. *Journal of Virology,* 76(11), 5759-5768.

BECKER, A. M., MICHAEL, D. G., SATPATHY, A. T., SCIAMMAS, R., SINGH, H. & BHATTACHARYA, D. 2012. IRF-8 extinguishes neutrophil production and promotes dendritic cell lineage commitment in both myeloid and lymphoid mouse progenitors. *Blood,* 119(9), 2003-2012.

BEEKES, M. & MCBRIDE, P. A. 2000. Early accumulation of pathological PrP in the enteric nervous system and gut-associated lymphoid tissue of hamsters orally infected with scrapie. *Neuroscience Letters,* 278(3), 181-184.

BERGMAN, M. P., ENGERING, A., SMITS, H. H., VAN VLIET, S. J., VAN BODEGRAVEN, A. A., WIRTH, H.-P., KAPSENBERG, M. L.,

VANDENBROUCKE-GRAULS, C. M. J. E., VAN KOOYK, Y. & APPELMELK, B. J. 2004. Helicobacter pylori modulates the T helper cell 1/T helper cell 2 balance through phase-variable interaction between lipopolysaccharide and DC-SIGN. *Journal of Experimental Medicine,* 200(8), 979-990.

BERGTOLD, A., DESAI, D. D., GAVHANE, A. & CLYNES, R. 2005. Cell surface recycling of internalized antigen permits dendritic cell priming of B cells. *Immunity,* 23(5), 503-514.

BERNEY, C., HERREN, S., POWER, C. A., GORDON, S., MARTINEZ-POMARES, L. & KOSCO-VILBOIS, M. H. 1999. A member of the dendritic cell family that enters B cell follicles and stimulates primary antibody responses identified by a mannose receptor fusion protein. *Journal of Experimental Medicine,* 190(6), 851-860.

BILSLAND, C. A., DIAMOND, M. S. & SPRINGER, T. A. 1994. The leukocyte integrin p150,95 (CD11c/CD18) as a receptor for iC3b. Activation by a heterologous beta subunit and localization of a ligand recognition site to the I domain. *Journal of Immunology,* 152(9), 4582-9.

BINDELS, L. B., BECK, R., SCHAKMAN, O., MARTIN, J. C., DE BACKER, F., SOHET, F. M., DEWULF, E. M., PACHIKIAN, B. D., NEYRINCK, A. M., THISSEN, J.-P., VERRAX, J., CALDERON, P. B., POT, B., GRANGETTE, C., CANI, P. D., SCOTT, K. P. & DELZENNE, N. M. 2012. Restoring specific lactobacilli levels decreases inflammation and muscle atrophy markers in an acute leukemia mouse model. *PLoS ONE,* 7(6), e37971.

BLACKWELL, N. M. & ELSE, K. J. 2001. B cells and antibodies are required for resistance to the parasitic gastrointestinal nematode trichuris muris. *Infection and Immunity,* 69(6), 3860-3868.

BLANQUET-GROSSARD, F., THIELENS, N. M., VENDRELY, C., JAMIN, M. & ARLAUD, G. J. 2005. Complement protein C1q recognizes a conformationally modified form of the prion protein. *Biochemistry,* 44(11), 4349-4356.

BOLTON, D. C., MCKINLEY, M. P. & PRUSINER, S. B. 1982. Identification of a protein that purifies with the scrapie prion. *Science,* 218(4579), 1309-1311.

BRADFORD, B. & MABBOTT, N. 2012. Prion disease and the innate immune system. *Viruses,* 4(12), 3389-3491.

BRADFORD, B. M., BROWN, K. L. & MABBOTT, N. A. 2016. Prion pathogenesis is unaltered following down-regulation of SIGN-R1. *Virology,* 497(2016), 337-345.

BRADFORD, B. M., CROCKER, P. R. & MABBOTT, N. A. 2014. Peripheral prion disease pathogenesis is unaltered in the absence of sialoadhesin (Siglec-1/CD169). *Immunology,* 143(1), 120-9.

BRADFORD, B. M., SESTER, D. P., HUME, D. A. & MABBOTT, N. A. 2011. Defining the anatomical localisation of subsets of the murine mononuclear phagocyte system using integrin alpha X (Itgax, CD11c) and colony stimulating factor 1 receptor (Csf1r, CD115) expression fails to discriminate dendritic cells from macrophages. *Immunobiology,* 216(11), 1228-1237.

BRADFORD, B. M., TUZI, N. L., FELTRI, M. L., MCCORQUODALE, C., CANCELLOTTI, E. & MANSON, J. C. 2009. Dramatic reduction of PrPC level and glycosylation in peripheral nerves following PrP knock-out from Schwann cells does not prevent transmissible spongiform encephalopathy neuroinvasion. *Journal of Neuroscience,* 29(49), 15445-15454.

BRADLEY, L. M., DALTON, D. K. & CROFT, M. 1996. A direct role for IFN-gamma in regulation of Th1 cell development. *Journal of Immunology,* 157(4), 1350-8.

BRANDEL, J. P. 1999. Clinical aspects of human spongiform encephalopathies, with the exception of iatrogenic forms. *Biomedicine & Pharmacotherapy,* 53(1), 14-18.

BREITFELD, D., OHL, L., KREMMER, E., ELLWART, J., SALLUSTO, F., LIPP, M. & FORSTER, R. 2000. Follicular B helper T cells express CXC chemokine receptor 5, localize to B cell follicles, and support immunoglobulin production. *Journal of Experimental Medicine,* 192(11), 1545-1552.

BREMER, J., BAUMANN, F., TIBERI, C., WESSIG, C., FISCHER, H., SCHWARZ, P., STEELE, A. D., TOYKA, K. V., NAVE, K.-A., WEIS, J. & AGUZZI, A. 2010. Axonal prion protein is required for peripheral myelin maintenance. *Nature Neuroscience,* 13(3), 310-318.

BROWN, K. L., GOSSNER, A., MOK, S. & MABBOTT, N. A. 2012. The effects of host age on the transport of complement-bound complexes to the spleen and the pathogenesis of intravenous scrapie infection. *Journal of Virology,* 86(1), 25-35.

BROWN, K. L. & MABBOTT, N. A. 2014. Evidence of subclinical prion disease in aged mice following exposure to bovine spongiform encephalopathy. *Journal of General Virology,* 95(1), 231-243.

BROWN, K. L., RITCHIE, D. L., MCBRIDE, P. A. & BRUCE, M. E. 2000. Detection of PrP in extraneural tissues. *Microscopy Research and Technique,* 50(1), 40-45.

BROWN, K. L., STEWART, K., RITCHIE, D. L., MABBOTT, N. A., WILLIAMS, A., FRASER, H., MORRISON, W. I. & BRUCE, M. E. 1999. Scrapie replication in lymphoid tissues depends on prion protein-expressing follicular dendritic cells. *Nature Medicine,* 5(11), 1308-1312.

BROWN, K. L., WATHNE, G. J., SALES, J., BRUCE, M. E. & MABBOTT, N. A. 2009. The effects of host age on follicular dendritic cell status dramatically impair scrapie agent neuroinvasion in aged mice. *Journal of Immunology,* 183(8), 5199-5207.

BROWN, P. & GAJDUSEK, D. C. 1991. Survival of scrapie virus after 3 years interment. *Lancet,* 337(8736), 269-270.

BRUCE, M. & DICKINSON, A. 1987. Biological evidence that scrapie agent has an independent genome. *Journal of General Virology,* 68(1), 79-89.

BRUCE, M., MCBRIDE, P., JEFFREY, M. & SCOTT, J. 1994. PrP in pathology and pathogenesis in scrapie-infected mice. *Molecular Neurobiology,* 8(2), 105-112.

BRUCE, M. E. 1993. Scrapie strain variation and mutation. *British Medical Bulletin,* 49(4), 822-838.

BRUCE, M. E. 2003. TSE strain variation. *British Medical Bulletin,* 66(1), 99-108.

BRUCE, M. E., BOYLE, A. & MCCONNELL, I. 2004. TSE strain typing in mice. *In:* LEHMANN, S. & GRASSI, J. (eds.) *Techniques in Prion Research.* (10),132-146 Basel: Birkhäuser Basel.

BRUCE, M. E., BROWN, K. L., MABBOTT, N. A., FARQUHAR, C. F. & JEFFREY, M. 2000. Follicular dendritic cells in TSE pathogenesis. *Immunology Today,* 21(9), 442-446.

BUELER, H., AGUZZI, A., SAILER, A., GREINER, R. A., AUTENRIED, P., AGUET, M. & WEISSMANN, C. 1993. Mice devoid of PrP are resistant to scrapie. *Cell,* 73(7), 1339-1347.

BULLOCK, W. E. & WRIGHT, S. D. 1987. Role of the adherence-promoting receptors, CR3, LFA-1, and p150,95, in binding of Histoplasma capsulatum by human macrophages. *The Journal of Experimental Medicine,* 165(1), 195-210.

CAMPBELL, D., J. , KIM, C., H. & BUTCHER, E., C. 2003. Chemokines in the systemic organization of immunity. *Immunological Reviews,* 195(1), 58-71.

CARLSEN, H. S., BAEKKEVOLD, E. S., JOHANSEN, F. E., HARALDSEN, G. & BRANDTZAEG, P. 2002. B cell attracting chemokine 1 (CXCL13) and its receptor CXCR5 are expressed in normal and aberrant gut associated lymphoid tissue. *Gut,* 51(3), 364-371.

CARP, R. I. 1982. Transmission of scrapie by oral route: effect of ginigval scarification. *The Lancet,* 319(8264), 170-171.
CARRERAS, E., TURNER, S., FRANK, M. B., KNOWLTON, N., OSBAN, J., CENTOLA, M., PARK, C. G., SIMMONS, A., ALBEROLA-ILA, J. & KOVATS, S. 2010. Estrogen receptor signaling promotes dendritic cell differentiation by increasing expression of the transcription factor IRF4. *Blood,* 115(2), 238-246.
CASHMAN, N. R., LOERTSCHER, R., NALBANTOGLU, J., SHAW, I., KASCSAK, R. J., BOLTON, D. C. & BENDHEIM, P. E. 1990. Cellular isoform of the scrapie agent protein participates in lymphocyte activation. *Cell,* 61(1), 185-192.
CASTRO-SEOANE, R., HUMMERICH, H., SWEETING, T., TATTUM, M. H., LINEHAN, J. M., FERNANDEZ DE MARCO, M., BRANDNER, S., COLLINGE, J. & KLÖHN, P.-C. 2012. Plasmacytoid dendritic cells sequester high prion titres at early stages of prion infection. *PLoS Pathogens,* 8(2), e1002538.
CATON, M. L., SMITH-RASKA, M. R. & REIZIS, B. 2007. Notch-RBP-J signaling controls the homeostasis of $CD8^-$ dendritic cells in the spleen. *Journal of Experimental Medicine,* 204(7), 1653-1664.
CAUGHEY, B., RACE, R. E. & CHESEBRO, B. 1988. Detection of prion protein mRNA in normal and scrapie-infected tissues and cell lines. *Journal of General Virology,* 69(3), 711-716.
CAUGHEY, B., RAYMOND, G. J., ERNST, D. & RACE, R. E. 1991. N-terminal truncation of the scrapie-associated form of PrP by lysosomal protease(s): implications regarding the site of conversion of PrP to the protease-resistant state. *Journal of Virology,* 65(12), 6597-6603.
CAUX, C., AIT-YAHIA, S., CHEMIN, K., DE BOUTEILLER, O., DIEU-NOSJEAN, M.-C., HOMEY, B., MASSACRIER, C., VANBERVLIET, B., ZLOTNIK, A. & VICARI, A. 2000. Dendritic cell biology and regulation of dendritic cell trafficking by chemokines. *Springer Seminars in Immunopathology,* 22(4), 345-369.
CEROVIC, V., HOUSTON, S. A., SCOTT, C. L., AUMEUNIER, A., YRLID, U., MOWAT, A. M. & MILLING, S. W. F. 2013. Intestinal CD103- dendritic cells migrate in lymph and prime effector T cells. *Mucosal Immunology,* 6(1), 104-113.
CHANDLER, R. L. 1961. Encephalopathy in mice produced by inoculation with scrapie brain material. *The Lancet,* 277(7191), 1378-1379.
CHARI, R., LONERGAN, K. M., PIKOR, L. A., COE, B. P., ZHU, C. Q., CHAN, T. H., MACAULAY, C. E., TSAO, M.-S., LAM, S., NG, R. T. & LAM, W. L. 2010. A sequence-based approach to identify reference genes for gene expression analysis. *BMC Medical Genomics,* 3(1), 1-11.
CHEN, L. L., FRANK, A. M., ADAMS, J. C. & STEINMAN, R. M. 1978. Distribution of horseradish peroxidase (HRP)-anti-HRP immune complexes in mouse spleen with special reference to follicular dendritic cells. *Journal of Cell Biology,* 79(1), 184-199.
CHEN, M. & WANG, J. 2010. Programmed cell death of dendritic cells in immune regulation. *Immunological Reviews,* 236(1), 11-27.
CHIZZOLINI, C., CHICHEPORTICHE, R., BURGER, D. & DAYER, J.-M. 1997. Human Th1 cells preferentially induce interleukin (IL)-1β while Th2 cells induce IL-1 receptor antagonist production upon cell/cell contact with monocytes. *European Journal of Immunology,* 27(1), 171-177.
CINAMON, G., ZACHARIAH, M. A., LAM, O. M., FOSS, F. W. & CYSTER, J. G. 2008. Follicular shuttling of marginal zone B cells facilitates antigen transport. *Nature Immunology,* 9(1), 54-62.
CLIFFE, L. J. & GRENCIS, R. K. 2004. The Trichuris muris System: a Paradigm of Resistance and Susceptibility to Intestinal Nematode Infection. *Advances in Parasitology.*Volume 57(2004),255-307: Academic Press.

CLIFFE, L. J., POTTEN, C. S., BOOTH, C. E. & GRENCIS, R. K. 2007. An increase in epithelial cell apoptosis is associated with chronic intestinal nematode infection. *Infection and Immunity,* 75(4), 1556-1564.

COLLINGE, J., WHITFIELD, J., MCKINTOSH, E., BECK, J., MEAD, S., THOMAS, D. J. & ALPERS, M. P. 2006. Kuru in the 21st century—an acquired human prion disease with very long incubation periods. *The Lancet,* 367(9528), 2068-2074.

COLMENARES, M. A., PUIG-KRÖGER, A., PELLO, O. M., CORBí, A. L. & RIVAS, L. 2002. Dendritic cell (DC)-specific intercellular adhesion molecule 3 (ICAM-3)-grabbing nonintegrin (DC-SIGN, CD209), a c-type surface lectin in human DCs, is a receptor for leishmania amastigotes. *Journal of Biological Chemistry,* 277(39), 36766-36769.

COLTEN, H. R., OOI, Y. M. & EDELSON, P. J. 1979. Synthesis and secretion of complement proteins by macrophages. *Annals of the New York Academy of Sciences,* 332(1), 482-490.

COLTEN, H. R., PERLMUTTER, R. C., SCHLESSINGER, D. H. & COLE, F. S. 1986. Regulation of Complement Protein Biosynthesis in Mononuclear Phagocytes. *In:* D. EVERED J. NUGENT, M. O. C. (ed.) *Ciba Foundation Symposium* 118-Biochemistry of Macrophages(10),141-154 Chichester: John Wiley & Sons, Ltd.

COOK, D. N., PROSSER, D. M., FORSTER, R., ZHANG, J., KUKLIN, N. A., ABBONDANZO, S. J., NIU, X.-D., CHEN, S.-C., MANFRA, D. J., WIEKOWSKI, M. T., SULLIVAN, L. M., SMITH, S. R., GREENBERG, H. B., NARULA, S. K., LIPP, M. & LIRA, S. A. 2000. CCR6 mediates dendritic cell localization, lymphocyte homeostasis, and immune responses in mucosal tissue. *Immunity,* 12(5), 495-503.

CORDIER-DIRIKOC, S. & CHABRY, J. 2008. Temporary depletion of $CD11c^+$ dendritic cells delays lymphoinvasion after intraperitonal scrapie infection. *Journal of Virology,* 82(17), 8933-8936.

CROCKER, P. R. 2002. Siglecs: sialic-acid-binding immunoglobulin-like lectins in cell-cell interactions and signalling. *Current Opinion in Structural Biology,* 12(5), 609-615.

CROCKER, P. R. & GORDON, S. 1986. Properties and distribution of a lectin-like hemagglutinin differentially expressed by murine stromal tissue macrophages. *Journal of Experimental Medicine,* 164(6), 1862-1875.

CROCKER, P. R., KELM, S., DUBOIS, C., MARTIN, B., MCWILLIAM, A. S., SHOTTON, D. M., PAULSON, J. C. & GORDON, S. 1991. Purification and properties of Sialoadhesin, a sialic acid-binding receptor of murine tissue macrophages. *EMBO Journal,* 10(7), 1661-1669.

CUILLE, J. & CHELLE, P. L. 1936. La maladie dite tremblante du mouton est-elle inocuulable? *Comptes Rendus de 'Academie des Sciences,* 1936(203), 1552-1554.

CUPEDO, T. & MEBIUS, R. E. 2003. Role of chemokines in the development of secondary and tertiary lymphoid tissues. *Seminars in Immunology,* 15(5), 243-248.

CYSTER, J. G. 1999. Chemokines and cell migration in secondary lymphoid organs. *Science,* 286(5447), 2098-2102.

CYSTER, J. G. 2000. Leukocyte migration: scent of the T zone. *Current Biology,* 10(1), R30-R33.

DAWOUD AL-BADER, M. & ALI AL-SARRAF, H. 2005. Housekeeping gene expression during fetal brain development in the rat—validation by semi-quantitative RT-PCR. *Developmental Brain Research,* 156(1), 38-45.

DE ALMEIDA, C. J. G., CHIARINI, L. B., DA SILVA, J. P., E SILVA, P. M. R., MARTINS, M. A. & LINDEN, R. 2005. The cellular prion protein modulates phagocytosis and inflammatory response. *Journal of Leukocyte Biology,* 77(2), 238-246.

DE SOUSA-CANAVEZ, J. M., DE OLIVEIRA MASSOCO, C., DE MORAES-VASCONCELOS, D., CORNETA, E. C., LEITE, K. R. M. & CAMARA-LOPES, L.

H. 2009. Retinoic acid inhibits dendritic cell differentiation driven by interleukin-4. *Cellular Immunology,* 259(1), 41-48.

DE WITTE, L., DE VRIES, R. D., VAN DER VLIST, M., YÜKSEL, S., LITJENS, M., DE SWART, R. L. & GEIJTENBEEK, T. B. H. 2008. DC-SIGN and CD150 have distinct roles in transmission of measles virus from dendritic cells to T-lymphocytes. *PLoS Pathogens,* 4(4), e1000049.

DEL RIO, M.-L., RODRIGUEZ-BARBOSA, J.-I., BOLTER, J., BALLMAIER, M., DITTRICH-BREIHOLZ, O., KRACHT, M., JUNG, S. & FORSTER, R. 2008. CX_3CR1^+c-kit^+ bone marrow cells give rise to $CD103^+$ and $CD103^-$ dendritic cells with distinct functional properties. *Journal of Immunology,* 181(9), 6178-6188.

DELAMARRE, L., PACK, M., CHANG, H., MELLMAN, I. & TROMBETTA, E. S. 2005. Differential lysosomal proteolysis in antigen-presenting cells determines antigen fate. *Science,* 307(5715), 1630-1634.

DENNING, T. L., WANG, Y.-C., PATEL, S. R., WILLIAMS, I. R. & PULENDRAN, B. 2007. Lamina propria macrophages and dendritic cells differentially induce regulatory and interleukin 17-producing T cell responses. *Nature Immunology,* 8(10), 1086-1094.

DIAMOND, M. S., STAUNTON, D. E., DE FOUGEROLLES, A. R., STACKER, S. A., GARCIA-AGUILAR, J., HIBBS, M. L. & SPRINGER, T. A. 1990. ICAM-1 (CD54): a counter-receptor for Mac-1 (CD11b/CD18). *The Journal of Cell Biology,* 111(6), 3129-3139.

DICKINSON, A. G., MEIKLE, V. M. H. & FRASER, H. 1986. Identification of a gene which controls the incubation period of some strains of scrapie agent in mice. *Journal of Comparative Pathology,* 78(3), 293-299.

DICKINSON, A. G. & TAYLOR, D. M. 1978. Resistance of scrapie agent to decontamination. *New England Journal of Medicine,* 299(25), 1413-1414.

DIEDRICH, J. F., BENDHEIM, P. E., KIM, Y. S., CARP, R. I. & HAASE, A. T. 1991. Scrapie-associated prion protein accumulates in astrocytes during scrapie infection. *Proceedings of the National Academy of Sciences of the United States of America,* 88(2), 375-379.

DIEU, M.-C., VANBERVLIET, B., VICARI, A., BRIDON, J.-M., OLDHAM, E., AIT-YAHIA, S., BRIERE, F., ZLOTNIK, A., LEBECQUE, S. & CAUX, C. 1998. Selective recruitment of immature and mature dendritic cells by distinct chemokines expressed in different anatomic sites. *Journal of Experimental Medicine,* 188(2), 373-386.

DINARELLO, C. A. 1999. IL-18: A TH1 -inducing, proinflammatory cytokine and new member of the IL-1 family. *Journal of Allergy and Clinical Immunology,* 103(1), 11-24.

DOBNER, T., WOLF, I., EMRICH, T. & LIPP, M. 1992. Differentiation-specific expression of a novel G protein-coupled receptor from Burkitt's lymphoma. *European Journal of Immunology,* 22(11), 2795-2799.

DODELET, V. C. & CASHMAN, N. R. 1998. Prion protein expression in human leukocyte differentiation. *Blood,* 91(5), 1556-1561.

DONALDSON, D. S., ELSE, K. J. & MABBOTT, N. A. 2015. The gut-associated lymphoid tissues in the small intestine, not the large intestine, play a major role in oral prion disease pathogenesis. *Journal of Virology,* 89(18), 9532-9547.

DONALDSON, D. S., KOBAYASHI, A., OHNO, H., YAGITA, H., WILLIAMS, I. R. & MABBOTT, N. A. 2012. M cell-depletion blocks oral prion disease pathogenesis. *Mucosal Immunology,* 5(2), 216-225.

DORBAN, G., DEFAWEUX, V., LEVAVASSEUR, E., DEMONCEAU, C., THELLIN, O., FLANDROY, S., PIRET, J., FALISSE, N., HEINEN, E. & ANTOINE, N. 2007. Oral

scrapie infection modifies the homeostasis of Peyer's patches' dendritic cells. *Histochemistry and Cell Biology,* 128(3), 243-251.

DZIENNIS, S., VAN ETTEN, R., PAHL, H., MORRIS, D., ROTHSTEIN, T., BLOSCH, C., PERLMUTTER, R. & TENEN, D. 1995. The CD11b promoter directs high-level expression of reporter genes in macrophages in transgenic mice. *Blood,* 85(2), 319-329.

EBISAWA, M., HASE, K., TAKAHASHI, D., KITAMURA, H., KNOOP, K. A., WILLIAMS, I. R. & OHNO, H. 2011. CCR6hiCD11cint B cells promote M-cell differentiation in Peyer's patch. *International Immunology,* 23(4), 261-9.

EDELSON, B. T., KC, W., JUANG, R., KOHYAMA, M., BENOIT, L. A., KLEKOTKA, P. A., MOON, C., ALBRING, J. C., ISE, W., MICHAEL, D. G., BHATTACHARYA, D., STAPPENBECK, T. S., HOLTZMAN, M. J., SUNG, S.-S. J., MURPHY, T. L., HILDNER, K. & MURPHY, K. M. 2010. Peripheral CD103+ dendritic cells form a unified subset developmentally related to CD8α+ conventional dendritic cells. *Journal of Experimental Medicine,* 207(4), 823-836.

EKLUND, C. M., KENNEDY, R. C. & HADLOW, W. J. 1967. Pathogenesis of scrapie virus infection in the mouse. *Journal of Infectious Diseases,* 117(1), 15-22.

EL SHIKH, M. E. & PITZALIS, C. 2012. Follicular dendritic cells in health and disease. *Frontiers in Immunology,* 3(2012), 292.

ELSE, K. J., FINKELMAN, F. D., MALISZEWSKI, C. R. & GRENCIS, R. K. 1994. Cytokine-mediated regulation of chronic intestinal helminth infection. *Journal of Experimental Medicine,* 179(1), 347-351.

ELSE, K. J. & GRENCIS, R. K. 1996. Antibody-independent effector mechanisms in resistance to the intestinal nematode parasite Trichuris muris. *Infection and Immunity,* 64(8), 2950-4.

EMARA, M., ROYER, P.-J., MAHDAVI, J., SHAKIB, F. & GHAEMMAGHAMI, A. M. 2012. Retagging identifies dendritic cell-specific intercellular adhesion molecule-3 (ICAM3)-grabbing non-integrin (DC-SIGN) protein as a novel receptor for a major allergen from house dust mite. *Journal of Biological Chemistry,* 287(8), 5756-5763.

ENDRES, R., ALIMZHANOV, M. B., PLITZ, T., FUTTERER, A., KOSCO-VILBOIS, M. H., NEDOSPASOV, S. A., RAJEWSKY, K. & PFEFFER, K. 1999. Mature follicular dendritic cell networks depend on expression of lymphotoxin β receptor by radioresistant stromal cells and of lymphotoxin β and tumor necrosis factor by B cells. *Journal of Experimental Medicine,* 189(1), 159-168.

ERBLICH, B., ZHU, L., ETGEN, A. M., DOBRENIS, K. & POLLARD, J. W. 2011. Absence of colony stimulation factor-1 receptor results in loss of microglia, disrupted brain development and olfactory deficits. *PLoS ONE,* 6(10), e26317.

FACCI, M. R., AURAY, G., MEURENS, F., BUCHANAN, R., VAN KESSEL, J. & GERDTS, V. 2011. Stability of expression of reference genes in porcine peripheral blood mononuclear and dendritic cells. *Veterinary Immunology and Immunopathology,* 141(1–2), 11-15.

FAULKNER, H., RENAULD, J.-C., VAN SNICK, J. & GRENCIS, R. K. 1998. Interleukin-9 enhances resistance to the intestinal nematode trichuris muris. *Infection and Immunity,* 66(8), 3832-3840.

FERREIRA, M., DOMINGUES, R. G. & VEIGA-FERNANDES, H. 2012. Stroma cell priming in enteric lymphoid organ morphogenesis. *Frontiers in Immunology,* 3(2012), 219.

FEVRIER, B., VILETTE, D., ARCHER, F., LOEW, D., FAIGLE, W., VIDAL, M., LAUDE, H. & RAPOSO, G. 2004. Cells release prions in association with exosomes. *Proceedings of the National Academy of Sciences of the United States of America,* 101(26), 9683-9688.

FILLATREAU, S. & GRAY, D. 2003. T Cell Accumulation in B Cell Follicles Is Regulated by Dendritic Cells and Is Independent of B Cell Activation. *The Journal of Experimental Medicine,* 197(2), 195-206.

FILLATREAU, S., GRAY, D. & ANDERTON, S. M. 2008. Not always the bad guys: B cells as regulators of autoimmune pathology. *Nature Reviews Immunology,* 8(5), 391-397.

FLORES-LANGARICA, A., SEBTI, Y., MITCHELL, D. A., SIM, R. B. & MACPHERSON, G. G. 2009. Scrapie pathogenesis: the role of complement C1q in scrapie agent uptake by conventional dendritic cells. *Journal of Immunology,* 182(3), 1305-1313.

FORD, M. J., BURTON, L. J., LI, H., GRAHAM, C. H., FROBERT, Y., GRASSI, J., HALL, S. M. & MORRIS, R. J. 2002a. A marked disparity between the expression of prion protein and its message by neurones of the CNS. *Neuroscience,* 111(3), 533-551.

FORD, M. J., BURTON, L. J., MORRIS, R. J. & HALL, S. M. 2002b. Selective expression of prion protein in peripheral tissues of the adult mouse. *Neuroscience,* 113(1), 177-192.

FORSTER, R., DAVALOS-MISSLITZ, A. C. & ROT, A. 2008. CCR7 and its ligands: balancing immunity and tolerance. *Nature Reviews Immunology,* 8(5), 362-371.

FORSTER, R., MATTIS, A. E., KREMMER, E., WOLF, E., BREM, G. & LIPP, M. 1996. A putative chemokine receptor, BLR1, directs B cell migration to defined lymphoid organs and specific anatomic compartments of the spleen. *Cell,* 87(6), 1037-47.

FOSTER, J. D., GOLDMANN, W., MCKENZIE, C., SMITH, A., PARNHAM, D. W. & HUNTER, N. 2004. Maternal transmission studies of BSE in sheep. *Journal of General Virology,* 85(10), 3159-3163.

FOTI, M., GRANUCCI, F., AGGUJARO, D., LIBOI, E., LUINI, W., MINARDI, S., MANTOVANI, A., SOZZANI, S. & RICCIARDI-CASTAGNOLI, P. 1999. Upon dendritic cell (DC) activation chemokines and chemokine receptor expression are rapidly regulated for recruitment and maintenance of DC at the inflammatory site. *International Immunology,* 11(6), 979-986.

FRASER, H., BROWN, K. L., STEWART, K., MCCONNELL, I., MCBRIDE, P. & WILLIAMS, A. 1996. Replication of scrapie in spleens of SCID mice follows reconstitution with wild-type mouse bone marrow. *Journal of General Virology,* 77(8), 1935-40.

FRASER, H. & DICKINSON, A. 1973. Scrapie in mice. Agent-strain differences in the distribution and intensity of grey matter vacuolation. *Journal of Comparative Pathology,* 83(1), 29 - 40.

FRASER, H. & DICKINSON, A. G. 1968. The sequential development of the brain lesions of scrapie in three strains of mice. *Journal of Comparative Pathology,* 78(3), 301-311.

FRASER, H. & DICKINSON, A. G. 1985. Targeting of scrapie lesions and spread of agent via the retino-tectal projection. *Brain Research,* 346(1), 32-41.

FU, Y.-X., HUANG, G., WANG, Y. & CHAPLIN, D. D. 1998. B lymphocytes induce the formation of follicular dendritic cell clusters in a lymphotoxin α-dependent fashion. *Journal of Experimental Medicine,* 187(7), 1009-1018.

FU, Y.-X., MOLINA, H., MATSUMOTO, M., HUANG, G., MIN, J. & CHAPLIN, D. D. 1997. Lymphotoxin-α (LTα) supports development of splenic follicular structure that is required for IgG responses. *Journal of Experimental Medicine,* 185(12), 2111-2120.

FUKUYAMA, S. & KIYONO, H. 2007. Neuroregulator RET initiates Peyer's-patch tissue genesis. *Immunity,* 26(4), 393-395.

GAJDUSEK, D. C. & GIBBS, C. J. 1964. Attempts to demonstrate a transmissible agent in Kuru, amyotrophic lateral sclerosis, and other sub-acute and chronic nervous system degenerations of man. *Nature,* 204(4955), 257-259.

GEIJTENBEEK, T. B. H. & VAN KOOYK, Y. 2003. DC-SIGN: A novel HIV receptor on DCs that mediates HIV-1 transmission. *In:* STEINKASSERER, A. (ed.) *Dendritic Cells and Virus Infection.*276(2),31-54: Springer Berlin Heidelberg.

GEIJTENBEEK, T. B. H., VAN VLIET, S. J., KOPPEL, E. A., SANCHEZ-HERNANDEZ, M., VANDENBROUCKE-GRAULS, C. M. J. E., APPELMELK, B. & VAN KOOYK, Y. 2003. Mycobacteria target DC-SIGN to suppress dendritic cell function. *Journal of Experimental Medicine,* 197(1), 7-17.

GEISSMANN, F., MANZ, M. G., JUNG, S., SIEWEKE, M. H., MERAD, M. & LEY, K. 2010. Development of monocytes, macrophages, and dendritic cells. *Science,* 327(5966), 656-661.

GILCH, S., SCHMITZ, F., AGUIB, Y., KEHLER, C., BÜLOW, S., BAUER, S., KREMMER, E. & SCHÄTZL, H., M. 2007. CpG and LPS can interfere negatively with prion clearance in macrophage and microglial cells. *FEBS Journal,* 274(22), 5834-5844.

GLATZEL, M. & AGUZZI, A. 2000. PrPC expression in the peripheral nervous system is a determinant of prion neuroinvasion. *Journal of General Virology,* 81(11), 2813-2821.

GLATZEL, M., HEPPNER, F. L., ALBERS, K. M. & AGUZZI, A. 2001. Sympathetic innervation of lymphoreticular organs is rate limiting for prion neuroinvasion. *Neuron,* 31(1), 25-34.

GLAYSHER, B. R. & MABBOTT, N. A. 2007. Role of the GALT in scrapie agent neuroinvasion from the intestine. *Journal of Immunology,* 178(6), 3757-3766.

GONZALEZ, M., MACKAY, F., BROWNING, J. L., KOSCO-VILBOIS, M. H. & NOELLE, R. J. 1998. The sequential role of lymphotoxin and B cells in the development of splenic follicles. *Journal of Experimental Medicine,* 187(7), 997-1007.

GONZALEZ, S. F., LUKACS-KORNEK, V., KULIGOWSKI, M. P., PITCHER, L. A., DEGN, S. E., KIM, Y.-A., CLONINGER, M. J., MARTINEZ-POMARES, L., GORDON, S., TURLEY, S. J. & CARROLL, M. C. 2010. Capture of influenza by medullary dendritic cells via SIGN-R1 is essential for humoral immunity in draining lymph nodes. *Nat Immunol,* 11(5), 427-434.

GORDON, W. S. 1957. Discussion to Palmer, A. C. Studies in scrapie. *Veterinary Record,* 1957(69), 1324-1327.

GOUSSET, K., SCHIFF, E., LANGEVIN, C., MARIJANOVIC, Z., CAPUTO, A., BROWMAN, D. T., CHENOUARD, N., DE CHAUMONT, F., MARTINO, A., ENNINGA, J., OLIVO-MARIN, J.-C., MANNEL, D. & ZURZOLO, C. 2009. Prions hijack tunnelling nanotubes for intercellular spread. *Nature Cell Biology,* 11(3), 328-336.

GRANER, E., MERCADANTE, A. F., ZANATA, S. M., FORLENZA, O. V., CABRAL, A. L. B., VEIGA, S. S., JULIANO, M. A., ROESLER, R., WALZ, R., MINETTI, A., IZQUIERDO, I., MARTINS, V. R. & BRENTANI, R. R. 2000. Cellular prion protein binds laminin and mediates neuritogenesis. *Molecular Brain Research,* 76(1), 85-92.

GRENCIS, R. K. 2001. Cytokine regulation of resistance and susceptibility to intestinal nematode infection — from host to parasite. *Veterinary Parasitology,* 100(1–2), 45-50.

GRIFFITH, J. S. 1967. Self-replication and Scrapie. *Nature,* 215(5105), 1043-1044.

GU, H., MARTH, J., ORBAN, P., MOSSMANN, H. & RAJEWSKY, K. 1994. Deletion of a DNA polymerase beta gene segment in T cells using cell type-specific gene targeting. *Science,* 265(5168), 103-106.

GUILLIAMS, M., GINHOUX, F., JAKUBZICK, C., NAIK, S. H., ONAI, N., SCHRAML, B. U., SEGURA, E., TUSSIWAND, R. & YONA, S. 2014. Dendritic cells, monocytes and macrophages: a unified nomenclature based on ontogeny. *Nat Rev Immunol,* 14(8), 571-578.

GUNN, M. D., NGO, V. N., ANSEL, K. M., EKLAND, E. H., CYSTER, J. G. & WILLIAMS, L. T. 1998. A B-cell-homing chemokine made in lymphoid follicles activates Burkitt's lymphoma receptor-1. *Nature,* 391(6669), 799-803.

HADDON, D. J., HUGHES, M. R., ANTIGNANO, F., WESTAWAY, D., CASHMAN, N. R. & MCNAGNY, K. M. 2009. Prion protein expression and release by mast cells after activation. *Journal of Infectious Diseases,* 200(5), 827-831.

HAJJ, G. N. M., LOPES, M. H., MERCADANTE, A. F., VEIGA, S. S., DA SILVEIRA, R. B., SANTOS, T. G., RIBEIRO, K. C. B., JULIANO, M. A., JACCHIERI, S. G., ZANATA, S. M. & MARTINS, V. R. 2007. Cellular prion protein interaction with vitronectin supports axonal growth and is compensated by integrins. *Journal of Cell Science,* 120(11), 1915-1926.

HAMILTON, J. A., WHITTY, G., WHITE, A. R., JOBLING, M. F., THOMPSON, A., BARROW, C. J., CAPPAI, R., BEYREUTHER, K. & MASTERS, C. L. 2002. Alzheimer's disease amyloid beta and prion protein amyloidogenic peptides promote macrophage survival, DNA synthesis and enhanced proliferative response to CSF-1 (M-CSF). *Brain Research,* 940(1–2), 49-54.

HARTSOUG, G. R. & BURGER, D. 1965. Encephalopathy of Mink .I. Epizootiologic and Clinical Observations. *Journal of Infectious Diseases,* 115(4), 387.

HARTUNG, H. P. & HADDING, U. 1983. Synthesis of complement by macrophages and modulation of their functions through complement activation. *Springer Seminars in Immunopathology,* 6(4), 283-326.

HASEBE, R., RAYMOND, G. J., HORIUCHI, M. & CAUGHEY, B. 2012. Reaction of complement factors varies with prion strains in vitro and in vivo. *Virology,* 423(2), 205-213.

HASNAIN, S. Z., WANG, H., GHIA, J. E., HAQ, N., DENG, Y., VELCICH, A., GRENCIS, R. K., THORNTON, D. J. & KHAN, W. I. 2010. Mucin gene deficiency in mice impairs host resistance to an enteric parasitic infection. *Gastroenterology,* 138(5-10), 1763-1771.e5.

HAYBAECK, J., HEIKENWALDER, M., KLEVENZ, B., SCHWARZ, P., MARGALITH, I., BRIDEL, C., MERTZ, K., ZIRDUM, E., PETSCH, B., FUCHS, T. J., STITZ, L. & AGUZZI, A. 2011. Aerosols transmit prions to immunocompetent and immunodeficient mice. *PLoS Pathogens,* 7(1), e1001257.

HEESTERS, BALTHASAR A., CHATTERJEE, P., KIM, Y.-A., GONZALEZ, SANTIAGO F., KULIGOWSKI, MICHAEL P., KIRCHHAUSEN, T. & CARROLL, MICHAEL C. 2013. Endocytosis and recycling of immune complexes by follicular dendritic cells enhances B cell antigen binding and activation. *Immunity,* 38(6), 1164-1175.

HEESTERS, B. A., MYERS, R. C. & CARROLL, M. C. 2014. Follicular dendritic cells: dynamic antigen libraries. *Nature Reviews Immunology,* 14(7), 495-504.

HEGDE, R. S., MASTRIANNI, J. A., SCOTT, M. R., DEFEA, K. A., TREMBLAY, P., TORCHIA, M., DEARMOND, S. J., PRUSINER, S. B. & LINGAPPA, V. R. 1998. A transmembrane form of the prion protein in neurodegenerative disease. *Science,* 279(5352), 827-34.

HEGGEBO, R., PRESS, C. M., GUNNES, G., INGE LIE, K., TRANULIS, M. A., ULVUND, M., GROSCHUP, M. H. & LANDSVERK, T. 2000. Distribution of prion protein in the ileal Peyer's patch of scrapie-free lambs and lambs naturally and experimentally exposed to the scrapie agent. *Journal of General Virology,* 81(9), 2327-2337.

HENG, T. S. P., PAINTER, M. W., ELPEK, K., LUKACS-KORNEK, V., MAUERMANN, N., TURLEY, S. J., KOLLER, D., KIM, F. S., WAGERS, A. J., ASINOVSKI, N., DAVIS, S., FASSETT, M., FEUERER, M., GRAY, D. H. D., HAXHINASTO, S., HILL, J. A., HYATT, G., LAPLACE, C., LEATHERBEE, K., MATHIS, D.,

BENOIST, C., JIANU, R., LAIDLAW, D. H., BEST, J. A., KNELL, J., GOLDRATH, A. W., JARJOURA, J., SUN, J. C., ZHU, Y., LANIER, L. L., ERGUN, A., LI, Z., COLLINS, J. J., SHINTON, S. A., HARDY, R. R., FRIEDLINE, R., SYLVIA, K. & KANG, J. 2008. The immunological genome project: networks of gene expression in immune cells. *Nature Immunology,* 9(10), 1091-1094.

HENRY, R. A. & KENDALL, P. L. 2010. CXCL13 blockade disrupts B lymphocyte organization in tertiary lymphoid structures without altering B cell receptor bias or preventing diabetes in nonobese diabetic mice. *Journal of Immunology,* 185(3), 1460-1465.

HEPPNER, F. L., CHRIST, A. D., KLEIN, M. A., PRINZ, M., FRIED, M., KRAEHENBUHL, J.-P. & AGUZZI, A. 2001a. Transepithelial prion transport by M cells. *Nature Medicine,* 7(9), 976-977.

HEPPNER, F. L., MUSAHL, C., ARRIGHI, I., KLEIN, M. A., RÜLICKE, T., OESCH, B., ZINKERNAGEL, R. M., KALINKE, U. & AGUZZI, A. 2001b. Prevention of scrapie pathogenesis by transgenic expression of anti-prion protein antibodies. *Science,* 294(5540), 178-182.

HOINVILLE, L. J., TONGUE, S. C. & WILESMITH, J. W. 2010. Evidence for maternal transmission of scrapie in naturally affected flocks. *Preventive Veterinary Medicine,* 93(2-3), 121-128.

HONDA, K., NAKANO, H., YOSHIDA, H., NISHIKAWA, S., RENNERT, P., IKUTA, K., TAMECHIKA, M., YAMAGUCHI, K., FUKUMOTO, T., CHIBA, T. & NISHIKAWA, S. I. 2001. Molecular basis for hematopoietic/mesenchymal interaction during initiation of Peyer's patch organogenesis. *Journal of Experimental Medicine,* 193(5), 621-630.

HOPKEN, U. E., ACHTMAN, A. H., KRUGER, K. & LIPP, M. 2004. Distinct and overlapping roles of CXCR5 and CCR7 in B-1 cell homing and early immunity against bacterial pathogens. *Journal of Leukocyte Biology,* 76(3), 709-18.

HOU, S., LANDEGO, I., JAYACHANDRAN, N., MILLER, A., GIBSON, I. W., AMBROSE, C. & MARSHALL, A. J. 2014. Follicular dendritic cell secreted protein FDC-SP controls IgA production. *Mucosal Immunology,* 7(4), 948-957.

HOUSTON, S. A., CEROVIC, V., THOMSON, C., BREWER, J., MOWAT, A. M. & MILLING, S. 2015. The lymph nodes draining the small intestine and colon are anatomically separate and immunologically distinct. *Mucosal Immunology,* doi:10.1038/mi.2015.77.

HSIEH, C., MACATONIA, S., TRIPP, C., WOLF, S., O'GARRA, A. & MURPHY, K. 1993. Development of TH1 CD4+ T cells through IL-12 produced by Listeria-induced macrophages. *Science,* 260(5107), 547-549.

HUANG, F.-P., FARQUHAR, C. F., MABBOTT, N. A., BRUCE, M. E. & MACPHERSON, G. G. 2002. Migrating intestinal dendritic cells transport PrP^{Sc} from the gut. *J Gen Virol,* 83(1), 267-271.

HUANG, F.-P. & MACPHERSON, G. G. 2004. Dendritic cells and oral transmission of prion diseases. *Advanced Drug Delivery Reviews,* 56(6), 901-913.

HUME, D. A. 2006. The mononuclear phagocyte system. *Current Opinion in Immunology,* 18(1), 49-53.

HUME, D. A. 2008a. Differentiation and heterogeneity in the mononuclear phagocyte system. *Mucosal Immunology,* 1(6), 432-441.

HUME, D. A. 2008b. Macrophages as APC and the dendritic cell myth. *Journal of Immunology,* 181(9), 5829-5835.

HUME, D. A. 2011. Applications of myeloid-specific promoters in transgenic mice support in vivo imaging and functional genomics but do not support the concept of distinct

macrophage and dendritic cell lineages or roles in immunity. *Journal of Leukocyte Biology,* 89(4), 525-538.

HUME, D. A., MABBOTT, N., RAZA, S. & FREEMAN, T. C. 2013. Can DCs be distinguished from macrophages by molecular signatures? *Nature Immunology,* 14(3), 187-189.

HUME, D. A., ROBINSON, A. P., MACPHERSON, G. G. & GORDON, S. 1983. The mononuclear phagocyte system of the mouse defined by immunohistochemical localization of antigen F4/80. Relationship between macrophages, Langerhans cells, reticular cells, and dendritic cells in lymphoid and hematopoietic organs. *Journal of Experimental Medicine,* 158(5), 1522-1536.

HUNTER, N., HOPE, J., MCCONNELL, I. & DICKINSON, A. G. 1987. Linkage of the scrapie-associated fibril protein (PrP) gene and sinc using congenic mice and festriction fragment length polymorphism analysis. *J. Gen. Virol.,* 68(10), 2711-2716.

ISAACS, J. D., JACKSON, G. S. & ALTMANN, D. M. 2006. The role of the cellular prion protein in the immune system. *Clinical and Experimental Immunology,* 146(1), 1-8.

ISHIKAWA, S., SATO, T., ABE, M., NAGAI, S., ONAI, N., YONEYAMA, H., ZHANG, Y.-Y., SUZUKI, T., HASHIMOTO, S.-I., SHIRAI, T., LIPP, M. & MATSUSHIMA, K. 2001. Aberrant high expression of B lymphocyte chemokine (Blc/Cxcl13) by C11b+Cd11c+ dendritic cells in murine lupus and preferential chemotaxis of B1 cells towards Blc. *Journal of Experimental Medicine,* 193(12), 1393-1402.

JANG, M. H., SOUGAWA, N., TANAKA, T., HIRATA, T., HIROI, T., TOHYA, K., GUO, Z., UMEMOTO, E., EBISUNO, Y., YANG, B.-G., SEOH, J.-Y., LIPP, M., KIYONO, H. & MIYASAKA, M. 2006. CCR7 is critically important for migration of dendritic cells in intestinal lamina propria to mesenteric lymph nodes. *Journal of Immunology,* 176(2), 803-810.

JUNG, S., UNUTMAZ, D., WONG, P., SANO, G.-I., DE LOS SANTOS, K., SPARWASSER, T., WU, S., VUTHOORI, S., KO, K., ZAVALA, F., PAMER, E. G., LITTMAN, D. R. & LANG, R. A. 2002. In vivo depletion of $CD11c^+$ dendritic cells abrogates priming of $CD8^+$ T cells by exogenous cell-associated antigens. *Immunity,* 17(2), 211-220.

KAMBAYASHI, T. & LAUFER, T. M. 2014. Atypical MHC class II-expressing antigen-presenting cells: can anything replace a dendritic cell? *Nature Reviews Immunology,* 14(11), 719-730.

KANG, Y.-S., DO, Y., LEE, H.-K., PARK, S. H., CHEONG, C., LYNCH, R. M., LOEFFLER, J. M., STEINMAN, R. M. & PARK, C. G. 2006. A dominant complement fixation pathway for pneumococcal polysaccharides initiated by SIGN-R1 interacting with C1q. *Cell,* 125(1), 47-58.

KANG, Y.-S., KIM, J. Y., BRUENING, S. A., PACK, M., CHARALAMBOUS, A., PRITSKER, A., MORAN, T. M., LOEFFLER, J. M., STEINMAN, R. M. & PARK, C. G. 2004. The C-type lectin SIGN-R1 mediates uptake of the capsular polysaccharide of Streptococcus pneumoniae in the marginal zone of mouse spleen. *Proceedings of the National Academy of Sciences of the United States of America,* 101(1), 215-220.

KANG, Y. S., YAMAZAKI, S., IYODA, T., PACK, M., BRUENING, S. A., KIM, J. Y., TAKAHARA, K., INABA, K., STEINMAN, R. M. & PARK, C. G. 2003. SIGN-R1, a novel C-type lectin expressed by marginal zone macrophages in spleen, mediates uptake of the polysaccharide dextran. *International Immunology,* 15(2), 177-186.

KHAN, W. I., RICHARD, M., AKIHO, H., BLENNERHASSET, P. A., HUMPHREYS, N. E., GRENCIS, R. K., VAN SNICK, J. & COLLINS, S. M. 2003. Modulation of intestinal muscle contraction by interleukin-9 (IL-9) or IL-9 neutralization: correlation

with worm expulsion in murine nematode infections. *Infection and Immunity,* 71(5), 2430-2438.
KIMBERLIN, R. H., COLE, S. & WALKER, C. A. 1987. Pathogenesis of scrapie is faster when infection is intraspinal instead of intracerebral. *Microbial Pathogenesis,* 2(6), 405-415.
KIMBERLIN, R. H., HALL, S. M. & WALKER, C. A. 1983. Pathogenesis of mouse scrapie: Evidence for direct neural spread of infection to the CNS after injection of sciatic nerve. *Journal of the Neurological Sciences,* 61(3), 315-325.
KIMBERLIN, R. H. & WALKER, C. A. 1978. Pathogenesis of mouse scrapie: Effect of route of inoculation on infectivity titres and dose-response curves. *Journal of Comparative Pathology,* 88(1), 39-47.
KIMBERLIN, R. H. & WALKER, C. A. 1986. Pathogenesis of scrapie (strain 263K) in hamsters infected intracerebrally, intraperitoneally or intraocularly. *Journal of General Virology,* 67(1986), 255-263.
KIMBERLIN, R. H. & WALKER, C. A. 1989. Pathogenesis of scrapie in mice after intragastric infection. *Virus Research,* 12(3), 213-220.
KITAMOTO, T., MURAMOTO, T., MOHRI, S., DOH-URA, K. & TATEISHI, J. 1991. Abnormal isoform of prion protein accumulates in follicular dendritic cells in mice with Creutzfeldt-Jakob disease. *Journal of Virology,* 65(11), 6292-6295.
KLAAS, M. & CROCKER, P. 2012. Sialoadhesin in recognition of self and non-self. *Seminars in Immunopathology,* 34(3), 353-364.
KLAAS, M., OETKE, C., LEWIS, L. E., ERWIG, L. P., HEIKEMA, A. P., EASTON, A., WILLISON, H. J. & CROCKER, P. R. 2012. Sialoadhesin promotes rapid proinflammatory and type I IFN responses to a sialylated pathogen, campylobacter jejuni. *Journal of Immunology,* 189(5), 2414-2422.
KLEIN, M. A., FRIGG, R., FLECHSIG, E., RAEBER, A. J., KALINKE, U., BLUETHMANN, H., BOOTZ, F., SUTER, M., ZINKERNAGEL, R. M. & AGUZZI, A. 1997. A crucial role for B cells in neuroinvasive scrapie. *Nature,* 390(6661), 687-690.
KLEIN, M. A., FRIGG, R., RAEBER, A. J., FLECHSIG, E., HEGYI, I., ZINKERNAGEL, R. M., WEISSMANN, C. & AGUZZI, A. 1998. PrP expression in B lymphocytes is not required for prion neuroinvasion. *Nature Medicine,* 4(12), 1429-1433.
KLEIN, M. A., KAESER, P. S., SCHWARZ, P., WEYD, H., XENARIOS, I., ZINKERNAGEL, R. M., CARROLL, M. C., VERBEEK, J. S., BOTTO, M., WALPORT, M. J., MOLINA, H., KALINKE, U., ACHA-ORBEA, H. & AGUZZI, A. 2001. Complement facilitates early prion pathogenesis. *Nature Medicine,* 7(4), 488-492.
KLEMENTOWICZ, J., TRAVIS, M. & GRENCIS, R. 2012. Trichuris muris: a model of gastrointestinal parasite infection. *Seminars in Immunopathology,* 34(6), 815-828.
KOCISKO, D. A., COME, J. H., PRIOLA, S. A., CHESEBRO, B., RAYMOND, G. J., LANSBURY, P. T. & CAUGHEY, B. 1994. Cell-free formation of protease-resistant prion protein. *Nature,* 370(6489), 471-474.
KONDO, Y. & DUNCAN, I. D. 2009. Selective reduction in microglia density and function in the white matter of colony-stimulating factor-1–deficient mice. *Journal of Neuroscience Research,* 87(12), 2686-2695.
KOYAMA, K., TAMAUCHI, H., TOMITA, M., KITAJIMA, T. & ITO, Y. 1999. B-cell activation in the mesenteric lymph nodes of resistant BALB/c mice infected with the murine nematode parasite Trichuris muris. *Parasitology Research,* 85(3), 194-199.
KRAUTLER, NIKE J., KANA, V., KRANICH, J., TIAN, Y., PERERA, D., LEMM, D., SCHWARZ, P., ARMULIK, A., BROWNING, JEFFREY L., TALLQUIST, M., BUCH, T., OLIVEIRA-MARTINS, JOSÉ B., ZHU, C., HERMANN, M., WAGNER,

U., BRINK, R., HEIKENWALDER, M. & AGUZZI, A. 2012. Follicular dendritic cells emerge from ubiquitous perivascular precursors. *Cell,* 150(1), 194-206.
KREBS, B., DORNER-CIOSSEK, C., SCHMALZBAUER, R., VASSALLO, N., HERMS, J. & KRETZSCHMAR, H. A. 2006. Prion protein induced signaling cascades in monocytes. *Biochemical and Biophysical Research Communications,* 340(1), 13-22.
KRETZSCHMAR, H. A., PRUSINER, S. B., STOWRING, L. E. & DEARMOND, S. J. 1986. Scrapie prion proteins are synthesized in neurons. *American Journal of Pathology,* 122(1), 1-5.
KRUG, A., FRENCH, A. R., BARCHET, W., FISCHER, J. A. A., DZIONEK, A., PINGEL, J. T., ORIHUELA, M. M., AKIRA, S., YOKOYAMA, W. M. & COLONNA, M. 2004. TLR9-dependent recognition of MCMV by IPC and DC generates coordinated cytokine responses that activate antiviral NK cell function. *Immunity,* 21(1), 107-119.
KRÜGER, D., THOMZIG, A., LENZ, G., KAMPF, K., MCBRIDE, P. & BEEKES, M. 2009. Faecal shedding, alimentary clearance and intestinal spread of prions in hamsters fed with scrapie. *Veterinary Research,* 40(1), 04.
KUBOSAKI, A., YUSA, S., NASU, Y., NISHIMURA, T., NAKAMURA, Y., SAEKI, K., MATSUMOTO, Y., ITOHARA, S. & ONODERA, T. 2001. Distribution of cellular isoform of prion protein in T lymphocytes and bone marrow, analyzed by wild-type and prion protein gene-deficient mice. *Biochemical and Biophysical Research Communications,* 282(1), 103-107.
KUJALA, P., RAYMOND, C. R., ROMEIJN, M., GODSAVE, S. F., VAN KASTEREN, S. I., WILLE, H., PRUSINER, S. B., MABBOTT, N. A. & PETERS, P. J. 2011. Prion uptake in the gut: identification of the first uptake and replication sites. *PLoS Pathogens,* 7(12), e1002449.
KUNZI, V., GLATZEL, M., NAKANO, M. Y., GREBER, U. F., VAN LEUVEN, F. & AGUZZI, A. 2002. Unhampered prion neuroinvasion despite impaired fast axonal transport in transgenic mice overexpressing four-repeat tau. *Journal of Neuroscience,* 22(17), 7471-7477.
LASMEZAS, C. I., CESBRON, J. Y., DESLYS, J. P., DEMAIMAY, R., ANJOU, K. T., RIOUX, R., LEMAIRE, C., LOCHT, C. & DORMONT, D. 1996. Immune system-dependent and -independent replication of the scrapie agent. *Journal of Virology,* 70(2), 1292-1295.
LAWSON, V. A., PRIOLA, S. A., WEHRLY, K. & CHESEBRO, B. 2001. N-terminal truncation of prion protein affects both formation and conformation of abnormal protease-resistant prion protein generated in vitro. *Journal of Biological Chemistry,* 276(38), 35265-71.
LEON, B., BALLESTEROS-TATO, A., BROWNING, J. L., DUNN, R., RANDALL, T. D. & LUND, F. E. 2012. Regulation of TH2 development by CXCR5+ dendritic cells and lymphotoxin-expressing B cells. *Nature Immunology,* 13(7), 681-690.
LEVAVASSEUR, E., METHAROM, P., DORBAN, G., NAKANO, H., KAKIUCHI, T., CARNAUD, C., SARRADIN, P. & AUCOUTURIER, P. 2007. Experimental scrapie in 'plt' mice: an assessment of the role of dendritic-cell migration in the pathogenesis of prion diseases. *Journal of General Virology,* 88(8), 2353-60.
LEWIS, V., HILL, A. F., HAIGH, C. L., KLUG, G. M., MASTERS, C. L., LAWSON, V. A. & COLLINS, S. J. 2009. Increased proportions of C1 truncated prion protein protect against cellular M1000 prion infection. *Journal of Neuropathology & Experimental Neurology,* 68(10), 1125-1135.
LIN, C.-L., SURI, R., M. , RAHDON, R., A. , AUSTYN, J., M. & ROAKE, J., A. 1998. Dendritic cell chemotaxis and transendothelial migration are induced by distinct chemokines and are regulated on maturation. *European Journal of Immunology,* 28(12), 4114-4122.

LIU, K., VICTORA, G. D., SCHWICKERT, T. A., GUERMONPREZ, P., MEREDITH, M. M., YAO, K., CHU, F.-F., RANDOLPH, G. J., RUDENSKY, A. Y. & NUSSENZWEIG, M. 2009. In vivo analysis of dendritic cell development and homeostasis. *Science,* 324(5925), 392-397.

LIU, T., LI, R., WONG, B.-S., LIU, D., PAN, T., PETERSEN, R. B., GAMBETTI, P. & SY, M.-S. 2001. Normal cellular prior protein is preferentially expressed on subpopulations of murine hemopoietic cells. *Journal of Immunology,* 166(6), 3733-3742.

LLEWELYN, C. A., HEWITT, P. E., KNIGHT, R. S. G., AMAR, K., COUSENS, S., MACKENZIE, J. & WILL, R. G. 2004. Possible transmission of variant Creutzfeldt-Jakob disease by blood transfusion. *The Lancet,* 363(9407), 417-421.

LÖTSCHER, M., RECHER, M., HUNZIKER, L. & KLEIN, M. A. 2003. Immunologically induced, complement-dependent up-regulation of the prion protein in the mouse spleen: follicular dendritic cells versus capsule and trabeculae. *Journal of Immunology,* 170(12), 6040-6047.

LU, C., TAKAGI, J. & SPRINGER, T. A. 2001. Association of the membrane proximal regions of the α and β subunit cytoplasmic domains constrains an integrin in the inactive state. *Journal of Biological Chemistry,* 276(18), 14642-14648.

LUHR, K. M., NORDSTROM, E. K., LOW, P., LJUNGGREN, H. G., TARABOULOS, A. & KRISTENSSON, K. 2004. Scrapie protein degradation by cysteine proteases in CD11c+ dendritic cells and GT1-1 neuronal cells. *Journal of Virology,* 78(9), 4776-82.

LUHR, K. M., WALLIN, R. P., LJUNGGREN, H. G., LOW, P., TARABOULOS, A. & KRISTENSSON, K. 2002. Processing and degradation of exogenous prion protein by CD11c(+) myeloid dendritic cells in vitro. *Journal of Virology,* 76(23), 12259-64.

LUNNON, K., TEELING, J. L., TUTT, A. L., CRAGG, M. S., GLENNIE, M. J. & PERRY, V. H. 2011. Systemic inflammation modulates Fc receptor expression on microglia during chronic neurodegeneration. *Journal of Immunology,* 186(12), 7215-7224.

LUTHER, S. A., ANSEL, K. M. & CYSTER, J. G. 2003. Overlapping roles of CXCL13, interleukin 7 receptor α, and CCR7 ligands in lymph node development. *Journal of Experimental Medicine,* 197(9), 1191-1198.

MABBOTT, N. A. 2004. The complement system in prion diseases. *Current Opinion in Immunology,* 16(5), 587-593.

MABBOTT, N. A. & BRADFORD, B. M. 2015. The good, the bad, and the ugly of dendritic cells during prion disease. *Journal of Immunology Research,* Article No. 168574(2015), 1-13.

MABBOTT, N. A., BROWN, K. L., MANSON, J. & BRUCE, M. E. 1997. T lymphocyte activation and the cellular form of the prion protein, PrP^c. *Immunology,* 92(2), 162-165.

MABBOTT, N. A. & BRUCE, M. E. 2001. The immunobiology of TSE diseases. *Journal of General Virology,* 82(10), 2307-2318.

MABBOTT, N. A. & BRUCE, M. E. 2004. Complement component C5 is not involved in scrapie pathogenesis. *Immunobiology,* 209(7), 545-549.

MABBOTT, N. A., BRUCE, M. E., BOTTO, M., WALPORT, M. J. & PEPYS, M. B. 2001. Temporary depletion of complement component C3 or genetic deficiency of C1q significantly delays onset of scrapie. *Nature Medicine,* 7(4), 485-487.

MABBOTT, N. A., DONALDSON, D. S., OHNO, H., WILLIAMS, I. R. & MAHAJAN, A. 2013. Microfold (M) cells: important immunosurveillance posts in the intestinal epithelium. *Mucosal Immunology,* 6(4), 666-677.

MABBOTT, N. A., KENNETH BAILLIE, J., HUME, D. A. & FREEMAN, T. C. 2010. Meta-analysis of lineage-specific gene expression signatures in mouse leukocyte populations. *Immunobiology,* 215(9–10), 724-736.

MABBOTT, N. A., KENNETH BAILLIE, J., KOBAYASHI, A., DONALDSON, D. S., OHMORI, H., YOON, S.-O., FREEDMAN, A. S., FREEMAN, T. C. & SUMMERS, K. M. 2011. Expression of mesenchyme-specific gene signatures by follicular dendritic cells: insights from the meta-analysis of microarray data from multiple mouse cell populations. *Immunology,* 133(4), 482-498.

MABBOTT, N. A., MACKAY, F., MINNS, F. & BRUCE, M. E. 2000. Temporary inactivation of follicular dendritic cells delays neuroinvasion of scrapie. *Nature Medicine,* 6(7), 719-720.

MABBOTT, N. A., MCGOVERN, G., JEFFREY, M. & BRUCE, M. E. 2002. Temporary blockade of the tumor necrosis factor receptor signaling pathway impedes the spread of scrapie to the brain. *Journal of Virology,* 76(10), 5131-5139.

MABBOTT, N. A., YOUNG, J., MCCONNELL, I. & BRUCE, M. E. 2003. Follicular dendritic cell dedifferentiation by treatment with an inhibitor of the lymphotoxin pathway dramatically reduces scrapie susceptibility. *Journal of Virology,* 77(12), 6845-54.

MACDONALD, K. P. A., PALMER, J. S., CRONAU, S., SEPPANEN, E., OLVER, S., RAFFELT, N. C., KUNS, R., PETTIT, A. R., CLOUSTON, A., WAINWRIGHT, B., BRANSTETTER, D., SMITH, J., PAXTON, R. J., CERRETTI, D. P., BONHAM, L., HILL, G. R. & HUME, D. A. 2010. An antibody against the colony-stimulating factor 1 receptor depletes the resident subset of monocytes and tissue- and tumor-associated macrophages but does not inhibit inflammation. *Blood,* 116(19), 3955-3963.

MACDONALD, K. P. A., ROWE, V., BOFINGER, H. M., THOMAS, R., SASMONO, T., HUME, D. A. & HILL, G. R. 2005. The colony-stimulating factor 1 receptor is expressed on dendritic cells during differentiation and regulates their expansion. *Journal of Immunology,* 175(3), 1399-1405.

MACPHERSON, A. J., MCCOY, K. D., JOHANSEN, F. E. & BRANDTZAEG, P. 2008. The immune geography of IgA induction and function. *Mucosal Immunology,* 1(1), 11-22.

MACPHERSON, A. J. & UHR, T. 2004. Induction of protective IgA by intestinal dendritic cells carrying commensal bacteria. *Science,* 303(5664), 1662-1665.

MADDUR, M. S., SHARMA, M., HEGDE, P., STEPHEN-VICTOR, E., PULENDRAN, B., KAVERI, S. V. & BAYRY, J. 2014. Human B cells induce dendritic cell maturation and favour Th2 polarization by inducing OX-40 ligand. *Nature communications,* 5(2014), 4092-4092.

MALLUCCI, G., DICKINSON, A., LINEHAN, J., KLOHN, P. C., BRANDNER, S. & COLLINGE, J. 2003. Depleting neuronal PrP in prion infection prevents disease and reverses spongiosis. *Science,* 302(5646), 871-874.

MANDELS, T. E., PHIPPSI, R. P., ABBOT, A. & TEW, J. G. 1980. The follicular dendritic cell: long term antigen retention during immunity. *Immunological Reviews,* 53(1), 29-59.

MANETTI, R., GEROSA, F., GIUDIZI, M. G., BIAGIOTTI, R., PARRONCHI, P., PICCINNI, M. P., SAMPOGNARO, S., MAGGI, E., ROMAGNANI, S. & TRINCHIERI, G. 1994. Interleukin 12 induces stable priming for interferon gamma (IFN-gamma) production during differentiation of human T helper (Th) cells and transient IFN-gamma production in established Th2 cell clones. *Journal of Experimental Medicine,* 179(4), 1273-1283.

MANETTI, R., PARRONCHI, P., GIUDIZI, M. G., PICCINNI, M. P., MAGGI, E., TRINCHIERI, G. & ROMAGNANI, S. 1993. Natural killer cell stimulatory factor (interleukin 12 [IL-12]) induces T helper type 1 (Th1)-specific immune responses and

inhibits the development of IL-4-producing Th cells. *Journal of Experimental Medicine,* 177(4), 1199-1204.
MANSON, J. C., CLARKE, A. R., HOOPER, M. L., AITCHISON, L., MCCONNELL, I. & HOPE, J. 1994. 129/Ola mice carrying a null mutation in PrP that abolishes mRNA production are developmentally normal. *Molecular Neurobiology,* 8(2-3), 121-7.
MANUELIDIS, L. 1997. Decontamination of Creutzfeldt-Jakob Disease and other transmissible agents. *Journal of Neurovirology,* 3(1), 62-65.
MAO, X., FUJIWARA, Y. & ORKIN, S. H. 1999. Improved reporter strain for monitoring Cre recombinase-mediated DNA excisions in mice. *Proceedings of the National Academy of Sciences of the United States of America,* 96(9), 5037-5042.
MARELLA, M. & CHABRY, J. 2004. Neurons and astrocytes respond to prion infection by inducing microglia recruitment. *Journal of Neuroscience,* 24(3), 620-627.
MARTINEZ, M. G., BIALECKI, M. A., BELOUZARD, S., CORDO, S. M., CANDURRA, N. A. & WHITTAKER, G. R. 2013. Utilization of human DC-SIGN and L-SIGN for entry and infection of host cells by the new world arenavirus, junín virus. *Biochemical and Biophysical Research Communications,* 441(3), 612-617.
MARZI, A., GRAMBERG, T., SIMMONS, G., MÖLLER, P., RENNEKAMP, A. J., KRUMBIEGEL, M., GEIER, M., EISEMANN, J., TURZA, N., SAUNIER, B., STEINKASSERER, A., BECKER, S., BATES, P., HOFMANN, H. & PÖHLMANN, S. 2004. DC-SIGN and DC-SIGNR Interact with the glycoprotein of marburg virus and the S protein of severe acute respiratory syndrome coronavirus. *Journal of Virology,* 78(21), 12090-12095.
MASCANFRONI, I. D., YESTE, A., VIEIRA, S. M., BURNS, E. J., PATEL, B., SLOMA, I., WU, Y., MAYO, L., BEN-HAMO, R., EFRONI, S., KUCHROO, V. K., ROBSON, S. C. & QUINTANA, F. J. 2013. IL-27 acts on DCs to suppress the T cell response and autoimmunity by inducing expression of the immunoregulatory molecule CD39. *Nature Immunology,* 14(10), 1054-1063.
MASTRIANNI, J. A. 2010. The genetics of prion diseases. *Genet Med,* 12(4), 187-195.
MAZZONE, A. & RICEVUTI, G. 1995. Leukocyte CD11/CD18 integrins: biological and clinical relevance. *Haematologica,* 80(2), 161-175.
MCBRIDE, P. A. & BEEKES, M. 1999. Pathological PrP is abundant in sympathetic and sensory ganglia of hamsters fed with scrapie. *Neuroscience Letters,* 265(2), 135-138.
MCBRIDE, P. A., EIKELENBOOM, P., KRAAL, G., FRASER, H. & BRUCE, M. E. 1992. PrP protein is associated with follicular dendritic cells of spleens and lymph nodes in uninfected and scrapie-infected mice. *Journal of Pathology,* 168(4), 413-418.
MCBRIDE, P. A., SCHULZ-SCHAEFFER, W. J., DONALDSON, M., BRUCE, M., DIRINGER, H., KRETZSCHMAR, H. A. & BEEKES, M. 2001. Early spread of scrapie from the gastrointestinal tract to the central nervous system involves autonomic fibers of the splanchnic and vagus nerves. *Journal of Virology,* 75(19), 9320-7.
MCCLOSKEY, M. L., CUROTTO DE LAFAILLE, M. A., CARROLL, M. C. & ERLEBACHER, A. 2011. Acquisition and presentation of follicular dendritic cell–bound antigen by lymph node–resident dendritic cells. *Journal of Experimental Medicine,* 208(1), 135-148.
MCCULLOCH, L., BROWN, K. L., BRADFORD, B. M., HOPKINS, J., BAILEY, M., RAJEWSKY, K., MANSON, J. C. & MABBOTT, N. A. 2011. Follicular dendritic cell-specific prion protein (PrP^c) expression alone is sufficient to sustain prion infection in the spleen. *PLoS Pathogens,* 7(12), e1002402.
MCCULLOCH, L., BROWN, K. L. & MABBOTT, N. A. 2013. Ablation of the cellular prion protein, PrPC, specifically on follicular dendritic cells has no effect on their maturation or function. *Immunology,* 138(3), 246-257.

MCDONALD, K. G., MCDONOUGH, J. S., DIECKGRAEFE, B. K. & NEWBERRY, R. D. 2010. Dendritic cells produce CXCL13 and participate in the development of murine small intestine lymphoid tissues. *American Journal of Pathology,* 176(5), 2367-2377.

MCGOVERN, G., MABBOTT, N. & JEFFREY, M. 2009. Scrapie affects the maturation cycle and immune complex trapping by follicular dendritic cells in mice. *PLoS ONE,* 4(12), e8186.

MCKINLEY, M. P., BOLTON, D. C. & PRUSINER, S. B. 1983. A protease-resistant protein is a structural component of the Scrapie prion. *Cell,* 35(1), 57-62.

MCLEAN, I. W. & NAKANE, P. K. 1974. Periodate-lysine-paraformaldehye fixative a new fixative for immunoelectron microscopy. *Journal of Histochemistry & Cytochemistry,* 22(12), 1077-1083.

MEBIUS, R. E. 2003. Organogenesis of lymphoid tissues. *Nature Reviews Immunology,* 3(4), 292-303.

METLAY, J. P., WITMER-PACK, M. D., AGGER, R., CROWLEY, M. T., LAWLESS, D. & STEINMAN, R. M. 1990. The distinct leukocyte integrins of mouse spleen dendritic cells as identified with new hamster monoclonal antibodies. *Journal of Experimental Medicine,* 171(5), 1753-1771.

MICHEL, B., MEYERETT-REID, C., JOHNSON, T., FERGUSON, A., WYCKOFF, C., PULFORD, B., BENDER, H., AVERY, A., TELLING, G., DOW, S. & ZABEL, M. D. 2012. Incunabular immunological events in prion trafficking. *Scientific Reports,* 2(2012), 440.

MINIKEL, E. V., VALLABH, S. M., LEK, M., ESTRADA, K., SAMOCHA, K. E., SATHIRAPONGSASUTI, J. F., MCLEAN, C. Y., TUNG, J. Y., YU, L. P. C., GAMBETTI, P., BLEVINS, J., ZHANG, S., COHEN, Y., CHEN, W., YAMADA, M., HAMAGUCHI, T., SANJO, N., MIZUSAWA, H., NAKAMURA, Y., KITAMOTO, T., COLLINS, S. J., BOYD, A., WILL, R. G., KNIGHT, R., PONTO, C., ZERR, I., KRAUS, T. F. J., EIGENBROD, S., GIESE, A., CALERO, M., DE PEDRO-CUESTA, J., HAÏK, S., LAPLANCHE, J.-L., BOUAZIZ-AMAR, E., BRANDEL, J.-P., CAPELLARI, S., PARCHI, P., POLEGGI, A., LADOGANA, A., O'DONNELL-LURIA, A. H., KARCZEWSKI, K. J., MARSHALL, J. L., BOEHNKE, M., LAAKSO, M., MOHLKE, K. L., KÄHLER, A., CHAMBERT, K., MCCARROLL, S., SULLIVAN, P. F., HULTMAN, C. M., PURCELL, S. M., SKLAR, P., VAN DER LEE, S. J., ROZEMULLER, A., JANSEN, C., HOFMAN, A., KRAAIJ, R., VAN ROOIJ, J. G. J., IKRAM, M. A., UITTERLINDEN, A. G., VAN DUIJN, C. M., DALY, M. J. & MACARTHUR, D. G. 2016. Quantifying prion disease penetrance using large population control cohorts. *Science Translational Medicine,* 8(322), 322ra9-322ra9.

MIRABILE, I., JAT, P. S., BRANDNER, S. & COLLINGE, J. 2014. Identification of clinical target areas in the brainstem of prion infected mice. *Neuropathology and Applied Neurobiology,* 41(5), 613-630.

MITCHELL, D. A., KIRBY, L., PAULIN, S. M., VILLIERS, C. L. & SIM, R. B. 2007. Prion protein activates and fixes complement directly via the classical pathway: Implications for the mechanism of scrapie agent propagation in lymphoid tissue. *Molecular Immunology,* 44(11), 2997-3004.

MIYASAKA, M. & TANAKA, T. 2004. Lymphocyte trafficking across high endothelial venules: dogmas and enigmas. *Nature Reviews Immunology,* 4(5), 360-370.

MOK, S. W. F., PROIA, R. L., BRINKMANN, V. & MABBOTT, N. A. 2012. B cell-specific S1PR1 deficiency blocks prion dissemination between secondary lymphoid organs. *Journal of Immunology,* 188(10), 5032–5040.

MONTRASIO, F., FRIGG, R., GLATZEL, M., KLEIN, M. A., MACKAY, F., AGUZZI, A. & WEISSMANN, C. 2000. Impaired prion replication in spleens of mice lacking functional follicular dendritic cells. *Science,* 288(5469), 1257-1259.

MOONEY, J. E., ROLFE, B. E., OSBORNE, G. W., SESTER, D. P., VAN ROOIJEN, N., CAMPBELL, G. R., HUME, D. A. & CAMPBELL, J. H. 2010. Cellular plasticity of inflammatory myeloid cells in the peritoneal foreign body response. *American Journal of Pathology,* 176(1), 369-380.

MOORE, R. C., HOPE, J., MCBRIDE, P. A., MCCONNELL, I., SELFRIDGE, J., MELTON, D. W. & MANSON, J. C. 1998. Mice with gene targetted prion protein alterations show that Prnp, Sinc and Prni are congruent. *Nature Genetics,* 18(2), 118-125.

MORI, S., NAKANO, H., ARITOMI, K., WANG, C.-R., GUNN, M. D. & KAKIUCHI, T. 2001. Mice lacking expression of the chemokines Ccl21-ser and Ccl19 (plt Mice) demonstrate delayed but enhanced T cell immune responses. *Journal of Experimental Medicine,* 193(2), 207-218.

MORRIS, J. A. & GAJDUSEK, D. C. 1963. Encephalopathy in mice following inoculation of scrapie sheep brain. *Nature,* 197(4872), 1084-1086.

MÜLLER, G., HÖPKEN, U., E. & LIPP, M. 2003. The impact of CCR7 and CXCR5 on lymphoid organ development and systemic immunity. *Immunological Reviews,* 195(1), 117-135.

MÜLLER, G. & LIPP, M. 2003. Concerted action of the chemokine and lymphotoxin system in secondary lymphoid-organ development. *Current Opinion in Immunology,* 15(2), 217-224.

MUZUMDAR, M. D., TASIC, B., MIYAMICHI, K., LI, L. & LUO, L. 2007. A global double-fluorescent Cre reporter mouse. *Genesis,* 45(9), 593-605.

MYONES, B. L., DALZELL, J. G., HOGG, N. & ROSS, G. D. 1988. Neutrophil and monocyte cell surface p150,95 has iC3b-receptor (CR4) activity resembling CR3. *Journal of Clinical Investigation,* 82(2), 640-651.

NAIK, S. H., SATHE, P., PARK, H.-Y., METCALF, D., PROIETTO, A. I., DAKIC, A., CAROTTA, S., O'KEEFFE, M., BAHLO, M., PAPENFUSS, A., KWAK, J.-Y., WU, L. & SHORTMAN, K. 2007. Development of plasmacytoid and conventional dendritic cell subtypes from single precursor cells derived in vitro and in vivo. *Nature Immunology,* 8(11), 1217-1226.

NAKAGAWA, R., TOGAWA, A., NAGASAWA, T. & NISHIKAWA, S.-I. 2013. Peyer's patch inducer cells play a leading role in the formation of B and T cell zone architecture. *Journal of Immunology,* 190(7), 3309-3318.

NEUTRA, M. R., FREY, A. & KRAEHENBUHL, J. P. 1996. Epithelial M cells: gateways for mucosal infection and immunization. *Cell,* 86(3), 345-8.

NIESS, J. H., BRAND, S., GU, X., LANDSMAN, L., JUNG, S., MCCORMICK, B. A., VYAS, J. M., BOES, M., PLOEGH, H. L., FOX, J. G., LITTMAN, D. R. & REINECKER, H.-C. 2005. CX_3CR1-mediated dendritic cell access to the intestinal lumen and bacterial clearance. *Science,* 307(5707), 254-258.

NISHIKAWA, S.-I., HONDA, K., VIEIRA, P. & YOSHIDA, H. 2003. Organogenesis of peripheral lymphoid organs. *Immunological Reviews,* 195(1), 72-80.

NISHIKAWA, Y., HIKIDA, M., MAGARI, M., KANAYAMA, N., MORI, M., KITAMURA, H., KUROSAKI, T. & OHMORI, H. 2006. Establishment of lymphotoxin β receptor signaling-dependent cell lines with follicular dendritic cell phenotypes from mouse lymph nodes. *Journal of Immunology,* 177(8), 5204-5214.

NOSSAL, G. J. V., ADA, G. L. & AUSTIN, C. M. 1965. Antigens in immunity: X. induction of immunologic tolerance to salmonella adelaide flagellin. *Journal of Immunology,* 95(4), 665-672.

NUVOLONE, M., HERMANN, M., SORCE, S., RUSSO, G., TIBERI, C., SCHWARZ, P., MINIKEL, E., SANOUDOU, D., PELCZAR, P. & AGUZZI, A. 2016. Strictly co-isogenic C57BL/6J-Prnp−/− mice: A rigorous resource for prion science. *The Journal of Experimental Medicine,* 213(3), 313-327.

NUVOLONE, M., KANA, V., HUTTER, G., SAKATA, D., MORTIN-TOTH, S. M., RUSSO, G., DANSKA, J. S. & AGUZZI, A. 2013. SIRPα polymorphisms, but not the prion protein, control phagocytosis of apoptotic cells. *Journal of Experimental Medicine,* 210(12), 2539-2552.

OESCH, B., WESTAWAY, D., WÄLCHLI, M., MCKINLEY, M. P., KENT, S. B. H., AEBERSOLD, R., BARRY, R. A., TEMPST, P., TEPLOW, D. B., HOOD, L. E., PRUSINER, S. B. & WEISSMANN, C. 1985. A cellular gene encodes scrapie PrP 27-30 protein. *Cell,* 40(4), 735-746.

OETKE, C., VINSON, M. C., JONES, C. & CROCKER, P. R. 2006. Sialoadhesin-deficient mice exhibit subtle changes in B- and T-cell populations and reduced immunoglobulin M levels. *Molecular and Cellular Biology,* 26(4), 1549-1557.

OHL, L., BERNHARDT, G., PABST, O. & FÖRSTER, R. 2003. Chemokines as organizers of primary and secondary lymphoid organs. *Seminars in Immunology,* 15(5), 249-255.

OKADA, T., NGO, V. N., EKLAND, E. H., FORSTER, R., LIPP, M., LITTMAN, D. R. & CYSTER, J. G. 2002. Chemokine Requirements for B Cell Entry to Lymph Nodes and Peyer's Patches. *Journal of Experimental Medicine,* 196(1), 65-75.

ONAI, N., MANZ, M. G. & SCHMID, M. A. 2010. Isolation of common dendritic cell progenitors (CDP) from mouse bone marrow.595: Methods in Molecular Biology: Dendritic Cell Protocols 2nd edition. New York: Shalin H Naik, 2010. Vol 595: 195-203.

ONAI, N., OBATA-ONAI, A., SCHMID, M. A., OHTEKI, T., JARROSSAY, D. & MANZ, M. G. 2007. Identification of clonogenic common Flt3+M-CSFR+ plasmacytoid and conventional dendritic cell progenitors in mouse bone marrow. *Nature Immunology,* 8(11), 1207-1216.

PAAR, C., WURM, S., PFARR, W., SONNLEITNER, A. & WECHSELBERGER, C. 2007. Prion protein resides in membrane microclusters of the immunological synapse during lymphocyte activation. *European Journal of Cell Biology,* 86(5), 253-264.

PABST, O., HERBRAND, H., FRIEDRICHSEN, M., VELAGA, S., DORSCH, M., BERHARDT, G., WORBS, T., MACPHERSON, A. J. & FORSTER, R. 2006. Adaptation of solitary intestinal lymphoid tissue in response to microbiota and chemokine receptor CCR7 signaling. *Journal of Immunology,* 177(10), 6824-32.

PABST, O., HERBRAND, H., WORBS, T., FRIEDRICHSEN, M., YAN, S., HOFFMANN, M., W., KÖRNER, H., BERNHARDT, G., PABST, R. & FÖRSTER, R. 2005. Cryptopatches and isolated lymphoid follicles: dynamic lymphoid tissues dispensable for the generation of intraepithelial lymphocytes. *European Journal of Immunology,* 35(1), 98-107.

PAN, T., WONG, B.-S., LIU, T., LI, R., PETERSEN, R. B. & SY, M.-S. 2002. Cell-surface prion protein interacts with glycosaminoglycans. *Biochemical Journal,* 368(1), 81-90.

PAQUET, S., DAUDE, N., COURAGEOT, M. P., CHAPUIS, J., LAUDE, H. & VILETTE, D. 2007. PrPc does not mediate internalization of PrPSc but is required at an early stage for de novo prion infection of Rov cells. *Journal of Virology,* 81(19), 10786-91.

PASPARAKIS, M., KOUSTENI, S., PESCHON, J. & KOLLIAS, G. 2000. Tumor Necrosis Factor and the p55TNF Receptor Are Required for Optimal Development of the Marginal Sinus and for Migration of Follicular Dendritic Cell Precursors into Splenic Follicles. *Cellular Immunology,* 201(1), 33-41.

PATTISON, I. H. 1957. Myopathy in sheep. *The Lancet,* 269(6959), 104-105.

PATTISON, I. H. 1965. Resistance of the scrapie agent to formalin. *Journal of Comparative Pathology,* 75(2), 159-164.
PATTISON, I. H., GORDON, W. S. & MILLSON, G. C. 1959. Experimental production of scrapie in goats. *Journal of Comparative Pathology,* 1959(69), 300-312.
PATTISON, I. H. & MILLSON, G. C. 1961. Scrapie Produced Experimentally in Goats With Special Reference To the Clinical Syndrome. *Journal of Comparative Pathology and Therapeutics,* 1961(71), 101-108.
PAVLI, P., WOODHAMS, C. E., DOE, W. F. & HUME, D. A. 1990. Isolation and characterization of antigen-presenting dendritic cells from the mouse intestinal lamina propria. *Immunology,* 70(1), 40-47.
PAYNE, R. J. H. & KRAKAUER, D. C. 1998. The spatial dynamics of prion disease. *Proceedings of the Royal Society of London B: Biological Sciences,* 265(1412), 2341-2346.
PERRIGOUE, J. G., SAENZ, S. A., SIRACUSA, M. C., ALLENSPACH, E. J., TAYLOR, B. C., GIACOMIN, P. R., NAIR, M. G., DU, Y., ZAPH, C., VAN ROOIJEN, N., COMEAU, M. R., PEARCE, E. J., LAUFER, T. M. & ARTIS, D. 2009. MHC class II-dependent basophil-CD4$^+$ T cell interactions promote T_H2 cytokine-dependent immunity. *Nature Immunology,* 10(7), 697-705.
PHAN, T. G., GREEN, J. A., GRAY, E. E., XU, Y. & CYSTER, J. G. 2009. Immune complex relay by subcapsular sinus macrophages and noncognate B cells drives antibody affinity maturation. *Nature Immunology,* 10(7), 786-793.
PHAN, T. G., GRIGOROVA, I., OKADA, T. & CYSTER, J. G. 2007. Subcapsular encounter and complement-dependent transport of immune complexes by lymph node B cells. *Nature Immunology,* 8(9), 992-1000.
PHYTHIAN-ADAMS, A. T., COOK, P. C., LUNDIE, R. J., JONES, L. H., SMITH, K. A., BARR, T. A., HOCHWELLER, K., ANDERTON, S. M., HÄMMERLING, G. J., MAIZELS, R. M. & MACDONALD, A. S. 2010. CD11c depletion severely disrupts Th2 induction and development in vivo. *Journal of Experimental Medicine,* 207(10), 2089-2096.
PRABAGAR, M. G., DO, Y., RYU, S., PARK, J. Y., CHOI, H. J., CHOI, W. S., YUN, T. J., MOON, J., CHOI, I. S., KO, K., KO, K., YOUNG SHIN, C., CHEONG, C. & KANG, Y. S. 2013. SIGN-R1, a C-type lectin, enhances apoptotic cell clearance through the complement deposition pathway by interacting with C1q in the spleen. *Cell Death Differentiation,* 20(4), 535-545.
PRINZ, M., HEIKENWALDER, M., JUNT, T., SCHWARZ, P., GLATZEL, M., HEPPNER, F. L., FU, Y.-X., LIPP, M. & AGUZZI, A. 2003a. Positioning of follicular dendritic cells within the spleen controls prion neuroinvasion. *Nature,* 425(6961), 957-962.
PRINZ, M., HEIKENWALDER, M., SCHWARZ, P., TAKEDA, K., AKIRA, S. & AGUZZI, A. 2003b. Prion pathogenesis in the absence of Toll-like receptor signalling. *EMBO Reports,* 4(2), 195-9.
PRINZ, M., HUBER, G., MACPHERSON, A. J. S., HEPPNER, F. L., GLATZEL, M., EUGSTER, H.-P., WAGNER, N. & AGUZZI, A. 2003c. Oral prion infection requires normal numbers of Peyer's patches but not of enteric lymphocytes. *American Journal of Pathology,* 162(4), 1103-1111.
PRINZ, M., MONTRASIO, F., KLEIN, M. A., SCHWARZ, P., PRILLER, J., ODERMATT, B., PFEFFER, K. & AGUZZI, A. 2002. Lymph nodal prion replication and neuroinvasion in mice devoid of follicular dendritic cells. *Proceedings of the National Academy of Sciences of the United States of America,* 99(2), 919-924.
PRUSINER, S. B. 1982. Novel proteinaceous infectious particles cause scrapie. *Science,* 216(4542), 136-144.

RANDOLPH, G. J. 2001. Dendritic cell migration to lymph nodes: cytokines, chemokines, and lipid mediators. *Seminars in Immunology,* 13(5), 267-274.
RAYMOND, C. R., AUCOUTURIER, P. & MABBOTT, N. A. 2007. In vivo depletion of $CD11c^+$ cells impairs scrapie agent neuroinvasion from the intestine. *Journal of Immunology,* 179(11), 7758-7766.
RENNERT, P. D., BROWNING, J. L., MEBIUS, R., MACKAY, F. & HOCHMAN, P. S. 1996. Surface lymphotoxin alpha/beta complex is required for the development of peripheral lymphoid organs. *Journal of Experimental Medicine,* 184(5), 1999-2006.
RIEMER, C., SCHULTZ, J., BURWINKEL, M., SCHWARZ, A., MOK, S. W., GULTNER, S., BAMME, T., NORLEY, S., VAN LANDEGHEM, F., LU, B., GERARD, C. & BAIER, M. 2008. Accelerated prion replication in, but prolonged survival times of, prion-infected CXCR3-/- mice. *Journal of Virology,* 82(24), 12464-71.
RIESNER, D. 2003. Biochemistry and structure of PrPC and PrPSc. *British Medical Bulletin,* 66(1), 21-33.
RITCHIE, G. E., MOFFATT, B. E., SIM, R. B., MORGAN, B. P., DWEK, R. A. & RUDD, P. M. 2002. Glycosylation and the complement System. *Chemical Reviews,* 102(2), 305-320.
ROSSI, D. & ZLOTNIK, A. 2000. The biology of chemokines and their receptors. *Annual Review of Immunology,* 18(1), 217-242.
RUBTSOV, A. V., RUBTSOVA, K., KAPPLER, J. W., JACOBELLI, J., FRIEDMAN, R. S. & MARRACK, P. 2015. CD11c-expressing B cells are located at the T cell/B cell border in spleen and are potent APCs. *Journal of Immunology,* 195(1), 71-9.
RUDD, P. M., WORMALD, M. R., WING, D. R., PRUSINER, S. B. & DWEK, R. A. 2001. Prion glycoprotein: structure, dynamics, and roles for the sugars. *Biochemistry,* 40(13), 3759-66.
RYBNER-BARNIER, C., JACQUEMOT, C., CUCHE, C., DORE, G., MAJLESSI, L., GABELLEC, M. M., MORIS, A., SCHWARTZ, O., DI SANTO, J., CUMANO, A., LECLERC, C. & LAZARINI, F. 2006. Processing of the bovine spongiform encephalopathy-specific prion protein by dendritic cells. *Journal of Virology,* 80(10), 4656-63.
RYBNER, C., HILLION, J., SAHRAOUI, T., LANOTTE, M. & BOTTI, J. 2002. All-trans retinoic acid down-regulates prion protein expression independently of granulocyte maturation. *Leukemia,* 16(5), 940-948.
SAEKI, H., MOORE, A. M., BROWN, M. J. & HWANG, S. T. 1999. Cutting edge: secondary lymphoid-tissue chemokine (SLC) and CC chemokine receptor 7 (CCR7) participate in the emigration pathway of mature dendritic cells from the skin to regional lymph nodes. *Journal of Immunology,* 162(5), 2472-2475.
SAEKI, H., WU, M. T., OLASZ, E. & HWANG, S. T. 2000. A migratory population of skin-derived dendritic cells expresses CXCR5, responds to B lymphocyte chemoattractant in vitro, and co-localizes to B cell zones in lymph nodes in vivo. *European Journal of Immunology,* 30(10), 2808-2814.
SALLUSTO, F., SCHAERLI, P., LOETSCHER, P., SCHANIEL, C., LENIG, D., MACKAY, C., R, QIN, S. & LANZAVECCHIA, A. 1998. Rapid and coordinated switch in chemokine receptor expression during dendritic cell maturation. *European Journal of Immunology,* 28(9), 2760-2769.
SÁNCHEZ-MARTÍN, L., ESTECHA, A., SAMANIEGO, R., SÁNCHEZ-RAMÓN, S., VEGA, M. Á. & SÁNCHEZ-MATEOS, P. 2011. The chemokine CXCL12 regulates monocyte-macrophage differentiation and RUNX3 expression. *Blood,* 117(1), 88-97.
SARMA, J. V. & WARD, P. A. 2010. The complement system. *Cell and Tissue Research,* 343(1), 227-235.

SASMONO, R. T., OCEANDY, D., POLLARD, J. W., TONG, W., PAVLI, P., WAINWRIGHT, B. J., OSTROWSKI, M. C., HIMES, S. R. & HUME, D. A. 2003. A macrophage colony-stimulating factor receptor-green fluorescent protein transgene is expressed throughout the mononuclear phagocyte system of the mouse. *Blood,* 101(3), 1155-1163.

SASSA, Y., INOSHIMA, Y. & ISHIGURO, N. 2010. Bovine macrophage degradation of scrapie and BSE PrPSc. *Veterinary Immunology and Immunopathology,* 133(1), 33-39.

SATPATHY, A. T., KC, W., ALBRING, J. C., EDELSON, B. T., KRETZER, N. M., BHATTACHARYA, D., MURPHY, T. L. & MURPHY, K. M. 2012. Zbtb46 expression distinguishes classical dendritic cells and their committed progenitors from other immune lineages. *Journal of Experimental Medicine,* 209(6), 1135-1152.

SAUER, B. & HENDERSON, N. 1988. Site-specific DNA recombination in mammalian cells by the Cre recombinase of bacteriophage P1. *Proceedings of the National Academy of Sciences of the United States of America,* 85(14), 5166-5170.

SAUNDERSON, S. C., DUNN, A. C., CROCKER, P. R. & MCLELLAN, A. D. 2014. CD169 mediates the capture of exosomes in spleen and lymph node. *Blood,* 123(2), 208-216.

SCHMITT-ULMS, G., LEGNAME, G., BALDWIN, M. A., BALL, H. L., BRADON, N., BOSQUE, P. J., CROSSIN, K. L., EDELMAN, G. M., DEARMOND, S. J., COHEN, F. E. & PRUSINER, S. B. 2001. Binding of neural cell adhesion molecules (N-CAMs) to the cellular prion protein. *Journal of Molecular Biology,* 314(5), 1209-1225.

SCHULZ-SCHAEFFER, W. J., TSCHÖKE, S., KRANEFUSS, N., DRÖSE, W., HAUSE-REITNER, D., GIESE, A., GROSCHUP, M. H. & KRETZSCHMAR, H. A. 2000. The paraffin-embedded tissue blot detects PrPSc early in the incubation time in prion diseases. *American Journal of Pathology,* 156(1), 51-56.

SCHULZ, O., JAENSSON, E., PERSSON, E. K., LIU, X., WORBS, T., AGACE, W. W. & PABST, O. 2009. Intestinal $CD103^+$, but not CX_3CR1^+, antigen sampling cells migrate in lymph and serve classical dendritic cell functions. *Journal of Experimental Medicine,* 206(13), 3101-3114.

SCHWAEBLE, W., SCHÄFER, M. K., PETRY, F., FINK, T., KNEBEL, D., WEIHE, E. & LOOS, M. 1995. Follicular dendritic cells, interdigitating cells, and cells of the monocyte-macrophage lineage are the C1q-producing sources in the spleen. Identification of specific cell types by in situ hybridization and immunohistochemical analysis. *Journal of Immunology,* 155(10), 4971-8.

SEDER, R. A., GAZZINELLI, R., SHER, A. & PAUL, W. E. 1993. Interleukin 12 acts directly on CD4+ T cells to enhance priming for interferon gamma production and diminishes interleukin 4 inhibition of such priming. *Proceedings of the National Academy of Sciences of the United States of America,* 90(21), 10188-10192.

SETHI, S., KERKSIEK, K. M., BROCKER, T. & KRETZSCHMAR, H. 2007. Role of the $CD8^+$ dendritic cell subset in transmission of prions. *Journal of Virology,* 81(9), 4877-4880.

SHREFFLER, W. G., CASTRO, R. R., KUCUK, Z. Y., CHARLOP-POWERS, Z., GRISHINA, G., YOO, S., BURKS, A. W. & SAMPSON, H. A. 2006. The major glycoprotein allergen from arachis hypogaea, Ara h 1, is a ligand of dendritic cell-specific ICAM-grabbing nonintegrin and acts as a Th2 adjuvant In vitro. *Journal of Immunology,* 177(6), 3677-3685.

SIGURDSON, C. J. & MILLER, M. W. 2003. Other animal prion diseases. *British Medical Bulletin,* 66(1), 199-212.

SIGURDSON, C. J., WILLIAMS, E. S., MILLER, M. W., SPRAKER, T. R., O'ROURKE, K. I. & HOOVER, E. A. 1999. Oral transmission and early lymphoid tropism of chronic

wasting disease PrPres in mule deer fawns (Odocoileus hemionus). *Journal of General Virology,* 80(10), 2757-2764.

SIGURDSSON, B. 1954. Rida, a chronic encephalitis of sheep with general remarks on infections which develop slowly and some of their special characteristics. *Brit Vet Jour,* 110(9), 341-354.

SIGURDSSON, B. & PALSSON, P. A. 1958. Visna of sheep - a slow, demyleinating infection. *British Journal of Experimental Pathology,* 39(5), 519.

SIMMONS, G., REEVES, J. D., GROGAN, C. C., VANDENBERGHE, L. H., BARIBAUD, F., WHITBECK, J. C., BURKE, E., BUCHMEIER, M. J., SOILLEUX, E. J., RILEY, J. L., DOMS, R. W., BATES, P. & PÖHLMANN, S. 2003. DC-SIGN and DC-SIGNR bind ebola glycoproteins and enhance infection of macrophages and endothelial cells. *Virology,* 305(1), 115-123.

SMITH, K. A., HARCUS, Y., GARBI, N., HÄMMERLING, G. J., MACDONALD, A. S. & MAIZELS, R. M. 2012. Type 2 innate immunity in helminth infection is induced redundantly and acts autonomously following CD11c+ cell depletion. *Infection and Immunity,* 80(10), 3481-3489.

SOZZANI, S. 2005. Dendritic cell trafficking: More than just chemokines. *Cytokine & Growth Factor Reviews,* 16(6), 581-592.

SPIELHAUPTER, C. & SCHÄTZL, H. M. 2001. PrPC Directly Interacts with Proteins Involved in Signaling Pathways. *Journal of Biological Chemistry,* 276(48), 44604-44612.

SPRINGER, T., GALFRÉ, G., SECHER, D. S. & MILSTEIN, C. 1979. Mac-1: a macrophage differentiation antigen identified by monoclonal antibody. *European Journal of Immunology,* 9(4), 301-306.

SRIVASTAVA, S., MAKARAVA, N., KATORCHA, E., SAVTCHENKO, R., BROSSMER, R. & BASKAKOV, I. V. 2015. Post-conversion sialylation of prions in lymphoid tissues. *Proceedings of the National Academy of Sciences of the United States of America,* 112(48), E6654-E6662.

STAHL, N., BORCHELT, D. R., HSIAO, K. & PRUSINER, S. B. 1987. Scrapie prion protein contains a phosphatidylinositol glycolipid. *Cell,* 51(2), 229-240.

STAMP, J. T. 1962. Scrapie: a transmissible disease of sheep. *Veterinary Record,* 74(1962), 357-362.

STEINMAN, R. M., GRANELLI-PIPERNO, A., POPE, M., TRUMPFHELLER, C., IGNATIUS, R., ARRODE, G., RACZ, P. & TENNER-RACZ, K. 2003. The interaction of immunodeficiency viruses with dendritic cells. *In:* STEINKASSERER, A. (ed.) *Dendritic Cells and Virus Infection.*2003(1),1-30 Berlin, Heidelberg: Springer-Verlag.

STEINMAN, R. M. & WITMER, M. D. 1978. Lymphoid dendritic cells are potent stimulators of the primary mixed leukocyte reaction in mice. *Proceedings of the National Academy of Sciences of the United States of America,* 75(10), 5132-5136.

STIMSON, E., HOPE, J., CHONG, A. & BURLINGAME, A. L. 1999. Site-specific characterization of the N-linked glycans of murine prion protein by high-performance liquid chromatography/electrospray mass spectrometry and exoglycosidase digestions. *Biochemistry,* 38(15), 4885-4895.

SUZUKI, K., GRIGOROVA, I., PHAN, T. G., KELLY, L. M. & CYSTER, J. G. 2009. Visualizing B cell capture of cognate antigen from follicular dendritic cells. *Journal of Experimental Medicine,* 206(7), 1485-1493.

SUZUKI, K., KAWAMOTO, S., MARUYA, M. & FAGARASAN, S. 2010. GALT: organization and dynamics leading to IgA synthesis. *In:* SIDONIA, F. & ANDREA, C. (eds.) *Advances in Immunology.*Volume 107(2010),153-185: Academic Press.

SZAKAL, A. K., KOSCO, M. H. & TEW, J. G. 1988. A novel in vivo follicular dendritic cell-dependent iccosome-mediated mechanism for delivery of antigen to antigen-processing cells. *Journal of Immunology,* 140(2), 341-53.

TAMOUTOUNOUR, S., HENRI, S., LELOUARD, H., DE BOVIS, B., DE HAAR, C., VAN DER WOUDE, C. J., WOLTMAN, A. M., REYAL, Y., BONNET, D., SICHIEN, D., BAIN, C. C., MOWAT, A. M., REIS E SOUSA, C., POULIN, L. F., MALISSEN, B. & GUILLIAMS, M. 2012. CD64 distinguishes macrophages from dendritic cells in the gut and reveals the Th1-inducing role of mesenteric lymph node macrophages during colitis. *European Journal of Immunology,* 42(12), 3150-3166.

TAMURA, T., TAILOR, P., YAMAOKA, K., KONG, H. J., TSUJIMURA, H., O'SHEA, J. J., SINGH, H. & OZATO, K. 2005. IFN regulatory factor-4 and -8 govern dendritic cell subset development and their functional diversity. *The Journal of Immunology,* 174(5), 2573-2581.

TASSANEETRITHEP, B., BURGESS, T. H., GRANELLI-PIPERNO, A., TRUMPFHELLER, C., FINKE, J., SUN, W., ELLER, M. A., PATTANAPANYASAT, K., SARASOMBATH, S., BIRX, D. L., STEINMAN, R. M., SCHLESINGER, S. & MAROVICH, M. A. 2003. DC-SIGN (CD209) mediates dengue virus infection of human dendritic cells. *Journal of Experimental Medicine,* 197(7), 823-829.

TAYLOR, D. M. 1993. Bovine spongiform encephalopathy and its association with the feeding of ruminant-derived protein. *Developments in biological standardization,* 80(1993), 215-214.

TAYLOR, D. M. 2000. Inactivation of Transmissible Degenerative Encephalopathy Agents: A Review. *The Veterinary Journal,* 159(1), 10-17.

TAYLOR, D. M., FRASER, H., MCCONNELL, I., BROWN, D. A., BROWN, K. L., LAMZA, K. A. & SMITH, G. R. A. 1994. Decontamination studies with the agents of bovine spongiform encephalopathy and scrapie. *Archives of Virology,* 139(3-4), 313-326.

TAYLOR, D. M., MCCONNELL, I. & FRASER, H. 1996. Scrapie infection can be established readily through skin scarification in immunocompetent but not immunodeficient mice. *Journal of General Virology,* 77(7), 1595-1599.

TAYLOR, P. R., PICKERING, M. C., KOSCO-VILBOIS, M. H., WALPORT, M. J., BOTTO, M., GORDON, S. & MARTINEZ-POMARES, L. 2002. The follicular dendritic cell restricted epitope, FDC-M2, is complement C4; localization of immune complexes in mouse tissues. *European Journal of Immunology,* 32(7), 1883-1896.

THADANI, V., PENAR, P. L., PARTINGTON, J., KALB, R., JANSSEN, R., SCHONBERGER, L. B., RABKIN, C. S. & PRICHARD, J. W. 1988. Creutzfeldt-Jakob disease probably acquired from a cadaveric dura mater graft. *Journal of Neurosurgery,* 69(5), 766-769.

TOBLER, I., GAUS, S. E., DEBOER, T., ACHERMANN, P., FISCHER, M., RULICKE, T., MOSER, M., OESCH, B., MCBRIDE, P. A. & MANSON, J. C. 1996. Altered circadian activity rhythms and sleep in mice devoid of prion protein. *Nature,* 380(6575), 639-642.

TROMBETTA, E. S., EBERSOLD, M., GARRETT, W., PYPAERT, M. & MELLMAN, I. 2003. Activation of lysosomal function during dendritic cell maturation. *Science,* 299(5611), 1400-3.

TSUTSUI, S., HAHN, J. N., JOHNSON, T. A., ALI, Z. & JIRIK, F. R. 2008. Absence of the cellular prion protein exacerbates and prolongs neuroinflammation in experimental autoimmune encephalomyelitis. *American Journal of Pathology,* 173(4), 1029-1041.

TUZI, N. L., CLARKE, A. R., BRADFORD, B., AITCHISON, L., THOMSON, V. & MANSON, J. C. 2004. Cre-loxP mediated control of PrP to study transmissible spongiform encephalopathy diseases. *Genesis,* 40(1), 1-6.

VAN DEN BROECK, W., DERORE, A. & SIMOENS, P. 2006. Anatomy and nomenclature of murine lymph nodes: Descriptive study and nomenclatory standardization in BALB/cAnNCrl mice. *Journal of Immunological Methods,* 312(1-2), 12-19.

VAN LIEMPT, E., VAN VLIET, S. J., ENGERING, A., GARCÍA VALLEJO, J. J., BANK, C. M. C., SANCHEZ-HERNANDEZ, M., VAN KOOYK, Y. & VAN DIE, I. 2007. Schistosoma mansoni soluble egg antigens are internalized by human dendritic cells through multiple C-type lectins and suppress TLR-induced dendritic cell activation. *Molecular Immunology,* 44(10), 2605-2615.

VEERHUIS, R., NIELSEN, H. M. & TENNER, A. J. 2011. Complement in the brain. *Molecular Immunology,* 48(14), 1592-1603.

VEIGA-FERNANDES, H., COLES, M. C., FOSTER, K. E., PATEL, A., WILLIAMS, A., NATARAJAN, D., BARLOW, A., PACHNIS, V. & KIOUSSIS, D. 2007. Tyrosine kinase receptor RET is a key regulator of Peyer's patch organogenesis. *Nature,* 446(7135), 547-551.

VERMI, W., LONARDI, S., BOSISIO, D., UGUCCIONI, M., DANELON, G., PILERI, S., FLETCHER, C., SOZZANI, S., ZORZI, F., ARRIGONI, G., DOGLIONI, C., PONZONI, M. & FACCHETTI, F. 2008. Identification of CXCL13 as a new marker for follicular dendritic cell sarcoma. *Journal of Pathology,* 216(3), 356-364.

VOIGT, I., CAMACHO, S. A., DE BOER, B. A., LIPP, M., FÖRSTER, R. & BEREK, C. 2000. CXCR5-deficient mice develop functional germinal centers in the splenic T cell zone. *European Journal of Immunology,* 30(2), 560-567.

VON POSER-KLEIN, C., FLECHSIG, E., HOFFMANN, T., SCHWARZ, P., HARMS, H., BUJDOSO, R., AGUZZI, A. & KLEIN, M. A. 2008. Alteration of B-cell subsets enhances neuroinvasion in mouse scrapie infection. *Journal of Virology,* 82(7), 3791-3795.

WALZ, R., AMARAL, O. B., ROCKENBACH, I. C., ROESLER, R., IZQUIERDO, I., CAVALHEIRO, E. A., MARTINS, V. R. & BRENTANI, R. R. 1999. Increased sensitivity to seizures in mice lacking cellular prion protein. *Epilepsia,* 40(12), 1679-1682.

WANG, S., MIYAZAKI, Y., SHINOZAKI, Y. & YOSHIDA, H. 2007. Augmentation of antigen-presenting and Th1-promoting functions of dendritic cells by WSX-1(IL-27R) deficiency. *Journal of Immunology,* 179(10), 6421-6428.

WANG, X., CHO, B., SUZUKI, K., XU, Y., GREEN, J. A., AN, J. & CYSTER, J. G. 2011. Follicular dendritic cells help establish follicle identity and promote B cell retention in germinal centers. *Journal of Experimental Medicine,* 208(12), 2497-2510.

WANG, Y. M., SZRETTER, K. J., VERMI, W., GILFILLAN, S., ROSSINI, C., CELLA, M., BARROW, A. D., DIAMOND, M. S. & COLONNA, M. 2012. IL-34 is a tissue-restricted ligand of CSF1R required for the development of Langerhans cells and microglia. *Nature Immunology,* 13(8), 753-760.

WATHNE, G. J., KISSENPFENNIG, A., MALISSEN, B., ZURZOLO, C. & MABBOTT, N. A. 2012. Determining the role of mononuclear phagocytes in prion neuroinvasion from the skin. *Journal of Leukocyte Biology,* 91(5), 817-828.

WATHNE, G. J. & MABBOTT, N. A. 2012. The diverse roles of mononuclear phagocytes in prion disease pathogenesis. *Prion,* 6(2), 124-133.

WEISE, J., SANDAU, R., SCHWARTING, S., CROME, O., WREDE, A., SCHULZ-SCHAEFFER, W., ZERR, I. & BÄHR, M. 2006. Deletion of cellular prion protein results in reduced Akt activation, enhanced postischemic caspase-3 activation, and exacerbation of ischemic brain injury. *Stroke,* 37(5), 1296-1300.

WILL, R. G. & IRONSIDE, J. W. 1999. Oral infection by the bovine spongiform encephalopathy prion. *Proceedings of the National Academy of Sciences,* 96(9), 4738-4739.

WILLIAMS, A. E., LAWSON, L. J., PERRY, V. H. & FRASER, H. 1994. Characterization of the microglial response in murine scrapie. *Neuropathology and Applied Neurobiology,* 20(1), 47-55.

WILLIAMS, J. W., TJOTA, M. Y., CLAY, B. S., LUGT, B. V., BANDUKWALA, H. S., HRUSCH, C. L., DECKER, D. C., BLAINE, K. M., FIXSEN, B. R., SINGH, H., SCIAMMAS, R. & SPERLING, A. I. 2013. Transcription factor IRF4 drives dendritic cells to promote Th2 differentiation. *Nature communications,* 4(2013), 2990-2990.

WRIGHT, S. D. & JONG, M. T. 1986. Adhesion-promoting receptors on human macrophages recognize Escherichia coli by binding to lipopolysaccharide. *The Journal of Experimental Medicine,* 164(6), 1876-1888.

WRIGHT, S. D., WEITZ, J. I., HUANG, A. J., LEVIN, S. M., SILVERSTEIN, S. C. & LOIKE, J. D. 1988. Complement receptor type three (CD11b/CD18) of human polymorphonuclear leukocytes recognizes fibrinogen. *Proceedings of the National Academy of Sciences of the United States of America,* 85(20), 7734-7738.

WROE, S. J., PAL, S., SIDDIQUE, D., HYARE, H., MACFARLANE, R., JOINER, S., LINEHAN, J. M., BRANDNER, S., WADSWORTH, J. D. F., HEWITT, P. & COLLINGE, J. 2006. Clinical presentation and pre-mortem diagnosis of variant Creutzfeldt-Jakob disease associated with blood transfusion: a case report. *The Lancet,* 368(9552), 2061-2067.

WU, C., OROZCO, C., BOYER, J., LEGLISE, M., GOODALE, J., BATALOV, S., HODGE, C. L., HAASE, J., JANES, J., HUSS, J. W. & SU, A. I. 2009. BioGPS: an extensible and customizable portal for querying and organizing gene annotation resources. *Genome Biology,* 10(11), R130-R130.

WU, C. Y., DEMEURE, C., KINIWA, M., GATELY, M. & DELESPESSE, G. 1993. IL-12 induces the production of IFN-gamma by neonatal human CD4 T cells. *Journal of Immunology,* 151(4), 1938-49.

WU, M.-T. & HWANG, S. T. 2002. CXCR5-transduced bone marrow-derived dendritic cells traffic to B cell zones of lymph nodes and modify antigen-specific immune responses. *Journal of Immunology,* 168(10), 5096-5102.

WU, M., SAEKI, H. & HWANG, S. 2001. Subcutaneously (SC)-injected, CXCR5-transduced bone marrow-derived dendritic cells (BMDC) traffic to B cells zones of lymph nodes (LN) and modify antigen-specific immune responses. *Journal of Investigative Dermatology,* 117(2), 350.

WU, Y., SUKUMAR, S., EL SHIKH, M. E., BEST, A. M., SZAKAL, A. K. & TEW, J. G. 2008. Immune complex-bearing follicular dendritic cells deliver a late antigenic signal that promotes somatic hypermutation. *Journal of Immunology,* 180(1), 281-290.

WYKES, M., POMBO, A., JENKINS, C. & MACPHERSON, G. G. 1998. Dendritic cells interact directly with naive B lymphocytes to transfer antigen and initiate class switching in a primary T-dependent response. *Journal of Immunology,* 161(3), 1313-1319.

YADAVALLI, R., GUTTMANN, R. P., SEWARD, T., CENTERS, A. P., WILLIAMSON, R. A. & TELLING, G. C. 2004. Calpain-dependent endoproteolytic cleavage of PrPSc modulates scrapie prion propagation. *Journal of Biological Chemistry,* 279(21), 21948-21956.

YAMAMOTO, M., YOSHIZAKI, K., KISHIMOTO, T. & ITO, H. 2000. IL-6 is required for the development of Th1 cell-mediated murine colitis. *Journal of Immunology,* 164(9), 4878-4882.

YANAMADALA, V. & FRIEDLANDER, R. M. 2010. Complement in neuroprotection and neurodegeneration. *Trends in Molecular Medicine,* 16(2), 69-76.

YEWDALL, A. W., DRUTMAN, S. B., JINWALA, F., BAHJAT, K. S. & BHARDWAJ, N. 2010. CD8+ T cell priming by dendritic cell vaccines requires antigen transfer to endogenous antigen presenting cells. *PLoS ONE,* 5(6), e11144.

YIN, S., PHAM, N., YU, S., LI, C., WONG, P., CHANG, B., KANG, S.-C., BIASINI, E., TIEN, P., HARRIS, D. A. & SY, M.-S. 2007. Human prion proteins with pathogenic mutations share common conformational changes resulting in enhanced binding to glycosaminoglycans. *Proceedings of the National Academy of Sciences of the United States of America,* 104(18), 7546-7551.

YOSHIDA, H., HONDA, K., SHINKURA, R., ADACHI, S., NISHIKAWA, S., MAKI, K., IKUTA, K. & NISHIKAWA, S.-I. 1999. IL-7 receptorα^{+} CD3^{-} cells in the embryonic intestine induces the organizing center of Peyer's patches. *International Immunology,* 11(5), 643-655.

YU, P., WANG, Y., CHIN, R. K., MARTINEZ-POMARES, L., GORDON, S., KOSCO-VIBOIS, M. H., CYSTER, J. & FU, Y.-X. 2002. B cells control the migration of a subset of dendritic cells into B cell follicles via CXC chemokine ligand 13 in a lymphotoxin-dependent fashion. *Journal of Immunology,* 168(10), 5117-5123.

ZABEL, M. D., HEIKENWALDER, M., PRINZ, M., ARRIGHI, I., SCHWARZ, P., KRANICH, J., VON TEICHMAN, A., HAAS, K. M., ZELLER, N., TEDDER, T. F., WEIS, J. H. & AGUZZI, A. 2007. Stromal complement receptor CD21/35 facilitates lymphoid prion colonization and pathogenesis. *Journal of Immunology,* 179(9), 6144-6152.

ZANATA, S. M., LOPES, M. H., MERCADANTE, A. F., HAJJ, G. N. M., CHIARINI, L. B., NOMIZO, R., FREITAS, A. R. O., CABRAL, A. L. B., LEE, K. S., JULIANO, M. A., DE OLIVEIRA, E., JACHIERI, S. G., BURLINGAME, A., HUANG, L., LINDEN, R., BRENTANI, R. R. & MARTINS, V. R. 2002. Stress-inducible protein 1 is a cell surface ligand for cellular prion that triggers neuroprotection. *EMBO Journal,* 21(13), 3307-3316.

ZHAO, C., CANTIN, R., BRETON, M., PAPADOPOULOU, B. & TREMBLAY, M. J. 2005. DC-SIGN-mediated transfer of HIV-1 is compromised by the ability of leishmania infantum to exploit DC-SIGN as a ligand. *Journal of Infectious Diseases,* 191(10), 1665-1669.

ZHOU, L., LIM, Q.-E., WAN, G. & TOO, H.-P. 2010. Normalization with genes encoding ribosomal proteins but not GAPDH provides an accurate quantification of gene expressions in neuronal differentiation of PC12 cells. *BMC Genomics,* 11(1), 1-13.

ZLOTNIK, I. & RENNIE, J. C. 1963. Further observations on the experimental transmission of scrapie from sheep and goats to laboratory mice. *Journal of Comparative Pathology,* 73(1963), 150-62.

ZOMOSA-SIGNORET, V., MAYORAL, M., LIMÓN, D., ESPINOSA, B., CALVILLO, M., ZENTENO, E., MARTÍNEZ, V. & GUEVARA, J. 2011. Sialylated and O-glycosidically linked glycans in prion protein deposits in a case of Gerstmann-Sträussler-Scheinker disease. *Neuropathology,* 31(2), 162-169.

Appendices

Appendix 1. Publications

BRADFORD, B. M., SESTER, D. P., HUME, D. A. & MABBOTT, N. A. 2011. Defining the anatomical localisation of subsets of the murine mononuclear phagocyte system using integrin alpha X (Itgax, CD11c) and colony stimulating factor 1 receptor (Csf1r, CD115) expression fails to discriminate dendritic cells from macrophages. *Immunobiology,* 216(11), 1228-1237.

BRADFORD, B. & MABBOTT, N. 2012. Prion disease and the innate immune system. *Viruses,* 4(12), 3389-3491.

BRADFORD, B. M., CROCKER, P. R. & MABBOTT, N. A. 2014. Peripheral prion disease pathogenesis is unaltered in the absence of sialoadhesin (Siglec-1/CD169). *Immunology,* 143(1), 120-9.

MABBOTT, N. A. & BRADFORD, B. M. 2015. The good, the bad, and the ugly of dendritic cells during prion disease. *Journal of Immunology Research,* Article No. 168574(2015), 1-13.

BRADFORD, B. M., BROWN, K. L. & MABBOTT, N. A. 2016. Prion pathogenesis is unaltered following down-regulation of SIGN-R1. Virology, 497(2016), 337-345.